

LONDON  
SCHOOL of  
HYGIENE  
& TROPICAL  
MEDICINE



LSHTM Research Online

Sparkes, PC; (2023) Exploring energy metabolism in male and female *Plasmodium falciparum* gametocytes. PhD thesis, London School of Hygiene & Tropical Medicine. DOI: <https://doi.org/10.17037/PUBS.04671600>

Downloaded from: <https://researchonline.lshtm.ac.uk/id/eprint/4671600/>

DOI: <https://doi.org/10.17037/PUBS.04671600>

**Usage Guidelines:**

Please refer to usage guidelines at <https://researchonline.lshtm.ac.uk/policies.html> or alternatively contact [researchonline@lshtm.ac.uk](mailto:researchonline@lshtm.ac.uk).

Available under license. To note, 3rd party material is not necessarily covered under this license: <http://creativecommons.org/licenses/by-nc-nd/4.0/>

<https://researchonline.lshtm.ac.uk>

LONDON  
SCHOOL of  
HYGIENE  
& TROPICAL  
MEDICINE



**Exploring energy metabolism in male and female  
*Plasmodium falciparum* gametocytes**

**Penny Chantal Sparkes**

Thesis submitted in accordance with the requirements  
for the degree of Doctor of Philosophy

University of London

October 2023

**Department of Infection Biology**

**Faculty of Infectious and Tropical Diseases**

**London School of Hygiene and Tropical Medicine**

**Primary supervisor:** Michael Delves

**Secondary supervisor:** David Baker

**Funded by the MRC-LID Doctoral Training Programme**

**Declaration**

I, Penny Chantal Sparkes, confirm that the work presented in this thesis is my own. Where information has been derived from other sources, I confirm that this has been indicated in the thesis.

## Abstract

Gametocytes are essential for human-to-mosquito transmission of the malaria parasite *Plasmodium falciparum*, but despite their importance, many aspects of their cell biology remain poorly understood, including energy metabolism. It is known that gametocytes upregulate mitochondrial energy metabolism, but not how this is regulated. In addition, it has not previously been investigated whether energy metabolism differs between male and female gametocytes.

Quantitative image analysis of functional mitochondrial labelling demonstrated that male gametocyte mitochondria are less active than those of females. Susceptibility of male and female gametocytes to mitochondrial electron transport chain (mETC) inhibitors was compared by two readouts: mitochondrial activity (MitoTracker labelling) and gamete formation (dual-gamete formation assay). Changes in mitochondrial activity were found to result in arrest of gametogenesis. Addition of oligomycin A with no pre-incubation also markedly reduced gametogenesis, suggesting that mitochondrial respiration is essential for optimal gametogenesis. Parasites expressing ATP nanosensors revealed that in excess glucose, intracellular ATP concentrations in gametocytes are insensitive to oligomycin A, demonstrating that glycolysis is sufficient to meet the energy needs of mature gametocytes. This supports the notion that upregulation of mitochondrial energy metabolism is to meet the energy demands of gametogenesis in males and onward mosquito stage development in females.

Data mining of published proteomic data and bioinformatics approaches identified six proteins of interest, two of which were taken forward for characterisation. One of these proteins, a putative ADP-forming acetyl-CoA synthetase (ACS-ADP), was found to be mitochondrially localised and expressed throughout the life cycle. A second protein, phosphofructokinase 11 (PFK11), was successfully disrupted using CRISPR gene editing, resulting in a marked reduction in oocyst production, suggesting it is critical for ookinete development into oocysts. While further experiments are required to determine their exact function, this work has identified several potential regulators of gametocyte energy metabolism.

## **Acknowledgments**

Foremost, I would like to thank my primary supervisor, Michael Delves, for giving me the opportunity to undertake my PhD in his lab and for his constant support and encouragement over the course of the project. I couldn't have asked for a better mentor and I have learned so much from you. Thank you also to my second supervisor, David Baker, for his helpful advice and guidance and interesting discussions throughout the PhD project.

I am grateful to the other members of the Delves lab, Eduardo and Toyin, for your advice, support and invaluable help with my experiments. Together with Michael, thank you for making the group such a fun place to work – despite the difficulties that working with gametocytes throws at us.

Thank you to all the members of the Moon, Baker, Sutherland, van Ooij and Conway labs and everyone in 380 for their guidance and support during the PhD project. In particular I would like to acknowledge James Thomas and Avnish Patel for their help and advice with troubleshooting my transfections (and all the times I had to borrow WR!). I would also like give special thanks to the members of the Malaria Transmission Facility past and present, chiefly Mojca Kristan, Harry Pollard and Prisca Hill, without whom my mosquito feeding experiments would not have been possible.

In addition to practical help and advice, I am grateful for the friendships I have made during my time at LSHTM, in particular Giulia Pianta, Tansy Vallintine, Aline Freville and the rest of the 'Malaria Girls' and 'London Walking' groups (you know who you are). Sometimes putting the world to rights at the Pump Handle Bar or the Institute is exactly what you need as a PhD student to keep your spirits up.

Finally, I would like to thank my friends and family. Thank you all for entertaining my enthusiasm for parasites and encouraging me to keep going and never give up. I could not have done it without you. Special thanks go to my friend Robyn Tucker for the inspiration to undertake this challenge and someone to vent to about the PhD experience during, and to my partner Jockum for his love, encouragement and support.

# Table of Contents

|  |    |
|--|----|
| List of figures .....  | 9  |
| List of tables .....   | 15 |
| Abbreviations .....  | 16 |
| List of Appendices .....   | 20 |
| Chapter 1 Introduction .....   | 21 |
| 1.1 Malaria as a public health problem .....   | 21 |
| 1.2 Aetiological agent and vector .....  | 22 |
| 1.3 The <i>Plasmodium</i> life cycle .....   | 22 |
| 1.3.1 The liver stage .....  | 22 |
| 1.3.2 The blood stage .....  | 23 |
| 1.3.3 Gametocytogenesis .....  | 24 |
| 1.3.4 The mosquito stages .....  | 27 |
| 1.4 Targeting transmission – why target gametocytes? .....                                     | 28 |
| 1.5 Energy metabolism in <i>Plasmodium</i> parasites .....                                     | 31 |
| 1.6 Sexual dimorphism in male and female gametocytes .....                                     | 36 |
| 1.7 Research Aims and Objectives .....   | 39 |
| 1.6.1 Aim 1 .....  | 39 |
| 1.6.2 Aim 2 .....  | 40 |
| 1.6.3 Aim 3 .....  | 40 |
| Chapter 2 Materials and Methods .....  | 41 |
| 2.1 Selection of candidate proteins .....  | 41 |
| 2.2.1 Data Sources .....   | 41 |
| 2.1.2 Protein selection workflow .....   | 41 |
| 2.1.3 Bioinformatic analysis .....   | 42 |
| 2.2 Molecular biology techniques .....   | 42 |
| 2.2.1 Polymerase chain reaction (PCR) .....  | 42 |
| 2.2.2 Primer design .....  | 42 |
| 2.2.3 Restriction digests .....  | 42 |
| 2.2.4 Generation of selection-linked integration (SLI) constructs for tagging<br>and TGD ..... | 43 |
| 2.2.5 Generation of CRISPR-Cas9 constructs for KO of PFK11 .....                               | 48 |
| 2.2.6 Generation of CRISPR-Cas9 vector for mNG-tagging of PFK11 .....                          | 52 |
| 2.2.6 Colony PCR screening .....   | 55 |
| 2.2.7 Sequencing .....   | 55 |
| 2.2.8 Plasmid purification .....   | 56 |

|           |   |    |
|-----------|---|----|
| 2.3       | Parasite culture .....  | 56 |
| 2.3.1     | Asexual blood stage parasite culture .....  | 56 |
| 2.3.2     | Gametocyte culture .....  | 56 |
| 2.3.3     | Gametocyte purification .....   | 57 |
| 2.3.4     | Percoll and sorbitol purification .....   | 58 |
| 2.3.5     | Ethanol precipitation of plasmid DNA .....  | 58 |
| 2.3.6     | Schizont-stage transfections .....  | 58 |
| 2.3.7     | Pre-loading transfections .....   | 58 |
| 2.3.8     | Mycoplasma screening .....  | 59 |
| 2.4       | Immunohistochemistry and imaging techniques .....   | 59 |
| 2.4.1     | Generation of custom antibodies .....   | 59 |
| 2.4.2     | MitoTrackerRed CMXRos labelling .....   | 59 |
| 2.4.3     | Fixation of gametocytes for immunofluorescence microscopy .....   | 59 |
| 2.4.4     | Immunofluorescence analysis (IFA) .....   | 60 |
| 2.4.5     | Immunofluorescence microscopy .....   | 61 |
| 2.4.6     | Quantitative image analysis .....   | 61 |
| 2.4.7     | Förster resonance energy transfer (FRET) microscopy .....   | 62 |
| 2.5       | Phenotyping of transgenic lines .....   | 64 |
| 2.5.1     | Asexual growth assay .....  | 64 |
| 2.5.2     | Quantification of gametocytaemia .....  | 64 |
| 2.5.3     | Quantification of gametogenesis .....   | 64 |
| 2.5.4     | Mosquito feeding assays .....   | 64 |
| 2.6       | Parasite assays .....   | 65 |
| 2.6.1     | MitoTracker drug assay .....  | 65 |
| 2.6.2     | Dual gamete formation assay (DGFA) .....  | 66 |
| 2.6.4     | Exflagellation IFAs – effect of glucose availability .....  | 66 |
| 2.6.5     | Plate-based exflagellation and female activation assays .....   | 67 |
| 2.6.6     | Serum and glucose titrations .....  | 67 |
| Chapter 3 | Investigation of mitochondrial structure and function in male and female <i>P. falciparum</i> gametocytes ..... | 69 |
| 3.1       | Introduction .....  | 69 |
| 3.2       | Results .....   | 70 |
| 3.2.1     | Development of a specific antibody marker to discriminate between male and female gametocytes .....             | 70 |
| 3.2.2     | Development of and validation of image analysis methodology .....   | 76 |
| 3.2.3     | Comparison of male and female gametocyte mitochondrial morphology .....   | 86 |
| 3.2.4     | Quantifying the mitochondrial activity of mature male and female gametocytes .....                              | 87 |

|            |   |     |
|------------|---|-----|
| 3.2.5      | Susceptibility of male and female gametocytes to inhibitors of the mETC   | 90  |
| 3.3        | Discussion.....   | 105 |
| Chapter 4  | Investigation into the essentiality of mitochondrial respiration for gametogenesis for <i>P. falciparum</i> gametocytes ..... | 113 |
| 4.1        | Introduction.....   | 113 |
| 4.2        | Results.....  | 118 |
| 4.2.1      | Initial experiments comparing exflagellation under differing glucose availability .....                                       | 118 |
| 4.2.2      | Defining the minimum human serum concentration for exflagellation..   | 121 |
| 4.2.3      | Defining the minimum glucose level concentration required for exflagellation.....   | 123 |
| 4.2.4      | Is mitochondrial respiration required for exflagellation? .....   | 124 |
| 4.2.5      | Importance of glycolysis and mitochondrial respiration for female gametogenesis.....  | 128 |
| 4.2.6      | Real time visualisation of ATP utilisation in <i>P. falciparum</i> gametocytes by FRET  | 129 |
| 4.3        | Discussion.....   | 135 |
| Chapter 5  | Identification and characterisation of putative regulators of gametocyte energy metabolism .....                              | 142 |
| 5.1        | Introduction.....   | 142 |
| 5.2        | Results.....  | 143 |
| 5.2.1      | Identification of candidate proteins.....   | 143 |
| 5.2.2      | Bioinformatic analysis of candidate proteins .....  | 144 |
| 5.2.3      | Characterisation of ACS-ADP expression.....   | 158 |
| 5.2.4      | Successful generation of an ACS-ADP-KO line.....  | 166 |
| 5.2.5      | Preliminary phenotyping of PFK11-KO parasites .....   | 166 |
| 5.2.5      | PFK11 antibody.....   | 174 |
| 5.2.6      | Preliminary localisation of a mitochondrial FAD-dependent G3PDH in <i>P. falciparum</i> .....                                 | 175 |
| 5.3        | Discussion.....   | 177 |
| Chapter 6  | Conclusions .....   | 185 |
| 6.1        | Male and female gametocytes differ in their energy metabolism.....  | 185 |
| 6.2        | Energy for exflagellation – a role for increased mitochondrial energy metabolism in male gametocytes?.....                    | 187 |
| 6.3        | Avoiding oxidative stress – a model for regulation of gametocyte energy metabolism .....                                      | 189 |
| 6.4        | Final conclusions.....  | 192 |
| References | .....   | 194 |
| Appendix   | .....   | 219 |

|  |            |
|--|------------|
| <b>Appendix 1. List of primers .....</b>   | <b>219</b> |
| <b>Appendix 2. Exflagellation IFAs of make gametocytes incubation for 24 hours with mETC inhibitors.....</b> | <b>222</b> |
| <b>Appendix 3. Table of oocyst counts for PFK11-KO vs NF54 WT mosquito feeding experiments .....</b>         | <b>224</b> |
| <b>Appendix 4. IFA showing that PFK11 antibody is not specific.....</b>                                      | <b>226</b> |

## List of figures

Figure 1.1. The *Plasmodium falciparum* life cycle originally from Nilsson *et al.* (2015).

Figure 1.2. Gametocyte development in *P. falciparum*.

Figure 1.3. Summary of known changes in energy metabolism across the life cycle of *P. falciparum*.

Figure 2.1. Selection-linked integration (SLI) tagging strategy.

Figure 2.2. Schematic of the selectable targeted gene disruption strategy (SLI-TGD) adapted from Birnbaum *et al.* (2017)

Figure 2.3. Schematic of restriction digestion of the SLI-mNG plasmid.

Figure 2.4. Restriction digest of pSLI-mNG backbone with KpnI and NotI.

Figure 2.5. Amplification of insert DNA for the SLI tagging vectors from NF54 genomic DNA.

Figure 2.6. CRISPR-Cas9 strategy for knockout of PFK11.

Figure 2.7. Amplification of the 5' and 3' homology regions for the CRISPR-Cas9 PFK11-KO vector from NF54 genomic DNA.

Figure 2.8. Restriction digest of PFK11-KO plasmids from 3 colonies (clone 1-3) of transformed *E. coli* with Aval and SacI.

Figure 2.9. Restriction digestion of the repair plasmid with NheI and PstI to confirm insertion of GFP-skip-BSD into the PFK11-KO plasmid.

Figure 2.10. CRISPR-Cas9 strategy for tagging of PFK11.

Figure 2.11. PCR Amplification of 3' homology region with SpeI overhang for mNG tagging of PFK11.

Figure 2.12. Diagnostic digests of colonies following Gibson assembly of the PFK11 tagging plasmid.

Figure 2.13. Protocol for seeding of gametocyte cultures from continuous asexual feeder cultures, adapted from Delves *et al.* (2016)

Figure 2.14. Gametocyte purification using a Gentodenz density gradient.

Figure 3.1. Anti-LDH2 staining in stage V gametocytes.

Figure 3.2. Co-staining of stage V gametocytes with anti-LDH2 and anti-G377.

Figure 3.3. Anti-LDH2 labelling post-activation.

Figure 3.4. Anti-LDH2 labelling across gametocyte development.

Figure 3.5. Anti-LDH2 and MitoTracker can be used in combination in IFAs.

Figure 3.6. Lattice SIM-squared image showing a 3D reconstruction of a male and a female gametocyte.

Figure 3.7. Schematic showing the process of drawing regions of interest (ROIs) for the image analysis.

Figure 3.8. Illustrations of the morphological parameters used to analyse the mitochondria.

Figure 3.9. Schematic showing the image analysis workflow.

Figure 3.10. Comparison of ability of anti-LDH2 and anti-alpha tubulin II to separate gametocytes into two populations.

Figure 3.11. Anti-LDH2 intensity (x axis) plotted against four examples of nuclear parameters (y axis).

Figure 3.12. Comparison of nuclear morphological parameters between male and female gametocytes.

Figure 3.13. Comparisons of mitochondrial morphology between male and female gametocytes.

Figure 3.14. Comparison of the fluorescence intensity of MitoTracker staining between males and females.

Figure 3.15. Titration of MitoTracker staining.

Figure 3.16. Regions of interest and calculation of mitochondrial staining for the modified image analysis method.

Figure 3.17. Comparison of MitoTracker staining (mitochondrial activity) between males and females.

Figure 3.18. Figure adapted from Lane *et al.* (2018). Diagram of the *Plasmodium* mitochondrial electron transport chain.

Figure 3.20. Mitochondrial activity in male and female gametocytes treated with complex III inhibitors.

Figure 3.21. Mitochondrial activity in male and female gametocytes treated with the DHODH inhibitor, DSM-265.

Figure 3.22. Mitochondrial activity in male and female gametocytes treated with the complex V/ATP synthase inhibitor, oligomycin A.

Figure 3.23. Dose-response curve showing inhibition of male and female gametogenesis by DSM-265.

Figure 3.24. Dose-response curve showing inhibition of male and female gametogenesis by atovaquone (ATQ).

Figure 3.25. Dose-response curve showing inhibition of male and female gametogenesis by ELQ-300.

Figure 3.26. Dose-response curves showing inhibition of male and female gametogenesis by oligomycin A.

Figure 3.27. Exflagellation IFAs of male gametocytes incubated for 24 hours with the mETC and respiration inhibitors showing representative morphology.

Figure 4.1. Molecular structure of glucose and 2-deoxyglucose (2DG) originally from Pajak *et al.*, (2020).

Figure 4.2. Inhibition of glycolysis by 2-deoxyglucose (2DG).

Figure 4.3. The principle of Förster resonance energy transfer (FRET).

Figure 4.4. Schematic of the ATeam FRET-based ATP probes, adapted from Imamura *et al.* (2009).

Figure 4.5. Exflagellation male gametocytes pre-incubated for 1 hour in media with different glucose availability.

Figure 4.6. Exflagellating male gametocytes pre-incubated for 24 hours in media with different glucose availability.

Figure 4.7. Comparison of exflagellation of male gametocytes at different human serum concentrations.

Figure 4.8. Dose response analysis of the effect of glucose concentration on exflagellation.

Figure 4.9. Comparison of exflagellation in the absence of glucose and inhibition of mitochondrial respiration.

Figure 4.10. Exflagellating male gametocytes in media with and without glucose and with inhibition of mitochondrial respiration.

Figure 4.11. Female gamete activation with and without glucose and with inhibition of mitochondrial respiration.

Figure 4.12. Images of stage V gametocytes expressing the ATeam1.03YEMK sensor.

Figure 4.13. Comparison of the FRET ratio (ATP/ADP) in gametocytes incubated in glucose versus no glucose (long-term pilot experiment.)

Figure 4.14. Comparison of the FRET ratio (ATP/ADP) in gametocytes in media with and without glucose over 20 minutes.

Figure 4.15. Possible changes in intracellular ATP concentrations that might be observed on induction of male gametogenesis.

Figure 5.1. Workflow for selection of candidate proteins.

Figure 5.2. Comparison of predicted domain architecture and active sites for PFK11 and PFK9.

Figure 5.4. Bioinformatic analysis of putative phosphoglucomutase in *P. falciparum*.

Figure 5.5. Bioinformatic analysis of PGM3 (PF3D7\_0310300) in *P. falciparum*.

Figure 5.6. Glycerol metabolism and the function of FAD-G3PDH.

Figure 5.7. Comparison of predicted domain architecture and motifs in PF3D7\_0306400 in *P. falciparum* and the FAD-dependent G3PDH in *Saccharomyces cerevisiae* (baker's yeast), GUT 2.

Figure 5.8. Bioinformatic analysis of GDH3 in *P. falciparum*.

Figure 5.9. Acetate formation in parasitic protozoa and helminths.

Figure 5.10. Comparison of ACS-ADP and ACS-ATP in *P. falciparum*.

Figure 5.11. Integration primers for the ACS-ADP mNG line.

Figure 5.12. Integration PCR gel for the ACS-ADP mNG-tagged line.

Figure 5.13. Live images of asexual blood stage ACS-ADP mNG parasites showing mNG fluorescence.

Figure 5.14. Expression of ACS-ATP mNG in 3D7-iGP *P. falciparum* parasites.

Figure 5.15. Subcellular localisation of ACS-ATP in stage V gametocytes.

Figure 5.16. Localisation of ACS-ADP in stage V gametocytes.

Figure 5.17. ACS-ADP expression in activated female gametes and *in vitro* generated retorts.

Figure 5.18. Fluorescence image of an ACS-ADP mNG oocyst in the midgut of a mosquito dissected at day 7.

Figure 5.19. Live image of ACS-ADP mNG sporozoites showing co-localisation between ACS-ADP mNG (green) and MitoTrackerRed CMX Ros (red).

Figure 5.20. Successful gene disruption of ACS-ADP by SLI-TGD.

Figure 5.21. Live imaging of asexual blood stage parasites and gametocytes of the PFK11-KO line.

Figure 5.22. Integration PCR showing successful KO of PFK11 by CRISPR gene editing.

Figure 5.23. Asexual blood stage growth in NF54 WT and PFK11-KO parasites.

Figure 5.24. Images of *in vivo* activated female gametes and midgut retorts of WT NF54 and PFK11-KO parasites.

Figure 5.25. Live fluorescence images of ookinetes from midguts of mosquitoes fed PFK11-KO and NF54 WT gametocytes.

Figure 5.26. Oocyst prevalence and intensity on NF54 WT and PFK11-KO parasites.

Figure 5.27. Staining of stage V gametocytes with an antibody raised to PFK11.

Figure 5.28. FAD-G3PDH expression in asexual blood stage parasites in the 3D7-iGP *P. falciparum* line.

Figure 5.29. FAD-G3PDH expression and localisation in *P. falciparum* gametocytes.

Figure 5.30. Model of a possible role of ACS-ADP in *P. falciparum* gametocytes.

Figure 5.31. Model for the role of PFK11 in *P. falciparum* gametocytes.

Figure 6.1. Summary of known changes in energy metabolism across the life cycle of *P. falciparum*.

Figure 6.2. Models for the increased activity of female gametocyte mitochondria compared to those of males.

Figure 6.3. Model for the increased susceptibility of male gametocytes to chemical inhibition of the mETC.

Figure 6.4. Model of possible roles of candidate proteins in regulating gametocyte energy metabolism.

## List of tables

Table 1.1. Summary of differences between male and female *P. falciparum* gametocytes which indicate they could differ in their energy metabolism.

Table 2.1. Candidate genes selected for genetic investigation in *P. falciparum* gametocytes.

Table 2.2. Non-gametocyte specific or non-gametocyte upregulated isoforms of proteins of interest.

Table 2.3 Custom antibodies generated against LDH2 (PF3D7\_1325200) and PFK11 (PF3D7\_1123800) for the study.

Table 2.4. List of primary and secondary antibodies used for immunofluorescence analysis.

Table 2.5. Peak excitation and emission values for all fluorophores and tags used in the study. ‘

Table 2.6. Morphological parameters for analysis of mitochondrial morphology in ICY BioImage Analysis Software.

Table 3.1. Activity of inhibitors of the mitochondrial electron transport chain (mETC) and respiration against *P. falciparum* asexual blood stages and gametocytes.

Table 4.1. % exflagellation with inhibition in the absence of glucose and inhibition of mitochondrial respiration.

Table 4.2. % female activation with and without glucose and with inhibition of mitochondrial respiration.

Table 5.1. List of candidate proteins of interest.

Table 5.2. Comparison of catalytic residues between PFK9 and PFK11 orthologues in different Plasmodium species.

Table 5.3. Gametocytaemia and exflagellation of 3 independent, matched NF54 WT and PFK11-KO gametocyte cultures.

Table 5.4. % female activation of 2 independent, matched NF54 WT and PFK11-KO gametocyte cultures.

## Abbreviations

|           |   |
|-----------|---|
| 2DG       | 2-deoxyglucose  |
| ACS       | acetyl-CoA synthetase (also known as acetate-CoA ligase)  |
| ACS-ADP   | ADP-forming acetyl-CoA synthetase                         |
| ACS-ATP   | ATP-forming acetyl-CoA synthetase                         |
| ACT       | Artemisin combination therapy                             |
| Aco       | aconitase   |
| ADP       | adenosine diphosphate                                     |
| ASCT      | acetate:succinate CoA-transferase                         |
| ATP       | adenosine triphosphate                                    |
| ATQ       | atovaquone  |
| BCKDH     | branched chain ketoacid dehydrogenase                     |
| BLAST     | Basic Local Alignment Tool                                |
| BLASTP    | Protein BLAST   |
| Cas9      | CRISPR associated protein 9                               |
| CDC       | Centers for Disease Control and Prevention                |
| CDD       | Conserved Domain Database                                 |
| CoA       | coenzyme A  |
| CRISPR    | clustered regularly interspaced short palindromic repeats |
| CSP       | circumsporozoite protein                                  |
| DHODH     | dihydroorotate dehydrogenase                              |
| DNA       | deoxyribonucleic acid                                     |
| EM        | electron microscopy                                       |
| FAD-G3PDH | FAD-dependent glycerol-3-phosphate dehydrogenase          |
| FH        | fumarate hydratase  |

|                  |  |
|------------------|--|
| G3PDH            | glycerol-3-phosphate dehydrogenase     |
| G6PD             | glucose-6-phosphate dehydrogenase      |
| gDNA             | genomic DNA                            |
| GDH              | glutamate dehydrogenase                |
| GDH1             | glutamate dehydrogenase 1              |
| GDH2             | glutamate dehydrogenase 2              |
| GDH3             | glutamate dehydrogenase 3              |
| GFP              | green fluorescent protein              |
| GO               | gene ontology                          |
| HDAD2            | histone deacetylase 2                  |
| HPI              | heterochromatin 1                      |
| HR               | homology region                        |
| HS               | human serum                            |
| IC <sub>50</sub> | half maximal inhibitory concentration  |
| IDH              | isocitrate dehydrogenase               |
| IRS              | Indoor residual spraying               |
| ITN              | Insecticide-treated bed net            |
| KDH              | α-ketoglutarate dehydrogenase          |
| KO               | knockout                               |
| LDH2             | lactate dehydrogenase 2                |
| LysoPC           | Lysophosphatidylcholine                |
| mETC             | mitochondrial electron transport chain |
| Mg <sup>2+</sup> | magnesium                              |
| MitoTracker      | MitoTrackerRed CMXRos                  |
| mNG              | mNeonGreen                             |
| MQO              | malate quinone oxidoreductase          |

|          |  |
|----------|--|
| NAD      | nicotinamide adenine dinucleotide                                    |
| NADP     | nicotinamide adenine dinucleotide phosphate                          |
| NADPH    | nicotinamide adenine dinucleotide phosphate hydrogen                 |
| NAFAc    | sodium fluoroacetate   |
| NDH2     | type II NADH dehydrogenase or type II NADH:ubiquinone oxidoreductase |
| NHEJ     | non-homologous end joining   |
| PBS      | phosphate buffered saline  |
| PCR      | polymerase chain reaction  |
| PFK      | phosphofructokinase  |
| PFK9     | phosphofructokinase 9  |
| PFK11    | phosphofructokinase 11   |
| PGM      | phosphoglucomutase   |
| PGM1     | phosphoglycerate mutase 1  |
| PGM2     | phosphoglycerate mutase 2  |
| PGM3     | putative phosphoglycerate mutase                                     |
| PlasmoDB | <i>Plasmodium</i> database   |
| PM       | Plasma membrane  |
| PV       | Parasitophorous vacuole  |
| PVM      | Parasitophorous vacuole membrane                                     |
| RBC      | red blood cell   |
| RNA      | ribonucleic acid   |
| ROI      | region of interest   |
| ROS      | reactive oxygen species  |
| SDH      | succinate dehydrogenase  |
| sgRNA    | single guide RNA   |
| SLI      | selection-linked integration   |

|         |  |
|---------|--|
| SLI-TGD | selectable targeted gene deletion                        |
| TBD     | Transmission blocking drug                               |
| TBV     | Transmission blocking vaccine                            |
| TCA     | Tricarboxylic acid                                       |
| TMPD    | N,N,N',N'-Tetramethyl-p-phenylenediamine Dihydrochloride |
| WHO     | World Health Organization                                |
| WT      | wild type  |

## List of Appendices

Appendix 1. List of primers.

Appendix 2. Exflagellation IFAs of make gametocytes incubation for 24 hours with mETC inhibitors.

Appendix 3. Table of oocyst counts for PFK11-KO vs NF54 WT mosquito feeding experiments.

Appendix 4. IFA showing that PFK11 antibody is not specific.

# Chapter 1 Introduction

## 1.1 Malaria as a public health problem

Malaria is a life-threatening parasitic disease to which nearly half the world's population is at risk (Geneva: World Health Organisation, 2022). Despite global efforts towards eradication, malaria remains a significant public health problem. An estimated 247 million cases and 619,000 deaths occurred worldwide in 2021, with disruptions due to the COVID-19 pandemic leading to approximately 13 million more cases and 63,000 additional deaths (Geneva: World Health Organisation, 2022). The WHO Africa Region shoulders a disproportionately high share of the global malaria burden, being home to 95% of malaria cases and 96% of malaria deaths, with 80% of deaths occurring in children under five years (Geneva: World Health Organisation, 2022). In addition to loss of life, malaria imposes a substantial social and economic burden. The direct costs of malaria (prevention and treatment) have been estimated to be at least 12 billion US dollars per year and the cost in lost economic growth (due to absence from work and school) is many times more than this (CDC - Centers for Disease Control and Prevention, 2021).

The principal malaria control strategies are provision of insecticide treated bed nets (ITNs), indoor residual spraying (IRS) of homes with insecticide and prompt treatment of clinical cases with artemisinin combination therapies (ACTs) (Bhatt *et al.*, 2015). ITNs and IRS were shown to be by far the most important interventions in Africa in terms of reducing malaria prevalence (Bhatt *et al.*, 2015). Preventive chemotherapies are also used to prophylactically treat vulnerable groups (such as children or pregnant women) during periods of greatest malarial risk (Geneva: World Health Organisation, 2022). As of October 2021, WHO recommended the RTS,S/AS01 malaria vaccine for broad use among children living in regions with moderate to high *Plasmodium falciparum* malaria transmission (Geneva: World Health Organisation, 2022). RTS,S/AS01 is a recombinant pre-erythrocytic vaccine containing the *P. falciparum* circumsporozoite protein (CSP), which has been shown to reduce clinical and severe malaria in young children and infants (RTS'S Clinical Trials Partnership, 2015) but shows a modest efficacy (36% in children and 26% in infants with three doses and a booster) (Arora, C Anbalagan and Pannu, 2021). Recently, the R21/Matrix-M vaccine (77% efficacy), also based on CSP, was approved for use in Ghana in April 2023 (Moorthy and Binka, 2021; Dattoo *et al.*, 2022) and is now the second malaria vaccine to be recommended for global use (WHO, 2023).

However, drug resistance in the parasites (including to artemisinin and partner drugs) (Noedl *et al.*, 2008; Ashley *et al.*, 2014; Mairet-Khedim *et al.*, 2021) and insecticide resistance in the

mosquito vector threaten the significant progress made in malaria control between ~2000-2015 which has now stalled. Therefore, effective interventions are urgently needed to continue to combat the disease.

## **1.2 Aetiological agent and vector**

Malaria is caused by protozoan parasites of the genus *Plasmodium* and transmitted between vertebrate hosts by female *Anopheles* mosquitoes. *Plasmodium* parasites are part of the Apicomplexa, a large phylum of parasitic alveolates (Levine, 1970). Six species of *Plasmodium* parasites are known to infect humans, namely *P. falciparum*, *Plasmodium vivax*, *Plasmodium ovale curtisi*, *Plasmodium ovale wallikeri*, *Plasmodium malariae* and *Plasmodium knowlesi*. Of these, *P. falciparum* is responsible for the most severe clinical manifestations (Mackintosh, Beeson and Marsh, 2004), and is the most lethal malaria parasite (Geneva: World Health Organisation, 2022). The zoonotic malaria *P. knowlesi* has also been shown to cause fatal disease in humans, due to its ability to reach high parasitaemia in a short window of time (Cox-Singh and Singh, 2008). Malaria caused by *P. vivax*, *P. ovale* and *P. malariae* is rarely fatal but can still cause considerable morbidity e.g. recurring infections with *P. vivax* and *P. ovale* due to reactivation of dormant hypnozoite forms (Krotoski *et al.*, 1982; Cogswell, 1992; Richter *et al.*, 2010), nephrotic syndrome from chronic or repeated *P. malariae* infection (Hendrickse and Adeniyi, 1979) and rare incidences of splenic rupture with *P. vivax* (Zingman and Viner, 1993; Jiménez *et al.*, 2007; Imbert, Rapp and Buffet, 2009; Siqueira *et al.*, 2012).

## **1.3 The *Plasmodium* life cycle**

*Plasmodium* parasites have a complex life cycle involving two hosts: a vertebrate host and a female *Anopheles* mosquito (Figure 1.1).

### **1.3.1 The liver stage**

Infection of the mammalian host occurs when an infected mosquito takes a blood meal, releasing saliva and inoculating infectious sporozoites into the skin (Sidjanski and Vanderberg, 1997; Kappe, Kaiser and Matuschewski, 2003). Sporozoites travel through the dermis using a form of locomotion termed gliding motility (Amino *et al.*, 2006; Montagna, Matuschewski and Buscaglia, 2012; Santos *et al.*, 2017), until they penetrate the capillaries and lymphatic vessels (Vanderberg and Frevert, 2004; Amino *et al.*, 2006). They enter the bloodstream and are carried to liver, where they penetrate a layer of endothelial cells and macrophages known as the sinusoidal wall (Pradel and Frevert, 2001; Tavares *et al.*, 2013). They subsequently traverse a number of hepatocytes before selecting a hepatocyte to invade (Frevert *et al.*, 2005). Here, they take up residence within a parasitophorous vacuole

(PV) (Mota *et al.*, 2001). The parasite then undergoes multiple rounds of asynchronous nuclear replication (schizogony) to form hepatic schizonts containing thousands of merozoites (Sturm *et al.*, 2006; Baer *et al.*, 2007). Once mature, which takes ~6-7 days in the case of *P. falciparum* (Vaughan *et al.*, 2012), the parasite's parasitophorous vacuole membrane (PVM) ruptures and packets of hepatic merozoites in host-derived vesicles known as merozoites, are released from the liver (Sturm *et al.*, 2006; Baer *et al.*, 2007). The merozoites protect the merozoites from phagocytic clearance by sinusoidal Kupffer cells in the liver and, once in the bloodstream, the merozoites disintegrate, releasing free merozoites (Sturm *et al.*, 2006; Baer *et al.*, 2007).

Following invasion in *P. vivax* and *P. ovale*, a proportion of sporozoites develop into dormant forms called hypnozoites which can persist in the liver for months or more before reactivating and giving rise to a new blood stage infection (Krotoski *et al.*, 1982; Cogswell, 1992; Richter *et al.*, 2010; Dembélé *et al.*, 2014). These relapsing infections can produce gametocytes which can be transmitted to mosquitoes and re-infect others, presenting a further obstacle to malaria elimination efforts (Dembélé *et al.*, 2014; Adams and Mueller, 2017).

### **1.3.2 The blood stage**

On release into the bloodstream, merozoites rapidly invade erythrocytes where they reside within a PV (Bannister *et al.*, 1975; Aikawa *et al.*, 1978). Following invasion, merozoites transform into immature trophozoites termed 'ring stage' parasites (Bannister *et al.*, 2000) which subsequently develop into trophozoites that feed on haemoglobin from the host cell (Goldberg *et al.*, 1990). Trophozoites undergo multiple rounds of schizogony to form blood stage schizonts containing 16-32 merozoites (Chris J. Janse *et al.*, 1986; Bannister *et al.*, 2000; Cowman and Crabb, 2006). Once matured (24-72 hours depending on the species, 48 hours for *P. falciparum*), the parasitophorous vacuole membrane (PVM) and subsequently the host erythrocyte membrane rupture, releasing free merozoites into the bloodstream, a process termed egress (Hale *et al.*, 2017). The free merozoites rapidly re-invade new host erythrocytes within minutes of egress (Boyle *et al.*, 2010). This cycle of replication and egress from host erythrocytes, which results in their lysis, is responsible for the clinical symptoms of malaria (Srivastava *et al.*, 2016) which range from a mild-flu like illness to complications such as severe anaemia, respiratory failure and coma, leading to death (Mackintosh, Beeson and Marsh, 2004; Idro *et al.*, 2010; Bartoloni and Zammarchi, 2012).

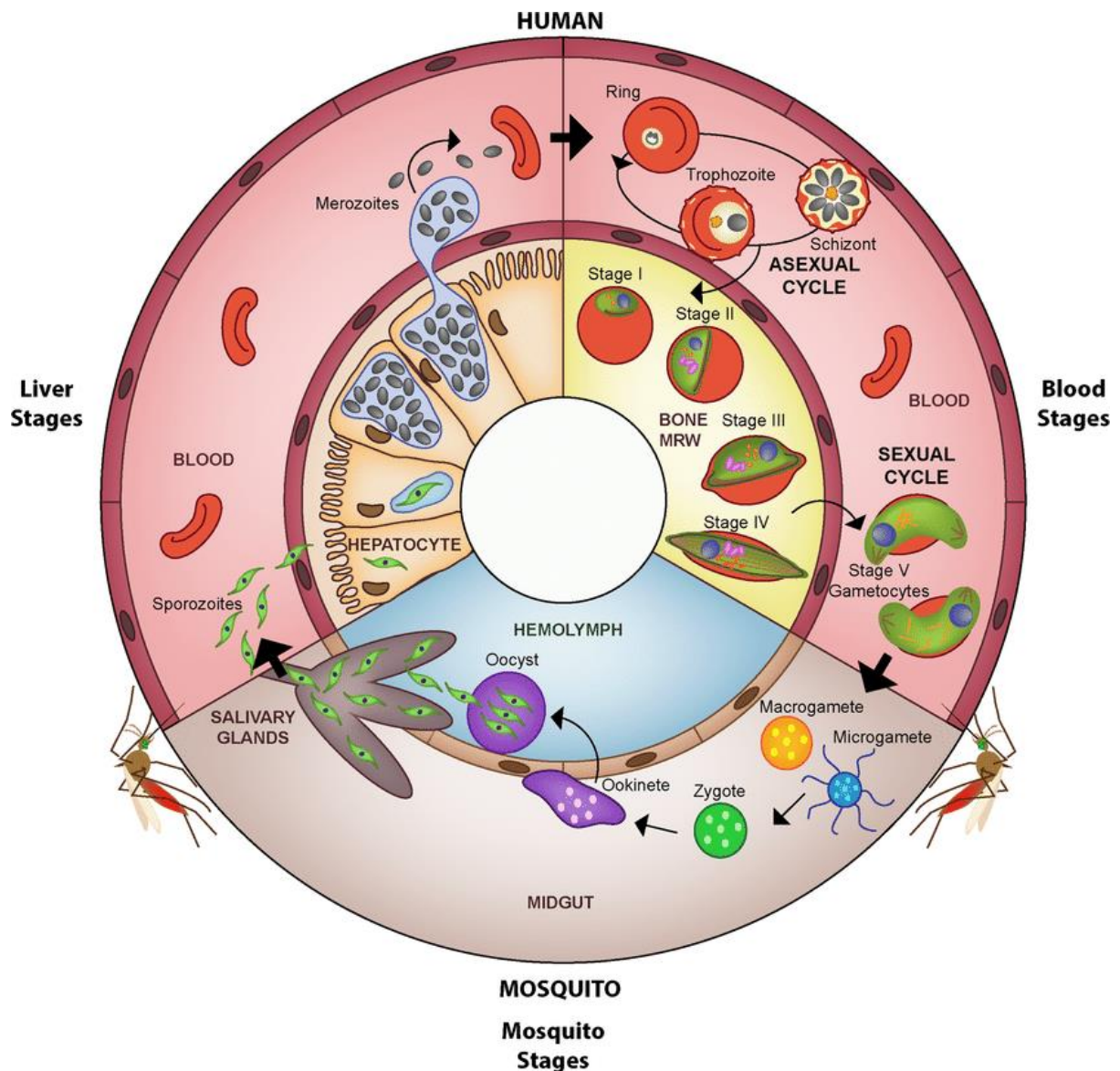


Figure 1.1. The *Plasmodium falciparum* life cycle originally from Nilsson *et al.* (2015).

### 1.3.3 Gametocytogenesis

With each intraerythrocytic cycle, a small proportion (<1% (Eichner *et al.*, 2001)) of ring stage parasites commit to develop into male and female gametocytes, (the sexual blood stages) in a process termed gametocytogenesis (Sinden, 1983; Bruce *et al.*, 1990). Gametocytes are solely responsible for human-to-mosquito transmission of malaria.

The malaria parasite undergoes several dramatic changes in environment across its complex life cycle. However, one life cycle transition that does not require a change in location or host is commitment to sexual development (Baker, 2010). Earlier research into the triggers for sexual commitment focused on environmental factors. Factors correlated with increased gametocyte production include haematological disruption (Drakeley *et al.*, 1999;

Trager, 2005; Stepniewska *et al.*, 2008; Baker, 2010), high asexual parasitaemia (Bruce *et al.*, 1990; Nacher *et al.*, 2002), stress (Chaubey, Grover and Tatu, 2014) and drug treatment (Butcher, 1997; Puta and Manyando, 1997; Hogh *et al.*, 1998). Gametocyte conversion rates *in vitro* have also been shown to be suppressed by the host lipid lysophosphatidylcholine (LysoPC) in serum or the addition of choline to serum-free medium (Brancucci *et al.*, 2017; Harris *et al.*, 2023). A recent study of *ex vivo* cultures of clinical samples in Ghana showed that gametocyte conversion correlated positively with level of parasitaemia and negatively with LysoPC concentration in patient plasma, suggesting that metabolic stress may trigger gametocytogenesis during natural infections also (Usui *et al.*, 2019).

The molecular mechanisms governing sexual differentiation are becoming better understood. The stage-specific transcription factor AP2-G was identified as an essential regulator of gametocyte formation in malaria parasites and acts as a developmental switch by activating the transcription of early gametocyte genes (Kafsack *et al.*, 2014; Sinha *et al.*, 2014). AP2-G is a member of the ApiAP2 family, which had previously been found to regulate several developmental transitions in the parasite including ookinete formation, oocyst sporozoite maturation and liver stage development (Kafsack *et al.*, 2014). The *ap2-g* locus is normally held in a silenced state by two epigenetic factors, histone deacetylase 2 (HDAD2) (Coleman *et al.*, 2014) and heterochromatin 1 (HP1) (Brancucci *et al.*, 2014). In *P. falciparum*, the effector protein GDV1 targets heterochromatin and triggers HPI eviction, allowing expression of *ap2-g* (Eksi *et al.*, 2012; Filarsky *et al.*, 2018) which induces irreversible commitment to the sexual pathway (Kafsack *et al.*, 2014).

Additional ApiAP2 proteins, AP2-G2 and AP2-G3, have been shown to co-regulate gametocytogenesis in conjunction with AP2-G (Sinha *et al.*, 2014; Yuda *et al.*, 2015; Zhang *et al.*, 2017; Kent *et al.*, 2018). Recently in 2021, Shang and colleagues identified six new ApiAP2 members associated with gametocytogenesis in *P. falciparum*. One of these, AP2-G5, suppresses the expression levels of *ap2-g* via binding to the upstream regulatory region directly or through recruitment to the exonic gene body involved in the maintenance of local heterochromatin structure, preventing sexual commitment (Shang *et al.*, 2021). This suggests that a regulatory network involving ApiAP2 proteins regulates sexual commitment and gametocyte development (Shang *et al.*, 2021).

Sexual conversion can occur by two different routes: one where PfAP2-G-expressing asexual blood stage parasites complete a replicative cycle before converting into gametocytes upon re-invasion, or a second route where conversion occurs within the same cycle (Bancells *et al.*, 2019).

In *P. falciparum*, gametocyte maturation takes ~10 days (Talman *et al.*, 2004; Alano, 2007; Dixon *et al.*, 2008; Baker, 2010; Bousema and Drakeley, 2011; Josling and Llinás, 2015). This extended period of development is unique to *P. falciparum* and the closely related primate parasite *Plasmodium reichenowi* (Garnham, 1966; Baker, 2010). In other *Plasmodium* species, gametocyte maturation is much faster, taking only a few days (Boyd and Kitchen, 1937; Wernsdorfer and McGregor, 1988; Galinski, Meyer and Barnwell, 2013; Bantuchai, Imad and Nguitragool, 2022).

Over the course of their development, *P. falciparum* gametocytes transition through a series of distinct morphological stages termed I-V (Hawking, Wilson and Gammage, 1971) (Figure 1.2), which are well-characterised by ultrastructural studies. Stage I gametocytes are rounded and difficult to distinguish from young trophozoites in Giemsa-stained blood films (Baker, 2010). By EM, it can be observed that, unlike erythrocytes infected by asexual parasites, there is no visible alteration of the erythrocyte plasmalemma (Sinden, 1982a). A subpellicular membrane and microtubule complex forms in stage I gametocytes and expands over stages II and III, elongating the parasite cell and distorting the red blood cell until stage IV where it surrounds the cell completely (Sinden, 1982a). The assembly of this network is thought to provide rigidity which allows stage I-IV gametocytes to sequester in the bone marrow and spleen (Thomson, 1914; Aguilar *et al.*, 2014; Joice *et al.*, 2014, 2014; Parkyn Schneider *et al.*, 2017; De Niz *et al.*, 2018). This sequestration is thought to allow developing gametocytes to avoid clearance by the spleen (Joice *et al.*, 2014). Membrane bound osmiophilic bodies first appear at stage IV along with obvious sexual dimorphism between males and females, though morphological differences (larger nucleus in males, greater numbers of ribosomes and ER in females) can be observed from stage III (Sinden, 1982a).

By stage V, male gametocytes show greatly reduced ribosomal density and a large nucleus with a kinetochore complex attached to the nuclear envelop, whereas females have more ribosomes and osmiophilic bodies and the nucleus is relatively small with a nucleolus (transcription factory) (Sinden, 1982a).

On maturity, the subpellicular membrane is lost by depolymerisation and the microtubular network is disassembled (Sinden, 1982a; Dearnley *et al.*, 2012; Tibúrcio *et al.*, 2012). The gametocytes become deformable and are no longer retained in the bone marrow and enter the peripheral circulation (Tibúrcio *et al.*, 2012). Here they circulate for a media of 6 days (range 1.3-22.2) (Eichner *et al.*, 2001) where they may be imbibed by a blood-feeding mosquito.

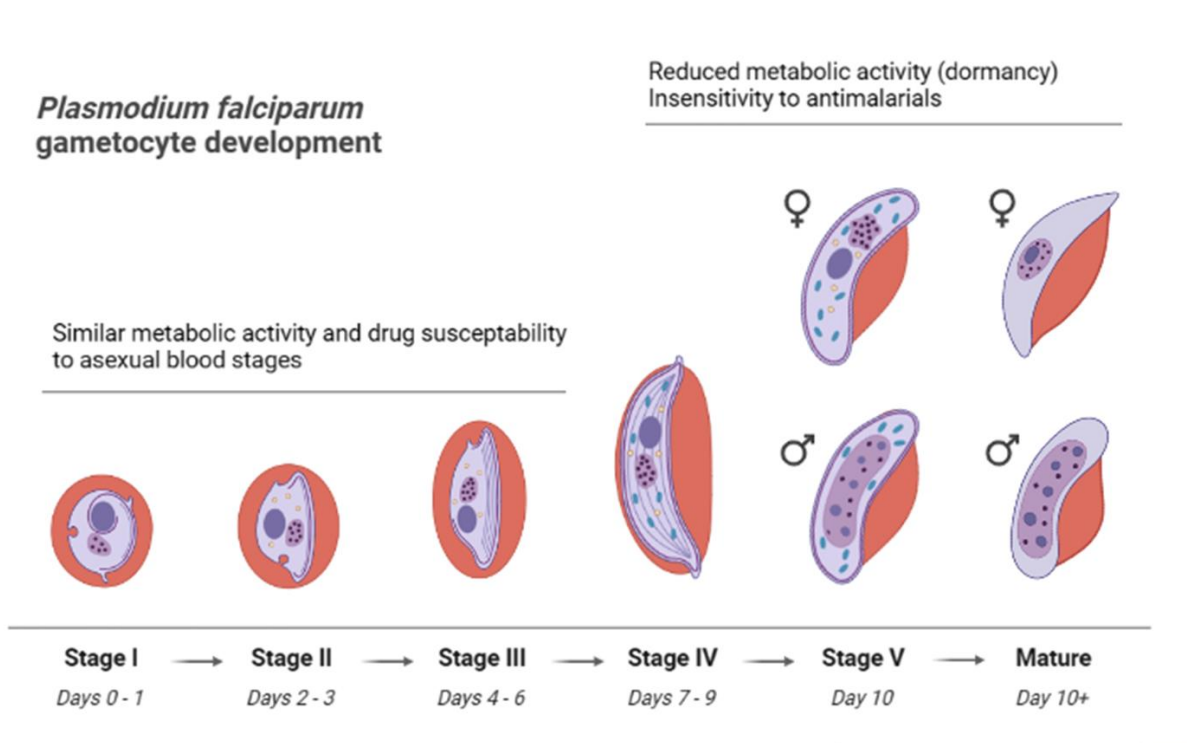


**Figure 1.2. Gametocyte development in *P. falciparum*.** Created in BioRender.

### 1.3.4 The mosquito stages

Upon uptake by the mosquito, gametocytes sense the decrease in temperature, increase in pH (Billker *et al.*, 1997) and the presence of xanthurenic acid (Billker *et al.*, 1998; Garcia *et al.*, 1998) in the mosquito midgut and rapidly differentiate into gametes. Male gametogenesis (exflagellation) requires *de novo* synthesis of DNA, three rounds of mitosis (Toyé, Sinden and Canning, 1977; C.J. Janse *et al.*, 1986; Raabe *et al.*, 2009), axoneme assembly (Ponzi *et al.*, 2009) and the formation and release of up to eight motile gametes, all within ~15-20 minutes (Delves *et al.*, 2013). Female gametogenesis requires translation of ~370 mRNA transcripts previously kept under translational repression by the DDX-6 class helicase DOZI and egress from the erythrocyte (Mair, Braks, Garver, Dimopoulos, *et al.*, 2006; Mair, Braks, Garver, Wiegant, *et al.*, 2006). The relative complexity of male gametogenesis compared to female gametogenesis likely explains why male gametocytes show greater susceptibility to antimalarial drugs than females (Delves *et al.*, 2013).

Cell-cell adhesion of male and females gamete is mediated by Pfs48/45-P230 (van Dijk *et al.*, 2001), and membrane fusion occurs in a HAP2-dependent process to initiate fertilization (Liu *et al.*, 2008; Delves *et al.*, 2013). Fertilisation forms diploid zygotes which subsequently undergo meiosis to become tetraploid and transform into motile ookinetes (Sinden, 1982b; Chris J. Janse *et al.*, 1986; Janse *et al.*, 1988). These ookinetes travel through the midgut

using gliding motility and invade the midgut wall, traversing midgut epithelial cells to reach the midgut basal lamina (Vlachou *et al.*, 2004) where they subsequently develop into oocysts (Sinden, Hartley and Winger, 1985) over 10-14 days (Alano and Carter, 1990). Oocysts produce 3,000 haploid sporozoites by uninuclear budding (Chris J. Janse *et al.*, 1986; Rosenberg and Rungsiwongse, 1991). Once mature, oocysts rupture, releasing sporozoites into the haemolymph where they migrate to the mosquito salivary glands and invade gland cells, eventually coming to rest in the secretory cavity. Here they remain viable for weeks, until the female mosquito takes its next blood meal and transmit the parasites to a new vertebrate host (Kappe, Kaiser and Matuschewski, 2003).

#### **1.4 Targeting transmission – why target gametocytes?**

Asexual blood stage parasites are responsible for the pathology of malaria. Consequently, most antimalarials are targeted towards these stages. However, it has long been accepted that interventions which block transmission between humans and mosquitoes are required for malaria elimination at country-level and ultimately, for global eradication of malaria (Delves, Angrisano and Blagborough, 2018; Birkholtz, Alano and Leroy, 2022).

The most obvious advantage of targeting transmission is to break the cycle of infection by clearing gametocyte reservoirs both in symptomatic patients and asymptomatic carriers (Birkholtz, Alano and Leroy, 2022), the latter of which can contribute to as high as 84% of persistent transmission (Andolina *et al.*, 2021). Targeting transmission could also act as a barrier to the spread of drug resistant alleles (Delves *et al.*, 2013, 2018; Delves, Angrisano and Blagborough, 2018). Transmission is a significant population bottleneck for *P. falciparum* (Delves, Angrisano and Blagborough, 2018; Birkholtz, Alano and Leroy, 2022) with natural mosquito infections producing only 3-5 oocysts (Medley *et al.*, 1993; Baton and Ranford-Cartwright, 2012), compared to  $\sim 10^{11}$  asexual blood stage parasites in a human host during severe malaria (Sinden, 2017). Therefore, selective pressure is applied to the much smaller, non-replicating gametocyte population, which may make resistance less likely to occur (Delves *et al.*, 2013, 2018).

Transmission-blocking interventions can be broadly divided into two categories: transmission-blocking drugs and transmission-blocking vaccines. Transmission-blocking drugs (TBDs) are antimalarial drugs which show activity against parasitic sexual stages (gametocytes, gametes and ookinetes). Transmission-blocking vaccines (TBVs) are vaccines designed to generate immune responses against antigens expressed by parasitic sexual stages (Delves, Angrisano and Blagborough, 2018). A wide range of parasite proteins have been examined as TBV targets over previous decades, but only five immunogens have

been shown to reproducibly demonstrate transmission blocking immunity and efficacy, namely Pfs230, Pfs48/45, HAP2, Pfs25 and Pfs28 (Delves, Angrisano and Blagborough, 2018). The rest of the section will focus on TBDs.

TBDs can target the parasite at different stages of sexual development. Dual active compounds are compounds which are active against both asexual blood stage parasites and transmission stages. 'Transmission-specific' compounds include those that 1) kill gametocytes, 2) render gametocytes sterile or unable to transmit once in the mosquito, 3) are active against gametes in the mosquito or 4) are active further downstream in the mosquito development against ookinetes, oocysts or sporozoites (Delves, Angrisano and Blagborough, 2018; Birkholtz, Alano and Leroy, 2022).

The 'ideal' TBD might appear to be one that is dual active. However, the amount of drug required to kill gametocytes is often much higher than for asexual blood stages which could cause problems with finding a safe, appropriate dose (Delves *et al.*, 2018). Dual activity compounds would also have the same target so resistance could be selected for during asexual blood stage replication (Birkholtz, Alano and Leroy, 2022). Resistance acquired in the asexual blood stage is readily transmitted (Ng *et al.*, 2016; Witmer *et al.*, 2020; Posayapisit *et al.*, 2021) unless the specific mechanism of action abrogates transmission further down in the mosquito, as seen with atovaquone (Goodman *et al.*, 2016). Therefore, it has been suggested that transmission-specific compounds which target gametocyte-specific biology might be a preferential approach (Delves, Angrisano and Blagborough, 2018; Birkholtz, Alano and Leroy, 2022). These drugs would need to be combined with two different asexual blood stage active drugs with different targets. This triple drug approach would provide transmission-blocking activity while protecting each of the partner drugs from resistance, extending the lifespan of the therapy (Delves, Angrisano and Blagborough, 2018; Birkholtz, Alano and Leroy, 2022).

Drugs which kill gametocytes or render them sterile may be preferable to a drug that only targets gametes, ookinetes or oocysts, as gametocytes in human blood are more accessible to pharmaceutical intervention (Birkholtz, Alano and Leroy, 2022). A drug administered to humans which is unable to kill or sterilise gametocytes would need a very long plasma half-life and potency to be effective against later sexual stages in the mosquito (Delves, Angrisano and Blagborough, 2018; Birkholtz, Alano and Leroy, 2022). A 2019 study showed that direct exposure of mosquitoes on surfaces treated with atovaquone blocked transmission which could be an approach suitable to target later mosquito stages (Paton *et al.*, 2019). However, additional factors including compound toxicity, formulation, cost, stability and choice of compound (so as not to contribute to drug resistance to drugs needed

to treat clinical malaria in humans) would need to be evaluated before such a strategy could be deployed (Paton *et al.*, 2019). In addition, pharmaceutical companies may not fund the expensive clinical testing of a drug with no direct therapeutic value to the patient, even if it would be beneficial at the population level. For now, gametocytes in the human host remain the most 'accessible' targets for transmission-blocking drugs.

However, gametocyte biology presents significant challenges for malaria control through chemotherapy. Early (stage I-III) gametocytes are thought to utilise erythrocyte haemoglobin as a major amino acid source, sharing similar metabolic activity to asexual blood stage parasites (Lamour *et al.*, 2014), and so are similarly sensitive to chloroquine which inhibits haem detoxification (Sinden, 1982b). However, as gametocytes mature, they reduce their metabolic activity and become quiescent (Sinden and Smalley, 1979). In this arrested state, mature gametocytes are insensitive to most currently used antimalarials (Smalley, 1977; Kumar and Zheng, 1990; Chutmongkonkul, Maier and Seitz, 1992) thus individuals can be cured of their asexual blood stage infection but still have circulating gametocytes which can still contribute to transmission, allowing the disease to continue to spread (Nilsson *et al.*, 2015). In addition, asymptomatic gametocyte carriers are unlikely to seek treatment.

Three approved antimalarials are known to possess transmission-blocking activity. Primaquine is effective against gametocytes (Burgess and Bray, 1961) but its use is limited as it causes haemolytic anaemia in glucose-6-phosphate dehydrogenase (G6PD) deficient individuals, a widespread mutation in Sub-Saharan Africa (Howes *et al.*, 2012). Nonetheless, WHO now recommends low dose primaquine for transmission-blocking following the demonstration of safety and efficacy in field trials (Gonçalves *et al.*, 2016; Delves, Angrisano and Blagborough, 2018; Dicko *et al.*, 2018). Methylene blue is effective against asexual blood stages, gametocytes and mosquito stages and is thought to function by perturbing the redox balance within the parasite (Färber *et al.*, 1998; Buchholz *et al.*, 2008). Atovaquone was also shown to have potent activity against ookinete and oocyst formation when carried across in the bloodmeal (Fowler, Sinden and Pudney, 1995). More recently, low dose tafenoquine showed transmission blocking activity in healthy volunteers experimentally infected with *P. falciparum*, showing a decline in oocysts and sporozoites in mosquitoes fed on the volunteers after 4 days of treatment, as well as a reduction in gametocyte density in patients (Webster *et al.*, 2023). Nonetheless, options for clearing gametocytes in patients remain limited.

In summary, gametocytes represent an important target for transmission-blocking drugs. However, despite their importance, many aspects of gametocyte biology remain poorly

understood. Improved understanding of the biology of these stages is essential for the discovery of new transmission-blocking drug targets.

## 1.5 Energy metabolism in *Plasmodium* parasites

Gametocytes possess unique aspects of their biology which could be exploited for transmission-blocking drug targets, one of which is energy metabolism. Energy metabolism refers to reactions involved in generating adenosine triphosphate (ATP) from nutrients.

The energy metabolism of *Plasmodium* and other protozoan parasites is considered an attractive drug target, as it is often divergent from their mammalian hosts (Sánchez, Galperin and Müller, 2000; Tielens *et al.*, 2010; Torrentino-Madamet *et al.*, 2010; Cobbold *et al.*, 2013; Oppenheim *et al.*, 2014; Ke *et al.*, 2015). For example, *P. falciparum* possesses divergent enzymes involved in energy metabolism which are not found in humans. Examples include: type II NADH dehydrogenase (NDH2), branched chain  $\alpha$ -ketoacid dehydrogenase (BCKDH) (Cobbold *et al.*, 2013; Oppenheim *et al.*, 2014) and malate quinone oxidoreductase (MQO) (Rajaram *et al.*, 2022). Apicomplexans, members of the phylum to which *Plasmodium* belongs, also show highly divergent mitochondrial electron transport chain (mETC) complexes (Nixon *et al.*, 2013; Maclean *et al.*, 2022) with complexes II, IV and V in apicomplexans having significantly more subunits than their equivalents in opisthokonts (the eukaryotic group that includes yeast and humans) (Maclean *et al.*, 2022). These differences allow for selective inhibition of enzymes involved in energy metabolism without toxicity to mammalian cells.

*Plasmodium* parasites encounter multiple, different nutritional environments across their complex, two-host life cycle (Srivastava *et al.*, 2016). The parasite's energy metabolism undergoes a series of changes during sexual development (MacRae *et al.*, 2013; Ke *et al.*, 2015; Srivastava *et al.*, 2016).

Asexual blood stage parasites rely primarily on glycolysis for energy generation (Sherman, 1979). *Plasmodium*-infected erythrocytes accelerate their glucose uptake up to 100-fold to support increased glucose consumption (McKee *et al.*, 1946; Warren and Manwell, 1954; Roth, 1987). *Plasmodium* parasites lack the enzymes for gluconeogenesis (Srivastava *et al.*, 2016) and due to the lack of fructose biphosphatase, they cannot synthesize energy stores such as glycogen. Therefore continuous glucose uptake is essential for parasite metabolism and survival (Krishna, Webb and Woodrow, 2001; Jiang, 2022). Deprivation of glucose led to a reduction in glycolytic flux and a rapid decline in ATP levels in *P. falciparum*, severely perturbing metabolic homeostasis (Saliba and Kirk, 1999; Saliba, Krishna and Kirk, 2004; van Niekerk *et al.*, 2016). Disruption of glucose uptake by genetic and chemical disruption of

the hexose transporter in *P. falciparum* and *P. berghei* has also been shown to be detrimental to asexual blood stage growth (Blume *et al.*, 2011; Slavic *et al.*, 2011).

It might seem counterintuitive for a parasite to choose a fermentative metabolism in the glucose-rich environment of human blood but in fact this may be advantageous (Oliveira and Oliveira, 2002; Salcedo-Sora *et al.*, 2014). Firstly, it has been hypothesized that reliance on glycolysis and limited mitochondrial respiration in asexual blood stage parasites has evolved as a strategy to support their rapid proliferation in the human host, analogous to the Warburg effect in cancer cells and other rapidly proliferating cells such as yeasts (Salcedo-Sora *et al.*, 2014) and bloodstream African trypanosomes (Jacot *et al.*, 2016). *Plasmodium* has several adaptations, comparable to those of cancer cells, which allow dysregulated glycolysis for rapid generation of glycolysis intermediates for rapid biomass generation for schizogony, (Salcedo-Sora *et al.*, 2014).

Secondly, oxidative stress is an unavoidable consequence of aerobic metabolism. Minimising mitochondrial ROS would be especially important for an organism which metabolises haemoglobin as free inorganic iron and haem are also potent generators of ROS. Therefore, choosing glycolysis may be a strategy to avoid oxidative stress in an environment already under stress from haemoglobin degradation (Oliveira and Oliveira, 2002).

Despite their dependence on glycolysis, asexual parasites possess a small, poorly cristate mitochondrion (Das *et al.*, 1997; Srivastava *et al.*, 2016). However, this has been shown to only be required for the re-oxidation of ubiquinol to support the function of the ubiquinone-dependent dihydroorotate dehydrogenase (DHODH) (Painter *et al.*, 2007; Srivastava *et al.*, 2016). DHODH is an essential enzyme for pyrimidine biosynthesis which is also involved in mitochondrial respiration. Providing ubiquinone turnover for DHODH is maintained (which minimally requires complex III), the initial two complexes (NDH2 and SDH) of the mETC are dispensable in *Plasmodium* (Painter *et al.*, 2007; Sturm *et al.*, 2015; Jacot *et al.*, 2016). In transgenic parasites expressing yeast DHODH, which does not require ubiquinone as an electron acceptor (Nagy, Lacroute and Thomas, 1992), disruption of mitochondrial respiration does not affect asexual blood stage parasites (Painter *et al.*, 2007).

It is now known that the tricarboxylic acid (TCA) cycle does operate in asexual parasites, with a low proportion of pyruvate being converted to acetyl-CoA by BCKDH (Oppenheim *et al.*, 2014) with major flux from glutamine (MacRae *et al.*, 2013; Srivastava *et al.*, 2016). However, knocking out six of the eight TCA cycle enzymes has no discernible effect on intraerythrocytic growth of *P. falciparum* (Ke *et al.*, 2015). In that study, fumarate hydratase

(FH) and MQO could not be successfully knocked out in asexual blood stage parasites (Ke *et al.*, 2015). However, more recent work using CRISPR gene editing has shown these enzymes to also be dispensable for the asexual replicative cycle (Rajaram *et al.*, 2022). Similarly, chemical inhibition of the TCA cycle with the aconitase inhibitor sodium fluoroacetate (NAFAc) had no effect on asexual blood stage parasites, suggesting the TCA cycle is dispensable in these stages (MacRae *et al.*, 2013). An asexual growth defect was observed in isocitrate dehydrogenase (IDH) knockout (KO) parasites but it was nonetheless found to be dispensable for asexual blood stage parasite survival (Yang *et al.*, 2022).

In contrast to the reliance on glycolysis for ATP generation in asexual blood stage parasites, gametocytes shift their energy metabolism towards an oxidative metabolism (MacRae *et al.*, 2013; Srivastava *et al.*, 2016). Metabolomic studies have demonstrated that *P. falciparum* gametocytes drive an active TCA cycle utilising glucose (major flux) and glutamine (minor flux) as carbon skeletons, opposite of the case in asexual parasites (MacRae *et al.*, 2013; Ke *et al.*, 2015). Asexual blood stage parasites secrete >93% of internalised glucose as lactate, whereas this figure decreases to 80% in gametocytes, suggesting increased flux of glucose-derived pyruvate into the TCA cycle (MacRae *et al.*, 2013). The increased importance of TCA metabolism in gametocytes is supported by the upregulation of TCA cycle enzyme genes (Young *et al.*, 2005) as well as the enlargement of the parasite mitochondrion into a multi-lobed structure with complex, tubular cristae (Krungkrai, Prapunwattana and Krungkrai, 2000a; Evers *et al.*, 2021), indicative of increased mitochondrial function (MacRae *et al.*, 2013).

Whereas TCA cycle enzymes are dispensable in asexual blood stage parasites, genetic and chemical disruption of TCA cycle genes has been shown to impact gametocyte development or abrogate transmission downstream in the mosquito (MacRae *et al.*, 2013; Ke *et al.*, 2015; Srivastava *et al.*, 2016; Yang *et al.*, 2022). KO of  $\alpha$ -ketoglutarate dehydrogenase (KDH), which prevents glutamine-derived carbon from entering the TCA cycle, were able to form mature stage V gametocytes and undergo exflagellation but could not produce oocysts when fed to mosquitoes (Ke *et al.*, 2015). Aconitase (Aco) KO blocks full utilization of glucose as a TCA carbon source at an early step (Ke *et al.*, 2015). Aco KO parasites showed an even more severe phenotype, arresting gametocyte development at stage III (Ke *et al.*, 2015), consistent with the effect of treatment of parasites with 10 mM sodium fluoroacetate, a direct inhibitor of Aco (MacRae *et al.*, 2013). In *P. berghei*, Aco mutants were able to form gametocytes but not able to undergo exflagellation (Srivastava *et al.*, 2016). Similarly, IDH KO parasites cannot develop beyond stage III/IV (Yang *et al.*, 2022). Two possible causes for this phenotype were explored by the authors, 1) accumulation of reactive oxygen species

(ROS) within the parasite mitochondrion due to reduced production of mitochondrial NADPH during the 10-14 days of gametocyte development and 2) build-up of toxic citrate upstream of IDH (Yang *et al.*, 2022). However, antioxidants did not rescue the phenotype, nor did amount of citrate affect gametocytogenesis or gamete formation (Yang *et al.*, 2022). Interestingly, Yang and colleagues (2022) found that both Aco and IDH KO parasites showed a fragmented mitochondrial morphology. These experiments demonstrate that disruption of the TCA cycle results in failure to progress through the insect stages of the life cycle, making TCA metabolism essential for transmission.

Many of the complexes of the mitochondrial electron transport chain (mETC) are also dispensable in asexual blood stage parasites but their loss is not tolerated by gametocytes or mosquito stages. Type II NADH dehydrogenase (NDH2) is dispensable in asexual blood stage parasites (Boysen and Matuschewski, 2011; Ke *et al.*, 2019) but KO parasites in *P. berghei* failed to develop into oocysts in the mosquito midgut (Boysen and Matuschewski, 2011). Similarly, KO of succinate dehydrogenase (SDH) showed this complex to be dispensable for asexual blood stage growth (Hino *et al.*, 2012; Ke *et al.*, 2015) but essential for oocyst formation in *P. berghei* (Hino *et al.*, 2012). Disruption of the  $\beta$  subunit gene of the ATP synthase (complex V) in *P. berghei* marginally reduced asexual blood-stage parasite growth but were unable to produce oocysts (Sturm *et al.*, 2015). Another species-specific difference in essentiality was observed with ATP synthase, as attempts to disrupt this gene in *P. falciparum* have been unsuccessful (Nina *et al.*, 2011). It has previously been demonstrated that the mETC in asexual blood stage parasites is not for ATP generation (Painter *et al.*, 2007), so this suggests that ATP synthase may have another essential role in asexual blood stage parasites independent of the mETC in *P. falciparum*.

It is still unknown why gametocytes upregulate mitochondrial energy metabolism in this way. Several hypotheses have been put forward to explain why this metabolic switch occurs.

The first of these is readiness for the environment within the mosquito. Gametocytes are found at the interface between the human and mosquito host. Therefore, gametocyte biology must be able to support the rapid changes that occur in the mosquito upon feeding. The parasites experience a change in temperature, pH, salt composition (Baker, 2010), increased oxygen (Boysen and Matuschewski, 2011) and the parasites are extracellular from gametogenesis onwards (Talman *et al.*, 2004). The composition of the bloodmeal is also altered by mosquito factors such as serine proteases and chymotrypsins (Vizioli *et al.*, 2001). Finally, of particular importance for energy metabolism, the mosquito midgut is a glucose-deprived environment (Boysen and Matuschewski, 2011). Once inside the mosquito, the bloodmeal begins to be digested, so the parasites must compete for glucose with the

mosquito itself and resident microbiota in the mosquito gut. One might speculate that greatly reduced concentrations of glucose would be available to the parasites, so it makes sense to upregulate mitochondrial energy metabolism (which is more efficient than glycolysis (Kadenbach, 2003; Zheng, 2012)) to maximise ATP generated from available glucose. As the process of exflagellation only takes 15-20 minutes in the newly ingested bloodmeal, it seems unlikely that male gametocytes would experience substantially depleted glucose during this time frame. However, this may be an important factor for post-fertilisation stages. In addition, once extracellular, the parasites are exposed to the mosquito immune system and may need extra ATP for processes such as antioxidant defence.

The second is that the shift towards mitochondrial energy metabolism reflects the increased energy requirements of sexual stage progression in the mosquito, including differentiation of gametes into ookinetes, invasions of the midgut epithelium, oocysts formation and eventually differentiation into sporozoites (Jacot *et al.*, 2016). In addition, although quiescent in the human host, gametocytes undergo explosive development once in the mosquito, suggesting they are in some way 'primed' for onward development whilst in the human host (Delves *et al.*, 2012, 2013). Male gametogenesis (exflagellation) is known to require glycolysis (Slavic *et al.*, 2011; Srivastava *et al.*, 2016) but it is rapid and complex and may require support from mitochondrial respiration. If this is the case, perhaps the upregulation of mitochondrial respiration contributes to a 'pool' of extra ATP which can be drawn upon to support the energy demands of onward development. It is not currently known whether such a 'pool' exists.

Conditions in the human host may also play a role. A previous transcriptional study (Daily *et al.*, 2007) identified at least two physiological states of parasites *in vivo*, a glycolysis-dependent state strongly correlated with ring stages *in vitro* and a state weakly correlated with gametocytes which showed upregulated TCA metabolism, oxidative phosphorylation, fatty acid metabolism and glycerol metabolism (Daily *et al.*, 2007; Lovegrove *et al.*, 2008; LeRoux, Lakshmanan and Daily, 2009). The latter was compared to a starvation response observed in yeast, so it has been suggested that *P. falciparum* parasites produce gametocytes when glucose is limited to escape the starved host and require alternative methods of energy metabolism until uptake by the mosquito (Daily *et al.*, 2007; Lovegrove *et al.*, 2008). Hypoglycaemia can occur during severe malaria (White *et al.*, 1987; Madrid *et al.*, 2015), which could be an instance where glucose availability is restricted and the gametocytes benefit from their upregulated mitochondrial energy metabolism to use glucose more efficiently and survive to be transmitted to a new host.

In summary, current data indicates increased importance of mitochondrial respiration in gametocytes and that mosquito transmission cannot tolerate loss of oxidative phosphorylation (Figure 1.3) but it is not known why. In addition, increased mitochondrial respiration may lead to increased production of reactive oxygen species (ROS) (Oliveira and Oliveira, 2002) which it could be speculated could harm the gametocytes during their long development. It is conceivable that gametocytes must balance longevity in the human host while awaiting uptake and readiness for the mosquito environment where mitochondrial respiration is known to be essential. My hypothesis is that gametocytes upregulate their mitochondrial energy metabolism to be ready for the mosquito environment, but that this is kept to a minimum or otherwise controlled (for example through regulatory proteins which interact with energy metabolism enzymes, or by proteins involved in antioxidant defence) to minimize potential damage by ROS. If such regulation exists, preventing it in gametocytes in the human host could result in damage to gametocytes which may render them unable to develop further in the mosquito. To date, no regulators of gametocyte energy metabolism have been identified. If such regulators were found, they could be attractive targets for transmission-blocking drugs.

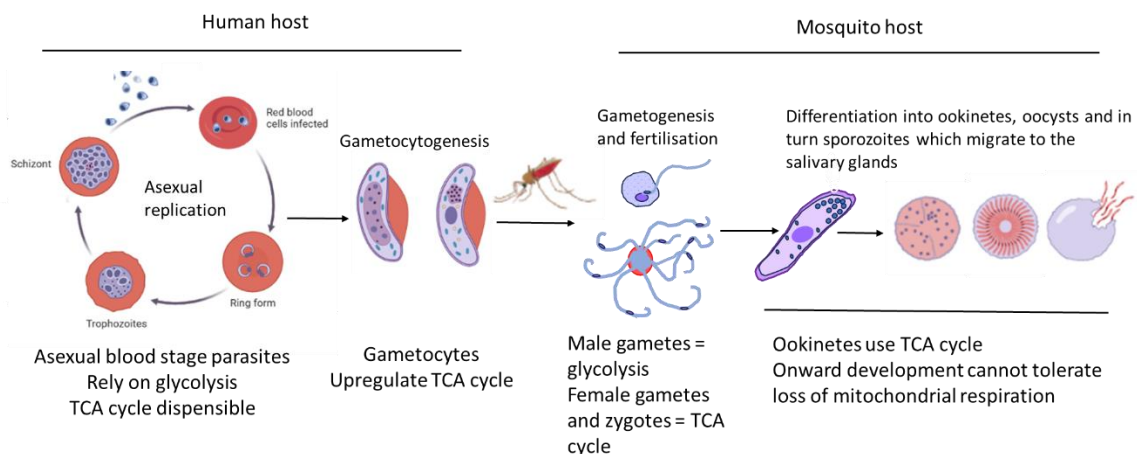


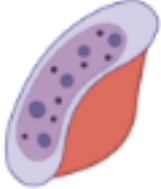
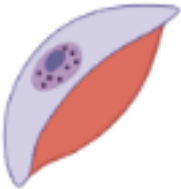
**Figure 1.3. Summary of known changes in energy metabolism across the life cycle of *P. falciparum*.** Data sources for this diagram: Srivastava *et al.* (2016), MacRae *et al.* (2013), Ket *et al.* (2015), Talman *et al.* (2014) Abbreviations: TCA cycle = tricarboxylic acid cycle. Created with BioRender.

## 1.6 Sexual dimorphism in male and female gametocytes

To add further complexity, gametocytes are sexually dimorphic. In the human host, male and female gametocytes have a common goal of surviving for up to 22 days (Eichner *et al.*, 2001) to be transmitted, which they achieve through quiescence. However, once taken up by a mosquito they undergo sex-specific developmental programmes and have divergent roles

in progressing the life cycle (Table 1.1). Male gametocytes are designed to produce male gametes whose sole purpose is to fertilise females (which includes contributing to genetic diversity through meiosis), whereas female gametocytes are preparing for both fertilisation and onward development in the mosquito (Talman *et al.*, 2004; Delves *et al.*, 2013).

The differences in biology between male and female gametes are stark. *Plasmodium* male gametes are among the simplest of all eukaryotic cells, composed of a nucleus containing a condensed haploid genome, an axoneme attached to a modified basal body and a plasma membrane (Sinden *et al.*, 1978). To transform into male gametes, male gametocytes shed their mitochondrion, apicoplast and all other organelles (Okamoto *et al.*, 2009) and their motility has been shown to be powered exclusively by glycolysis (Talman *et al.*, 2014). In addition, male gametes only contribute DNA to the new zygote, the female gamete provides the bulk of the cellular biomass including the mitochondrion and all other organelles for onward development in the mosquito. Therefore, the female gametocyte ‘biomass’ is long-lived in the vector and extracellular for ~24 hours until the mature ookinete penetrates the midgut wall. This contrasts the lifespan of the male gametes, which is short, around 30-40 minutes (Sinden and Croll, 1975). Labelling experiments have shown that unfertilised female gametes and ookinetes drive an active TCA cycle (Srivastava *et al.*, 2016) and as previously mentioned, insect stages cannot tolerate loss of mitochondrial respiration.

| Male gametocyte  | Female gametocyte   |
|--|---|
|   |    |
| Provide only <b>DNA</b> <sup>1</sup> to new zygote (according to current knowledge).   | Provide bulk of <b>cellular ‘biomass’ and all other organelles</b> for <b>onward development</b> <sup>1</sup> .   |
| Male gametes have <b>no mitochondria</b> <sup>1</sup> and use <b>glycolysis</b> <sup>2</sup> .   | Female gametes, zygotes and ookinetes use the <b>TCA cycle</b> <sup>3</sup> .   |
| Enrichment of proteins required for <b>male gametogenesis</b> ; proteins involved DNA replication, chromatin organisation and axoneme formation <sup>4,5</sup> . | Enrichment of proteins required for <b>zygote formation</b> and functions <b>after fertilisation</b> ; protein-, lipid- and <b>energy metabolism</b> <sup>4,5</sup> . |
| <b>Male gametes</b> have <b>30-40-minute</b> <sup>2</sup> lifespan: <b>‘short-lived’</b> in the vector   | <b>Female ‘biomass’</b> must persist <b>11-16 days</b> <sup>6</sup> in the vector survive to generate infectious sporozoites: <b>‘long-lived’</b> in the vector       |

|   |   |
|---|---|
| <b>Exflagellation</b> takes place in the newly ingested bloodmeal: <b>similar glucose to in human host?</b> | <b>Female ‘biomass’</b> must persist in vector as bloodmeal is depleted: <b>low glucose environment?</b> <sup>8</sup> |
|---|---|

**Table 1.1. Summary of differences between male and female *P. falciparum* gametocytes which indicate they could differ in their energy metabolism.** Data sources for this table: 1) Okamoto *et al.* (2009), 2) Talman *et al.* (2014), 3) Srivastava *et al.* (2016), 4) Lasonder *et al.* (2016), 5) Miao *et al.* (2017), 7) Meis *et al.* (1992), 8) Boysen & Matuschewski (2011). Images of male and female gametocytes from BioRender.

These differences in biology are reflected in transcriptomic and proteomic analyses of purified male and female *P. falciparum* and *P. berghei* gametocytes (Khan *et al.*, 2005; Lasonder *et al.*, 2016; Miao *et al.*, 2017). The male proteome is enriched in proteins involved in DNA replication, chromatin organisation and axoneme formation (required for the formation of the haploid, flagellated gametes), whereas the female proteome is enriched in proteins involved in the mitochondria, protein synthesis, translation, protein, lipid and energy metabolism (required for zygote formation, ookinete development and motility) (Khan *et al.*, 2005; Lasonder *et al.*, 2016; Miao *et al.*, 2017). This suggests that the mitochondria may be more important in female gametocytes. Despite these differences in the male and female proteomes, it has not been investigated whether the sexes differ in their energy metabolism.

A striking aspect of gametocyte development which is common to both sexes is the enlargement of the mitochondrion into an elaborate, multi-lobed structure, shown by electron microscopy (EM) to be cristate (Krungkrai, Prapunwattana and Krungkrai, 2000b; Evers *et al.*, 2021). In early EM studies, female mitochondria were reported to have more mitochondria than males (Sinden, 1982c; Krungkrai, Prapunwattana and Krungkrai, 2000b). A study by Okamoto and colleagues (2009) indicated that gametocytes had a single, highly complex mitochondrion and that previous accounts of gametocytes having multiple mitochondria (Sinden, 1982a) could be accounted for by varied angle of sectioning of EM. However, this has been challenged by a recent study examining *P. falciparum* ultrastructure using high-resolution volumetric electron microscopy which suggested the presence of multiple, distinct mitochondria in gametocytes (Evers *et al.*, 2023). It has not previously been investigated whether male and female mitochondria differ in their morphology.

Despite the markedly different fates of male and female gametocytes during transmission, it has not been investigated whether they differ in their mitochondrial energy metabolism. My overarching hypothesis is that gametocytes keep mitochondrial energy metabolism to a minimum in the human host, but they are ready to switch once taken up by a mosquito. If increased mitochondrial energy metabolism is important for survival in the mosquito host, it

might be expected that this would be more important for female gametocytes. As male gametes are shorter-lived in the vector and do not require mitochondrial respiration to complete their role, male gametocytes may be able to limit their mitochondrial respiration (and in turn ROS production) even lower than females. It has been shown that male gametogenesis is more vulnerable to drug treatment than female gametogenesis, suggesting male gametogenesis is more vulnerable to disruption (Delves *et al.*, 2013). Therefore, male gametocytes might benefit from even more limited ROS production due to their relative fragility. Alternatively, the mitochondria of both sexes might have the same activity but for different reasons i.e., in males it is only for exflagellation whereas for females it is for post-fertilisation development. It seems plausible that exflagellation is an energy intensive process due to its complexity. However, disruption of KDH (prevents entry of glutamine-derived carbon from entering the TCA cycle) did not affect exflagellation in *P. falciparum* (Ke *et al.*, 2015), suggesting mitochondrial respiration is not required for male gametogenesis. Similarly, treatment with 100 nM atovaquone, which inhibits cytochrome bc<sub>1</sub> (complex III of the mETC), did not affect male gametogenesis (Ke *et al.*, 2015). The relative importance of glycolysis and mitochondrial respiration for exflagellation needed to be revisited.

## **1.7 Research Aims and Objectives**

Metabolomic studies have demonstrated that energy metabolism differs between asexual blood stage parasites and gametocytes. However, it is unknown how gametocytes regulate their energy metabolism to make the transition from human to mosquito and whether energy metabolism differs between the male and female gametocytes. Improved understanding of gametocyte energy metabolism could provide a rich source of new antimalarial transmission-blocking drug targets.

### **1.6.1 Aim 1**

The divergent biological roles and protein expression between male and female gametocytes suggests energy metabolism may differ between the sexes, an area which remains thus far unexplored. The first aim of the project is to develop tools to determine whether energy metabolism differs between male and female *P. falciparum* gametocytes.

Research objectives:

1. Identify a robust biomarker for accurately distinguishing male and female gametocytes in immunofluorescence assay (IFA) images.

2. Develop an image analysis method using this biomarker and functional mitochondrial labelling to determine whether male and female gametocyte mitochondria differ in their morphology and activity.
3. Test whether male and female gametocytes differ in their susceptibility to inhibitors targeting the mitochondrial electron transport chain (mETC).

### 1.6.2 Aim 2

Mitochondrial respiration is known to be essential for mosquito stages, but it is unknown whether it has a role in gametocytes or the process of gametogenesis. The second aim of the project was to determine whether mitochondrial respiration is required for gametogenesis. It has also not previously been investigated whether gametogenesis is 'energy intensive' compared to the 'resting' state of mature gametocytes in the human host. An additional component to this aim was to develop methods to investigate intracellular ATP concentrations in gametocytes in response to glucose deprivation.

1. Determine whether mitochondrial energy metabolism is required for gametogenesis.
2. Generate transgenic parasites with a genetically encoded ATP indicator to investigate ATP utilisation in gametocytes.

### 1.6.3 Aim 3

Gametocytes are solely responsible for human-to-mosquito transmission and their biology must be able to support this sudden change in host environment. However, how they regulate their energy metabolism to allow survival in both these environments remains unclear. The third aim was to identify and characterise *P. falciparum* proteins with evidence to suggest a role in gametocyte energy metabolism, with a particular interest in those proteins differentially expressed between males and females.

Research objectives:

1. Use data mining of published proteomic data and bioinformatics analysis to identify candidate proteins putatively important for gametocyte energy metabolism.
2. Generate transgenic parasite lines with the proteins of interest tagged with the green fluorescent protein mNeonGreen to characterize their expression and determine their subcellular localisations.
3. Generate transgenic parasite lines with the proteins of interest knocked out to investigate their role in gametocyte energy metabolism.

## Chapter 2

## Materials and Methods

### 2.1 Selection of candidate proteins

#### 2.2.1 Data Sources

Candidate proteins putatively important for gametocyte energy metabolism were selected by data mining of published gametocyte proteomic and phenotyping data. The following data sources were used for the data mining:

Lasonder *et al.* (2016) – An integrated transcriptomic and proteomic analysis of sex-separated male and female *P. falciparum* N54 strain gametocytes was used to identify proteins differentially expressed between the sexes.

Silvestrini *et al.* (2010) – A proteomic study comparing *P. falciparum* trophozoites, early (stage I-II) and mature (stage V) gametocytes was used to investigate whether the proteins of interest were specifically expressed or upregulated in gametocytes (indicative of a gametocyte specific function) or more widely expressed across the life cycle.

Zhang *et al.* (2018) – Essentiality screen which generated *P. falciparum* NF54 mutants via random piggyBac transposon mutagenesis, with the resulting 38,000 mutants being genetically identical except for a single randomly inserted transposon at TTAA tetranucleotide sites which has the potential to disrupt normal gene function.

Bushell *et al.* (2017) – Essentiality screen which measured the competitive growth rates in mice of 2,578 barcoded *P. berghei* knockout mutants (representing >50% of the genome), with unsuccessful gene disruption indicating that the gene is essential for asexual growth.

#### 2.1.2 Protein selection workflow

Proteins identified in Lasonder and colleagues' (2016) proteome with a 10-fold or greater difference in protein expression between male and female gametocytes were investigated further and those proteins assigned GO Terms linked to energy metabolism (e.g., glycolysis, carbohydrate metabolic process, mitochondrial TCA cycle). Proteins which were already well-studied in gametocytes or predicted to be essential to all parasite stages according to essentiality screens in *P. falciparum* and *P. berghei* (Bushell *et al.*, 2017; Zhang *et al.*, 2018) were excluded to give the final shortlist of proteins to study. Essentiality in asexual blood stage parasites would suggest the protein's function is not gametocyte specific. Additional genes were also identified from literature searches.

### **2.1.3 Bioinformatic analysis**

Bioinformatic analysis was performed with a range of online tools. BLASTP (<https://blast.ncbi.nlm.nih.gov/Blast.cgi>) searches were used to search for genes with predicted protein sequences similar to the genes of interest. Pairwise comparisons of proteins sequences were performed with EMBOSS Needle ([https://www.ebi.ac.uk/Tools/psa/emboss\\_needle/](https://www.ebi.ac.uk/Tools/psa/emboss_needle/)). Multiple sequence alignments were performed in CLUSTAL Omega (<https://www.ebi.ac.uk/Tools/msa/clustalo/>). Reference sequences for multiple alignments were obtained from PlasmoDB (<https://plasmodb.org/plasmo/>) for *Plasmodium* species and Gen Bank (<https://www.ncbi.nlm.nih.gov/genbank/>) or Uniprot (<https://www.uniprot.org/>) for other organisms. Searches of InterPro (<https://www.ebi.ac.uk/interpro/>) and the Conserved Domain Database (CDD) (<https://www.ncbi.nlm.nih.gov/Structure/cdd/wrpsb.cgi>) were used to investigate family membership and predicted domains and motifs. Predicted physical properties of the proteins were investigated using web-based tools found on the ExPASy Bioinformatics Resource Portal (<https://www.expasy.org/>).

## **2.2 Molecular biology techniques**

### **2.2.1 Polymerase chain reaction (PCR)**

All PCR products for molecular cloning were amplified using CloneAmp HiFi polymerase (Takara Bio) from parasite genomic DNA (gDNA) or plasmid DNA. A typical reaction involved 30 cycles of: 10 seconds at 98 °C, 30 seconds at 52 °C and 60 seconds at 70 °C, followed by a final extension of 5 minutes at 70 °C.

### **2.2.2 Primer design**

Genomic sequences used for primer design were obtained from PlasmoDB. All primers were ordered from Integrated DNA Technologies (IDT). The online tool OligoCalc (Kibbe, 2007) was used to determine the annealing temperatures of the primers and avoid self-complementarity and hairpin formation. All primers used are listed in Appendix 1.

### **2.2.3 Restriction digests**

Restriction digests were set up with restriction enzymes from New England Biolabs (NEB) according to the manufacturer's instructions.

## 2.2.4 Generation of selection-linked integration (SLI) constructs for tagging and TGD

To investigate the subcellular localisation of the proteins of interest and characterise their expression, constructs were generated for mNeonGreen (mNG) tagging. The strategy chosen for the integration of these constructs was selection-linked integration (SLI) (Birnbaum *et al.*, 2017). In this approach, a promoterless targeting region on the plasmid to be integrated is linked with an additional selectable marker which can only be expressed after single crossover integration into the target locus so parasites can be selected by using the additional integration-linked resistance marker (Birnbaum *et al.*, 2017) (Figure 2.1). SLI constructs were generated for all six genes of interest identified by data mining of proteomic data, shown in Table 2.1.

| PlasmoDB<br>Gene ID | Predicted Gene<br>product                              | A. Successfully<br>disrupted in the<br>asexual life<br>cycle |     | B. Protein<br>expression data<br>(spectra) |    |    | C. Fold<br>difference in<br>expression<br>FG/MG |
|---------------------|--|--|-----|--|----|----|---|
|                     |  | Pf   | Pb  | T  | EG | LG |   |
| PF3D7_1128300       | Phosphofructokinase<br>11 (PFK11)                      | Yes  | Yes | N  | N  | 73 | 329.03  |
| PF3D7_1012500       | Phosphoglucomutase                                     | Yes  | Yes | 3  | 1  | 30 | 110.90  |
| PF3D7_0310300       | Phosphoglycerate<br>mutase                             | Yes  | Yes | 3  | 8  | 84 | 87.48   |
| PF3D7_0306400       | FAD-dependent<br>glycerol-3-phosphate<br>dehydrogenase | Yes  | Yes | 9  | 12 | 38 | 68.03   |
| PF3D7_0802000       | Glutamate<br>hydrogenase 3<br>(GDH3)                   | Yes  | Yes | 22   | 5  | 18 | 37.74   |
| PF3D7_1437700       | Acetyl-CoA<br>synthetase ADP-<br>forming (ACS-ADP)     | Yes  | Yes | N  | 8  | 31 | 0.76  |

**Table 2.1. Candidate genes selected for genetic investigation in *P. falciparum* gametocytes.**

Data sources: **A)** Asexual blood stage phenotyping data (Bushell *et al.*, 2017; Zhang *et al.*, 2018), **B)** Proteomic data in trophozoites and early gametocytes (Silvestrini *et al.*, 2010), **C)** Proteomic data in mature male and female gametocytes (Lasonder *et al.*, 2016). Abbreviations: Pf = *P. falciparum*, Pb = *P. berghei*, T = trophozoites, EG = stage I-II gametocytes, LG = stage V gametocytes, N = protein not

identified. ACS-ADP was not differentially expressed between the sexes but was selected to study a potential link between glycolysis and acetate formation in gametocytes.

### Selection-linked integration (SLI)

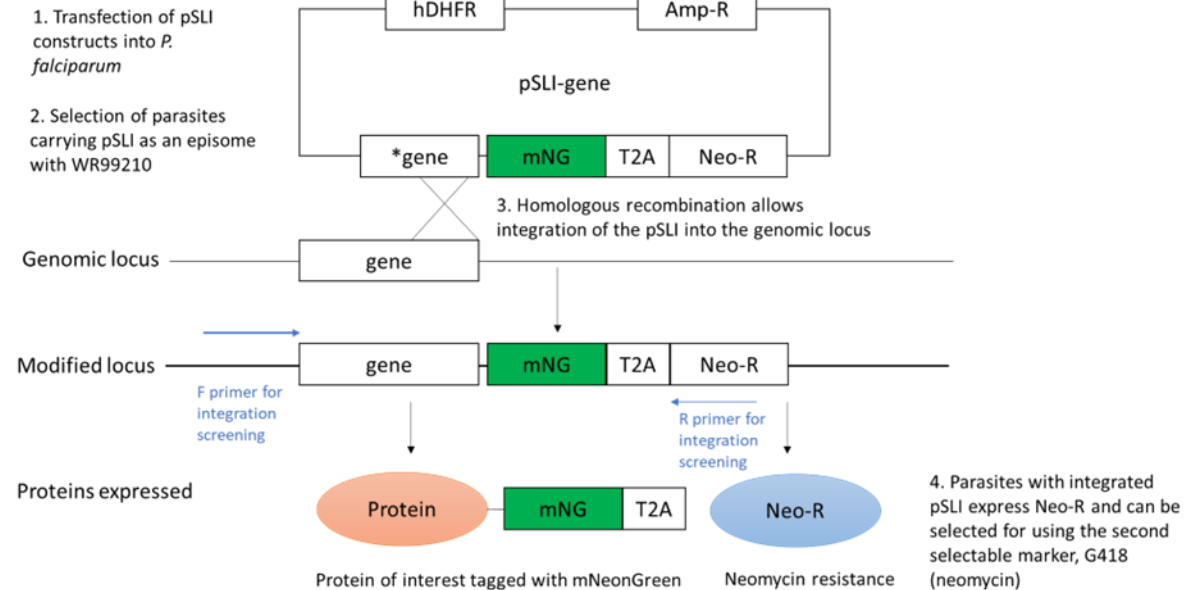


**Figure 2.1. Selection-linked integration (SLI) tagging strategy.** Recombination between regions of homology in the SLI cassette and genomic locus allows for selection-linked integration. The vector backbone carries the selectable markers: ampicillin resistance (Amp-R), neomycin resistance (neo-R) and human dihydrofolate reductase (hDHFR), which confers resistance to the drug WR99210. Parasites that have taken up the pSLI targeting vector as episome express hDHFR, which confers resistance to WR99210. The antibiotic geneticin (G418), an analog of neomycin sulphate with similar mechanisms to neomycin, selects for parasites in which successful integration of the SLI cassette into the genomic locus has occurred.

For PFK11 and ACS-ADP, additional SLI constructs were generated for targeted gene disruption (SLI-TGD) (Birnbbaum *et al.*, 2017) to determine whether knocking out either of these genes resulted in a phenotype in gametocytes or downstream mosquito stages, which would suggest the protein is important for transmission. The SLI-TGD plasmids function like the SLI tagging vectors except that the homology region in gene of interest is at the 5' region as opposed to the mNG tagging construct where it was at the 3' region. Recombination of the SLI-TGD cassette with the genomic locus results in the truncation of the target protein (in the case of ACS-ADP, the first 390 bp of the 2922 bp gene). This truncation likely severely compromises gene function, equivalent to deleting the entire gene. A schematic is shown in Figure 2.2.

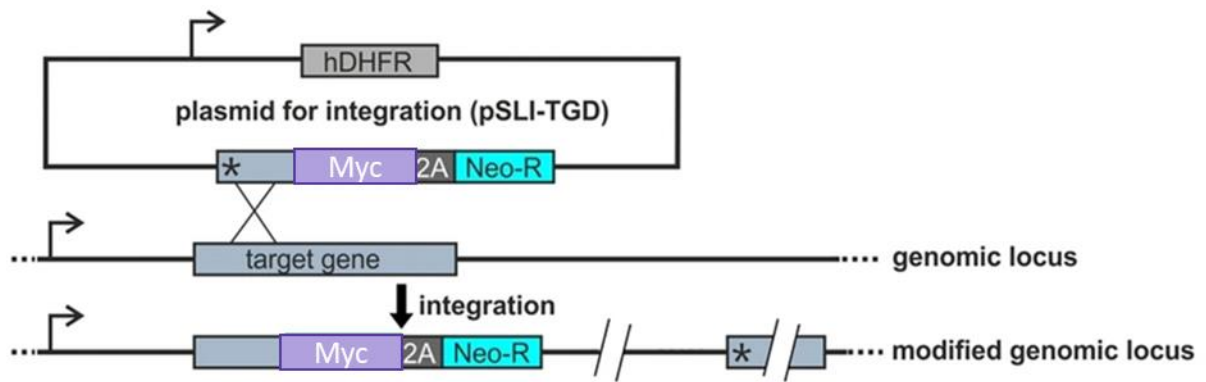


**Figure 2.2. Schematic of the selectable targeted gene disruption strategy (SLI-TGD) adapted from Birnbaum *et al.* (2017).** \* = 390 bp fragment of N-terminal region of target gene, in this case ACS-ADP; Myc = Myc tag, 2A: T2A skip peptide; arrows: promoters.

For five of the genes, SLI constructs were also generated to tag isoforms of the proteins of interest which were not gametocyte-specific or upregulated. Unlike the proteins of interest, these isoforms were expressed throughout the life cycle, to compare gametocyte-specific or upregulated isoforms with non-gametocyte specific isoforms (Table 2.2).

| Plasmid ID    | Gene Name | Gene product  | Counterpart to:                                  |
|---------------|-----------|---|--|
| PF3D7_0915400 | PFK9      | ATP-dependent phosphofruktokinase (catalyses step 3 in glycolysis)                                      | PFK11 (PF3D7_1128300)                            |
| PF3D7_0627800 | ACS-ATP   | Acetyl-CoA synthetase (ATP-forming) (activation of acetate to acetyl-CoA)                               | ACS (ADP-forming) PF3D7_1437700                  |
| PF3D7_1120100 | PGM1      | Co-factor dependent phosphoglycerate mutase (catalyses step 8 in glycolysis)                            | Putative phosphoglycerate mutase (PF3D7_0310300) |
| PF3D7_0413500 | PGM2      | Phosphatase with residual mutase activity   | Putative phosphoglycerate mutase (PF3D7_0310300) |
| PF3D7_1416500 | GDH1      | Glutamate dehydrogenase 1 (NADP <sup>+</sup> -dependent GDH, possibly involved in ammonia assimilation) | GDH3 (PF3D7_0802000)                             |

**Table 2.2. Non-gametocyte specific or non-gametocyte upregulated isoforms of proteins of interest.** References for the information in this table are as follows: PFK9 (Mony *et al.*, 2009), ACS

(ATP-forming) (Sánchez, Galperin and Müller, 2000; Tielens *et al.*, 2010), PGM1 and PGM2 (Hills *et al.*, 2011), GDH1 (Storm *et al.*, 2011; Zocher *et al.*, 2012)

To generate the tagging constructs, an existing SLI construct (pSLI-mNG) targeting an unrelated protein with an mNG tag was modified to excise the existing insert and replace it with the desired custom inserts (Figure 2.3). A restriction digest of the existing pSLI-mNG with KpnI and NotI yielded two fragments. Measured against the GeneRuler 1 kb DNA ladder, the larger fragment was between 5000-7000 bp and the smaller fragment between 700-1000 bp, consistent with the expected size of the vector backbone (6743 bp) and excised insert (918 bp), suggesting the vector had been cut correctly (Figure 2.4).

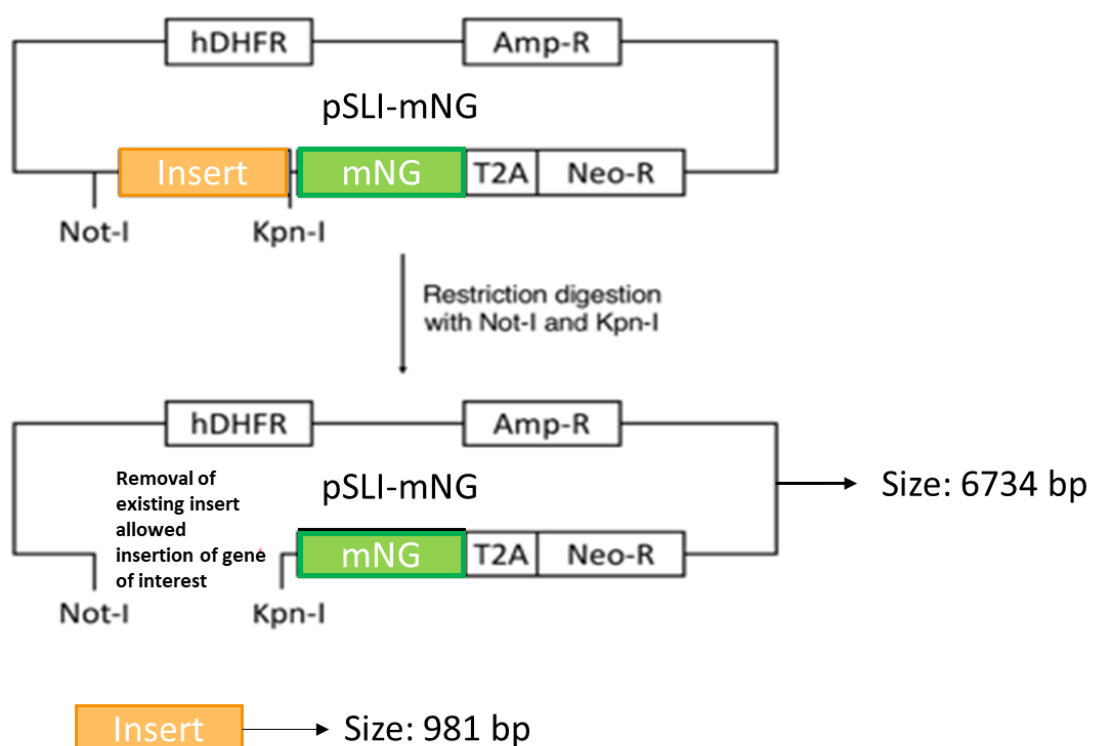


**Figure 2.3. Schematic of restriction digestion of the SLI-mNG plasmid.** Abbreviations: hDHFR = human dihydrofolate reductase (WR99210 resistance gene), Amp-R = ampicillin resistance gene, mNG = mNeonGreen, T2A = skip peptide, Neo-R = neomycin resistance gene. Neo-R enables parasites to grow in media containing the antibiotic geneticin (G418). The sizes of the cut vector backbone (6734 bp) and existing insert (981 bp) are shown in the figure.

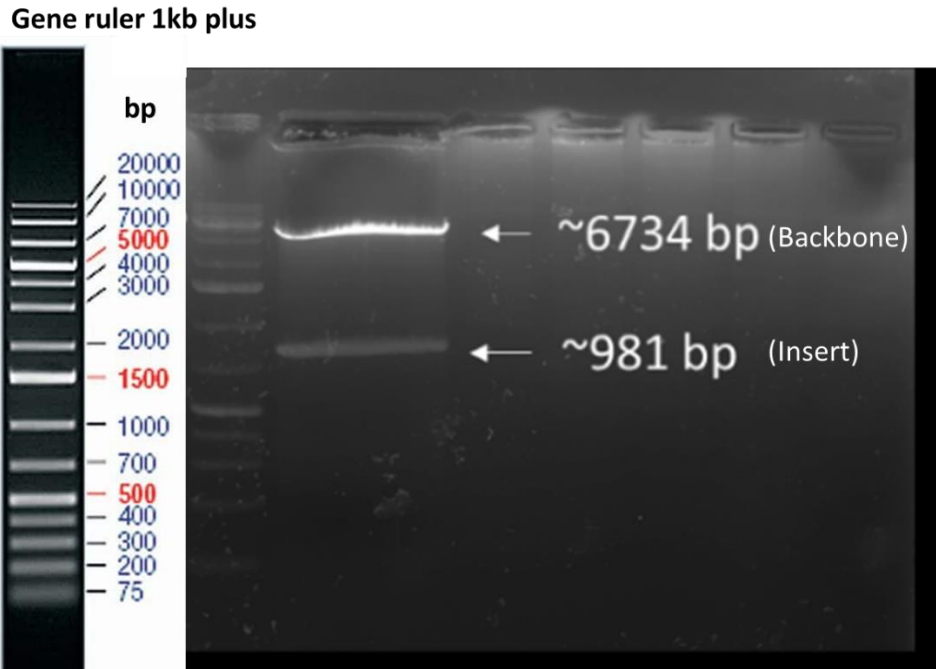


**Figure 2.4. Restriction digest of pSLI-mNG backbone with KpnI and NotI.** Bands were sized using a Gene Ruler 1 kb plus ladder, shown on the left.

Genomic DNA (gDNA) was extracted from NF54 asexual blood stage parasites and 3' regions of the genes of interest were subsequently amplified by PCR. Primers were designed to include 30 bp regions of overlap between the *P. falciparum* insert sequences and the adjacent sequences of the pSLI-mNG backbone. Bands of the expected sizes for the inserts were obtained by PCR. Examples are shown in Figure 2.5.

The inserts were then ligated into the pSLI-mNG vector backbone by Gibson Assembly using the designed homology regions. *Escherichia coli* competent cells were subsequently transformed with the Gibson cloning reactions and the transformed colonies screened by colony PCR. Colony PCR products from *E. coli* transformed with each construct were consistent with the expected insert sizes. Correct ligation of the inserts into the pSLI-mNG backbone was subsequently confirmed by sequencing.

### Gene ruler 1kb plus

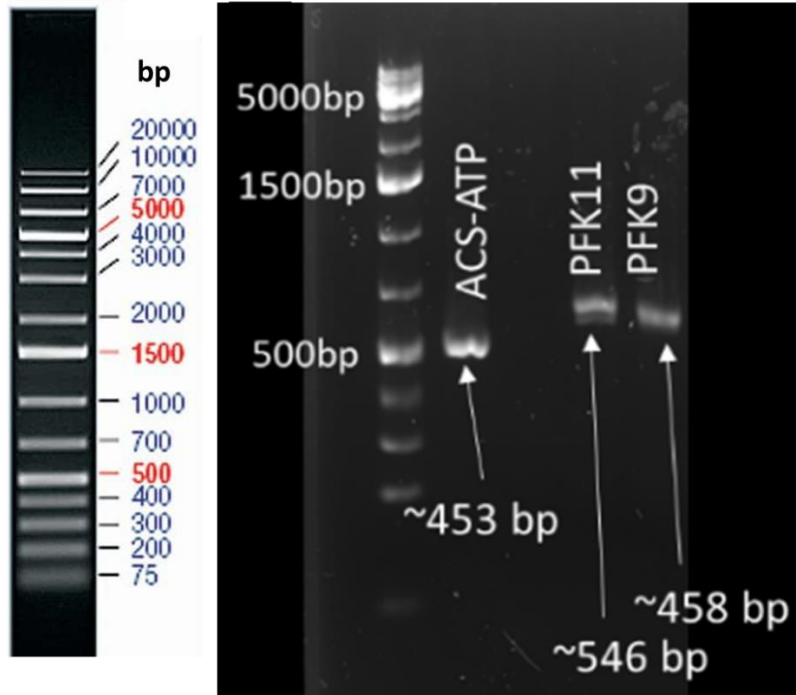


**Figure 2.5. Amplification of insert DNA for the SLI tagging vectors from NF54 genomic DNA.** Examples shown are for ACS-ATP, PFK11 and PFK9. Abbreviations: bp = base pair. Bands were sized using a Gene Ruler 1 kb plus ladder, shown on the left.

### 2.2.5 Generation of CRISPR-Cas9 constructs for KO of PFK11

The CRISPR gene editing strategy has been adapted for use in *P. falciparum* (Ghorbal *et al.*, 2014). CRISPR gene editing is based on the clustered, regularly interspaced, short palindromic repeat (CRISPR)–CRISPR-associated protein 9 (Cas9) system (CRISPR-Cas9), a bacterial immune mechanism against viruses. CRISPR gene editing involves introducing a plasmid which encodes the Cas9 endonuclease and a single guide RNA (sgRNA) which guides the Cas9 to the required site of the chromosomal target to cleave the DNA. A repair plasmid containing the desired genetic modification is also introduced which will integrate into the genome either by non-homologous end joining (NHEJ) or homologous recombination (Ghorbal *et al.*, 2014).

PFK11 could not be disrupted using SLI-TGD so a new CRISPR gene editing strategy was used instead. CRISPR-Cas9 mediated KO of PFK11 required two plasmids 1) a plasmid containing the Cas9 sequence and guide RNA (gRNA) and 2) a repair plasmid. An existing Cas9 and repair plasmid were kindly provided by James Thomas (LSHTM). The repair plasmid was modified to replace the existing insert with the custom insert for PFK11-KO. The custom insert consisted of 5' and 3' homology regions in the N-terminal region of PFK11 which would target and massively truncate PFK11 by CRISPR-Cas9. Between the two

homology regions, there was a GFP sequence, a skip peptide and a blasticidin resistance gene. A schematic of the CRISPR-Cas9 knockout strategy is shown in Figure 2.6.

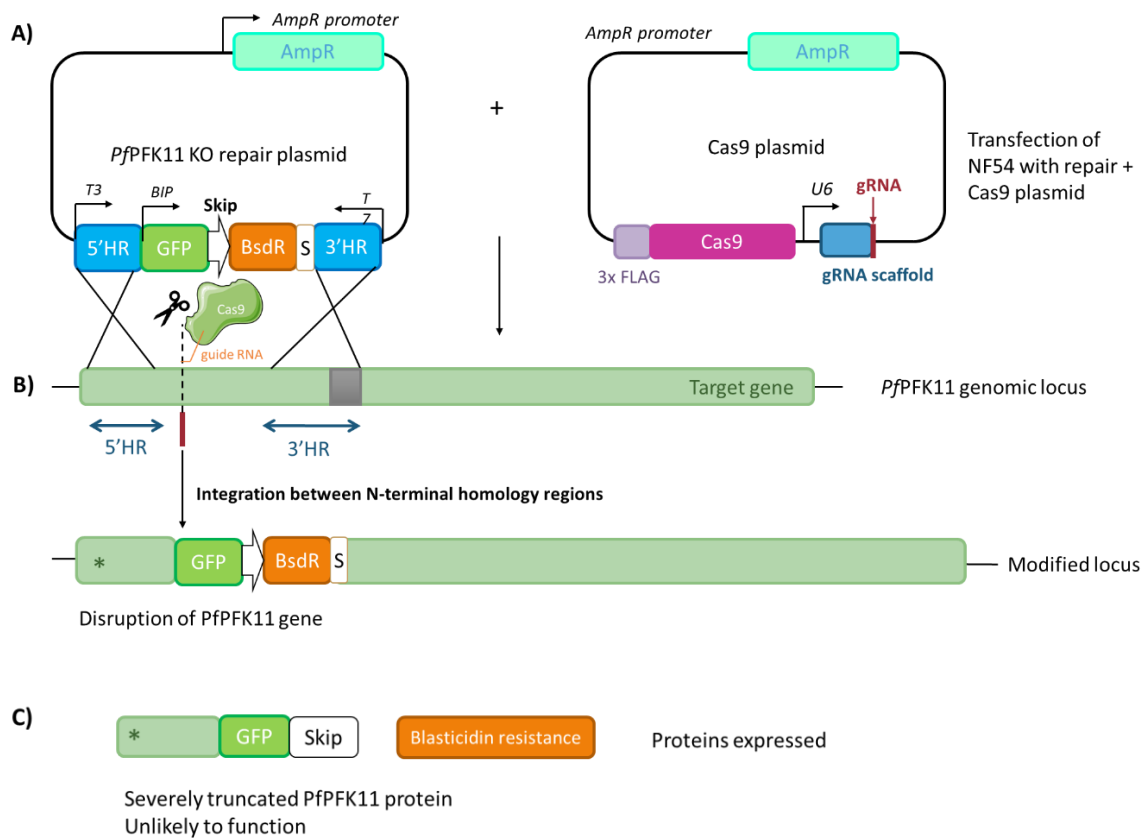


**Figure 2.6. CRISPR-Cas9 strategy for knockout of PFK11.** **A)** NF54 parasites are transfected with the PFK11-KO repair plasmid and Cas9 plasmid. **B)** The guide RNA (gRNA) guides the Cas9 enzyme to the appropriate site on the target gene where it cuts the DNA. The repair plasmid inserts into the genome by homologous recombination with the 5' and 3' homology regions (HRs) at the 5' region of the *PFK11* gene. This results in disruption of the *PFK11* gene as the insert integrates into the 5' region. The stop codon after the blasticidin resistance gene prevents the rest of the PFK11 protein from being expressed. **C)** A severely truncated version of the PFK11 protein is expressed and the transfected parasites will express GFP. Parasites with the construct integrated can be selected for using blasticidin (BSD). Abbreviations: HR = homology region, GFP = green fluorescent protein, skip = skip peptide, BsdR = blasticidin resistance gene, S = stop codon, AmpR = ampicillin resistance gene, gRNA = guide RNA.

The custom insert was generated as follows. PCR was used to amplify from genomic DNA the 5' (747 bp) and 3' (1043 bp) homology regions to target and massively truncate PFK11 by CRISPR gene editing. These regions were successfully amplified producing bands sizes of ~700 and ~1000 bp, consistent with the size of the 5' and 3' homology regions respectively (Figure 2.7.)

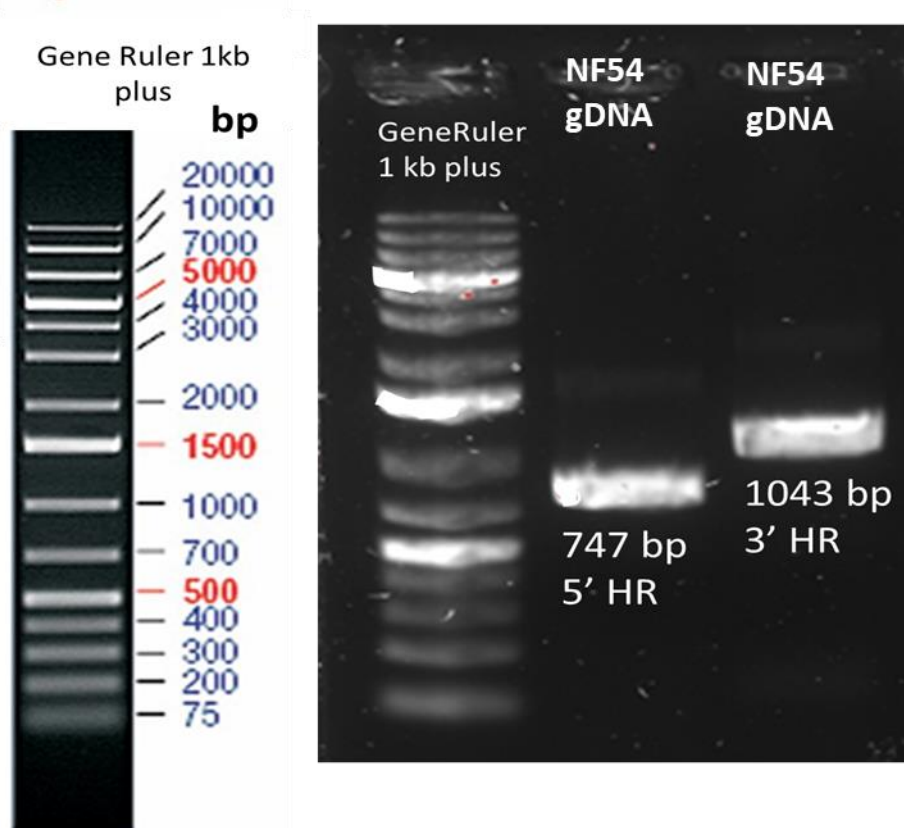


**Figure 2.7. Amplification of the 5' and 3' homology regions for the CRISPR-Cas9 PFK11-KO vector from NF54 genomic DNA.** Abbreviations: HR = homology region, gDNA = genomic DNA.

The 5' and 3' homology regions were then ligated into the vector backbone by Gibson Assembly and the products used to transform bacteria. The plasmid was then digested with *Ava*I and *Sac*I which would separate the vector backbone (2.8 kb) from the 5' and 3' homology regions and sequence between them (4.5 kb). Two bands were obtained, one at ~5 kb and ~3kb, suggesting the insert had successfully been ligated into the vector (Figure 2.8).

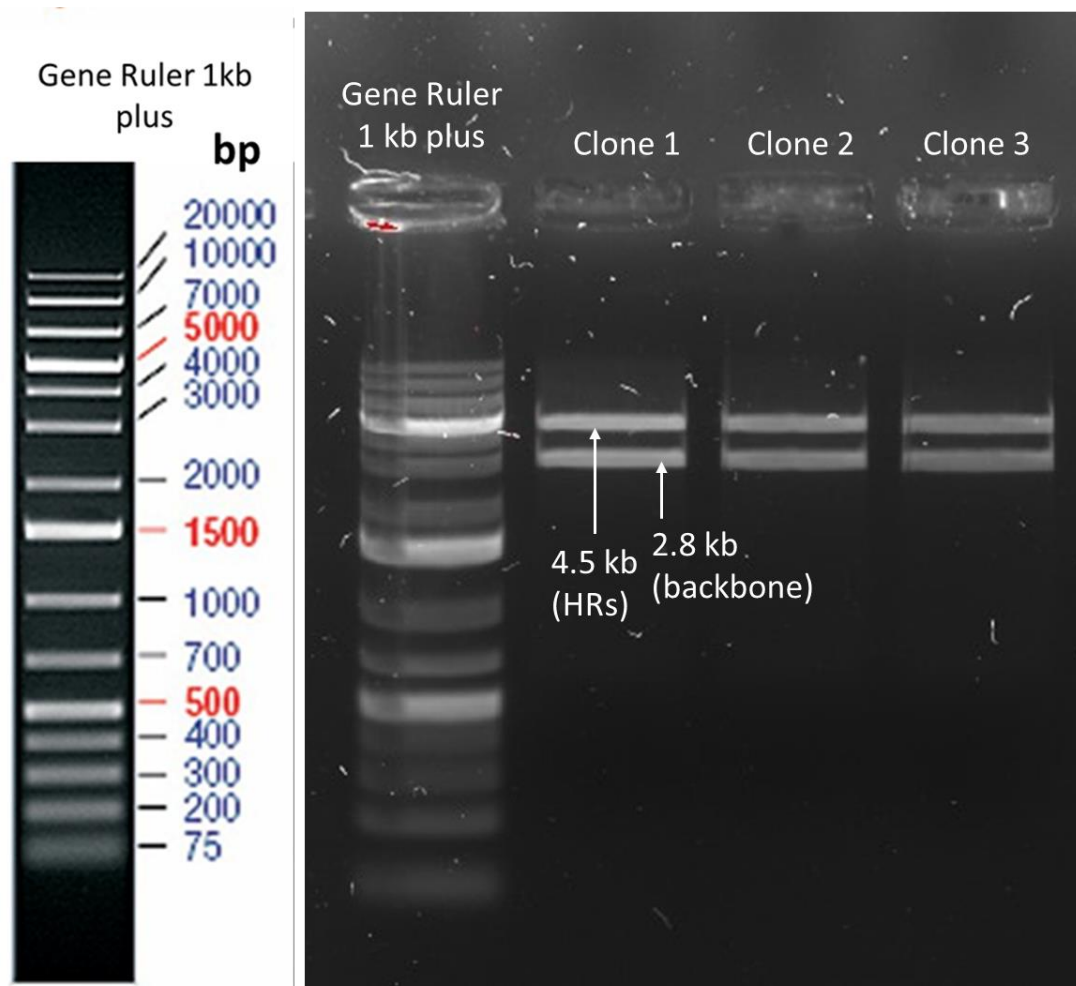


**Figure 2.8.** Restriction digest of PFK11-KO plasmids from 3 colonies (clone 1-3) of transformed *E. coli* with *Ava*I and *Sac*I. Abbreviations: HRs = homology regions.

Finally, a drug selectable marker, the blasticidin (BSD) resistance gene was added to the repair plasmid to make it more efficient to select for the repair event. The existing insert sequence between the 5' and 3' homology regions was digested out with *Nhe*I and *Pst*I. A replacement insert sequence of GFP followed by a skip peptide followed a BSD resistance gene (GFP-skip-BSD) was then amplified from a different plasmid gifted by Avnish Patel (LSHTM). The GFP-skip-BSD fragment was ligated into the repair plasmid by Gibson assembly. To confirm insertion of GFP-skip-BSD, the plasmid was digested with *Nhe*I and *Pst*I, giving band sizes of ~7 kb, ~700 bp and ~450 bp (Figure 2.9) The vector backbone is 6.6 kb, GFP is 717 bp and BSD fragment is 464 bp, therefore the bands observed are consistent with the expected product sizes. Correct ligation of the insert into the vector backbone was then confirmed by sequencing.

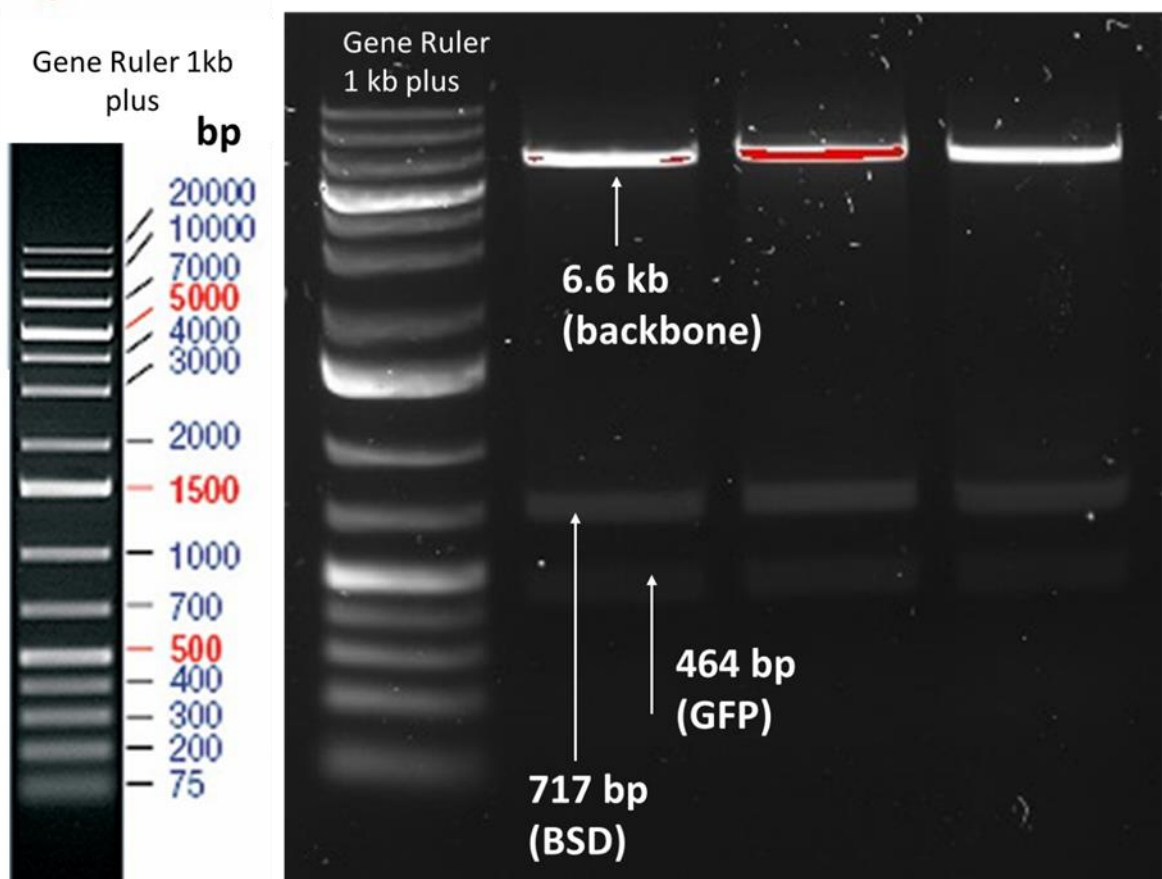


**Figure 2.9. Restriction digestion of the repair plasmid with NheI and PstI to confirm insertion of GFP-skip-BSD into the PFK11-KO plasmid.** Abbreviations: GFP = green fluorescent protein, BSD = blasticidin resistance.

### 2.2.6 Generation of CRISPR-Cas9 vector for mNG-tagging of PFK11

It was not possible to tag PFK11 using SLI despite multiple attempts. In a revised strategy, a CRISPR-Cas9 plasmid with the Cas9 and guide RNA integrated (kindly gifted by Ashley Vaughan, Seattle Children's Hospital) was modified (Figure 2.9). The repair template consisted of the following: an Aval restriction site, a 5' homology region (in the C-terminus of the PFK11 protein), an insert sequence (the recodonised C terminus from PFK11, an XhoI restriction site, the mNeonGreen (mNG) tag sequence and a stop codon), a 3' homology region and a PstI-SacI restriction site. The 5' homology region with a SpeI Gibson overhang (data not shown) and the 3' homology region with a Sall Gibson overhang (Figure 2.10) were amplified by PCR.

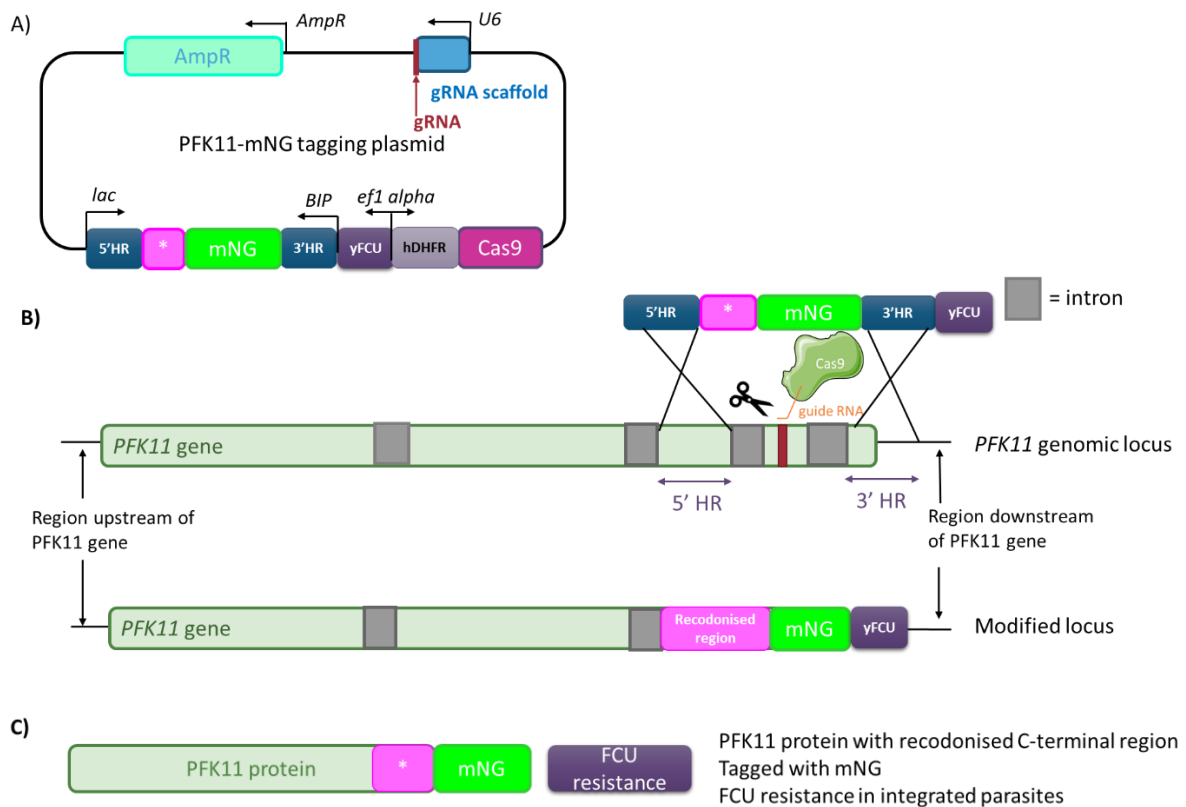


**Figure 2.10. CRISPR-Cas9 strategy for tagging of PFK11.** **A)** CRISPR-Cas9 vector for mNeonGreen (mNG) tagging of PFK11. Abbreviations: AmpR = ampicillin resistance, gRNA = guide RNA, HR = homology region, \* = recodonsed region between the 5' and 3' HRs with introns removed, yFCU = Fluorouracil (5-FU or FCU) resistance gene, hDHFR = human Dihydrofolate reductase. **B)** The plasmid encodes both the Cas9 and the repair template. When the plasmid is taken up the Cas9 enzyme is translated and is guided to the correct site to cut by the gRNA. The repair template then undergoes homologous recombination with the 5' and 3' HRs to repair the DNA. The repair template consists of the 5' HR, a recodonsed region with introns removed (prior to this the region proved impossible to amplify by PCR), the mNG tag and the 3'HR. Grey boxes represent introns in the PFK11 gene. **C)** The successful modification results in expression of the PFK11 protein tagged with mNG. Integrated parasites also express an FCU resistance selectable marker which can be used to select for parasites with the integrated construct.

To insert the gRNA, the plasmid was first cut to release the gRNA fragment with Esp3I. Complementary primers containing the gRNA and overhangs were used to clone the gRNA into the plasmid backbone by Gibson assembly. The multiple cloning site (MCS) was then opened by digestion with *SpeI* and *Sall*. The insert fragment was synthesised by GeneArt and consisted of the recodonsed C terminus from PFK11, a *XhoI* restriction site and the mNG sequence followed by a stop codon. The 5' homology region, the insert fragment with the recodonsed region with the mNG tag and stop codon and the 3' homology region and vector backbone were ligated together in a single Gibson assembly reaction. The Gibson

cloning products were then used to transform *E. coli* competent cells. Screening of 11 colonies from the plate by colony PCR for the 5' homology region (520 bp) revealed 5 positive colonies. The plasmids from the positive colonies were then miniprepped and diagnostic digests performed with XhoI and SacII. The XhoI restriction site is located just before the mNG tag and SacII just after the 3' homology region. The expected size of the fragment from the XhoI to SacII is 1723 bp and for the rest of the construct, 12440 bp. As shown in Figure 2.12, the digest gives a band of ~1700 bp and a higher band between 10 kb and 20 kb, consistent with the expected sizes, suggesting correct integration into the vector. Correct ligation of the plasmid was subsequently confirmed by sequencing.

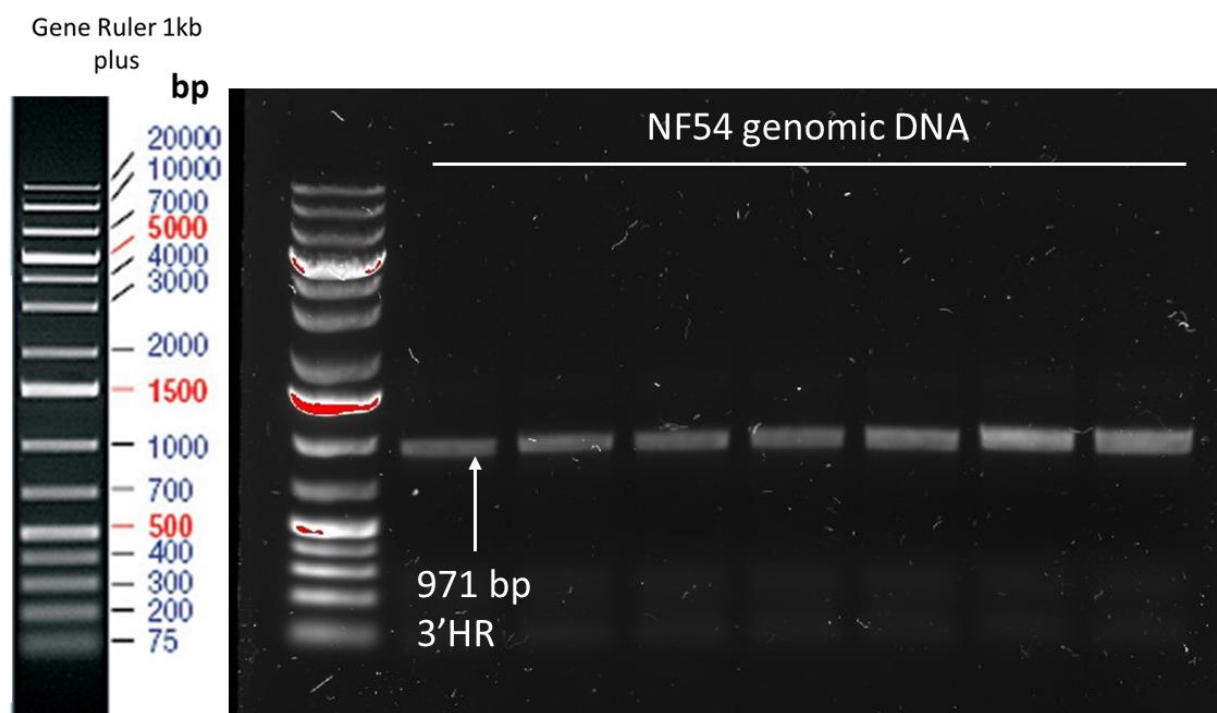


**Figure 2.11. PCR Amplification of 3' homology region with SpeI overhang for mNG tagging of PFK11.** Abbreviations: HR = homology region.

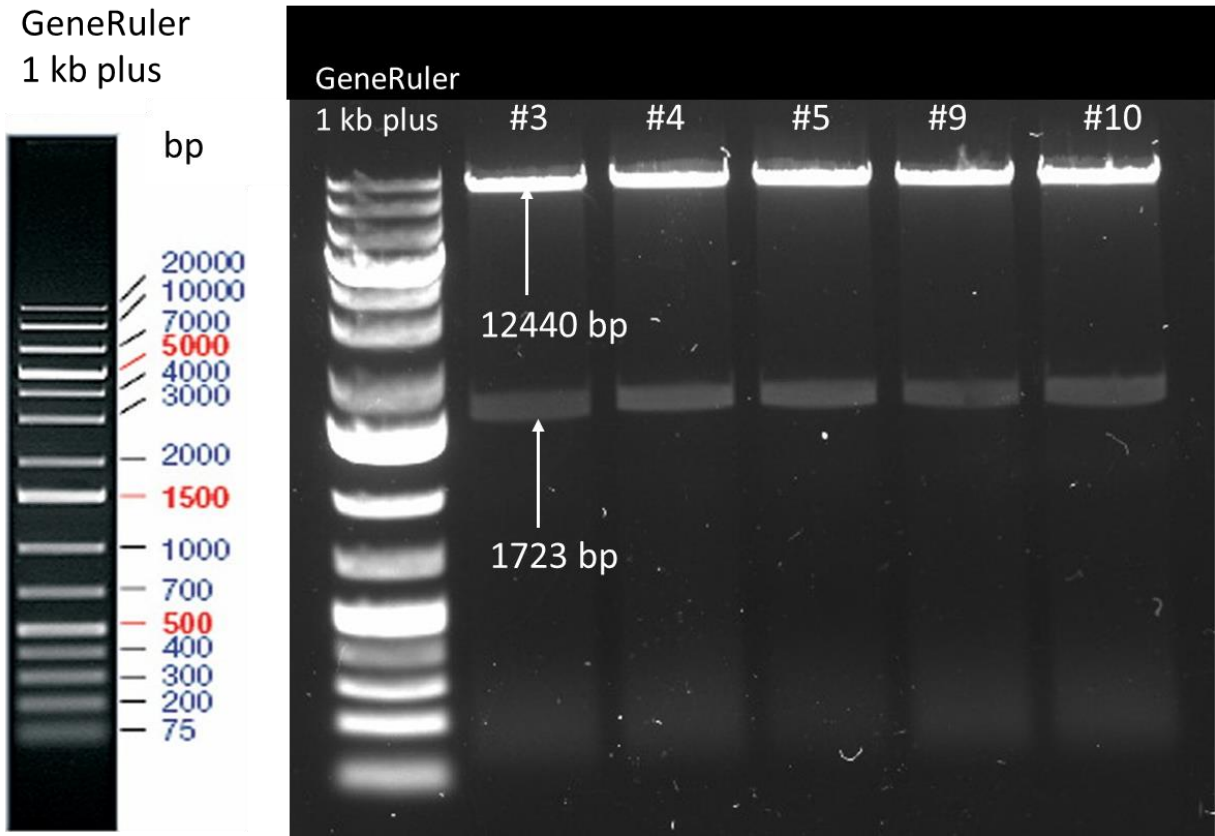


**Figure 2.12. Diagnostic digests of colonies following Gibson assembly of the PFK11 tagging plasmid.** Electrophoresis gel showing the digestion of 5 colonies (#3,4,5,9,10) with XhoI and SacII. XhoI is located just before the mNG and SacII just after the 3' HR. This region is 1723bp, consistent with the lower band on gel). The remainder of the plasmid is 12440 bp consistent with the higher band.

## 2.2.6 Colony PCR screening

Colonies of successful transformants were diluted in 100  $\mu$ l of phosphate buffered saline (PBS). Incubation at 90  $^{\circ}$ C was carried out for 3 minutes prior to commencement of PCR to ensure lysis of *E. coli* transformants and release of plasmids. PCR was carried out with GoTaq<sup>®</sup> Green Master Mix (Promega) according to the manufacturer's instructions. Primers for all constructs can be found in Appendix 1. The PCR products of NF54 gDNA amplified with the primers for each construct were used as positive controls for the colony PCR.

## 2.2.7 Sequencing

For SLI-tagging plasmids, Sanger sequencing was carried out by Eurofins (United Kingdom) to confirm correct integration of the insert fragments into the pSLI-mNG plasmid backbone. The primers used for sequencing can be found in Appendix 1. For the PFK11-KO and PFK11-mNG tagging plasmids, the whole plasmids were sequenced by Plasmidsaurus

(Oregon, USA) ([www.plasmidsaurus.com](http://www.plasmidsaurus.com)) to verify the plasmid had been constructed correctly.

### **2.2.8 Plasmid purification**

Isolation of plasmid DNA for molecular cloning was carried out using a Monarch® Plasmid Miniprep Kit (New England BioLabs). Large-scale plasmid preparation for transfection was carried out using a Genopure Plasmid Maxi Kit (Roche). Both kits were used according to the manufacturer's instructions.

## **2.3 Parasite culture**

### **2.3.1 Asexual blood stage parasite culture**

NF54 asexual blood stage parasites (a gift from Leiden University) were cultured in *P. falciparum* custom medium (RPMI-1640, 2.3 g/L sodium bicarbonate, 2 g/L dextrose, 5.9 g/L HEPES, 50 mg/L hypoxanthine, 1% Albumax II, 10% human AB+ serum, 30 mg/ml L-glutamine) and type O, A or AB human blood at 37 °C under 3% O<sub>2</sub>–5% CO<sub>2</sub>–92% N<sub>2</sub> (malaria gas.) Culture medium was replenished daily. Cultures were passaged to 0.5% parasitaemia and 4% haematocrit every 2-3 days. Culture parasitaemia of asexual maintenance cultures was kept under 5% as far as possible as exceeding this parasitaemia resulted in suboptimal gametocyte production.

### **2.3.2 Gametocyte culture**

The gametocyte culture protocol was adapted from Delves *et al.* (2016) (a schematic shown is in Figure 2.12). Gametocyte cultures were seeded from asexual blood stage cultures at 2% parasitaemia and 4% haematocrit in gametocyte medium (RPMI-1640 with 2 g/L dextrose, 5.9 g/L HEPES, 10% v/v human AB+ serum, 0.5% Albumax, 3.7% v/v HT supplement (Gibco), 30 mg/ml L-glutamine, 2.78g/L sodium bicarbonate) at 37 °C under malaria gas. Culture media was replaced daily for 14 days. All surfaces and reagents were maintained at 37 °C to maintain a ~37 °C temperature and prevent premature activation of gametocytes.

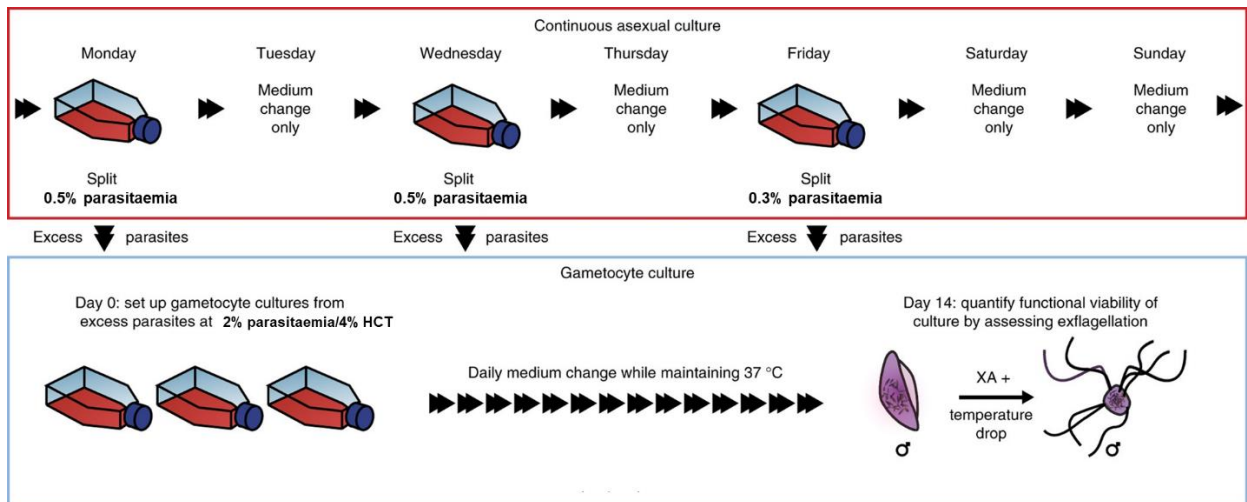


**Figure 2.13. Protocol for seeding of gametocyte cultures from continuous asexual feeder cultures, adapted from Delves *et al.* (2016).**

### 2.3.3 Gametocyte purification

To purify gametocytes from one 10 ml culture, 5 ml of pre-heated Gentodenz (Genprice Gentaur) 14% w/v solution was added to a low-binding 15 ml falcon tube and the 10 ml culture gently added to the top of the Gentodenz layer. Centrifugation at 20 minutes at 800 x g at 37 °C separated the culture into layers (Figure 2.14). The enriched gametocyte layer was then aspirated to obtain purified gametocytes without asexual parasites and uninfected erythrocytes.

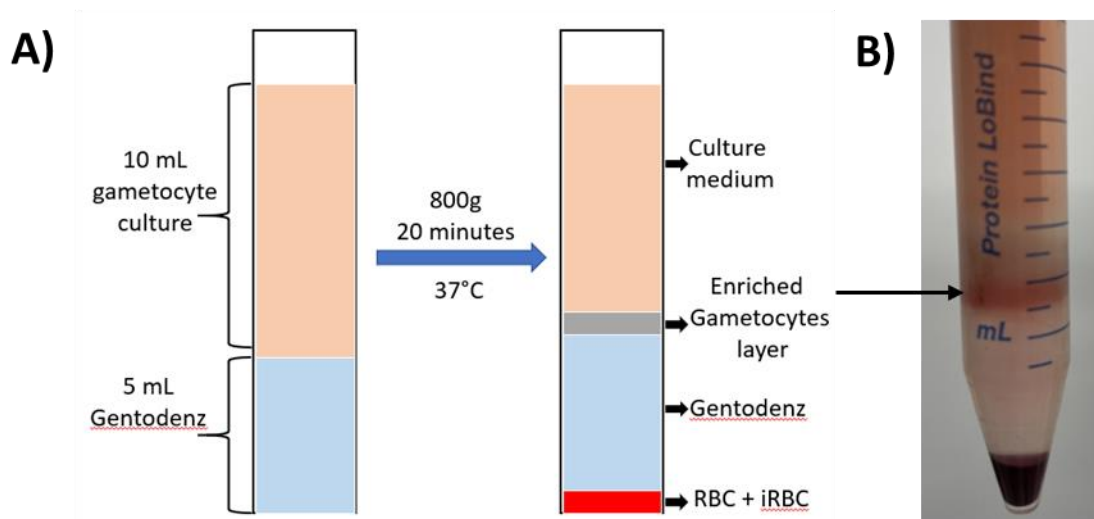


**Figure 2.14. Gametocyte purification using a Gentodenz density gradient. A)** Schematic showing the procedure for obtaining mature gametocytes using a Gentodenz density gradient. Abbreviations: RBC = red blood cells, iRBC = infected red blood cells. **B)** Image of a Gentodenz separated gametocyte culture. The enriched gametocyte layer is indicated by the black arrow.

### **2.3.4 Percoll and sorbitol purification**

To obtain tightly synchronous parasites for transfection, segmented schizonts were isolated on a 63% Percoll cushion (Rivadeneira, Wasserman and Espinal, 1983; Radfar *et al.*, 2009) and then allowed to re-invade fresh erythrocytes for 1-2 hours. Schizonts which did not rupture within the invasion window were lysed with 5% D-sorbitol (Sigma) for 15 minutes to give synchronous ring stage cultures (Lambros and Vanderberg, 1979).

### **2.3.5 Ethanol precipitation of plasmid DNA for transfection**

Plasmid DNA was ethanol precipitated with 1/10 volume 3 M sodium acetate and a minimum of 3 volumes of 100% ethanol and incubated for 30 minutes at -20 °C. Precipitated DNA was then washed in 70% ethanol and then dried in a sterile microbiology safety cabinet.

### **2.3.6 Schizont-stage transfections**

PFK11-KO parasites were generated by schizont-stage transfections. Parasites were synchronised by 2-3 rounds of Percoll/sorbitol purification. Late-stage segmented schizonts were purified on 63% Percoll cushion and transfected with 10 µg of linearized plasmid DNA using the Amaxa 4D electroporator (Lonza) the P3 Primary cell 4D Nucleofector X Kit L (Lonza) and program FP158 as previously described (Collins *et al.*, 2013). Transfected parasites were transferred into culture flasks of 10 ml gametocyte medium with 4% haematocrit. 24 hours later, the PFK11-KO transfectants were selected for using blasticidin (BSD). To obtain a pure population of PFK11-KO, cloning was carried out by plaque assay as previously described (Thomas *et al.*, 2016).

### **2.3.7 Pre-loading transfections**

The pre-loading transfection protocol was adapted from those previously described (Deitsch, Driskill and Wellems, 2001; Carrasquilla *et al.*, 2020). Briefly, 300 µl of packed fresh erythrocytes were mixed with 400 µl of plasmid DNA (100 µg per transfection) diluted in cytomix and electroporated using a BioRad Gene Pulser Xcell. Transfected erythrocytes were added to 4 ml pre-warmed culture medium and were left to recover for 30 min at 37 °C before being mixed with 500 µl of parasite culture containing 4-5% segmented schizonts. Culture medium was replaced 24 hours later. At 48 hours following transfection, the culture volume was adjusted to 10 ml and 4% haematocrit and drug selection started. ACS-ADP-mNG transfectants were selected for episomally using 2.5 nM WR99210 (gifted by the Baker and Moon labs, LSHTM), and subsequently for integration with 1000 µg/ml geneticin (G418) (Cayman Chemical.)

### 2.3.8 Mycoplasma screening

Parasite cultures were screened monthly to confirm the absence of *Mycoplasma* using an in-house PCR modified from one previously described (Hopert *et al.*, 1993).

## 2.4 Immunohistochemistry and imaging techniques

### 2.4.1 Generation of custom antibodies

A custom rat polyclonal antibody was raised to peptides from LDH2 (PF3D7\_1325200, a protein predicted to be specifically expressed in male gametocytes) by Eurogentec. The 28 Day Speedy service was used. Two rats were immunised with two peptides (both peptides immunised into both rats) which were predicted to be specific and immunogenic. A custom rabbit polyclonal antibody was also raised against PFK11 (PF3D7\_1123800) using the same service. The peptides used are shown in Table 2.3.

| Antibody        | Raised in | Peptides   |
|-----------------|-----------|--|
| $\alpha$ -LDH2  | Rat       | Peptide 1: C+NYKHETVVDENKPN-cooh<br>Peptide 2: C+HDFRKDLPKGRALDI |
| $\alpha$ -PFK11 | Rabbit    | Peptide 1: C+SKKDKNNTTDRVKKS<br>Peptide 2: CVSNEKSNNNIPYDN       |

**Table 2.3. Custom antibodies generated against LDH2 (PF3D7\_1325200) and PFK11 (PF3D7\_1123800) for the study.**

### 2.4.2 MitoTrackerRed CMXRos labelling

Gametocytes were transferred to a pre-warmed 1.5 ml tube in a 37 °C heater block and MitoTrackerRed CMXRos (Invitrogen) added to the culture at the desired concentration. For analysis of mitochondrial morphology, 200 nM was used according to the manufacturer's instructions. For analysis of mitochondrial activity, a titration of MitoTrackerRed CMXRos was performed to determine a more sensitive concentration with reduced background staining. The selected concentration was 12.5 nM. Gametocytes were incubated with MitoTrackerRed CMXRos for 25 minutes then pelleted in a warmed microcentrifuge to remove supernatant, before being washed twice with warm culture medium. Gametocytes were then resuspended in fresh medium and fixed as described below.

### 2.4.3 Fixation of gametocytes for immunofluorescence microscopy

Gametocytes for immunofluorescence assays (IFA) were fixed 1:1 with 8% paraformaldehyde (PFA) solution to give a final concentration of 4% PFA. Gametocytes were fixed for 30 minutes before 50  $\mu$ l of the fixed cell solution was added to pre-prepared polylysine-coated coverslips in 500  $\mu$ l PBS and allowed to settle overnight at 4 °C.

#### 2.4.4 Immunofluorescence analysis (IFA)

Fixed gametocytes were permeabilised with 0.1% v/v Triton X-100 and subsequently washed three times with PBS. Blocking with PBS + 10% foetal bovine serum (FBS) was carried out for 30 minutes to prevent non-specific antibody binding. 1-hour incubation was performed with primary antibodies. Washing with PBS was carried out prior to 45 minutes incubation with the secondary antibodies. A list of primary and secondary antibodies used in the study can be found in Table 2.4. Coverslips were then mounted on glass slides with DAPI-containing VectaShield (Vector Laboratories).

| <b>Primary antibodies</b>   |                  |                      |                              |
|---|------------------|----------------------|------------------------------|
| <b>Target</b>   | <b>Species</b>   | <b>Dilution used</b> | <b>Manufacturer/provider</b> |
| <b><math>\alpha</math>-LDH2</b>                                   | rat              | 1:10,000             | Custom antibody, Eurogentec  |
| <b><math>\alpha</math>-G377</b>                                   | guinea pig       | 1:10,000             | Custom antibody, Eurogentec  |
| <b><math>\alpha</math>-PFK11</b>                                  | rabbit           | 1:50,000             | Custom antibody, Eurogentec  |
| <b><math>\alpha</math>-alpha tubulin II</b>                       | mouse            | 1:500                | Sigma-Aldrich                |
| <b><math>\alpha</math>-Pfs25 coupled to Cy3</b>                   | mouse            | 1:500                | MR4                          |
| <b><math>\alpha</math>-Pfs230</b>                                 | mouse            | 1:1000               | MR4                          |
| <b>Secondary antibodies</b>                                       |                  |                      |                              |
| <b>Target</b>   | <b>Conjugate</b> | <b>Dilution used</b> | <b>Manufacturer/provider</b> |
| <b><math>\alpha</math>-rat IgG heavy light and chains (green)</b> | Alexa Fluor 488  | 1:1000               | Invitrogen Molecular Probes  |
| <b><math>\alpha</math>-rat IgG heavy light and chains (red)</b>   | Alexa Fluor 594  | 1:1000               | Invitrogen Molecular Probes  |

|  |                 |        |                             |
|--|-----------------|--------|-----------------------------|
| <b>α-mouse IgG heavy light and chains (green)</b>        | Alexa Fluor 488 | 1:1000 | Invitrogen Molecular Probes |
| <b>α-mouse IgG heavy light and chains (red)</b>          | Alexa Fluor 555 | 1:1000 | Invitrogen Molecular Probes |
| <b>α-rabbit IgG heavy light and chains (red)</b>         | Alexa Fluor 555 | 1:1000 | Invitrogen Molecular Probes |
| <b>α-guinea pig IgG heavy light and chains (far red)</b> | Alexa Fluor 647 | 1:1000 | Invitrogen Molecular Probes |

**Table 2.4. List of primary and secondary antibodies used for immunofluorescence analysis.**

Abbreviations: MR4 = The Malaria Research and Reference Reagent Resource Center.

<https://www.beiresources.org/MR4Home.aspx>

### 2.4.5 Immunofluorescence microscopy

Z-stack images of gametocytes were taken using a Nikon TiE Eclipse widefield microscope. Deconvolution was performed within the Nikon NIS Elements analysis software. Peak excitation and emission values for all fluorophores and tags used in the study are shown in Table 2.5.

| <b>Fluorophore or tag</b>    | <b>Excitation (nm)</b> | <b>Emission (nm)</b> |
|------------------------------|------------------------|----------------------|
| <b>mNeonGreen or GFP</b>     | 490                    | 525                  |
| <b>Alexa Fluor 488</b>       | 490                    | 525                  |
| <b>Alexa Fluor 555</b>       | 550                    | 580                  |
| <b>Alexa Fluor 594</b>       | 590                    | 617                  |
| <b>Alexa Fluor 647</b>       | 650                    | 671                  |
| <b>α-Pfs25-Cy3</b>           | 550                    | 570                  |
| <b>MitoTrackerRed CMXRos</b> | 590                    | 617                  |

**Table 2.5. Peak excitation and emission values for all fluorophores and tags used in the study.**

Abbreviations: nanometres

### 2.4.6 Quantitative image analysis

Images of gametocytes were processed in ICY BioImage Analysis software (ICY) (<https://icy.bioimageanalysis.org/>). Individual images of gametocytes were cropped using the Rectangle + Fast crop tools. For the morphological analysis, a region of interest (ROI) was

drawn around the perimeter of the gametocyte using the Polygon tool. ROIs around the mitochondria and nucleus were generated by thresholding using the HK-Means plugin. For analysis of mitochondrial activity, an ROI was drawn around the gametocyte and a second ROI was drawn in the cytoplasm of the gametocyte using the Rectangle tool which was used for background correction of MitoTrackerRed CMXRos fluorescence intensity. Morphological parameters (ROI statistics) and MitoTrackerRed CMXRos intensity were subsequently analysed in ICY and the data exported to Excel. Explanations of the morphological parameters used are shown in Table 2.6. The parameters were subsequently compared between the male and female groups (sex was determined using fluorescence intensity of anti-LDH2 labelling). Morphological parameters were compared between the male and female groups using a Student's t-test in Graph Pad PRISM 9. For mitochondrial activity, background corrected MitoTrackerRed CMXRos intensity was compared. As fluorescence intensity is a noisy variable, normalisation a reference group was necessary to identify there were consistent trends between males and females. As females had consistently higher readouts, the males were normalised to the female mean and the percentage reduction calculated for each replicate. However, the disadvantage of this approach is that variation in the female group becomes unavailable which precludes statistical analysis. The development of the image analysis methods used in the study, and potential improvements before publishing the data, are elaborated on in Chapter 3.

| <b>Parameter (unit)</b> | <b>Explanation</b>   |
|-------------------------|--|
| <b>Contour (px)</b>     | The perimeter (in 2D) or surface area (in 3D), expressed in pixels.  |
| <b>Interior (px)</b>    | The area (in 2D) or volume (in 3D), expressed in pixels.   |
| <b>Roundness (%)</b>    | Following the ISO 1101 standard: the normalised ratio between the radius of the minimum inscribed and largest circumscribed circles (or spheres), expressed as a percentage (100% for a circle or sphere).                               |
| <b>Elongation</b>       | A scale factor given by the ratio between the first and second ellipse diameters (the diameters (along each axis) of the best fitting ellipse (or ellipsoid)), expressed in pixels. The minimum value is 1 (for a non-elongated object). |

**Table 2.6. Morphological parameters for analysis of mitochondrial morphology in ICY BioImage Analysis Software.** Source: <https://icy.bioimageanalysis.org/plugin/roi-statistics/>

## 2.4.7 Förster resonance energy transfer (FRET) microscopy

NF54 asexual blood stage parasites were transfected with a plasmid encoding the ATeam1.03YEMK ATP nanosensor (Imamura *et al.*, 2009) using the erythrocyte pre-loading method described in section 2.3.7. Parasites expressing the sensor as an episome were selected using blasticidin. NF54-ATeam1.03YEMK gametocytes were cultured to maturity (day 14 post-seeding) and purified using a Gentodenz density gradient as previously described. Purified gametocytes were then washed twice with gametocyte medium. Both these steps are performed in a centrifuge heated to 38 °C to prevent gametocytes from activating. Samples of purified gametocytes for imaging were then washed three times with the following warm media for each of the experimental treatments: i) 'glucose' – glucose-free RPMI + 10 mM glucose + 0.1% human serum (HS), ii) 'no glucose' – glucose-free RPMI + 0.1% HS and iii) 'glucose + oligomycin A' – glucose-free RPMI + 10 mM glucose + 0.1% HS + 5 µM oligomycin A (ATP synthase inhibitor) and iv) 'no glucose + oligomycin A' – glucose-free RPMI + 0.1% HS + 5 µM oligomycin A (ATP synthase inhibitor). After the third wash in the different treatments, the gametocytes were washed in PBS or PBS-glucose immediately before imaging as the phenol red in the culture medium could potentially interfere with the fluorescence reading. If levels of background fluorescence were too high, this could prevent accurate measurement of the FRET ratio. Following washing, the pellet was resuspended in fresh, warm PBS and transferred to the surface of a pre-warmed slide and a coverslip placed on top. The slide was then transferred to the microscope stage, heated to 37 °C, ready for imaging.

FRET-based ATP imaging was carried out on a Nikon TiE widefield fluorescence microscope. Samples were excited at 435 nm and emission was measured at 430-480 nm for eCFP (donor; emission peak at 475 nm) and 500-550 nm for mVenus (acceptor, emission peak at 527 nm), using DAPI and GFP filters respectively. A 95-minute 'long' incubation was piloted first. For the 'glucose' and 'no glucose' conditions, a time lapse image was generated with images taken at 10-minute intervals over a 95-minute period. There was an initial lag of 10 minutes before the first measurement for the glucose treatment as this was the handling time for setting up for the slide and allowing the cells to settle sufficiently. Then while the first measurement for the 'glucose' treatment was made, the first 'no glucose' treatment slide was prepared for measurement. The glucose treatment was read at 10, 30, 50, 70 and 95 minutes from time 0 and the no glucose treatment at 20, 40, 60, 85 and 105 minutes. For subsequent experiments, images were taken at 1-minute intervals over a 20-minute period.

Deconvolution of time-lapse images was carried out in NIS Elements software (Version 4.0). Time-lapse images were background-corrected and subsequently split into separate images using the Extract Single Frame tool in ICY. ROIs were subsequently drawn around all the gametocytes in each separate image using the Polygon tool. Once all the images had

been processed, the ROIs were analysed in ICY, and the fluorescence intensity values of the FRET and CFP channels exported to Excel. The FRET ratio for each cell (Venus/eCFP) was calculated by dividing the mean intensity of the FRET channel (ATP bound to the sensor) by the CFP channel (ATP not bound). The mean FRET ratio for each time point was then calculated and compared between the experimental conditions.

## **2.5 Phenotyping of transgenic lines**

### **2.5.1 Asexual growth assay**

Asexual growth of WT and transgenic parasite lines was assessed by seeding WT and PFK11-KO parasites at 0.1% and counting parasitaemia in Giemsa-stained blood films for 5 days or until the parasitaemia became too high to count by eye.

### **2.5.2 Quantification of gametocytaemia**

To quantify gametocytaemia, WT and PFK11-KO gametocyte cultures were added 1:1 to gametocyte medium containing the PKG inhibitor ML10 (1  $\mu$ M) to prevent premature activation of gametocytes. The number of gametocytes and erythrocytes per ml were counted using a Neubauer haemocytometer. Gametocytaemia was calculated by the following formula: % gametocytaemia = (Number of gametocytes per ml / number of red blood cells per ml) x 100.

### **2.5.3 Quantification of gametogenesis**

To quantify gamete formation, WT and PFK11-KO gametocytes were pelleted and resuspended in gametocyte medium containing 100  $\mu$ M xanthurenic acid (Sigma-Aldrich) to induce gametogenesis. A sample of activated culture was transferred to a Neubauer haemocytometer and the number of exflagellation centres and red blood cells per ml. The % exflagellation was calculated by the following formula = (number of exflagellation centres per ml/ number of erythrocytes per ml) x 100. The remaining activated culture was left for 24 hours at room temperature and then labelled for 30 minutes with an anti-Pfs25-Cy3 antibody. Images were taken on the DIC and red channels of each well. Female gamete activation was calculated as: % female activation = (number of Pfs25+ve cells/number of red blood cells) x 100.

### **2.5.4 Mosquito feeding assays**

Mosquito feeding assays were adapted from protocols previously described (Churcher *et al.*, 2012; Miura *et al.*, 2013; Witmer *et al.*, 2018). WT and transgenic gametocytes were cultured to maturity and fed to female *Anopheles stephensi* mosquitoes. All culture manipulations were performed at 37 °C to prevent activation of the gametocytes. 10 ml gametocyte cultures were mixed with 200-300 µl of pre-warmed fresh human erythrocytes (RBC) and pelleted using a heated centrifuge at 500 x g for 5 minutes at 38 °C. The supernatant was removed, and the RBC/gametocyte pellet was mixed with pre-warmed human serum in a ratio of 2:3. Mosquitoes were fed using a 3D-printed feeder attached to a 38 °C circulating water bath chained in a loop with silicone tubing (total circulation loop = ~ 50 cm) (Witmer *et al.*, 2018). The feeders were pre-warmed and covered with Parafilm® stretched in both directions to make a thin membrane (Witmer *et al.*, 2018). The RBC/gametocyte/serum mixture was added into the membrane feeder and mosquitoes allowed to feed for 20–30 min at ambient room temperature of 21 °C. After feeding, mosquitoes were maintained at 26 °C and 80% humidity.

A proportion of mosquito midguts were dissected 24 hours post-feeding and labelled with an anti-Pfs25-Cy3 conjugated antibody (1:500 dilution). The presence/absence of Pfs25+ve ookinetes was confirmed in the WT and transgenic groups by live microscopy using a Nikon TiE widefield microscope. Midguts were dissected on day 7 post-feeding and stained in 0.1% mercurochrome in PBS for 15 minutes to identify oocysts. Oocysts per midgut were counted at 20x magnification using a light microscope. Oocyst production was quantified by two measures i) oocyst prevalence – whether oocysts were present in the mosquito midgut or not (% mosquitoes infected) and ii) oocyst intensity – the mean number of oocysts per midgut. Salivary glands were dissected from a final group of mosquitoes 16 days post-feeding to confirm the presence/absence of sporozoites by light microscopy (20x magnification). Sporozoites were imaged live using a Nikon TiE widefield microscope (100x magnification.)

## **2.6 Parasite assays**

### **2.6.1 MitoTracker drug assay**

Mature gametocyte cultures were incubated at 37 °C for 24 hours in gametocyte medium containing DMSO (drug vehicle control) or the following mETC inhibitors: i) atovaquone (ATQ) (concentrations tested: 1 nM, 10 nM, 100 nM, 1 µM and 10 µM), ii) ELQ-300 (concentrations tested: 1 nM, 10 nM, 100 nM, 1 µM and 10 µM), iii) 10 µM DSM-265 and iv) 50 µM oligomycin A. Gametocytes were subsequently labelled with 12.5 nM MitoTrackerRed CMXRos and co-labelled with the anti-LDH2 antibody. Quantitative image analysis of

MitoTrackerRed CMXRos labelling in untreated and treated male and female gametocytes was then carried out as described (2.4.6.) As previously mentioned, as fluorescence intensity is noisy, normalisation to a reference group was necessary. In this case, the female DMSO-treated group, which generally had the highest read outs, was used to compare all others to. However, the disadvantage of this approach is that variation in this group becomes unavailable which prevents statistical analyses.

### **2.6.2 Dual gamete formation assay (DGFA)**

Dual gamete formation assays were performed as previously described (Delves *et al.*, 2016). Briefly, exflagellation was first quantified by haemocytometer and % exflagellation calculated as: exflagellation centres per ml/erythrocytes per ml x 100. A cut-off of 0.2% or greater exflagellation was chosen. Triplicate 384-well assay plates were then prepared using an HP Tecan D300 digital dispenser (compound printer). A concentration range of 3 nM – 25 µM was printed for each of the four drugs (atovaquone, ELQ-300, DSM-265 and oligomycin A) as well as a column with the negative control (DMSO) and positive control (20 µM Gentian Violet.) Gametocytes were diluted to a 25 ml gametocyte inoculum at 12.5 million RBCs/ml per plate. Gametocytes were added to pre-warmed assay plates and incubated at 37 °C under malaria gas. Two incubation lengths were performed, 24 hours and 1 hour. Following incubation, gametocytes were activated with 10 µl/well ookinete medium containing an anti-Pfs25-Cy3 antibody at 1:500 dilution in PBS. The plate was then incubated at 4 °C for 4 minutes and subsequently at 28 °C for 5 minutes. The plate was then transferred to a Nikon TiE widefield microscope for readout of exflagellation 20 minutes after induction. Exflagellation was quantified using an automated JOBS algorithm in NIS Elements software which images each well sequentially on the 4x objective with a 1.5x zoom (effectively 6x) and records a 10-frame time-lapse image over 1 second. Plates were then incubated overnight in the dark at room temperature and then read with another automated JOBS algorithm which images each well sequentially at 6x on the tetramethylrhodamine (TRITC) channel. Exflagellation centres and Pfs25+ve cells (female gametes) were quantified using automated analysis scripts in the Icy Bioimage Analysis Program (<https://icy.bioimageanalysis.org/>). The % inhibition was calculated by comparing the inhibitory activity of the mETC inhibitors with that of DMSO and Gentian Violet control wells. Dose-response curves and IC<sub>50</sub> values were analysed by fitting a curve using a nonlinear regression in GraphPad Prism 9.

### **2.6.4 Exflagellation IFAs – effect of glucose availability**

Mature gametocytes were incubated for 1 hour and for 24 hours under the following conditions: i) glucose - medium containing 11 mM glucose + 10% human serum (~1.1 mM glucose), ii) low glucose – glucose-free medium + 10% human serum (~1.1 mM glucose) and iii) low glucose + 2-deoxyglucose (2DG) - glucose-free medium + 10% human serum (~1.1 mM glucose) + 11 mM 2DG. 2DG is an analog of glucose which has the 2-hydroxyl group replaced by hydrogen, which is taken up by the glucose transporters of cells. 2DG is converted to 2-deoxyglucose-6-phosphate (2DG-6P) by hexokinase, but 2DG-6P cannot be used by phosphoglucose isomerase in the next step of glycolysis (Schmidt and O'Donnell, 2021). Therefore, 2DG is a competitive inhibitor of glucose and so arrests glycolysis. Gametocytes were then activated in room temperature medium containing these conditions plus 100  $\mu$ M xanthurenic acid (condition-matched ookinete medium) to trigger exflagellation. Samples were fixed for IFAs after 20 minutes and labelled with DAPI and an anti-alpha tubulin II antibody to visualise exflagellation centres. Exflagellation centres were counted using an automated script in ICY BioImage Analysis Software and the data exported to Excel.

### **2.6.5 Plate-based exflagellation and female activation assays**

Mature gametocytes were transferred to pre-warmed 1.5 ml Eppendorf tubes (100  $\mu$ l gametocyte culture per tube) and washed three times with 200  $\mu$ l of the following media: i) 11 mM glucose + 0.1% human serum (HS) (at this concentration, HS provides ~0.1 mM glucose) ii) No glucose + 0.1% HS and iii) 11 mM glucose + 0.1% HS + 5  $\mu$ M oligomycin A. 100  $\mu$ l of each condition were transferred to 96 well plates in triplicate and activated with 50  $\mu$ l of condition-matched ookinete medium. Following 20 minutes incubation at room temperature, time lapse images of the wells (20 frames over 2 seconds) were taken using a Nikon TiE widefield microscope. An automated script in the ICY Bioimage Analysis Program was subsequently used to quantify the number of exflagellation centres in each well. The remaining activated gametocyte culture in the Eppendorf was incubated for 24 hours at room temperature and labelled with an anti-Pfs25-Cy3 antibody for 30 minutes the following day. Female gamete activation in each condition was then quantified as described (2.5.3).

### **2.6.6 Serum and glucose titrations**

Serum and glucose titrations were performed to determine the minimum concentrations for the assay in 2.6.5, For the serum titration, mature gametocytes were washed three times in standard (11 mM glucose) and glucose-free RPMI containing 10%, 2%, 1% and 0.1% HS. For the glucose titration, they were washed with glucose-free RPMI with 0.1% HS and the following concentrations of glucose added back: 1.11, 0.56, 0.29, 0.15, 0.08, 0.05, 0.03, 0

mM. In both cases, exflagellation was triggered with condition-matched ookinete medium then quantified as described above (2.6.4.)

# Chapter 3 Investigation of mitochondrial structure and function in male and female *P. falciparum* gametocytes

## 3.1 Introduction

Blood stage parasites that have committed to develop as gametocytes, upregulate their tricarboxylic acid (TCA) cycle (MacRae *et al.*, 2013; Ke *et al.*, 2015), a shift which coincides with the enlargement of the mitochondrion (Okamoto *et al.*, 2009) into a complex, cristate structure (Krungkrai, Prapunwattana and Krungkrai, 2000b; Evers *et al.*, 2021). The importance of this to the gametocyte stage is unknown, but mitochondrial respiration is essential in the transmission stages (MacRae *et al.*, 2013; Ke *et al.*, 2015; Srivastava *et al.*, 2016).

Interestingly, both male and female gametocytes enlarge their mitochondrion in this way, but only the female mitochondrion is retained in the zygote (Okamoto *et al.*, 2009). Male gametocytes shed theirs prior to becoming motile gametes which pass on only their DNA (Okamoto *et al.*, 2009). Lacking mitochondria, male gametes are powered solely by glycolysis (Talman *et al.*, 2014). Mitochondrial respiration can result in the production of harmful reactive oxygen species (ROS) (Oliveira and Oliveira, 2002). Increased mitochondrial respiration in gametocytes could result in increased production of ROS which could potentially affect the longevity of circulating gametocytes. Therefore, why does the male gametocyte invest in growing a large complex organelle only to discard it at the next developmental stage, particularly one that may damage the gametocyte during its long development in the human host? Despite the different fates of male and female gametocytes during transmission, it has not been investigated whether they differ in their mitochondrial energy metabolism.

The first aim of this work was to compare the mitochondrial morphology of male and female gametocytes, and then investigate any functional differences. A prerequisite for this was to develop a method to distinguish between male and female gametocytes. The mitochondria of gametocytes can be labelled using commercial dyes, for example MitoTrackerRed CMXRos (Gebru, Mordmüller and Held, 2014; Hliscs *et al.*, 2015; Plouffe *et al.*, 2016). However, distinguishing male and female gametocytes morphologically is challenging.

I adopted an immunofluorescence-based approach using sex-specific antibodies to allow easy classification of gametocytes into male and female groups in immunofluorescence assay (IFA) images. These sex-specific antibodies could be used in combination with functional mitochondrial labelling and image analysis used to compare morphological

parameters and intensity of MitoTrackerRed CMXRos labelling (as a readout of activity) between the sexes. However, previous studies have highlighted that commonly used male and female gametocyte markers can be ambiguous.

For example, Schwank and colleagues used an IFA-based approach using antibodies to G377 and alpha tubulin II to determine if these markers could be used to calculate sex ratios of gametocytes *in vitro* (Schwank, Sutherland and Drakeley, 2010). G377 (Alano *et al.*, 1995; Severini *et al.*, 1999) and alpha tubulin II (Rawlings *et al.*, 1992) were thought of as two established biomarkers for female and male gametocytes respectively. However, while alpha tubulin II was differentially expressed in mature male and female gametocytes, they also found it showed promiscuous expression in all stage I-IV gametocytes. It was also observed that some late-stage gametocytes which reacted with anti-G377 antibodies also reacted with anti-alpha tubulin II (Schwank, Sutherland and Drakeley, 2010). G377 has been shown to be specific to female osmiophilic bodies which are distinct from the male secretory organelles (termed male osmiophilic bodies or MOBs) in *P. berghei* gametocytes (Olivieri *et al.*, 2015). This suggests that G377 is female-specific and anti-alpha tubulin II can be found in females, as opposed to G377 being found in osmiophilic bodies in general and these being more abundant in females. New biomarkers which allow accurate distinction of gametocyte sex are needed to investigate sex-specific biology in *P. falciparum* gametocytes.

## **3.2 Results**

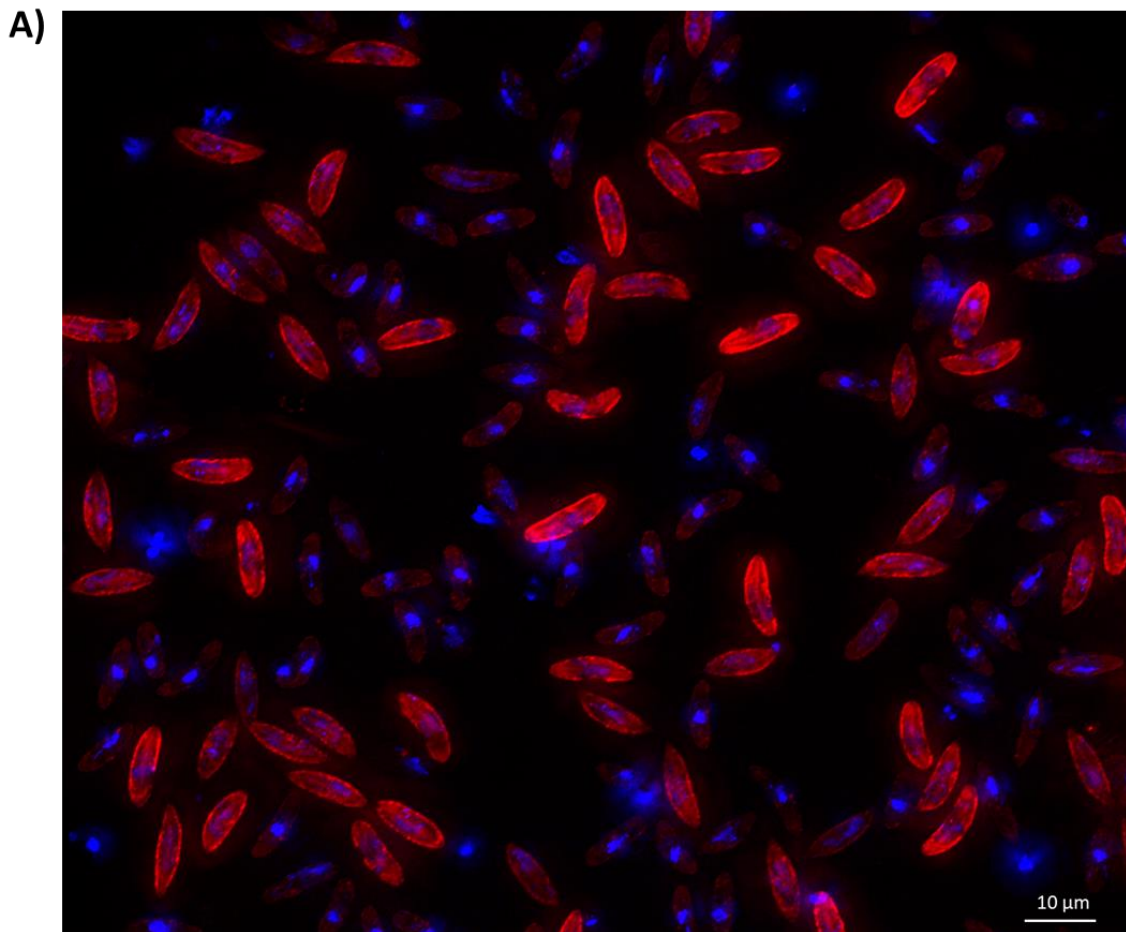
### **3.2.1 Development of a specific antibody marker to discriminate between male and female gametocytes**

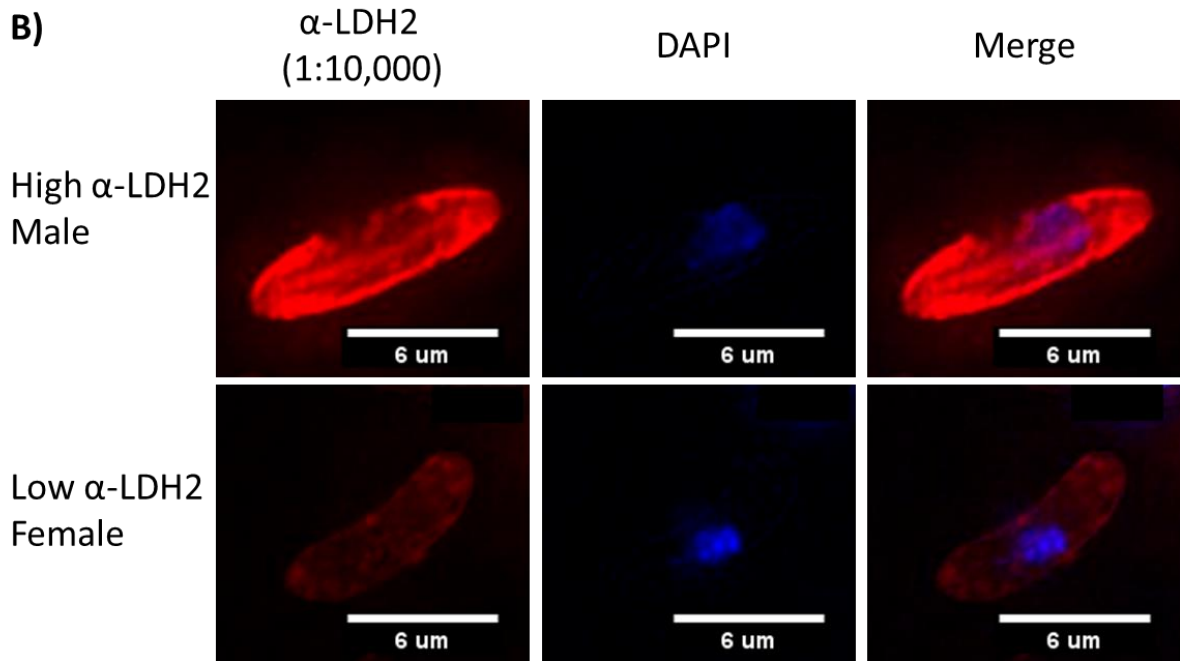
To reliably distinguish the sexes, robust new biomarkers which can be used to accurately distinguish male and female gametocytes in IFAs were needed. To meet this need, a rat polyclonal antibody was raised to peptides from PF3D7\_1325200 (LDH2) that were predicted to be specific and immunogenic. LDH2 is predicted to be a putative lactate or malate dehydrogenase (Evers *et al.*, 2021) and is reportedly upregulated in, or specific to, male gametocytes (Lasonder *et al.*, 2016). Previous work using antibodies to the *P. falciparum* LDH2 and the equivalent gene in *P. berghei* (PBANKA\_1340400) has shown that this protein is expressed in male gametocytes (Delves *et al.*, 2017; Grasso *et al.*, 2020, 2022).

#### **Cellular and stage expression of LDH2 by immunofluorescence**

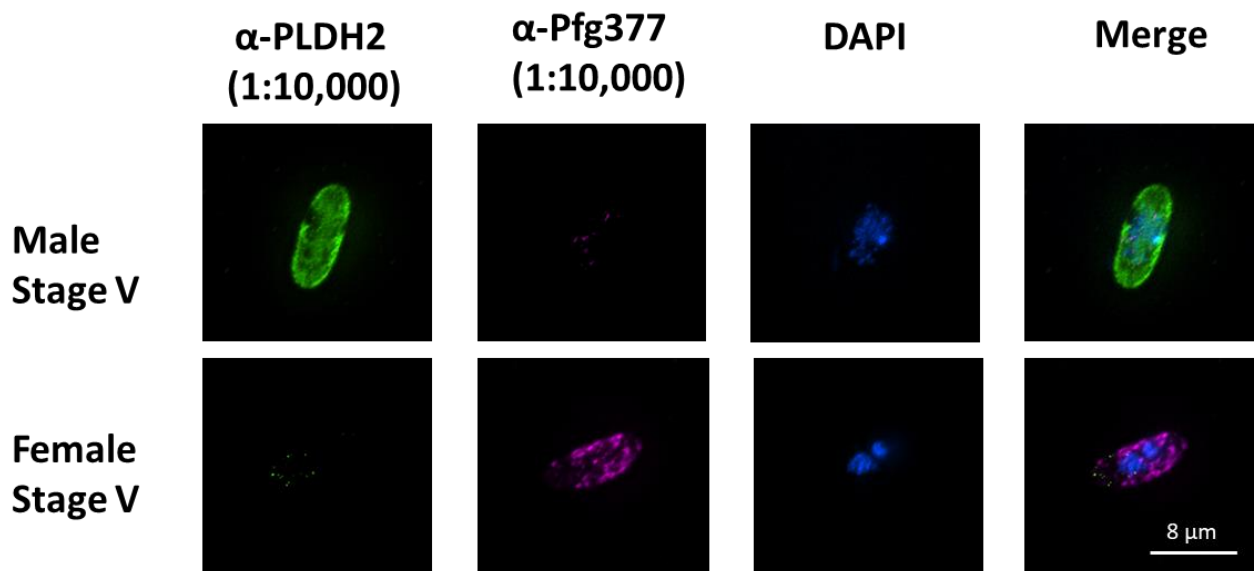
IFAs of mature stage V gametocytes showed that the LDH2 antibody selectively labels a subpopulation of gametocytes (Figure 3.1). The intensely stained population showed more diffuse DAPI staining which took up a greater volume of the cell. In contrast, the faint

population showed a smaller, compact nucleus with bright DAPI staining. This is consistent with published data which reports that female gametocytes have a smaller, less complex nucleus with a nucleolus, whereas males have a more complex nuclear shape and much higher nuclear volume (Evers *et al.*, 2023). The bright population also did not co-label with an antibody to G377 (Figure 3.2), a protein found only in the osmiophilic bodies of female gametocytes (Alano *et al.*, 1995; Severini *et al.*, 1999). This strongly suggests that anti-LDH2 accurately discriminates against male and female gametocytes.





**Figure 3.1. Anti-LDH2 staining in stage V gametocytes.** **A)** Immunofluorescence assay (IFA) image showing purified gametocytes labelled with DAPI (blue) and the anti-LDH2 antibody (red). **B)** Enlarged view of differentially labelled male and female gametocytes with anti-LDH2 (red). DNA is labelled with DAPI (blue). The female (low anti-LDH2) showed a smaller, denser nucleus whereas the DAPI staining in the male (high anti-LDH2) is more diffuse.



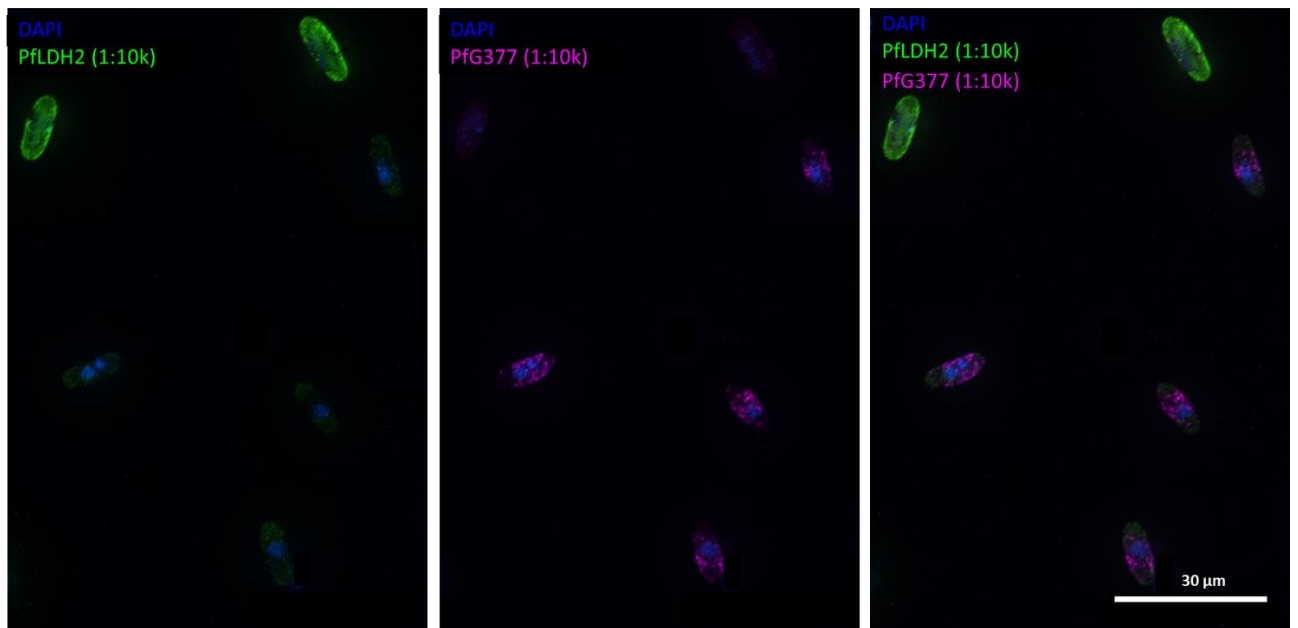
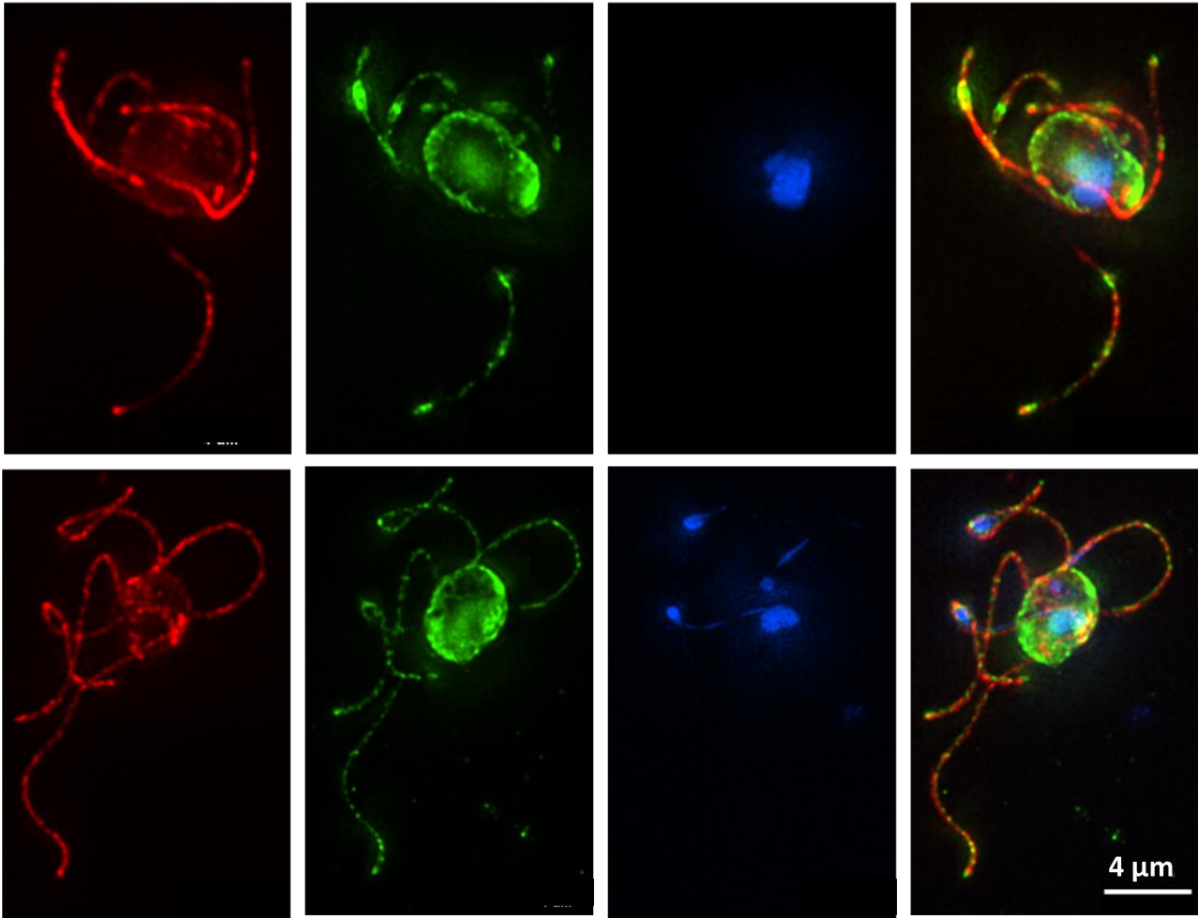


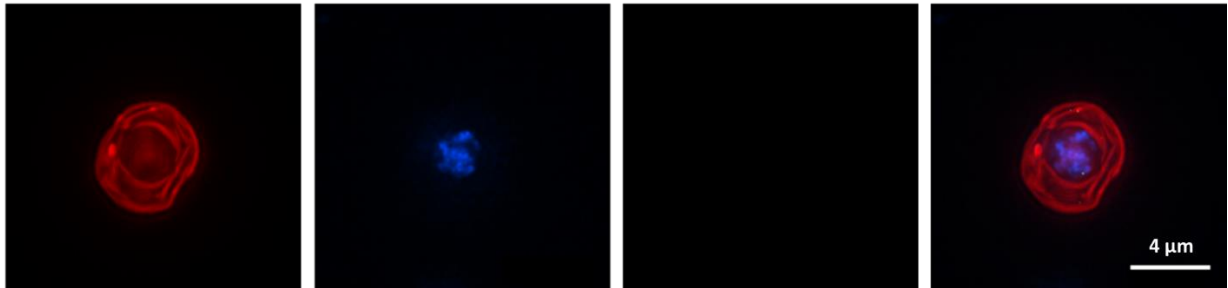
**Figure 3.2. Co-staining of stage V gametocytes with anti-LDH2 and anti-G377.** Top) IFA image of direct comparison of male and female gametocyte. Bottom) IFA image showing multiple males and females. DAPI is shown in blue, anti-LDH2 is in green and anti-G377 is in pink.

To further confirm the male-specific expression of LDH2, labelling in activated gametes was investigated. Exflagellating male gametocytes were fixed and co-stained with anti-LDH2 (visualised in green) and anti-alpha tubulin II (visualised in red) (Figure 3.3 A). Intense LDH2 staining was observed in exflagellating male gametocytes. Both LDH2 and alpha tubulin II are located on the flagella of the emerging male gametes, but their individual labelling patterns do not co-localise. Activated female gametes were labelled with an antibody to Pfs25 (red), a protein expressed on the surface of female gametes, zygotes and ookinetes (Farrance *et al.*, 2011), and co-labelled with anti-LDH2 (green) (Figure 3.3 B and C). Anti-LDH2 labelling was absent from all activated female gametes and retorts, an intermediate stage between a fertilised zygote and an ookinete, which further supports that the unlabelled subpopulation of gametocytes are female. These data show LDH2 is specific to male gametocytes and an anti-LDH2 antibody can be used to accurately distinguish male and female gametocytes in immunofluorescence assays (IFAs).

A) Alpha tubulin II (1:500)      LDH2 (1:10,000)      DAPI      Merge



B) α-Pfs25-Cy3      DAPI      LDH2      Merge



c)

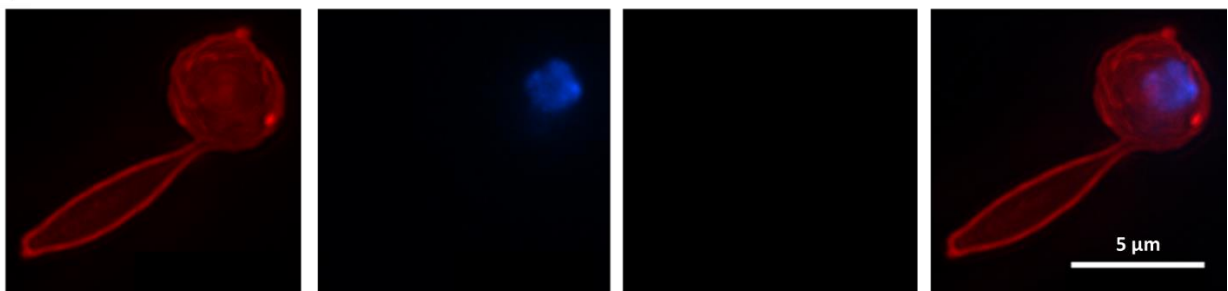


**Figure 3.3. Anti-LDH2 labelling post-activation. A)** Exflagellating male gametocytes expressing LDH2 as visualised by labelling with the anti-LDH2 antibody in green, alpha tubulin II in red and DAPI in blue. **B)** Activated female gamete labelled with an anti-Pfs25 antibody (red), DAPI (blue) and anti-LDH2 (green.) **C)** IFA showing a retort (fertilised female) with the same markers.

Having established the sex-specific expression of LDH2 in mature gametocytes and gametes, I then explored its pattern of expression during gametocyte development. Gametocytes of different stages of development were labelled with anti-LDH2 co-stained with anti-Pfs230. Pfs230 is a gametocyte surface protein localised to the plasma membrane which is a major antigen expressed on the surface of gametes during emergence (Lobo and Kumar, 1998; Brooks and Williamson, 2000; Eksi *et al.*, 2002). The protein is expressed in both gametocyte sexes (Eksi and Williamson, 2002).

Anti-Pfs230 staining becomes clearly visible in stage II gametocytes and is clearly visible throughout gametocyte development to mature stage V gametocytes (Figure 3.4 A). This allowed gametocytes to be staged and to determine the stage of development at which LDH2 labelling becomes visible. Anti-LDH2 staining becomes visible in gametocytes at stage IV of development. There were noticeably stage IVs which were differentially stained with anti-LDH2 which could reflect sex-specific expression. Anti-LDH2 was found to give superior identification of male gametocytes compared to previous markers and thus was adopted for subsequent experiments. From stage V, anti-LDH2 is clearly differential between male and female gametocytes.

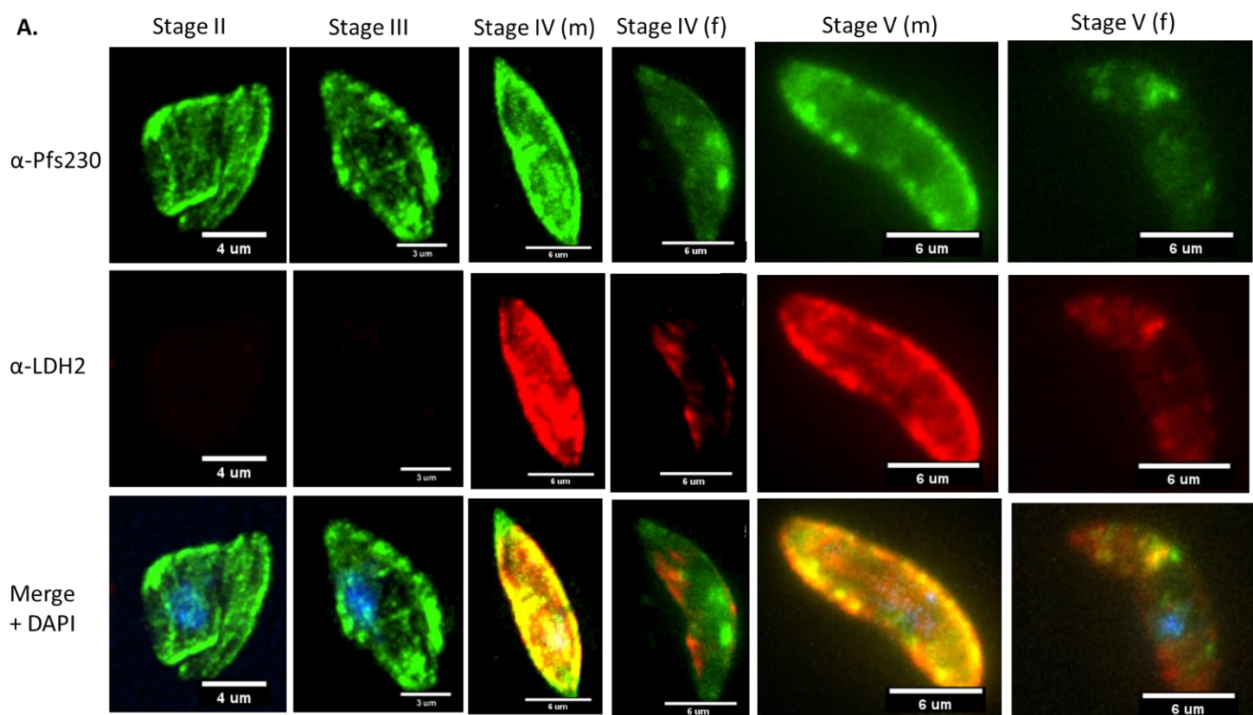


**Figure 3.4. Anti-LDH2 labelling across gametocyte development.** *P. falciparum* gametocytes across gametocyte development co-stained with anti-Pfs230 (green) and anti-LDH2 (red) showing Pfs230 is expressed in all stages of gametocytes whereas LDH2 begins being expressed from stage IV.

In summary, LDH2 is a robust marker for male gametocytes, suitable for distinguishing male and female gametocytes visually in IFAs.

### **3.2.2 Development of and validation of image analysis methodology**

The characterisation of the anti-LDH2 antibody established that it is as a suitable biomarker for distinguishing male and female gametocytes. The next step was to develop a reproducible image analysis method to compare mitochondrial morphology and activity between male and female gametocytes.

The proposed method was to analyse immunofluorescence images of mature stage V gametocytes co-labelled with the mitochondrial label MitoTrackerRed CMXRos (fluoresces red) for visualisation of mitochondria and the anti-LDH2 antibody (with a green secondary antibody) to distinguish gametocyte sex. MitoTrackerRed CMXRos labelling would allow measurement of mitochondrial size and shape and – as uptake of MitoTrackerRed is dependent on the mitochondrial membrane potential (Jogdand *et al.*, 2012) – the intensity of red fluorescence intensity could be used as a readout of mitochondrial activity.

An image analysis approach was chosen instead of flow cytometry as flow cytometry would only allow us to capture the overall MitoTracker fluorescence of the male and female groups but would not distinguish between fluorescence from the mitochondria itself and cytoplasmic background. Whereas with image analysis, a region of interest could be drawn around the mitochondria to analyse the mitochondria specifically. In addition, it would allow the exclusion of any immature (non-stage V) gametocytes from the analysis.

Several mitochondrial dyes have been developed, but MitoTrackerRed CMXRos was chosen for the following reasons. Uptake of this dye into the mitochondrion is dependent on the mitochondrial membrane potential so MitoTrackerRed CMXRos can be used to distinguish live, compromised and dead parasites (Jogdand *et al.*, 2012). Therefore, the fluorescence intensity can be used as an indicator of how active the mitochondria are, and this could be compared between males and females. In addition, as it was hoped that this image analysis methodology could be used to compare the susceptibility of male and female gametocytes to mitochondria-targeting drugs, being able to distinguish parasites with a collapsed mitochondrial membrane potential was essential. MitoTracker Red CMXRos has been successfully used for gametocyte viability assays previously (Hliscs *et al.*, 2015; Plouffe *et*

*al.*, 2016). Other mitochondrial stains, such as rhodamine-based dyes, have previously been shown to impact mitochondrial respiration and their uptake is not entirely dependent on membrane potential (Mai and Allison, 1983; Modica-Napolitano *et al.*, 1984; Jogdand *et al.*, 2012). This makes them unsuitable for detecting potentially subtle differences in the mitochondrial energy metabolism of males and females. Other advantages of MitoTracker Red CMXRos include that it is intrinsically fluorescent, does not require reduction or oxidation for fluorescence and is well retained after fixation so it can be used for fluorescence microscopy as well as flow cytometry (Jogdand *et al.*, 2012).

Test images of gametocytes taken on a widefield fluorescence microscope (Figure 3.5) and a lattice light sheet microscope (Figure 3.6) showed that the anti-LDH2 antibody could be used in the combination with MitoTrackerRed CMXRos to visualise the mitochondrial network. The lattice SIM<sup>2</sup> image in Figure 3.6 shows the typical multi-lobed morphology of gametocyte mitochondria. MitoTrackerRed CMXRos will be referred to as MitoTracker from here onwards.

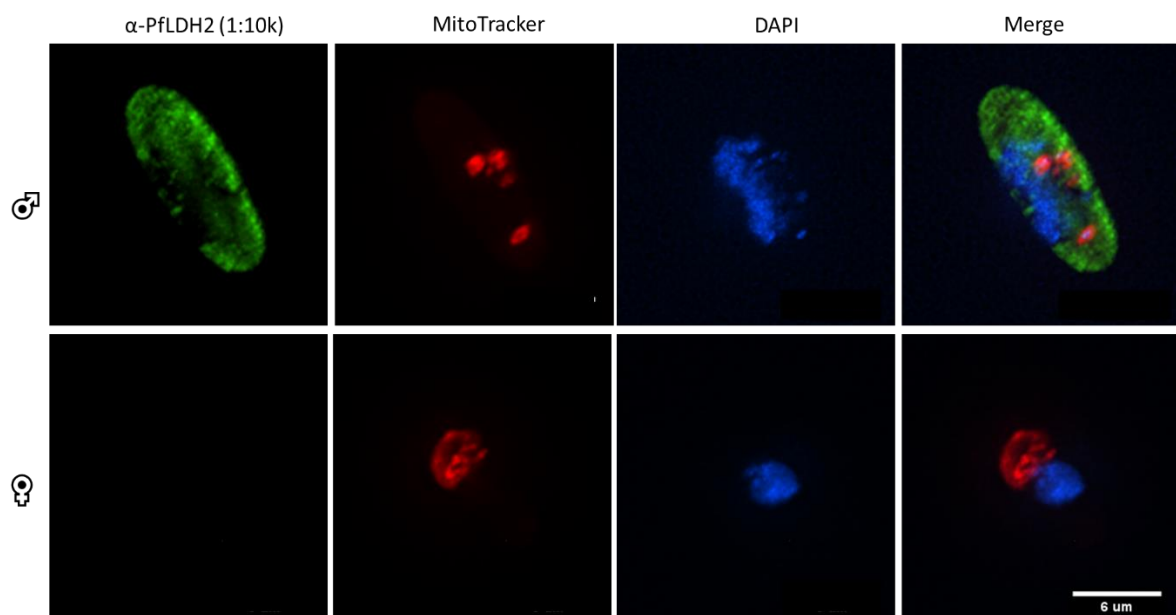


**Figure 3.5. Anti-LDH2 and MitoTracker can be used in combination in IFAs.** IFA images of stage V male (top) and female (bottom) gametocytes co-labelled with anti-LDH2 (green), DAPI (blue) and MitoTracker (red). Images taken on a Nikon TiE widefield fluorescence microscope.

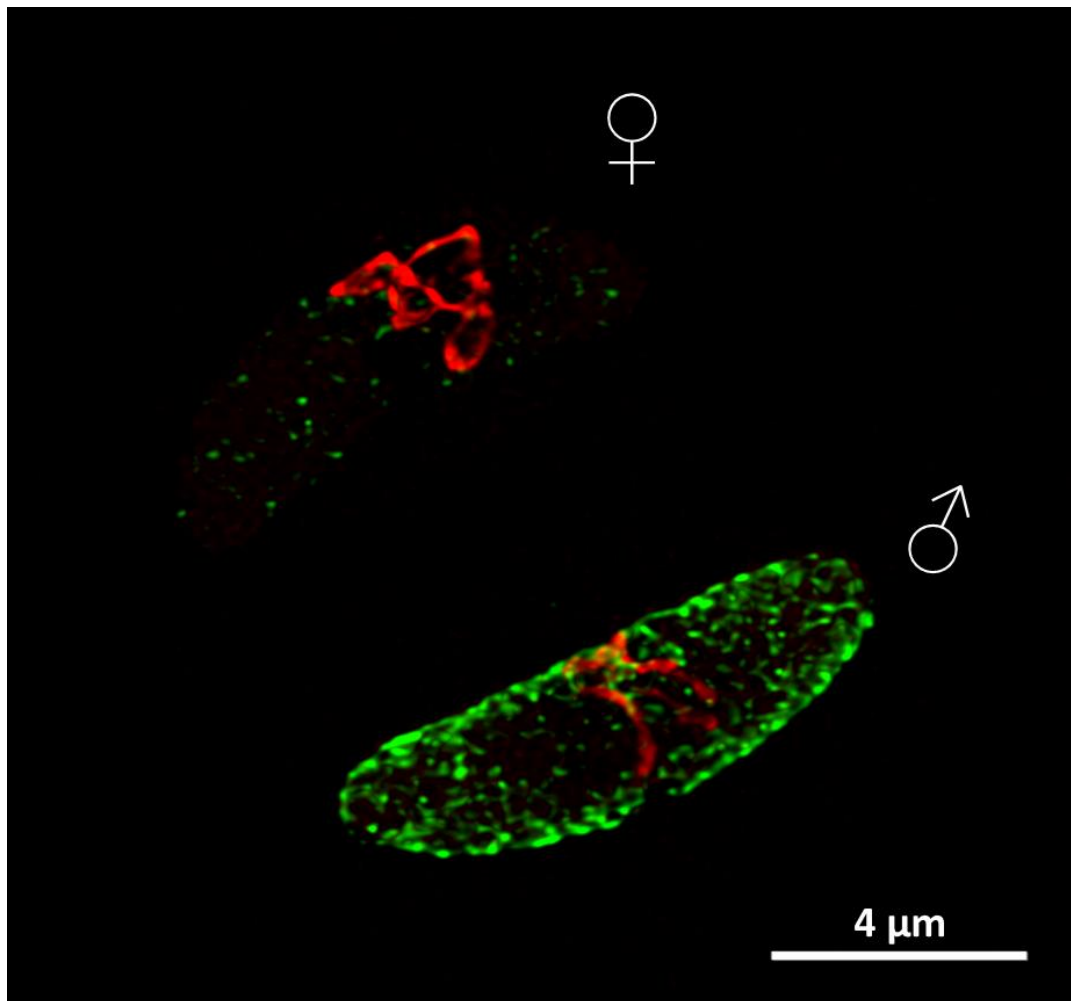


**Figure 3.6. Lattice SIM-squared image showing a 3D reconstruction of a male and a female gametocyte.** Anti-LDH2 is shown in green and MitoTracker in red. Image taken on an Elyra 7 lattice light sheet microscope as part of a demo session. This microscope is not routinely available at LSHTM.

The steps of the image analysis method were as follows. A schematic showing an overview of the method is shown in Figure 3.9.

### **Step 1: Preparation of gametocytes**

Gametocytes for image analysis were cultured to maturity and exflagellation tested to confirm the gametocytes were alive and functional.

By day 14 post-seeding, most of the gametocytes remaining in the culture were mature stage V gametocytes. This ensured the mitochondria of mature male and female gametocytes were being compared rather than immature stages. As mitochondrial activity was being compared, it was important to ensure healthy cells were being measured. To ensure optimal mitochondrial labelling, an incubation time of 25 minutes and working

concentration of 200 nM of MitoTrackerRed CMXRos was chosen in accordance with the manufacturer's instructions, with the view that concentration or incubation length could be adjusted if staining was found to be too faint or oversaturated. PFA fixation of gametocytes in solution was chosen over fixation of blood smears as the gametocyte morphology is better preserved. Gametocytes were then co-labelled with anti-LDH2 to distinguish sex and DAPI to label the nucleus. Although the aim was to compare male and female mitochondria, the nucleus was included as a control to validate the image analysis methodology, as differences between male and female gametocyte nuclei are well-characterised. Therefore, if the image analysis was able to detect known differences between male and female nuclei, this indicates that it should be able to detect differences between male and female mitochondria if present.

## **Step 2: Imaging and image processing**

Immunofluorescence images of gametocytes were taken on a widefield fluorescence microscope. The widefield microscope was chosen over confocal microscopy as resolution needed to be balanced with speed of image capture, and confocal microscopy is much slower to capture the images. Both methods were tested, and it was concluded that widefield fluorescence microscopy (with image deconvolution) was sufficient to visualise the mitochondrial structure and allowed the capture of many more images of gametocytes within the same time frame.

Gametocytes were imaged as z-stacks (n= typically 30 to 50 slices) to capture the entire multilobed mitochondrial structure. Initially, it was proposed that 3D reconstructions of the mitochondria could be generated to allow measurement of mitochondrial structure in detail, but there was not sufficient resolution for this on microscopes routinely available at LSHTM.

Images were subsequently processed on NIS Elements software. Images were deconvolved to increase the signal-to-noise ratio and clarify the image. Maximum intensity projections were then generated from the deconvolved z-stacks. This creates a 2D image where only the pixels with the highest intensity values of the Z-stack are displayed in the image, which clarifies the image and makes it easy to draw accurate regions of interest for analysis. All the images are processed consistently to provide a fair comparison within a given experiment.

The next step was to draw regions of interest (ROIs) around the mitochondria and nuclei so that the size, shape, and fluorescence intensity could be analysed. Images of individual gametocytes were cropped in ICY BioImage Analysis software (ICY) and ROIs drawn around the perimeter of the whole gametocyte, the nucleus, and the mitochondria. The

whole gametocyte ROIs were drawn manually using the Polygon tool as this was found to be more accurate than attempts to automate this step (Figure 3.7 A + B). The mitochondrial and nuclear ROIs were drawn by thresholding using the HK-Means plugin and could be visualised on the images as red and blue shaded areas respectively (examples are shown in Figure 3.7 C). Images were checked to confirm that the ROIs generated using this method were fair representations of the mitochondrial and nuclear morphology.

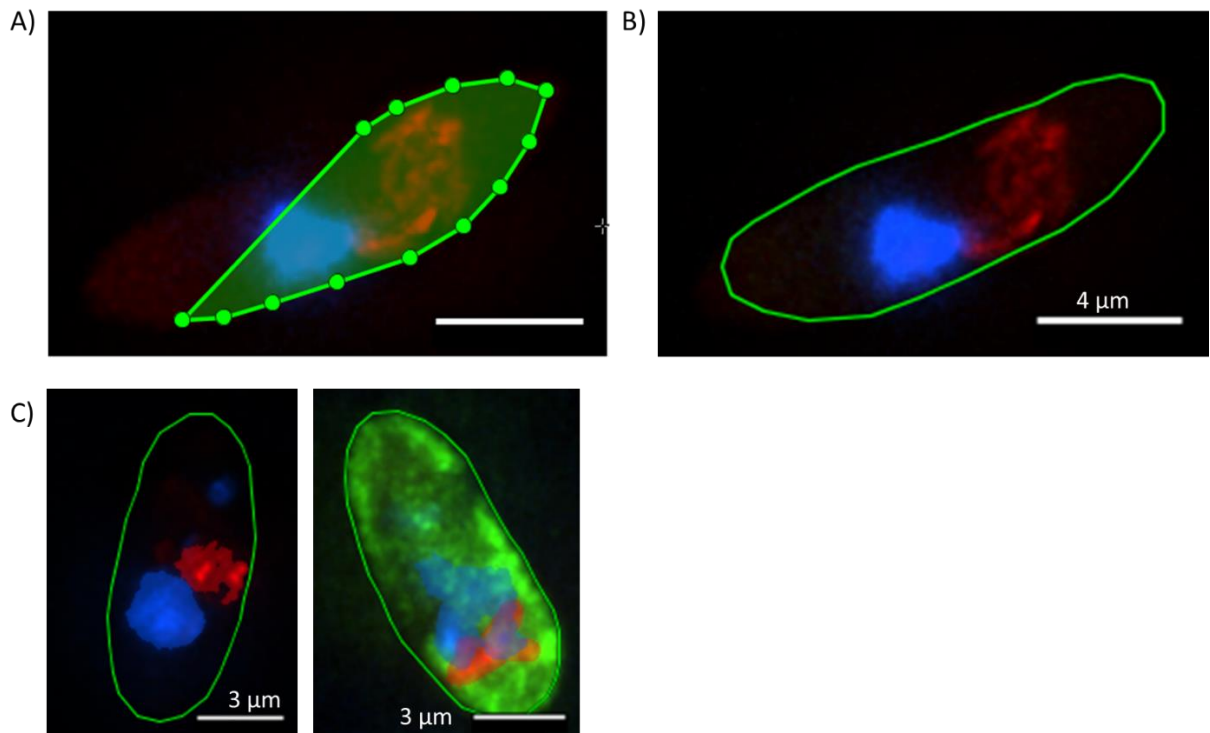


**Figure 3.7. Schematic showing the process of drawing regions of interest (ROIs) for the image analysis. A)** Whole gametocyte (GCT) region of interest (ROI) being drawn around a female gametocyte in ICY BioImage Analysis software using the Polygon tool. **B)** Finished whole GCT ROI around the same female gametocyte. **C)** An example of a male and female gametocyte with the finished whole GCT ROIs around the perimeter of the cells and the mitochondrial (red) and nuclear (blue) ROIs as selected by the thresholding tool.

### Step 3: Image analysis

Once all the ROIs had been drawn, a script was used to analyse all the ROIs and export the data to Microsoft Excel for analysis. Gametocytes were then assigned as either male or female based on anti-LDH2 staining (mean fluorescence intensity of the green channel). Once each cell was annotated as male or female, morphological parameters, and fluorescence intensity of MitoTrackerRed CMXRos (red channel) could be compared between the groups.

Definitions of all parameters used are available at <https://icy.bioimageanalysis.org/plugin/roi-statistics/>. Illustrations are shown in Figure 3.8. Contour and interior were the perimeter and area of the ROI respectively, expressed in pixels. This would allow comparison of the size of the mitochondria between the sexes. Roundness is a measure of how round the ROI is, defined as the normalised ratio between the radius of the minimum inscribed and largest circumscribed circles i.e. the maximum and minimum sizes for circles (or spheres for 3D shapes) that are just sufficient to fit inside and to enclose the shape (<https://www.iso.org/obp/ui/#iso:std:iso:12181:-1:ed-1:v1:en>). This value is expressed as a percentage (100% for a circle or sphere). Elongation is a measure of how elongated an object is, defined as the ratio between the first and second ellipse diameters. These are the diameters along each axis of the best fitting ellipse, expressed in pixels. The minimum value is 1, for a non-elongated object.

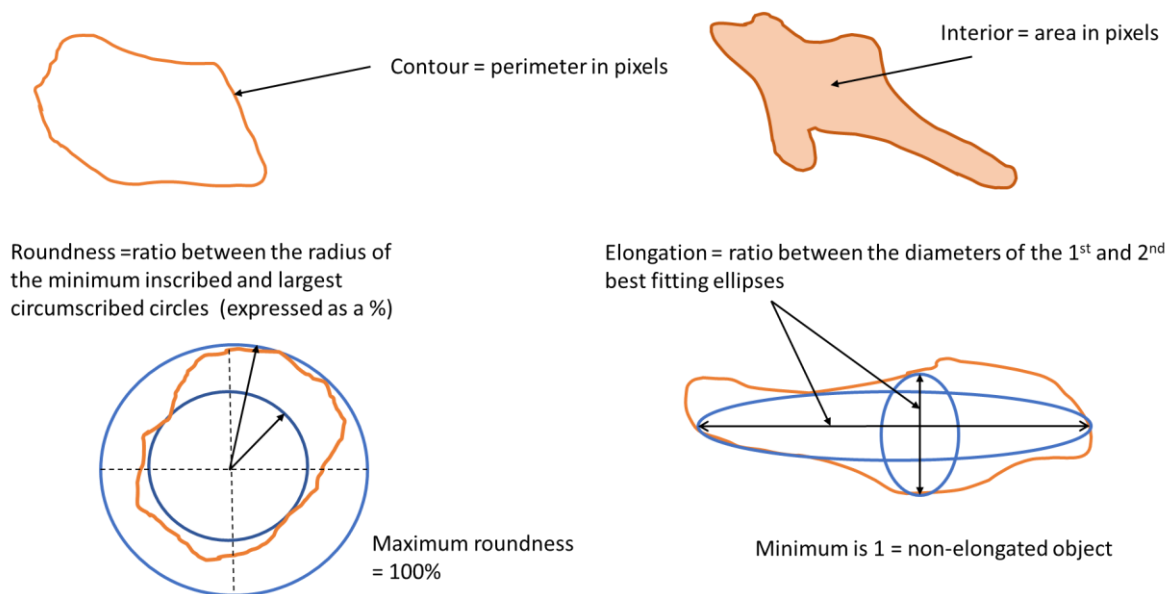


**Figure 3.8. Illustrations of the morphological parameters used to analyse the mitochondria.**

ICY provides different measurements of fluorescence intensity. Mean intensity is the average intensity across all pixels in the ROI. This measurement is not affected by the size of the ROI but could be skewed by a small number of very bright pixels. Sum intensity is the combined intensity of all pixels in the ROI, which captures all the red fluorescence but is affected by the area of the ROI. The measurement of fluorescence intensity selected was the sum intensity of the ROI divided by the interior (area in pixels) to control for size.

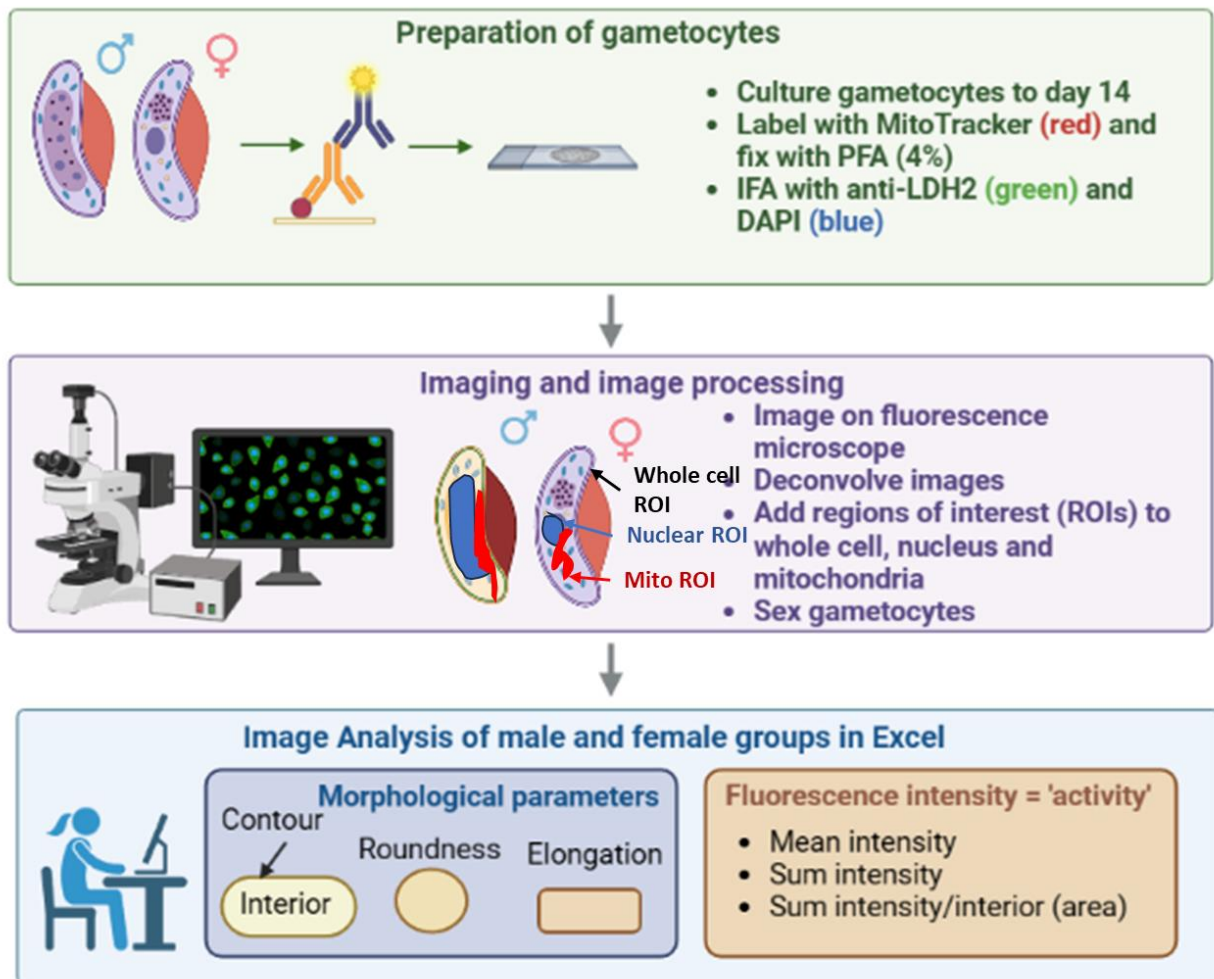


**Figure 3.9. Schematic showing the image analysis workflow.** The male gametocyte in the middle panel is a different colour to symbolise it stains more intensely with the anti-LDH2 antibody compared to the female. Abbreviations: PFA = paraformaldehyde, IFA = immunofluorescence assay, LDH2 = lactate dehydrogenase 2, DAPI = 4',6-diamidino-2-phenylindole (DNA stain), ROI = region of interest. Created with BioRender.com

#### Step 4: Validation

Before analysing the mitochondria, a pilot study was conducted to test the suitability of the analysis method.

The first of these aimed to investigate how LDH2 compared to the existing male gametocyte marker alpha tubulin II as a biomarker for distinguishing the sexes. Gametocytes were co-labelled with anti-LDH2 and anti-alpha tubulin II and the nuclear stain DAPI. Nuclear ROIs were generated as described in section 3.2.2. As shown in Figure 3.10, when other parameters were plotted against anti-alpha tubulin II and anti-LDH2 mean intensity, it was more difficult to distinguish two clear groups that might correspond to males and females

using alpha tubulin II as a marker than with LDH2. In addition, I observed that when trying to use alpha tubulin II to differentiate male and female stage V gametocytes by eye, there were many more ambiguous cells that were difficult to classify as male or female, compared to using LDH2.

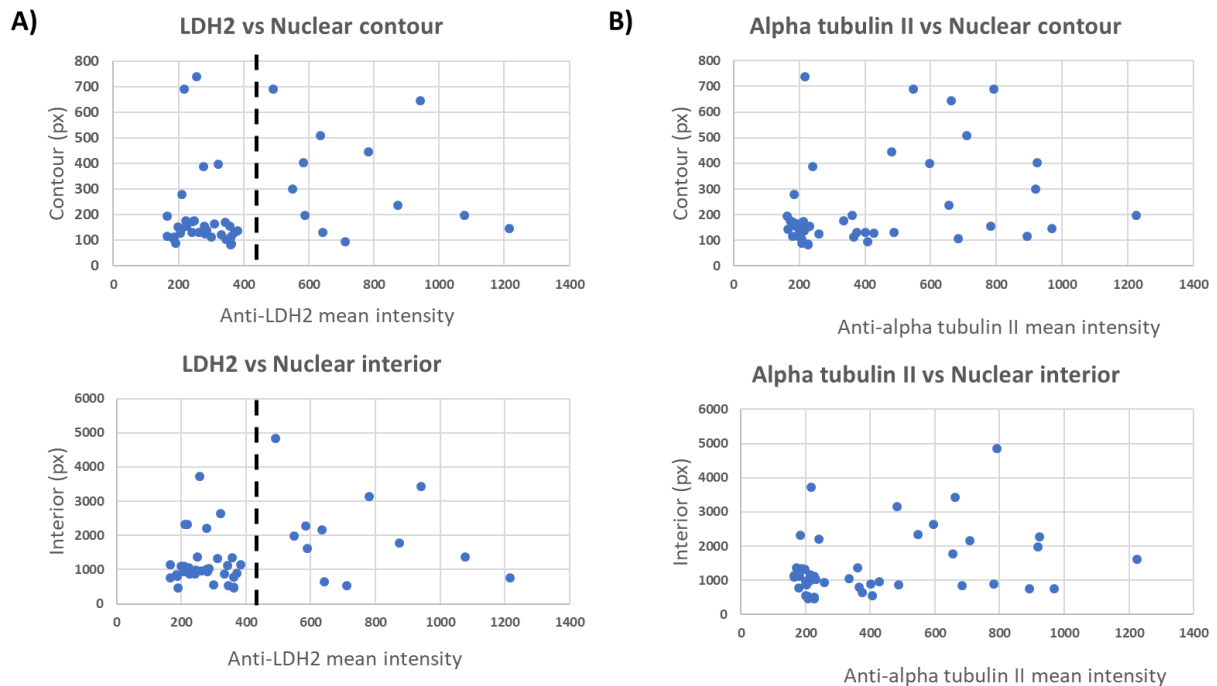


**Figure 3.10. Comparison of ability of anti-LDH2 and anti-alpha tubulin II to separate gametocytes into two populations. A)** Anti-LDH2 intensity (x axis) plotted against nuclear contour (top) and interior (bottom). **B)** Anti-alpha tubulin II mean intensity (x axis) plotted against nuclear contour (top) and interior (bottom). 1 of 3 replicates is shown here, n = 46 gametocytes.

The second pilot aimed to determine i) whether LDH2 fluorescence intensity values could be used to separate the gametocytes into two population and ii) whether the analysis could detect known differences in nuclear morphology between male and female gametocytes, which would indicate that the analysis method is suitable to compare the mitochondria between the sexes. Gametocytes were co-labelled with anti-LDH2 and DAPI.

The pilot study showed that anti-LDH2 fluorescence intensity values can successfully separate the gametocytes into two groups. The graphs in Figure 3.11 show anti-LDH2 mean intensity plotted on the x axis and nucleus morphology parameters on the y axis, and you can see clear separation into 'low LDH2' or 'high LDH2' groups which likely correspond to female and males respectively. The clear separation into two groups allows easy comparison of the different morphological parameters between male and female gametocytes.

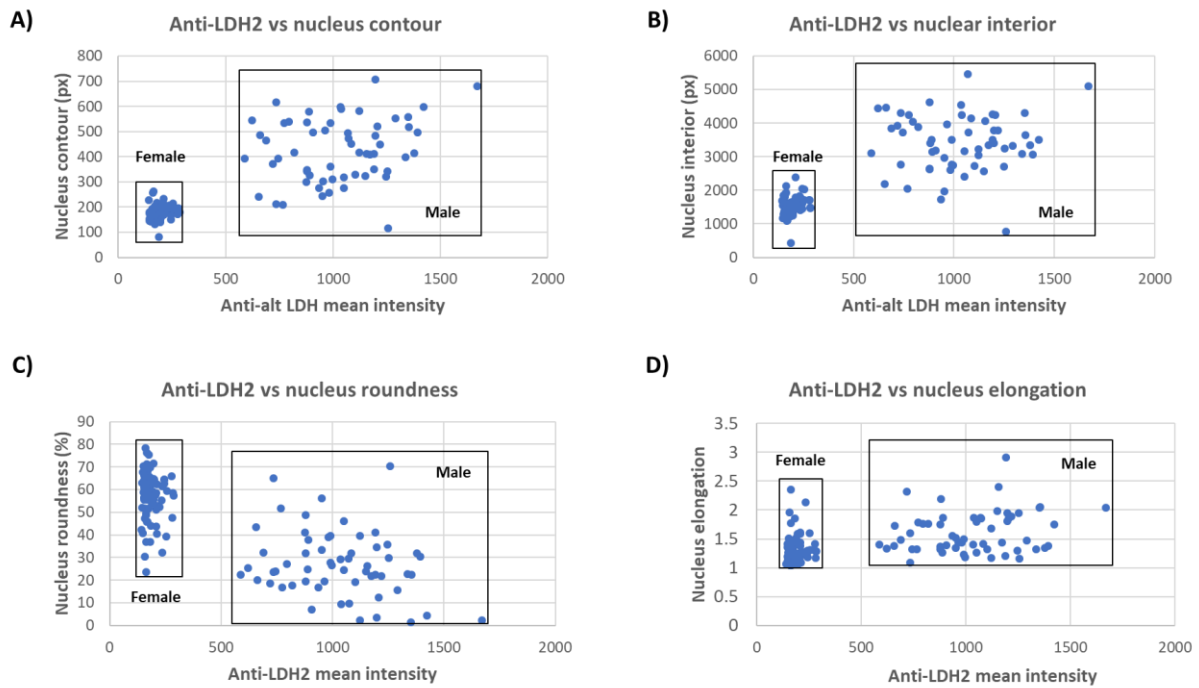


**Figure 3.11. Anti-LDH2 intensity (x axis) plotted against four examples of nuclear parameters (y axis). A) nuclear contour B) nuclear interior C) nuclear roundness and D) nuclear elongation.** Each point is a single gametocyte. Anti-LDH2 clearly separates the gametocytes into low LDH2 (female) and high LDH2 (male) populations, indicated by the rectangles. Data shown is from one example biological replicate n = 139 individual gametocytes.

The second test was to determine whether measurements of the nuclear parameters of the male and female groups matched sex differences in published literature. It is known that female gametocytes have a relatively small, compact nucleus whereas the male nucleus is larger and more diffuse. The image analysis method was able to detect these differences (Figure 3.12). Male gametocytes nuclei were found to have significantly higher contour (unpaired Student's t-test  $p = 0.0043$ ) and elongation ( $p = 0.0327$ ) values than females. Males had higher interior values but the difference was not significant. Female gametocytes had significantly higher roundness ( $p = 0.0003$ ) than males. The nuclear morphology trends reflect what we know about male and female nuclei which a) further suggests LDH2 is suitable for distinguishing males and females and b) that the analysis should be sufficient for finding sex differences in the mitochondria if they are there.

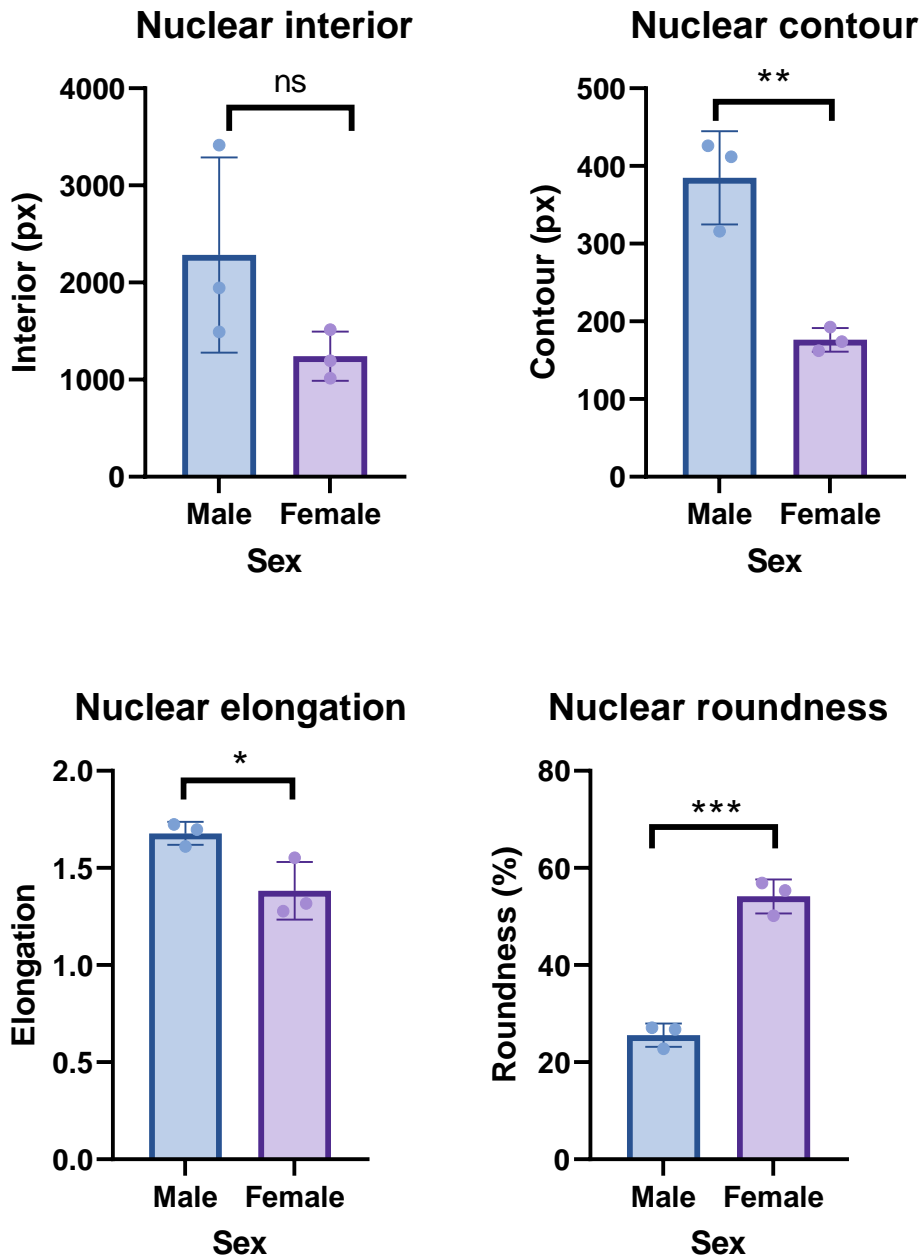


**Figure 3.12. Comparison of nuclear morphological parameters between male and female gametocytes.**  $n = 3$  independent experiments of between 45 and 139 gametocytes per replicate. All statistics are unpaired Student's t-tests. \* =  $p < 0.05$ , \*\* =  $p < 0.01$ , \*\*\* =  $p < 0.001$ . Error bars = SEM.

In summary, the anti-LDH2 antibody identifies two clear populations of gametocytes with known diagnostic features of male and female gametocytes. The anti-LDH2 has also been shown to be a superior marker for distinguishing the sexes compared to previous methods.

### 3.2.3 Comparison of male and female gametocyte mitochondrial morphology

The image analysis was then used to compare mitochondrial morphology in males and females. It was frequently observed that female gametocytes had a slightly larger mitochondrion than males (Figure 3.13). However, over subsequent replicates the difference was found not to be statistically significant.

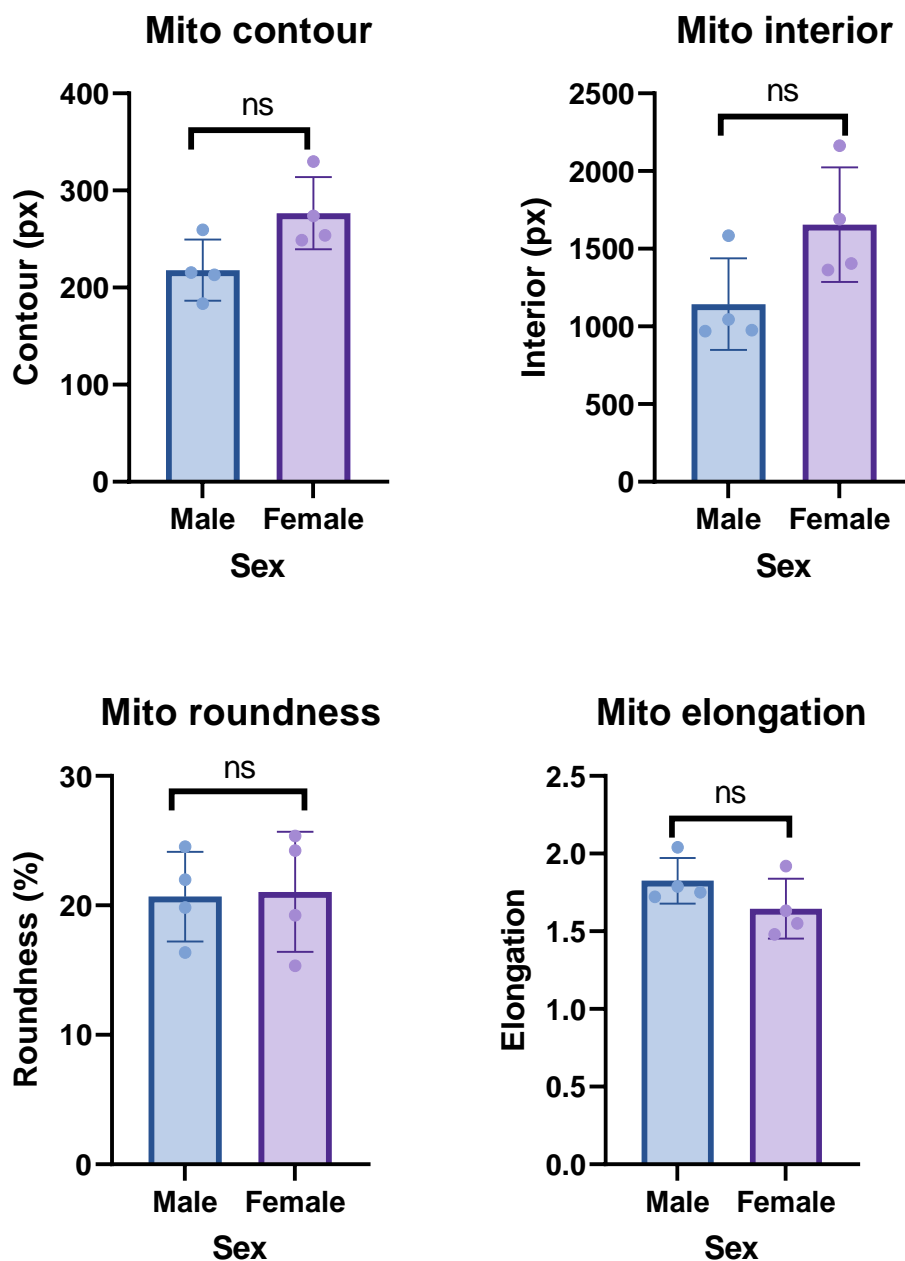


**Figure 3.13. Comparisons of mitochondrial morphology between male and female gametocytes.** n= 4 independent experiments of between 47 and 139 gametocytes per replicate. All were non-significant by unpaired Students' t-test. Error bars = SEM.

Using this methodology, there appears to be no difference in mitochondrial morphology between male and female gametocytes.

### 3.2.4 Quantifying the mitochondrial activity of mature male and female gametocytes

#### Modification of image analysis method to compare mitochondrial activity

Mitochondrial activity (which I define as the sum intensity of MitoTracker fluorescence per gametocyte divided by the interior area of the mitochondrion – essentially deriving the mean fluorescence per pixel), was measured by MitoTracker labelling of male and female gametocytes across three independent experiments. It was found that there was no statistically significant difference in mitochondrial staining per pixel between male and female gametocyte mitochondria, suggesting they are of a similar activity (Figure 3.14). However, it was observed that the mitochondrial labelling in the cells was very bright and could possibly be saturated, obscuring differences in uptake of the dye between male and female mitochondria.

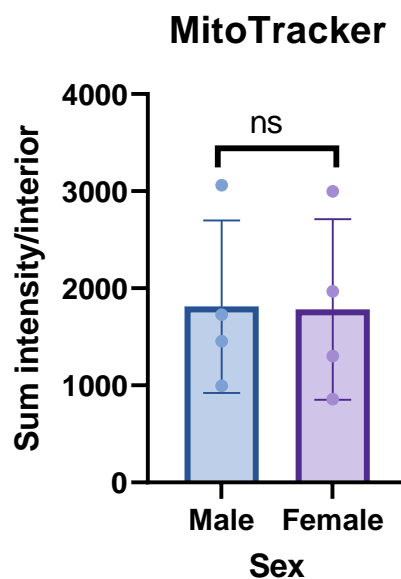


**Figure 3.14. Comparison of the fluorescence intensity of MitoTracker staining between males and females.**  $n = 4$  independent experiments of between 47 and 139 gametocytes per replicate. Mitochondrial staining was defined as the sum intensity of red fluorescence within the mitochondrial ROI divided by the interior (area in pixels) of the mitochondrial ROI. The male and female groups were compared by Student's unpaired t-test and no significant difference was found between the groups. Error bars = SEM.

I hypothesised that the MitoTracker concentration recommended by the manufacturer could be oversaturating the mitochondria and may account for similar activity observed. To test this, a titration of MitoTracker was performed to determine whether MitoTracker could still label the mitochondria label at more sensitive concentrations to reduce background staining. Concentrations of 100, 25 and 12.5 nM were compared to the original selected concentration of 200 nM. MitoTracker intensity decreased with increasing dilution of the dye as expected (Figure 3.15 A). It was found that structure of the mitochondria could still be clearly seen at the lower concentrations of 25 and 12.5 nM (Figure 3.15 B).

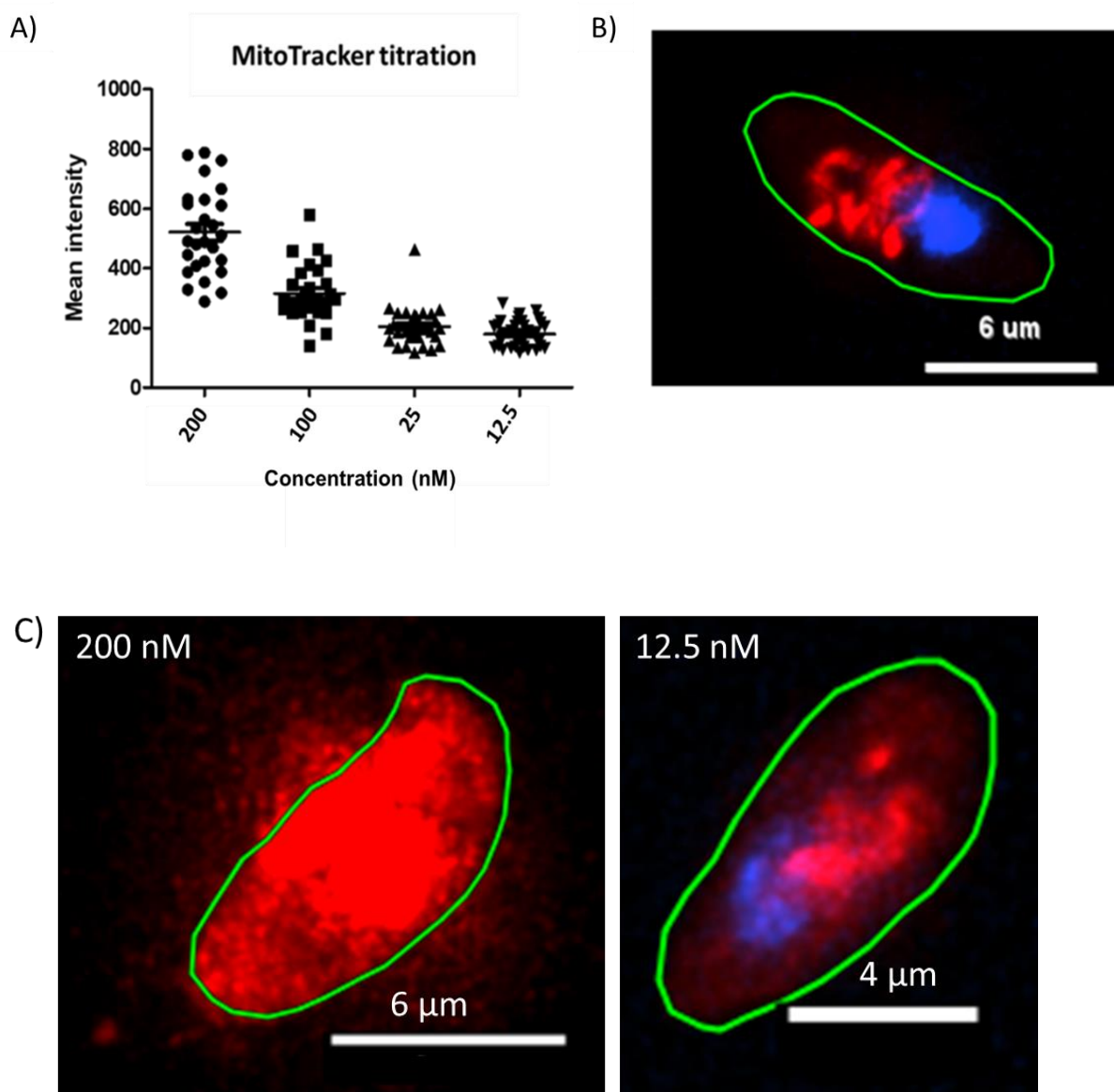


**Figure 3.15. Titration of MitoTracker staining.** **A)** Mean intensity of gametocyte mitochondria stained with different concentrations of MitoTracker **B)** IFA image showing a gametocyte labelled with MitoTracker at 12.5 nM in red and DAPI in blue. **C)** Comparison image of gametocytes labelled with

MitoTracker at 200 nM and 12.5 nM with synchronised look up tables (LUTs). LUTs are set to where the mitochondrion is visible at 12.5 nM.

Based on this, for the experiment comparing male and female mitochondrial activity was repeated using MitoTracker at the non-saturating concentration of 12.5 nM. In addition, the way the ROIs were drawn to measure the MitoTracker intensity was refined. An ROI was drawn around the perimeter of the gametocyte using the Polygon tool as shown before (Figure 3.7 A + B) but instead of generating a mitochondrial ROI using thresholding (Figure 3.7 C), a square ROI was drawn in a cytoplasmic area as demonstrated in Figure 3.16. In this modified method, the whole gametocyte ROI (A in Figure 3.16) allowed the capture of all red fluorescence in the gametocyte cell (from the cytoplasm and the mitochondria) and the background square (B in Figure 3.16) captured the 'background' fluorescence in the cytoplasm. Mitochondrial staining was calculated by taking the mean intensity of the background square, multiplying it by the interior of the whole gametocyte and then subtracting this value from the sum intensity of MitoTracker for the whole gametocyte. This background-corrected value is representative of the fluorescence that can be attributed to the mitochondria itself. This also streamlines the workflow as it removes the thresholding step to generate the mitochondrial and nuclear ROIs.

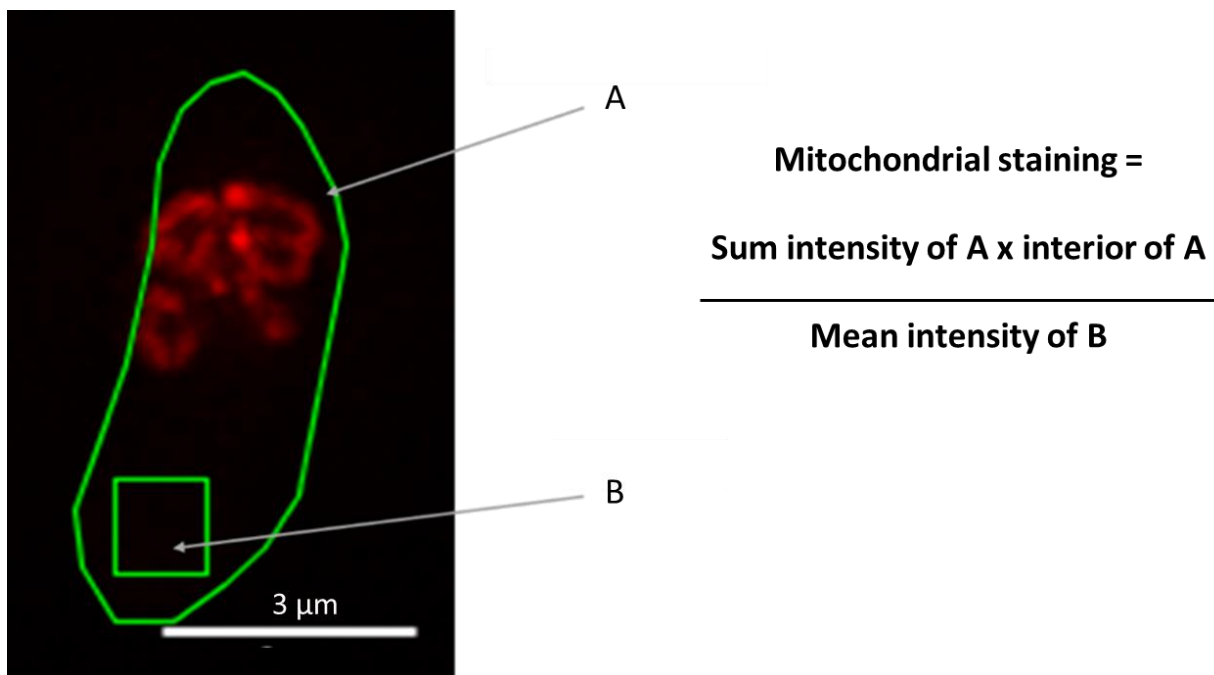


**Figure 3.16. Regions of interest and calculation of mitochondrial staining for the modified image analysis method.** ROI A is drawn around the entire gametocyte. ROI B is the smaller ROI in a non-mitochondrial area used to background correct the image. The formula for calculating the mitochondrial staining is the sum intensity x interior of A divided by the mean intensity of B. This gives the mitochondrial staining per pixel.

### Male gametocyte mitochondria have a lower activity than females

Male and female gametocyte mitochondria were subsequently analysed using the modified image analysis method. It was found males accumulated 43.4% less MitoTracker staining than females (Figure 3.17). Uptake of MitoTracker is dependent on the mitochondrial membrane potential and is used as a readout of mitochondrial activity. The increased uptake in female gametocyte mitochondria suggests they may be more active than males. The finding that male and female mitochondria appear to differ in their baseline mitochondrial activity has not been reported before and is the first observed difference in male and female gametocyte energy metabolism.

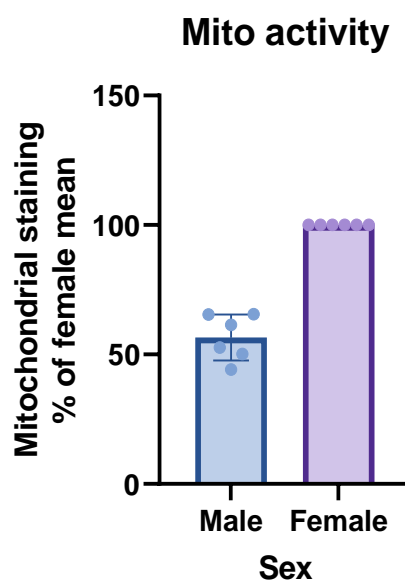


**Figure 3.17. Comparison of MitoTracker staining (mitochondria activity) between males and females.** n = 6 independent experiments measuring between 19 and 59 individual gametocytes per replicate. To control for variability between the experiments, mitochondrial staining was normalised to the female mean. Error bars = SEM.

### 3.2.5 Susceptibility of male and female gametocytes to inhibitors of the mETC

Having established the assay conditions which reproducibly showed that male gametocytes have a lower baseline mitochondrial activity than females, I then investigated how activity changed when gametocytes were treated with inhibitors of the mitochondrial electron transport chain (mETC).

Inhibitors were chosen that disrupt different points of the mETC. These were: the cytochrome bc1 (complex III) inhibitors atovaquone and ELQ-300, the DHODH inhibitor DSM-265 and the ATP synthase (complex V) inhibitor, oligomycin A (Figure 3.18.)

Inhibitors were tested at a range of concentrations that encompassed previously reported IC<sub>50</sub>s for male and female gametocytes or asexual blood stage parasites if gametocyte data was not available (Table 3.1). Based on this previous data, atovaquone and ELQ-300 were used at a concentration range of 1 nM through to 10 µM, in a 10-fold serial dilution. DSM-265 was tested at 10 µM. Oligomycin A was reported to be less potent with a reported IC<sub>50</sub> against asexual blood stage parasites of 1.45 µM (Fry, Webb and Pudney, 1990), as opposed to nanomolar concentrations for the other three inhibitors, so a higher concentration of 50 µM was used instead.

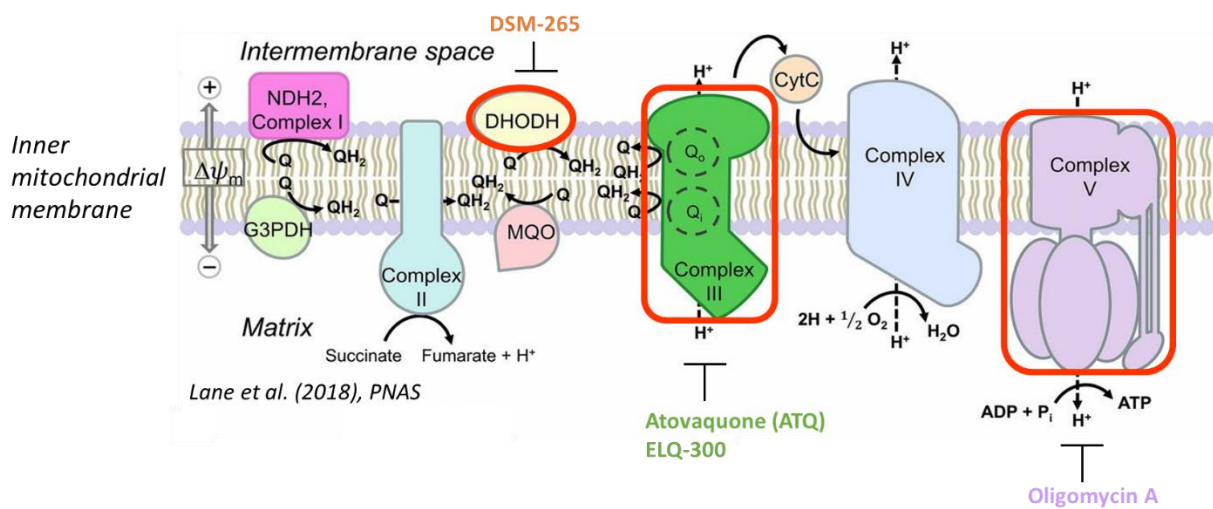


**Figure 3.18. Figure adapted from Lane *et al.* (2018). Diagram of the *Plasmodium* mitochondrial electron transport chain.** The complexes targeted for the mitochondrial activity assay and dual-gamete formation are indicated by the red bubbles.

| Inhibitor         | Activity of mitochondrial inhibitors                                  |                                  |                                 |  |
|-------------------|---|----------------------------------|---------------------------------|--|
|                   | (Values are reported IC <sub>50</sub> values unless otherwise stated) |                                  |                                 |  |
|                   | Asexual blood stage parasites   | Early stage GCT<br>(Stage I-III) | Late stage GCT<br>(Stage IV-V)  | Gametogenesis  |
| <b>Atovaquone</b> | < 1 nM  | >12.5 µM <sup>3</sup>            | Stage IV – 2.73 µM <sup>3</sup> | Exflagellation:<br>1 µM – 12.02% inhibition <sup>4</sup> |
|                   | 0.6 nM <sup>1</sup>   |                                  |                                 |  |
|                   | 0.7 nM <sup>2</sup>   |                                  | Stage V - >12.5 µM <sup>3</sup> |  |

|                     |                            |  |                                    |   |
|---------------------|----------------------------|--|------------------------------------|---|
|                     |                            |  | Stage IV-V – 16<br>µM <sup>2</sup> | Female<br>activation:<br><br>1 µM – 12.31%<br>inhibition <sup>4</sup><br><br>10 µM –<br>28.05%<br>inhibition <sup>4</sup> |
| <b>ELQ-300</b>      | 1.3 – 13.6 nM <sup>5</sup> | 0.1 µM<br>prevented<br>maturation past<br>stage III <sup>5</sup> | 71.9 nM <sup>5</sup>               |   |
| <b>DSM-265</b>      | 100 nM <sup>6</sup>        | No activity <sup>6</sup>   | No activity <sup>6</sup>           | No activity <sup>6</sup>  |
| <b>Oligomycin A</b> | 1.45 µM <sup>7</sup>       |  |                                    |   |

**Table 3.1. Activity of inhibitors of the mETC and respiration against *P. falciparum* asexual blood stages and gametocytes.** Data sources for the information in this table: 1) (Delves *et al.*, 2012) 2) (Lelièvre *et al.*, 2012), 3) (Plouffe *et al.*, 2016), 4) (Delves *et al.*, 2013), mean inhibition of gametogenesis compared to DMSO controls, 5) (Nilsen *et al.*, 2013), activity against sexual blood stage parasites and late gametocytes are IC<sub>50</sub> values, stage I-II gametocytes treated with 0.1 µM ELQ-300 failed to progress past stage III in their development, 6) (Phillips *et al.*, 2015), activity against gametogenesis was assessed by dual-gamete formation assay (DGFA) and found no activity 7) (Fry, Webb and Pudney, 1990).

Complex III was targeted using the antimalarial atovaquone and ELQ-300. Atovaquone inhibits the Qo site of the bc1 complex (Birth, Kao and Hunte, 2014) whereas ELQ-300 inhibits the Qi site (Stickles *et al.*, 2015). Treatment with these drugs inhibits mitochondrial electron transport and atovaquone is known to be able to collapse the mitochondria membrane potential (Srivastava, Rottenberg and Vaidya, 1997). If treatment with atovaquone and ELQ-300 in gametocytes depolarizes the mitochondrial membrane, it would be expected to observe a reduction in MitoTrackerRed CMXRos staining with increased concentration of these inhibitors.

DHODH was targeted directly using DSM-265, a potent, selective inhibitor of *P. falciparum* DHODH. Targeting DHODH has been previously shown not to have any transmission-blocking effects (Phillips *et al.*, 2015) so inhibition of gametogenesis would not be expected in the DGFA. However, even if DSM-265 is not transmission-blocking, its effect on mitochondrial activity has not been studied. Assuming that mitochondrial activity is not important for transmission, it could still have a non-essential effect.

Oligomycin A is a potent inhibitor of ATP synthase (complex V) (Lardy, Johnson and McMurray, 1958; Kagawa and Racker, 1966; Symersky *et al.*, 2012; Hearne *et al.*, 2020). It blocks the proton channel (Fo subunit) which is necessary for oxidative phosphorylation of ADP to ATP (Hearne *et al.*, 2020). Therefore, this drug inhibits ATP production, and the blocking of the proton channel causes an accumulation of protons outside the mitochondrion. Based on this mechanism of action, when gametocytes are treated with oligomycin A, the mitochondrial membrane would become hyperpolarized (a change in a membrane potential which makes it more negative) which could result in increased MitoTrackerRed CMXRos labelling relative to untreated gametocytes as uptake is dependent on a negative mitochondrial membrane potential.

Susceptibility of male and female gametocytes to these inhibitors was measured by two readouts 1) mitochondrial activity and 2) gametocyte viability i.e., their ability to form gametes.

To compare mitochondrial activity, mature gametocytes were treated with the inhibitors for 24 hours then labelled with MitoTracker. Fluorescence images of treated gametocytes were then analysed using the modified image analysis method described in section 3.2.4.

The ability to successfully form gametes was assessed using the dual gamete formation assay (DGFA) (Delves *et al.*, 2013; Ruecker *et al.*, 2014). This assay gives a dual readout which allows simultaneous comparison of the effect of an inhibitor on male and female gametocytes. Measuring the effect of mETC inhibitors on male and female gametogenesis is important because male and female gamete formation require different processes.

Exflagellation involves three rounds of DNA replication, assembly of axonemes and flagella of 6-8 motile gametes and egress from the host red blood cell, all completed in ~15-20 minutes. In contrast, female gametogenesis involves de-repression of translational repression and egress from the red blood cell. While it is known that gamete motility is driven solely by glycolysis, exflagellation is a rapid and complex series of processes. It is not known whether any of these processes require mitochondrially produced ATP.

If a link could be demonstrated between inhibition of the mitochondrial activity and inhibition of gamete formation, this would suggest that mitochondrial respiration is important for gametogenesis.

### **Mitochondrial activity in male and female gametocytes treated with mETC inhibitors**

The complex III inhibitors – atovaquone and ELQ-300 – showed a dose-dependent decrease in mitochondrial activity in males and females (Figure 3.20). Decreased mitochondrial staining with increased complex III inhibition would be expected as this should depolarize the mitochondrial membrane, increasingly preventing the mitochondria from being able to take up the dye. Depolarization of the mitochondrial membrane is a known consequence of atovaquone treatment (Srivastava, Rottenberg and Vaidya, 1997; Srivastava and Vaidya, 1999), so this is not unexpected. In the atovaquone treated gametocytes from 100 nM and higher, many of the gametocytes lacked MitoTracker staining or showed diffuse MitoTracker staining in the background of gametocyte cell, rather than uptake into the mitochondria (Figure 3.19). This phenotype is consistent with depolarization of the membrane and inability to take up the dye (Srivastava and Vaidya, 1999).

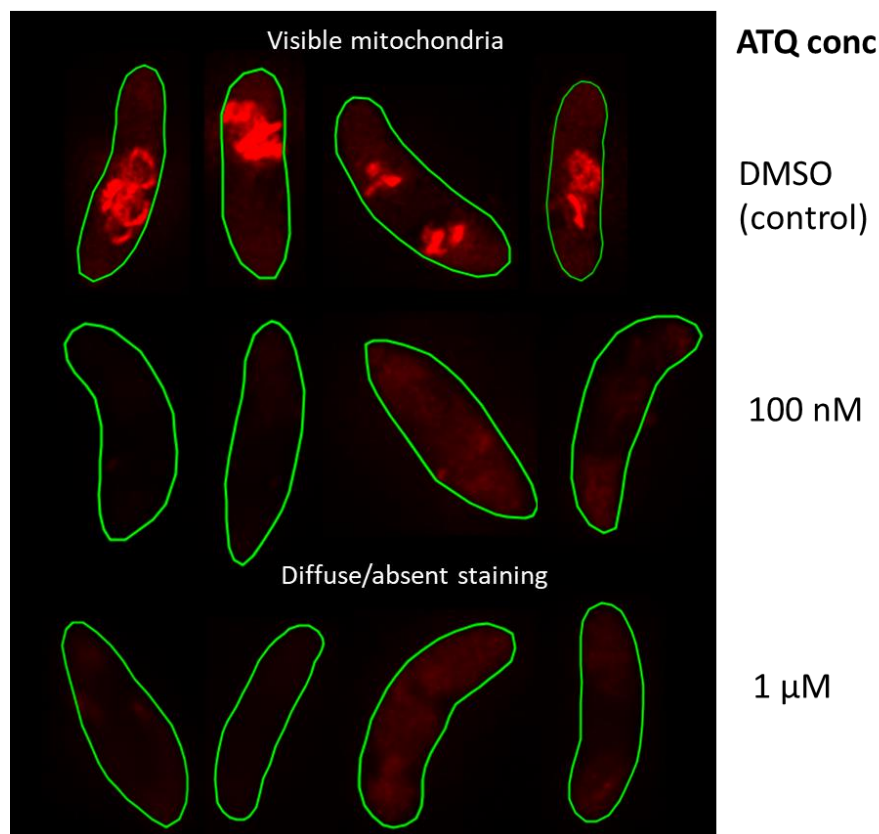


**Figure 3.19. Examples of absent or diffuse MitoTracker staining in atovaquone-treated gametocytes.** Top) DMSO-treated controls showing visible MitoTracker staining, middle) 100 nM atovaquone, bottom) 1  $\mu$ M atovaquone. Abbreviations: ATQ conc = atovaquone concentration.

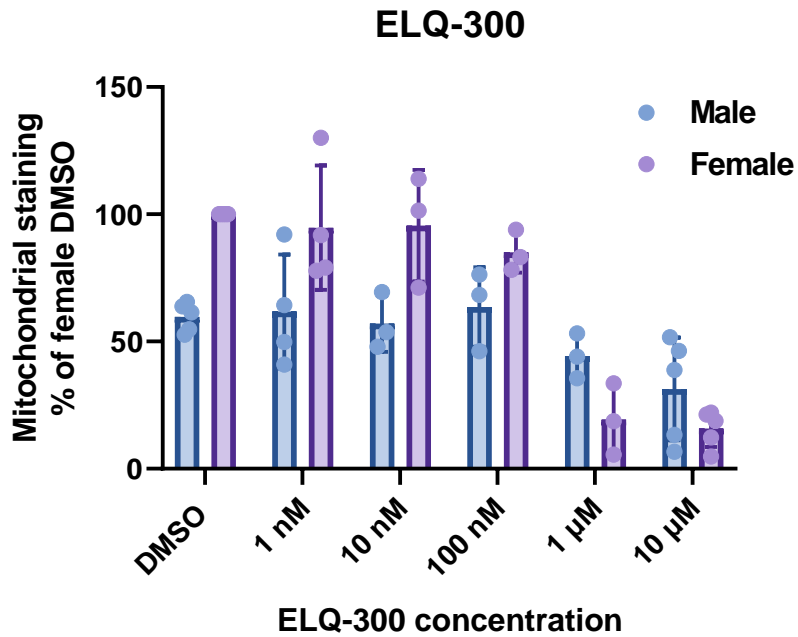
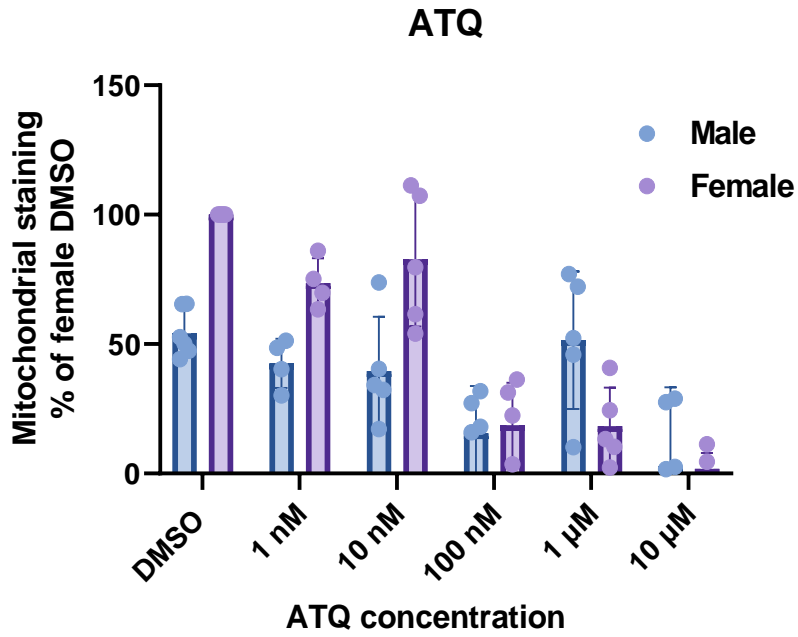


**Figure 3.20. Mitochondrial activity in male and female gametocytes treated with complex III inhibitors.** In each experimental replicate, mitochondrial staining was normalised to the female DMSO mean. Top) atovaquone (ATQ), n = 4-6 independent experiments (between 198-281 gametocytes measured per replicate). Bottom) ELQ-300, n =3-5 independent experiments (between 108-294 gametocytes measured per replicate). Error bars = SEM.

DSM-265 did not affect mitochondrial staining, even at the high starting concentration of 10  $\mu$ M, suggesting disruption of DHODH has little effect on the mitochondrial membrane potential (Figure 3.21). Based on this result, further lower concentrations were not tested as a difference would be unlikely to be observed.

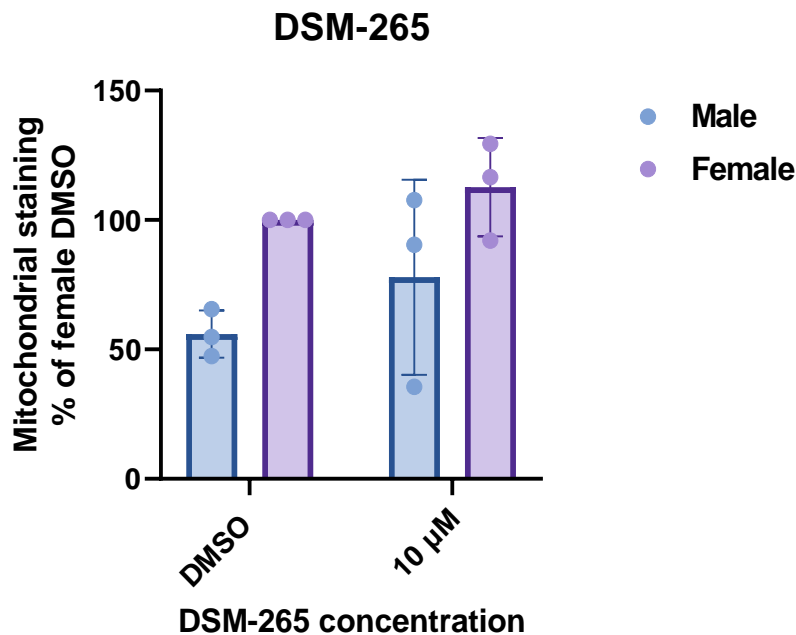


**Figure 3.21. Mitochondrial activity in male and female gametocytes treated with the DHODH inhibitor, DSM-265.**  $n = 3$  independent experiments (between 70-113 gametocytes measured per replicate.) In each experimental replicate, mitochondrial staining was normalised to the female DMSO mean. Error bars = SEM.

The ATP synthase inhibitor oligomycin A increased MitoTracker staining (Figure 3.22). The increase in MitoTracker staining suggests treatment with oligomycin A resulted in increased accumulation of the dye. Oligomycin A inhibits ATP synthase by blocking its proton channel which would lead to a build-up of protons in the intermembrane space. This accumulation of protons would result in a change in the membrane potential which makes the potential more negative – hyperpolarization. As previously mentioned, uptake of MitoTracker is dependent on a negative mitochondrial membrane potential. Therefore, the increase in MitoTracker staining observed in the treated gametocytes is consistent with membrane hyperpolarization.

While the effects on mitochondrial activity were observed at high drug concentrations, making it difficult to rule out the drugs having off-target effects, the effects of oligomycin A and the complex III inhibitors are consistent with the known effects of these inhibitors on mitochondrial respiration.

These results show that mitochondrial inhibitors can cause measurable changes in mitochondrial activity in gametocytes. The next step was to determine whether this change in activity affects their functionality i.e. their ability to form gametes. If gametocytes cannot form gametes, there is no transmission.

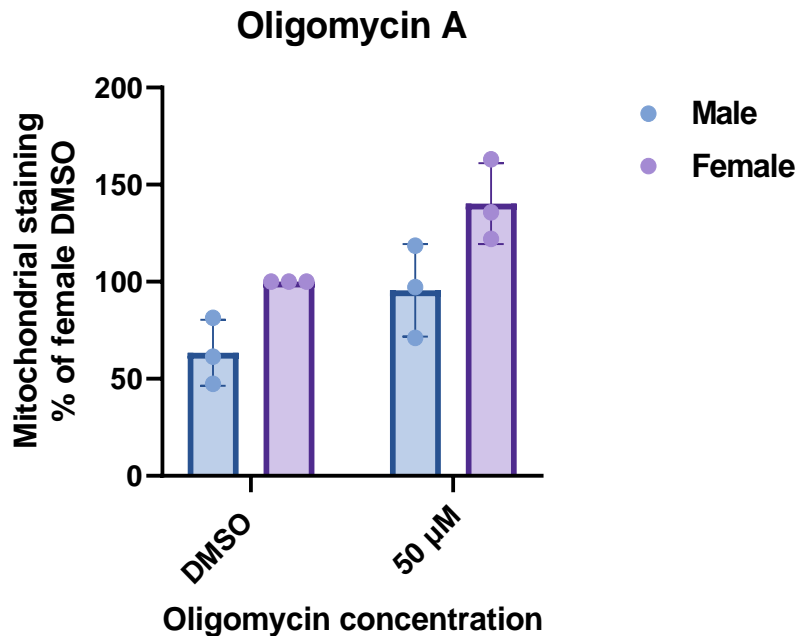


**Figure 3.22. Mitochondrial activity in male and female gametocytes treated with the complex V/ATP synthase inhibitor, oligomycin A.** n = 3 independent experiments (between 103-160 gametocytes measured per replicate). In each experimental replicate, mitochondrial staining was normalised to the female DMSO mean. Error bars = SEM.

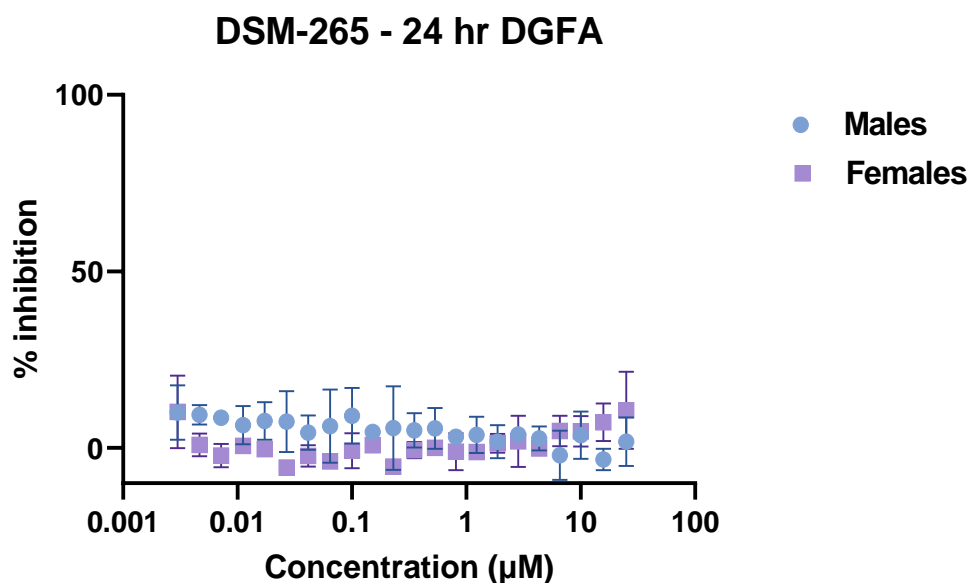
### Effect of mETC inhibitors on male and female gametogenesis

Image analysis of drug-treated MitoTracker-labelled gametocytes revealed that complex III inhibitors decreased mitochondrial activity and depolarised the mitochondrial membrane, whereas the complex V inhibitors increased MitoTracker staining compared to untreated controls, consistent with membrane hyperpolarization. However, these observations do not report on whether changes to mitochondrial activity affect the viability of gametocytes i.e. their ability to successfully form gametes once taken up by a mosquito.

Gamete formation when gametocytes were preincubated for 24 hours with the mETC inhibitors was investigated using a dual gamete formation assay (DGFA). The aim of this experiment was to i) determine if the mETC inhibitors had any effect on gamete formation, ii) calculate a dose-response curve and the  $IC_{50}$  value for each inhibitor against male and female gametogenesis, iii) investigate whether there is a link between a disrupted

mitochondrion (depolarization or hyperpolarization of the membrane, both resulting in reduced or/no ATP production) and a reduction in gamete production. To investigate the short-term effects of the mETC inhibitors, a DGFA was also carried out on gametocyte pre-incubated for 1 hour with the drugs.

The image analysis of MitoTracker-labelled DSM-265 treated gametocytes showed no effect on mitochondrial activity in either male or female gametocytes at 10  $\mu\text{M}$  (Figure 3.23). Consistent with previous reports (Phillips *et al.*, 2015), DSM-265 had no effect on male or female gametogenesis in either the 24-hour or 1-hour DGFA even at as high a concentration of 25  $\mu\text{M}$ , suggesting inhibition of DHODH does not have a transmission-blocking effect. As mentioned above, inhibition of DHODH in asexual blood stage parasites results in parasite death due to preventing *de novo* pyrimidine biosynthesis which is essential in asexual blood stage parasites but not in gametocytes (Painter *et al.*, 2007). However, it is interesting that inhibition of DHODH does not seem to affect the mitochondrial ETC. Possible explanations for this are proposed in the discussion (3.3).



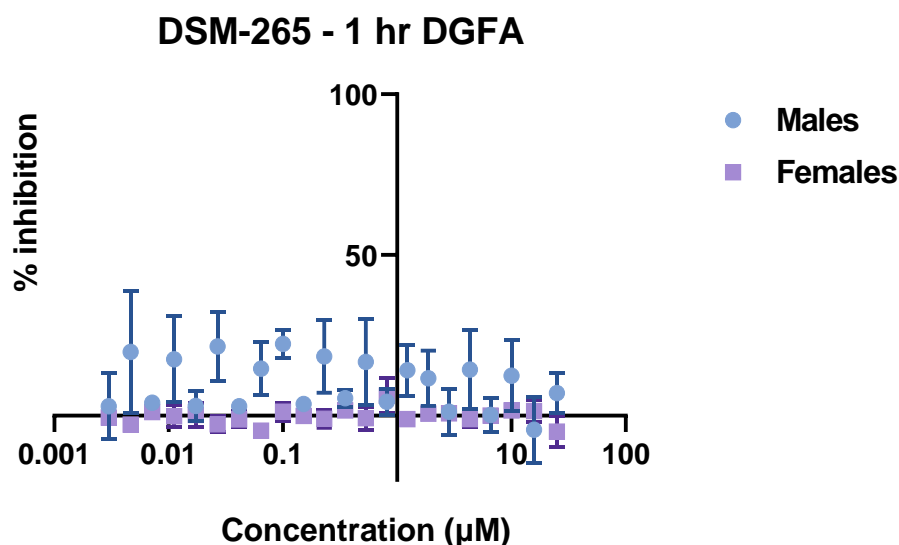


**Figure 3.23. Dose-response curve showing inhibition of male and female gametogenesis by DSM-265.** n = 3 independent experiments. Top) 24-hour preincubation, bottom) 1-hour preincubation. Errors bars = SEM.

In the 24-hour DGFA, the complex III inhibitors atovaquone (Figure 3.24) and ELQ-300 (Figure 3.25) showed dose-dependent inhibition of exflagellation with  $IC_{50}$  values of 68.5 nM and 42.2 nM respectively. This suggests that inhibition of complex III is having an inhibitory effect on male gametogenesis. The complex III inhibitors were less effective at inhibiting female gametogenesis. The  $IC_{50}$  values for atovaquone and ELQ-300 against female gametogenesis were calculated as 313.6 nM and 247.7 nM respectively, with inhibition plateauing at ~50% for both inhibitors.

In contrast, the 1-hour DGFA with the complex III inhibitors showed no inhibition of exflagellation. This suggests that the effect on the mitochondria and in turn exflagellation takes time to occur. Atovaquone and ELQ-300 are classed as a slow-acting antimalarials (Nilsen *et al.*, 2013; Mariebernard, Mohanty and Rajendran, 2022) so perhaps this is not an unexpected result. Inhibition was observed in the female assay. The  $IC_{50}$  against female gametogenesis was 1.43  $\mu$ M for atovaquone and 291.2 nM for ELQ-300. Once again inhibition plateaued at ~50% for both inhibitors. The female dose-response curve is likely similar to the 24-hour assay because the activated female gametes are left for 24 hours before staining with the anti-Pfs25 antibody to allow maximal expression of Pfs25 on the gamete surface (Delves *et al.*, 2013).

The image analysis of mitochondrial activity, as visualised by MitoTracker labelling, showed that mitochondrial activity did not differ compared to untreated gametocytes up to 10 nM but

by 100 nM, mitochondrial activity had dropped substantially in both male and female gametocytes. This reduction is consistent with depolarization of the mitochondrial membrane and suggests inhibition of mitochondrial activity occurs between 10 and 100 nM. The fact that the IC<sub>50</sub> values of atovaquone and ELQ-300 against exflagellation is in this range shows a link between decreased mitochondrial activity (and in turn reduced mitochondrial ATP production) and inhibition of exflagellation. This supports the hypothesis that that mitochondrial ATP production is important for male gametogenesis directly. A similar reduction in MitoTracker intensity was observed in females in the image analysis. However, this did not translate to as great an inhibitory effect on gamete formation. This suggests that male gametocytes are more susceptible to disruption of their mitochondria by complex III inhibitors (in terms of onward viability) than females.

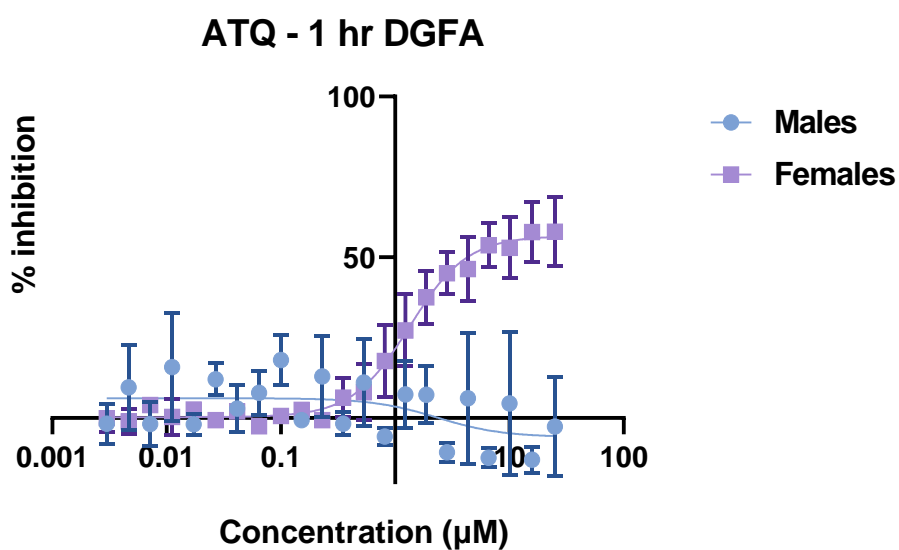
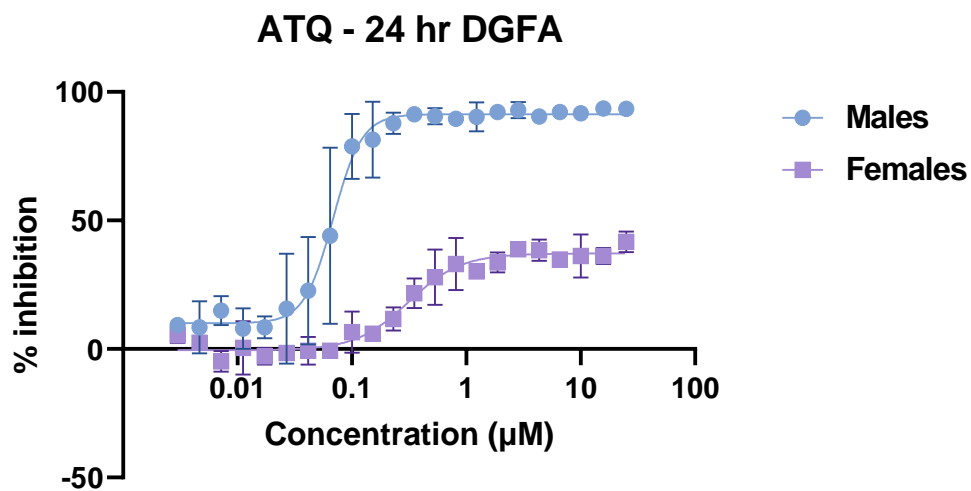


**Figure 3.24. Dose-response curve showing inhibition of male and female gametogenesis by atovaquone (ATQ).** n = 3 independent experiments. Top) 24-hour preincubation. Bottom) 1-hour preincubation. Error bars = SEM.

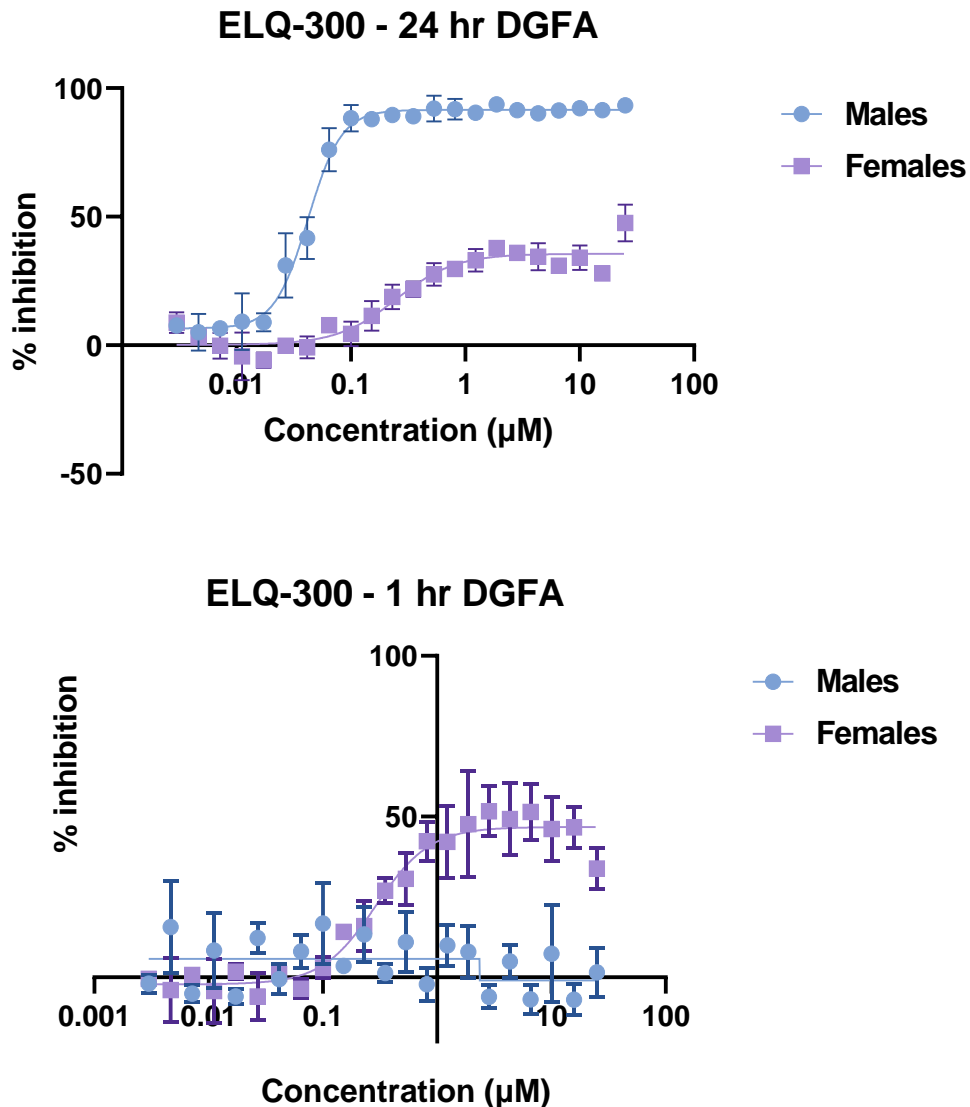


**Figure 3.25. Dose-response curve showing inhibition of male and female gametogenesis by ELQ-300.** n = 3 independent experiments. Top) 24-hour preincubation. Bottom) 1-hour preincubation. Error bars = SEM.

Inhibition of exflagellation was also observed for the complex V (ATP synthase) inhibitor oligomycin A in the 24-hour DGFA, albeit at a much higher  $IC_{50}$  of 303.9 nM (Figure 3.26). Oligomycin A is known to be less potent against *Plasmodium* asexual blood stage parasites than the complex III inhibitors (1.45 µM (Fry, Webb and Pudney, 1990)) so it is not unexpected the  $IC_{50}$  against exflagellation would be higher. Treatment with oligomycin A

blocks the proton channel which is required for production of mitochondrial ATP. This suggests that disruption of mitochondrial respiration is inhibiting male gametogenesis.

Oligomycin A showed inhibition of female gametogenesis in the 24-hour assay but did not reach a plateau, therefore an accurate  $IC_{50}$  could not be calculated in PRISM software based on the dose-response curve. However, the highest concentration of oligomycin A tested, 25  $\mu$ M, did give 100% inhibition of female gametogenesis so the  $IC_{50}$  could be speculated to be  $\sim$ 12.5  $\mu$ M. This is considerably higher than the  $IC_{50}$  against male gametogenesis of 303.9 nM, suggesting disruption of mitochondrial respiration is having less of an effect on female gametogenesis.

Unlike the complex III inhibitors, oligomycin A did show inhibition of exflagellation in the 1-hour assay, although inhibition plateaus at  $\sim$ 60-70% inhibition. The  $IC_{50}$  against exflagellation with 1-hour incubation was 12.7  $\mu$ M. It is possible that these concentrations can block mitochondrial respiration after 1-hour incubation, whereas with a longer incubation time this can happen at lower concentrations. As oligomycin A inhibits mitochondrial respiration, the fact that oligomycin A has an inhibitory effect on exflagellation after a short incubation supports that mitochondrial respiration is important for male gametogenesis. Inhibition against female gametogenesis plateaued at  $>$ 50% inhibition, with an  $IC_{50}$  of 25.5  $\mu$ M.

In the image analysis, oligomycin A treatment increased mitochondrial labelling compared to the untreated control, consistent with hyperpolarization of the membrane and resultant increased accumulation of the dye into the mitochondria. Again, these results show a link between an observed change in mitochondrial membrane potential and reduced ability to form gametes in male gametocytes, suggesting that mitochondrial energy metabolism may be more important for gametogenesis than previously thought. The hyperpolarization phenotype was also observed for female gametocytes in the image analysis but again this has not resulted in any substantial activity against female gametogenesis. This further suggests that male gametocytes are more susceptible to disruption of mitochondrial respiration (in terms of their ability to transmit to mosquitoes) than females.

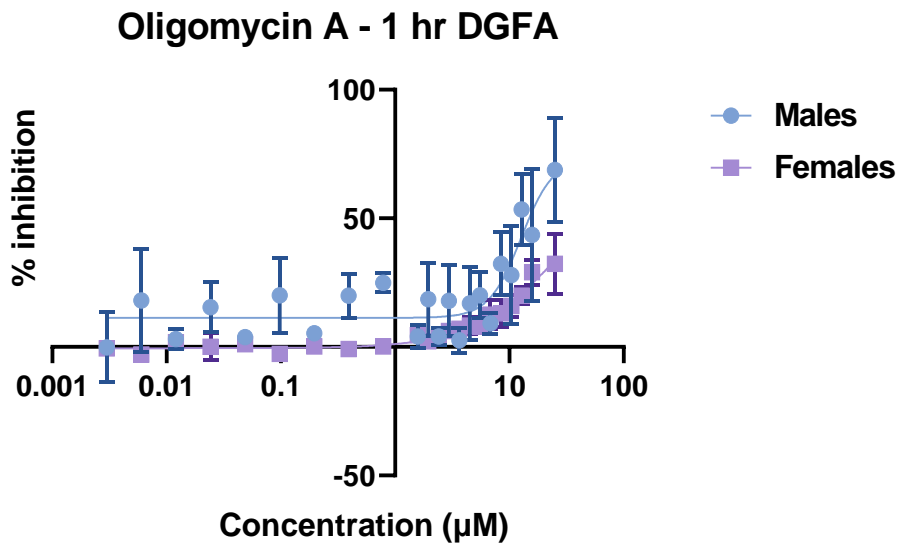
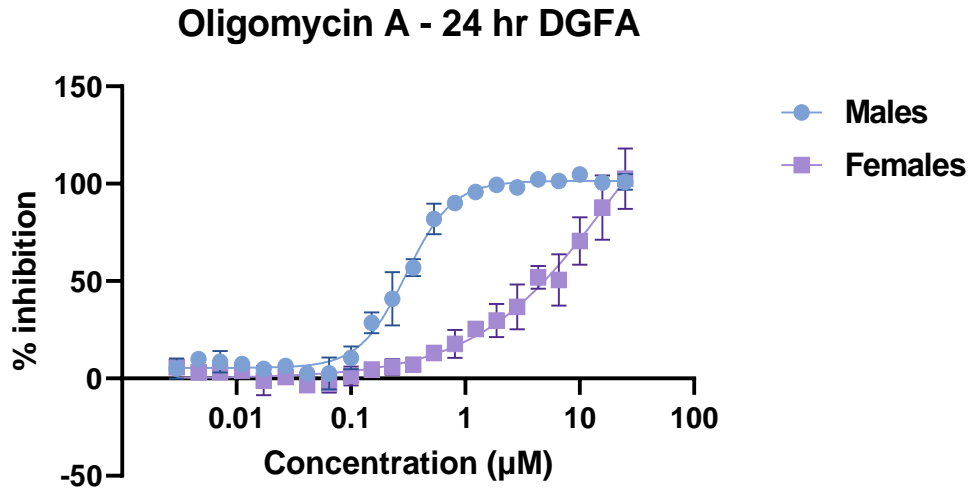


**Figure 3.26. Dose-response curves showing inhibition of male and female gametogenesis by oligomycin A.**  $n = 3$  independent experiments. Top) 24-hour preincubation. Bottom) 1-hour preincubation. Error bars = SEM.

In summary, these data demonstrate for the first time a link between the disruption of mitochondrial respiration and impaired male gametogenesis, suggesting that mitochondrial respiration is required for efficient exflagellation. Comparatively low inhibition of female gametogenesis was observed, demonstrating a difference between the sexes in their susceptibility to mETC inhibitors.

**Male gametocytes treated with mETC inhibitors start to undergo gametogenesis but show aberrant flagellar morphology**

Alongside the DGFAs, gametocytes pre-treated with the mETC incubators for 24 hours were triggered to exflagellate and fixed for IFAs. The parasites were then labelled with an anti-alpha tubulin II antibody and DAPI to visualise exflagellation centres and allow investigation of whether there was a particular point of arrest for gametogenesis.

The IFAs showed that gametocytes treated with the inhibitors do not arrest early in the process (Figure 3.27). Gametocytes treated with complex III and V inhibitors successfully replicated their DNA as shown by increased DAPI staining and formed flagella. It was frequently observed that the flagella had diffuse alpha tubulin II or aberrant morphology (montages are shown in Appendix 2). However, despite being in advanced stages of gametogenesis in the IFAs, high levels of inhibition at these concentrations (10  $\mu$ M for atovaquone and ELQ-300, 50  $\mu$ M for oligomycin A) were seen in the DGFA. The exflagellation readout for the DGFA is based on detection of the movement of the gametes emerging from the red blood cells. If inhibition is high at this concentration, it suggests that there was little detectable movement of exflagellation centres. This suggests that gametocytes treated with these inhibitors are not dead and can progress so far with exflagellation but that the gametes can't properly escape the host erythrocyte and/or move.

Taken together, the IFA and DGFA results suggest that insufficient mitochondrial respiration appears to lead to aberrant or stalled gametogenesis. This suggests that mitochondrial activity is important for male gametogenesis and that disruption of mitochondrial respiration could result in a block in transmission.

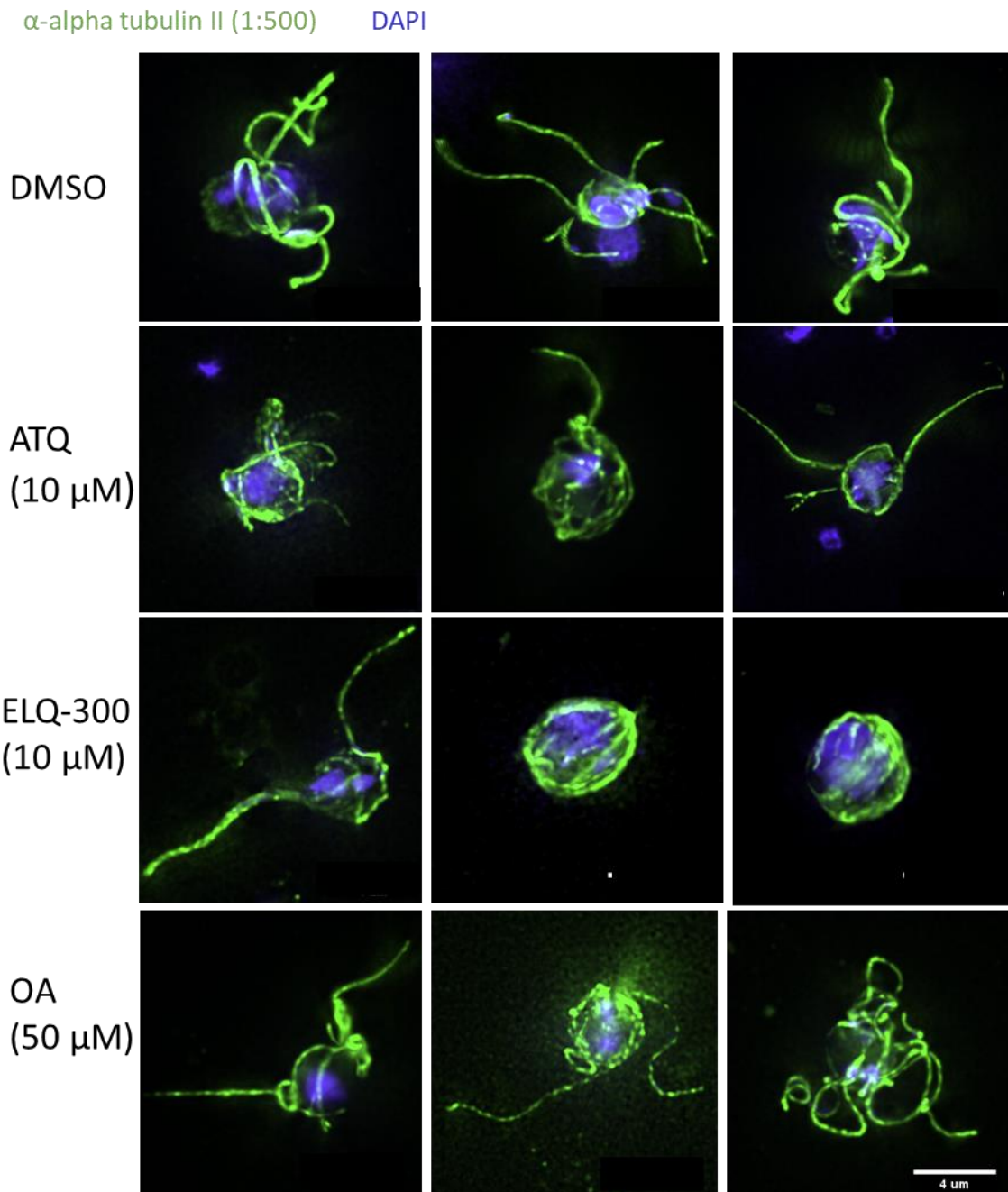


**Figure 3.27. Exflagellation IFAs of male gametocytes incubated for 24 hours with the mETC and respiration inhibitors showing representative morphology.** DMSO = control (normal exflagellation), Abbreviations: ATQ = atovaquone, OA = oligomycin A.

### 3.3 Discussion

Male and female gametocytes undergo markedly different developmental programmes during the life cycle. Notably, the female gametocyte retains its mitochondria whereas in males it is shed during the gametogenesis process and male gametes rely on glycolysis from then on (Okamoto *et al.*, 2009). Proteomic data also suggest that proteins involved in energy metabolism and the mitochondria are enriched in female gametocytes compared to

males (Khan *et al.*, 2005; Lasonder *et al.*, 2016; Miao *et al.*, 2017) . Despite these differences, it has not been previously investigated whether male and female gametocytes differ in their energy metabolism. To address this question, I developed methods to compare mitochondrial morphology and activity between males and females as well as their susceptibility to mETC-targeting drugs. The results presented in this chapter indicate for the first time that female mitochondria are more active than those of males and that disruption of mitochondrial respiration impacts male gametogenesis.

A challenge to this research was that existing markers of gametocyte sex can be ambiguous. An antibody to LDH2 was found to be able to distinguish male and female gametocytes accurately, both visually in IFAs and by fluorescence intensity, overcoming this challenge. The antibody is specific to male gametocytes from stage IV and does not label stage II and III gametocytes. This could provide advantages over existing markers such as alpha tubulin II which has previously been reported to be expressed in stage I-IV gametocytes and to be present in a population of stage V female gametocytes counterstained with a female marker G377 (Schwank, Sutherland and Drakeley, 2010). In contrast, I found no overlap with LDH2 expressing (male) and G377 expressing (female) gametocytes indicating that my developed antibody is superior to previous techniques to determine the sex of mature gametocytes. Indeed, anti-LDH2 appeared to also stain Stage IV gametocytes – consistent with recently published data that gametocytes are neither male or female until a transcriptional switch at the *md1* locus at around stage III which determines sex (Gomes *et al.*, 2022).

Providing further support to the sex-specificity of anti-LDH2, my image analysis method correctly identified known differences in nuclear methodology between males and females and enabled comparisons of mitochondrial morphology and activity. The image analysis method using anti-LDH2 to differentiate sex could have wider applications for studying sex specific biology outside of energy metabolism. Anti-LDH2 antibody labelling could be used in combination with other fluorescent probes. Examples could include probes for the endoplasmic reticulum and Golgi apparatus (e.g. ER-Tracker, CellLight Golgi-RFP) or lipophilic stains, such as Nile red (Greenspan, Mayer and Fowler, 1985; Tran *et al.*, 2014).

Using my developed image analysis methodology, I did not observe a measurable difference in mitochondrial morphology using the simple analysis parameters described in Section 3.2.2. My method relies on measuring 2D maximum intensity projections of deconvolved z-stack images of gametocytes. Cells are three dimensional structures and so future work to identify subtle differences in male and female mitochondrial organisation would require higher resolution microscopy techniques or EM.

Another possible extension to this work would be to use a machine learning approach to classify the mitochondria into phenotypes, to identify any subtle differences that are not obvious to the human observer. Automated image analysis of fluorescence microscopy images using artificial intelligence (AI) and machine learning (ML) techniques have already been widely adopted for drug screening (Aulner *et al.*, 2019). Recently, Tsebriy and colleagues developed an AI/ML pipeline called Phenotype Image Data and Digital Learning Innovation (PhIDDLI) which allowed them to characterise the activity of a panel of 40 transmission-blocking molecules through analysis of fluorescence images of gametocytes treated with the molecules and triggered to undergo exflagellation (Tsebriy *et al.*, 2023). This analysis pipeline can be applied to any fluorescence microscopy dataset containing cells delineated by bounding boxes (Tsebriy *et al.*, 2023), and so could be applied to fluorescence images of gametocyte mitochondria to classify them into phenotypes in an unbiased manner. It could then be determined whether any of the clusters corresponded to gametocyte sex.

Male gametocyte mitochondria were found to have 43% less MitoTracker staining than females at non-saturating concentrations of MitoTracker. Uptake of Mitotracker is dependent on the mitochondrial membrane potential and so is proportional to mitochondrial activity. As female gametocyte mitochondria were not significantly larger than those of males, this suggests male mitochondria are less active than those of females. This is consistent with published proteomic data which showed that proteins involved in energy metabolism are among those enriched in female gametocytes. These data provide the first exciting indication that male and female gametocytes differ in their energy metabolism.

MitoTracker fluorescence intensity was found to vary between biological replicates. For data variables that are particularly noisy, normalisation to a reference group was necessary. For comparisons of MitoTracker intensity in untreated and drug-treated male and female gametocytes, I used the group which consistently had the highest read outs, untreated female gametocytes, to compare the other groups to. However, the disadvantage of this approach is that variation in this group becomes unavailable which prevents statistical analyses. A different approach would be to normalise within each experimental replicate and to use 2-way ANOVA to simultaneously assess the effect of treatment and sex. Another approach would be to normalise the female treatment groups to the female DMSO control, and the male treatment groups to the male control. This would enable statistical analyses to specifically answer the question of whether the treatments have different effects on males and females.

Male and female gametocytes are found in the same environment in the human host and share the strategy of being inconspicuous and waiting to be taken up by a mosquito for

sexual development. Therefore, it seems unlikely this difference in baseline activity between the sexes is related to their time in the vertebrate host. It seems more likely to be due to the different fates of male and female gametocytes during transmission. Male gametes lack mitochondria, swim using a flagellum powered by ATP generated by glycolysis and have a maximum lifespan of 30-40 minutes in the vector (Talman *et al.*, 2014). *Plasmodium* male gametes are primarily composed of a nucleus and a flagellum and transfer only their DNA to the new zygote (according to our current knowledge), whereas female gametes provide the cytoplasm, mitochondria, and all other organelles to the new zygote (Okamoto *et al.*, 2009) which is then extracellular for 24 hours in the midgut (Delves, Angrisano and Blagborough, 2018). The parasites must then survive in the vector for a period of ~16 days to successfully complete their transformation into infectious sporozoites to infect a new host. Female gametes and ookinetes have also been demonstrated to have an active TCA cycle (Srivastava *et al.*, 2016). Considering these different fates in the mosquito, female mitochondria may have a higher activity for one or more of the following reasons.

Gametogenesis takes place in the newly ingested blood meal, where there may be comparable levels of glucose to those in the human host during the 15–20-minute period required for exflagellation, after which the male gametes have no mitochondria and use glycolysis for ATP to power their flagellum for motility (Talman *et al.*, 2014). Whereas, by the time fertilisation has occurred the glucose in the bloodmeal may be substantially depleted so perhaps the female gametocyte requires increased levels of mitochondrial respiration in preparedness for this so that the resultant zygote can optimise their use of glucose with the more efficient mitochondrial respiration. This could be investigated by allowing *Anopheles* mosquitoes to blood feed and then killing the mosquitoes at different time points to extract the bloodmeals. The amount of glucose in the blood meals at different time points post-feeding could then be measured. It would be interesting to quantify how much glucose is available to gametocytes undergoing gametogenesis versus an ookinete 24 hours post-feeding.

Exflagellation is relatively complex compared to female gametogenesis, and male gametocytes have previously been shown to be more susceptible to antimalarials than female gametocytes (Delves *et al.*, 2013), suggesting females have less 'targetable' biology. An alternative hypothesis could be that reduced mitochondrial activity in males is an adaptation to reduce oxidative stress which the male may be more susceptible to. Published data has shown methylene blue, a drug which is thought to affect the redox balance, to be more effective against male gametocytes than females (Delves *et al.*, 2013). If exflagellation is more sensitive to disruption of the redox balance than female gametogenesis, it makes

sense that male gametocytes may need to minimise ROS to remain viable and transmissible. However, my DGFA data showed that exflagellation is increasingly impaired with increasing inhibition of mitochondrial enzymes. It could be argued that if reduction in ROS is the purpose of lower mitochondrial activity in males, one could speculate that low concentrations of these drugs might temporarily be beneficial to exflagellation, and this not observed.

To validate this hypothesis, the amount of ROS produced by a male gametocyte and a female gametocyte would need to be quantified. This could be achieved through image analysis of gametocytes stained with CellROX which are fluorogenic probes which are non-fluorescent in a reduced state and exhibit bright, stable fluorescence upon oxidation by reactive oxygen species (ROS). The probes are formaldehyde fixable and so could be used in combination with the anti-LDH2 antibody to distinguish gametocyte sex. If males have relatively less CellROX labelling than females, males may be reducing mitochondrial energy metabolism to avoid oxidative stress.

Another consideration is that all previous metabolomic data studying mitochondrial energy metabolism is on mixed populations of gametocytes. The sex ratio is ~three to five females to every one male (Smalley and Sinden, 1977) so it is possible that our current understanding of gametocyte energy metabolism is female-biased. Sex-specific metabolomic analysis to compare  $^{13}\text{C}$ -glucose utilisation in male and female gametocytes could be used to determine whether the labelling of TCA cycle intermediates differs between male and female gametocytes. However, this would require the generation of transgenic lines which would allow the purification of sex-pure populations of gametocytes.

An example of such a line is the *PfDynGFP/PfP47mCHERRY* line generated by Lasonder and colleagues (2016) which expresses GFP (green) under the control of male gametocyte specific promoter and mCHERRY (red) under a female specific promoter. This line was successfully used to separate gametocytes into males and females by flow cytometry for their transcriptomic analysis (Lasonder *et al.*, 2016) and so males and females of this line could be separated for metabolomic analysis using the same method. An advantage of this line is that male and female gametocytes from the same culture could be directly compared, rather than having to use two separate transgenic lines. However, the authors noted that some gametocytes were both GFP and mCHERRY positive (thought to be stage IV) (Lasonder *et al.*, 2016) so a strict gating strategy would potentially have to be used during the sorting to ensure mature stage V male and female gametocytes were being compared.

This study also demonstrated, using MitoTracker labelling and DGFA analysis of gametocytes treated with mETC inhibitors (ATQ, ELQ-300 and oligomycin A), a direct link between inhibition of mitochondrial energy metabolism and impaired male gametogenesis. The fact that the mETC inhibitors showed a higher activity against male gametogenesis than female gametogenesis suggests that male gametogenesis may be more energy intensive. As previously mentioned, male gametogenesis appears to be more complex than female gametogenesis, therefore it seems plausible that the process might require greater support from mitochondrially produced ATP, whereas, if female gametogenesis is less energy intensive, perhaps glycolysis is sufficient to support it.

The observed  $IC_{50}$  values of ATQ and ELQ-300 against exflagellation in the DGFA are notably high compared to the nanomolar (subnanomolar in the case of atovaquone) activity of these drugs against asexual blood stage parasites. However, there are key differences in the action of these drugs against asexual parasites and gametocytes. Complex III in asexual blood stage parasites is only required to maintain ubiquinone turnover to support the function of the ubiquinone-dependent DHODH (Jacot *et al.*, 2016). Therefore, disruption of complex III results in disruption of DHODH and its essential role in pyrimidine biosynthesis, which asexual blood stage parasites cannot tolerate (Painter *et al.*, 2007; Ke *et al.*, 2015). However, disruption of DHODH has previously been reported to have no effect on gamete formation (Phillips *et al.*, 2015). This suggests that disruption of this process has no effect on gametocytes, which supports the notion that the observed effect of complex III inhibitors in the image analysis is due to disruption of mitochondrial ATP production rather than effects on other biosynthetic processes in the cell, such as pyrimidine biosynthesis by DHODH.

The finding that inhibition of mitochondrial respiration has an effect on exflagellation contradicts Ke and colleagues' previous finding (2015) that incubating WT NF54 gametocytes for 24 hours with 100 nM atovaquone had no effect on exflagellation. However, as 100 nM is close to the  $IC_{50}$  (~68 nM) for atovaquone, small variations in concentration or experimental setup could have a large effect on whether the parasites are able to exflagellate or not. Ke *et al.*, (2015) suggest that in addition to directly blocking mitochondrial energy production, mETC inhibition also prevents flux through the TCA cycle as well. Therefore, it is possible that the inhibition of gametogenesis with ATQ and ELQ-300 in my 24-hour DGFA could also be due to knock-on effects of perturbing other biosynthetic processes that rely on TCA cycle intermediates.

The  $IC_{50}$  of oligomycin A against male gametogenesis in the 24-hour DGFA was 303.9 nM, which is lower than a previously reported  $IC_{50}$  of 1.45  $\mu$ M against asexual blood stage parasites (Fry, Webb and Pudney, 1990). ATP synthase inhibitors are known to not be very

potent against asexual blood stage parasites, with  $IC_{50}$  values in the micromolar range (Basco and Le Bras, 1994). Asexual blood stages operate a minimal TCA cycle and the mETC is not for the purpose of generating ATP in these stages (Painter *et al.*, 2007; Sturm *et al.*, 2015). If mitochondrial ATP production is blocked, parasites can produce enough ATP for cellular processes through glycolysis. Whereas, if mitochondrially produced ATP is important for meeting the energy needs of exflagellation, then it makes sense that inhibition of this process would have a higher activity against exflagellation than asexual blood stage parasites. However, to date ATP synthase has not been successfully disrupted in *P. falciparum*, suggesting it is essential and has other roles outside of ATP production (Nina *et al.*, 2011). Perhaps, higher concentrations of ATP synthase inhibitors are required to disrupt these yet unknown processes to kill asexual blood stage parasites compared to the amount required to disrupt exflagellation. The fact that ATP synthase inhibitors show much higher activity against exflagellation than asexual blood stages suggests that inhibition of male gametogenesis is due to disruption of mitochondrial ATP production rather than off-target effects.

Interestingly, IFAs of gametocytes treated for 24 hours with the mETC inhibitors (10  $\mu$ M for ATQ and ELQ-300 and 50  $\mu$ M for oligomycin A) showed that while some had stalled at the 'rounding up' stage of male gametogenesis, many appeared to have progressed to the advanced stages of gametogenesis, having successfully formed flagella (although anti-alpha tubulin II labelling was frequently observed to be faint or punctate). Exflagellation centres in the DGFA are counted by an algorithm which detects the movement of the gametes egressing from the red blood cell. In the 24-hour DGFA 100% inhibition was observed by  $\sim$  5  $\mu$ M for oligomycin A and  $\sim$  1  $\mu$ M for the complex III inhibitors, suggesting that at concentrations higher than this, there would be little detectable movement of exflagellation centres. When the DGFA and IFA data is considered together, this shows that male gametocytes treated with these inhibitors can begin the process of gametogenesis, but the gametes can't properly escape the host erythrocyte and/or move. This demonstrates that the arrest of male gametogenesis observed in the DGFA is not because the mETC inhibitors have killed the gametocytes but that it is disrupting the process of exflagellation.

While it has been previously reported that DSM-265 does not have any effect on gametogenesis, it is surprisingly that inhibition of DHODH, even at a high concentration of 10  $\mu$ M, did not impact mitochondrial activity as measured by MitoTracker. DHODH is crucial to asexual blood stage parasite survival due its essential role in pyrimidine biosynthesis. However, in the mETC itself, DHODH is thought to function, at least in part, as a contributor of electrons to the downstream complexes, along with the other dehydrogenases at the start

of the mETC (Nixon *et al.*, 2013). If all these dehydrogenases have this role, then perhaps there is sufficient redundancy so that if one is inhibited, there are sufficient electrons provided by the others that the mitochondrial membrane potential can be maintained. It would be interesting to measure mitochondrial activity in gametocytes treated with DSM-265 in combination with inhibitors of NDH2, SDH (complex II), MQO and G3PDH. If mitochondrial activity is comparable to the control in gametocytes treated with DSM-265 alone but the mitochondrial membrane potential collapses when inhibitors of the other dehydrogenases are added, this suggests there is redundancy for the role of DHODH in the mETC.

In summary, the experiments presented in chapter 3 uncovered two key findings 1) male gametocyte mitochondria were found to be less active than those of females and 2) changes in mitochondrial activity resulted in arrest of gametogenesis. These results provide the first evidence that mitochondrial respiration is important for gametogenesis and that male and female gametocytes differ in their mitochondrial energy metabolism.

## **Chapter 4 Investigation into the essentiality of mitochondrial respiration for gametogenesis for *P. falciparum* gametocytes**

### **4.1 Introduction**

Despite entering a non-proliferative state, gametocytes of *P. falciparum* upregulate mitochondrial energy metabolism (MacRae *et al.*, 2013; Ke *et al.*, 2015). Mitochondrial respiration is a more efficient method of energy generation than glycolysis. Glycolysis generates a net total of 2 ATP molecules per glucose molecule, whereas oxidative phosphorylation can produce 34-36 (Kadenbach, 2003; Zheng, 2012). However, mature gametocytes are essentially dormant in the human host and greatly reduce their metabolic activity (Sinden and Smalley, 1979; Lamour *et al.*, 2014), which suggests that they require less ATP to fuel their reduced cellular processes. It is unknown whether the upregulation of mitochondrial respiration provides gametocytes with a 'buffer' or 'pool' of extra ATP which they could draw upon for onward development once taken up by a mosquito.

Whereas female gametocytes provide their mitochondrion and most of the cellular biomass to the new zygote (Okamoto *et al.*, 2009), male gametocytes are comparatively short-lived in the vector, shedding their mitochondrion during exflagellation and using glycolysis from then for their motility (Talman *et al.*, 2014). The fact that male gamete motility requires active glycolysis (Talman *et al.*, 2014) implies that male gametes cannot 'store' energy generated by the mitochondrion. If mitochondria aren't required for male gametocytes after exflagellation, one might imagine that if male gametocytes so possess an ATP 'pool', this might be used in combination with glycolysis to meet the energy demands of exflagellation, a highly complex, multi-step process.

The second aim of the project was to determine whether mitochondrial respiration was needed for gametogenesis. The data reported in the previous chapter suggests that mitochondrial respiration appears to be important for gametogenesis, which hasn't been shown previously. However, the gametocytes in the DGFAs were incubated for 24 hours with the inhibitors, so it could be argued that the inhibitors could be having other adverse effects on the gametocytes which are contributing to the observed reduction in exflagellation. To determine whether mitochondrial respiration is important for the process of gametogenesis itself, the effect of inhibition of mitochondrial respiration with no pre-incubation needed to be tested.

Glycolysis is known to be essential for male gametogenesis (Slavic *et al.*, 2011; Srivastava *et al.*, 2016). 2-deoxyglucose (2DG) is a commonly used tool in studying glycolysis. 2DG is an analog of glucose which has the 2-hydroxyl group replaced by hydrogen (Figure 4.1), which is taken up by the glucose transporters of cells. 2DG is converted to 2-deoxyglucose-6-phosphate (2DG-6P) by hexokinase, but 2DG-6P cannot be used by phosphoglucose isomerase in the next step of glycolysis (Schmidt and O'Donnell, 2021), making 2DG a competitive inhibitor of step 2 of glycolysis, the production of glucose-6-phosphate from glucose (Figure 4.2). Therefore, the addition of this inhibitor blocks glycolysis. In *P. berghei*, treatment with this inhibitor resulted in dose-dependent reduction in exflagellation, suggesting that glycolysis is essential for exflagellation (Srivastava *et al.*, 2016). Similarly, Slavic and colleagues found that treatment with a specific inhibitor of the *P. berghei* hexose transporter inhibited male gametogenesis (Slavic *et al.*, 2011). However, to date, this has not been confirmed for *P. falciparum*.

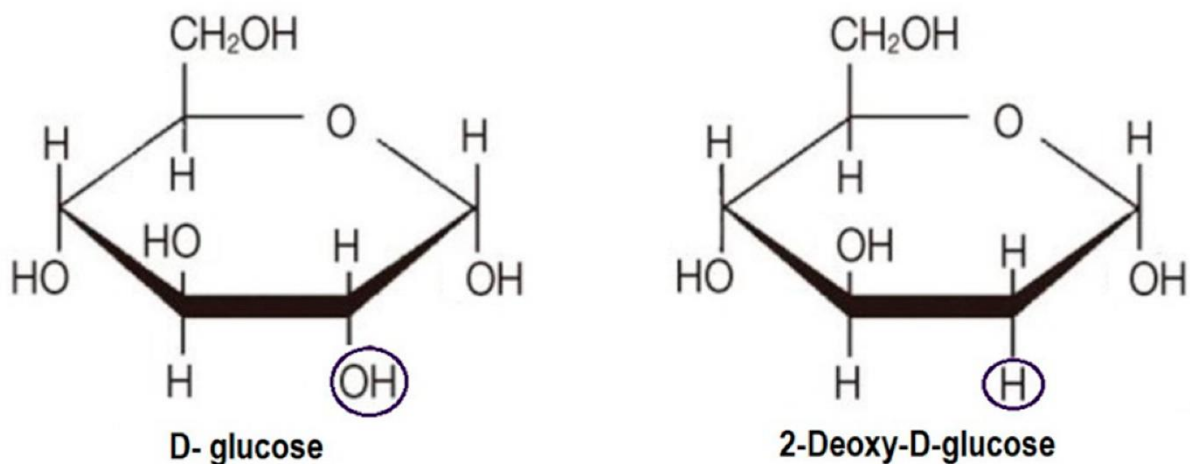


**Figure 4.1. Molecular structure of glucose and 2-deoxyglucose (2DG) originally from Pajak *et al.* (2020)** The position of the hydroxyl group in 2DG is indicated by the purple circle.

For female gametocytes, Srivastava and colleagues reported that *P. berghei* female gametogenesis was unaffected by treatment with 2DG, suggesting glycolysis was not required for female gametogenesis to occur (Srivastava *et al.*, 2016). However, they defined successful activation as emergence of the female gamete from the host red blood cell (egress). This measures whether the amount of egress is the same, not whether gametocytes have fully activated and can go on to be fertilised and undergo further development in the mosquito. This is important to determine as if the gametes egress but are non-functional then glycolysis is essential for female gametogenesis and transmission.

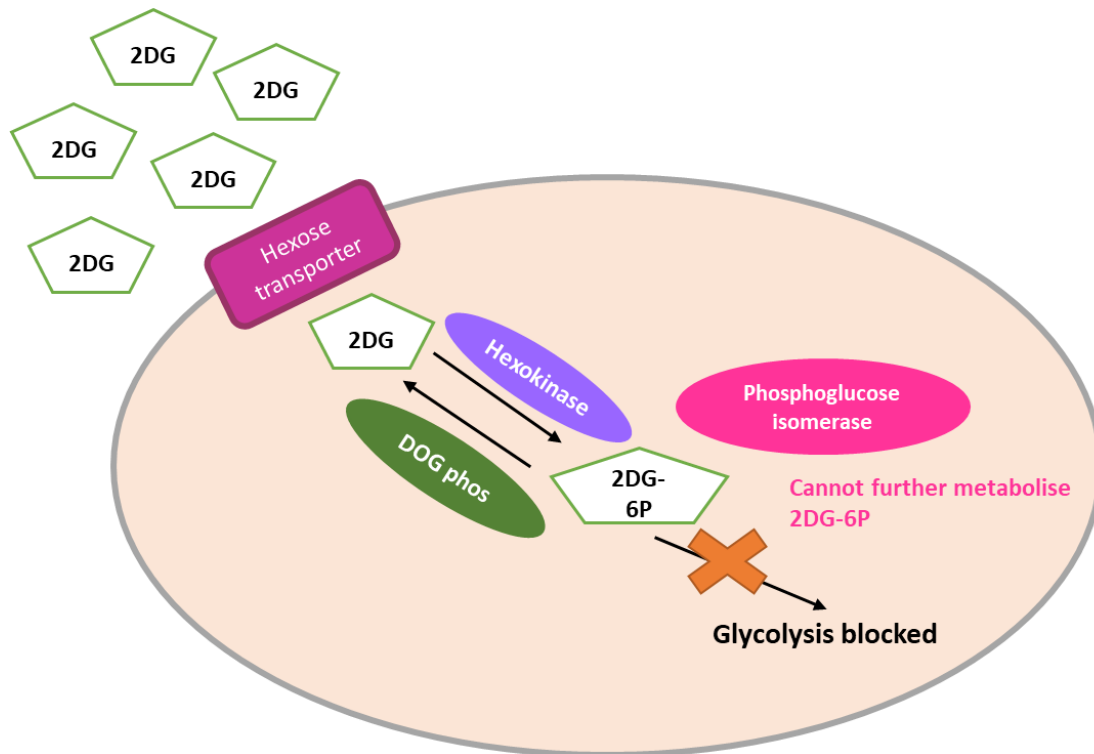


**Figure 4.2. Inhibition of glycolysis by 2-deoxyglucose (2DG).** Abbreviations: 2DG = 2-deoxyglucose, 2DG-6P = 2-deoxyglucose-6-phosphate, DOG phos = DOG (deoxyglucose) phosphatases.

In addition, metabolomic and experimental genetic studies of energy metabolism in *P. berghei* and *P. falciparum* have shown species-specific differences in the essentiality of enzymes and pathways on parasite survival, gametogenesis, and onward development in the insect vector. Therefore, the essentiality of glycolysis for male and female gametogenesis in *P. falciparum* also needed to be investigated specifically.

In the first part of this chapter, I aimed to address the following questions i) do male gametocytes have an 'energy store' that they can draw upon for exflagellation, ii) what is the minimum concentration of glucose required for exflagellation, iii) is glycolysis required for female activation and iv) is mitochondrial respiration required for normal gametogenesis in males and females or is glycolysis sufficient?

As previously mentioned, it is not known whether the increased use of mitochondrial energy metabolism in gametocytes (MacRae *et al.*, 2013; Ke *et al.*, 2015) allows them to build up a 'pool' of extra ATP which can be drawn upon for exflagellation by male gametocytes. To determine whether such a 'pool' is present, a method that allowed visualisation of changes in ATP levels in the gametocyte cell was required.

Genetically-encoded nanosensors have been developed for the measurement of ATP levels in cells (Imamura *et al.*, 2009; Tantama *et al.*, 2013; Lerchundi, Huang and Rose, 2020), which utilise Förster resonance energy transfer (FRET) between two fluorophores to visualise ATP levels.

FRET is a phenomenon where excitation is transferred from a donor to an acceptor fluorophore through long-range dipole-dipole coupling (Didenko, 2001; Sekar and Periasamy, 2003). As a result of this interaction the donor molecule fluorescence is quenched, and the acceptor molecule becomes excited and subsequently loses energy via heat or fluorescence emission (Didenko, 2001). When FRET occurs, the intensity of the donor fluorescence decreases, and the fluorescence intensity acceptor increases (Didenko, 2001). FRET can be used investigate biological phenomena that produce small changes in distance between two molecules (Sekar and Periasamy, 2003), for example, a protein-protein interaction. A schematic of the principle of FRET is shown in Figure 4.3.

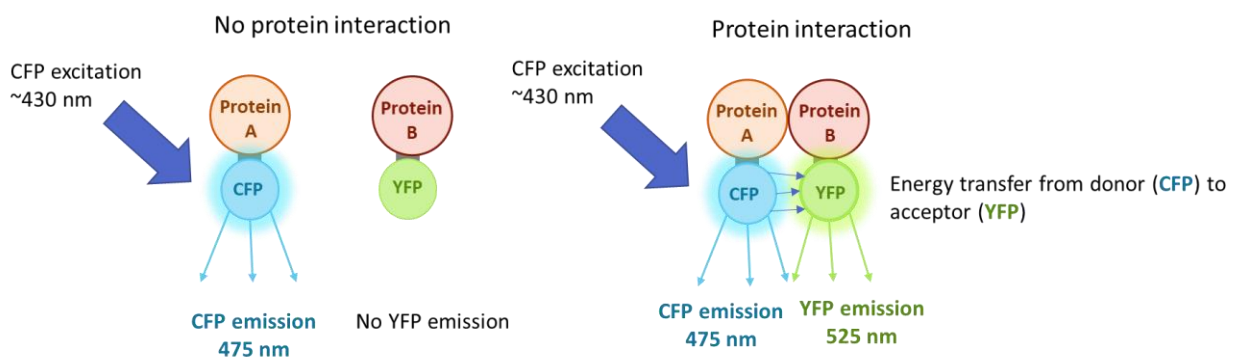


**Figure 4.3. The principle of Förster resonance energy transfer (FRET).** Abbreviations: CFP = cyan fluorescent protein, YFP = yellow fluorescent protein, nm = nanometers.

Examples of FRET-based ATP indicators are the ATeam sensors developed by Imamura and colleagues (Imamura *et al.*, 2009). The ATeams were generated by genetically linking mseCFP (variant of cyan fluorescent protein (CFP)) with mVenus (variant of yellow fluorescent protein (YFP)), each at either the N or C terminus of the  $\epsilon$  subunit of the Fo-F1-ATP synthase from *Bacillus subtilis* (Imamura *et al.*, 2009). A series of these nanosensors were generated with differing affinities to ATP ( $K_D$ ) by substituting the  $\epsilon$  subunit with that of a different bacteria species or by altering the amino acid residues at the domain interface (Imamura *et al.*, 2009).

The sensor functions as follows. The donor, eCFP, has a peak emission of 475 nm and the acceptor, mVenus, a peak emission of 527 nm (Imamura *et al.*, 2009; Lerchundi, Huang and Rose, 2020). The donor, eCFP, is excited at 435 nm (Imamura *et al.*, 2009). In the absence

of ATP, fluorescence emission of the donor at 475nm is high because less efficient transfer of energy occurs between the donor and the acceptor fluorophore. Whereas when ATP is bound to the ATP synthase  $\epsilon$  subunit, this results in a conformational change of the sensor protein which allows for more efficient energy transfer, leading to an increase in fluorescence emission at 527 nm (Imamura *et al.*, 2009; Lerchundi *et al.*, 2019). The eCFP/mVenus emission ratio can be calculated from CFP and YFP fluorescence images of individual cells captured on a widefield fluorescence microscope (Imamura *et al.*, 2009). A decrease the eCFP/mVenus emission ratio (the FRET ratio) indicates that ATP levels in the cell have decreased. A schematic drawing is shown in Figure 4.4.

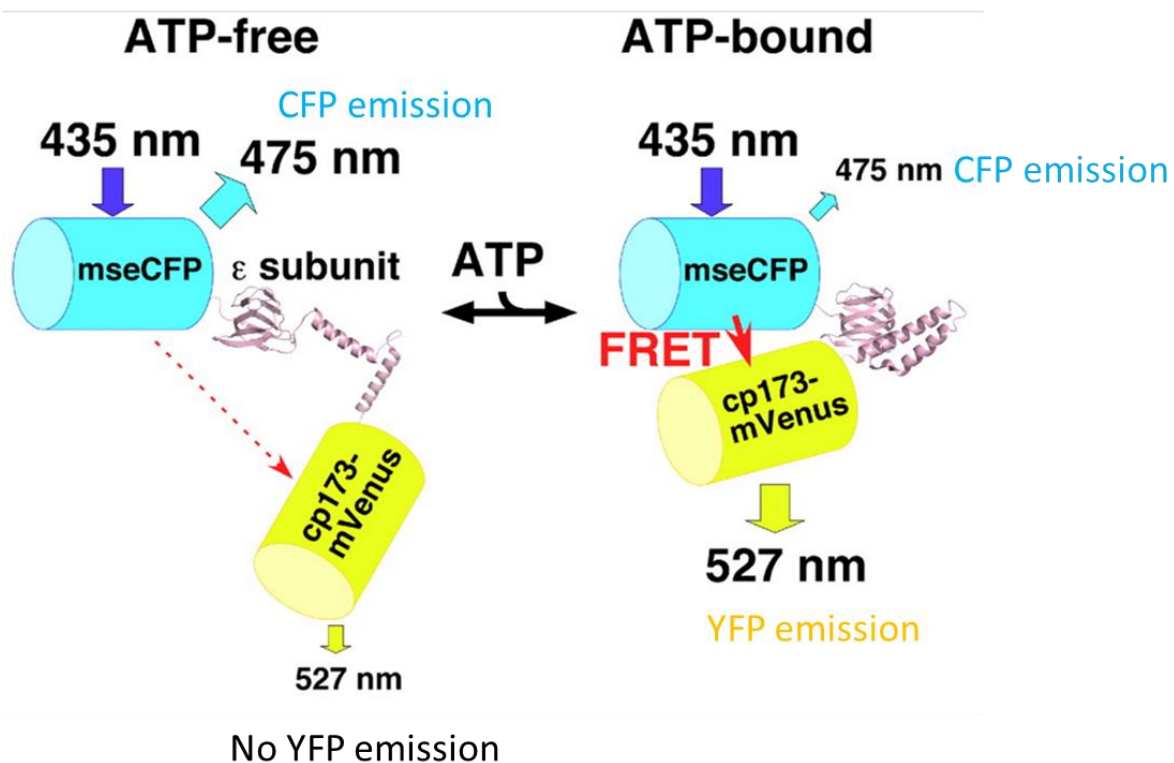


**Figure 4.4. Schematic of the ATeam FRET-based ATP probes, adapted from Imamura *et al.* (2009).** Abbreviations: nm = nanometre, mseCFP = variant of cyan fluorescent protein, cp173-mVenus = variant of yellow fluorescent protein,  $\epsilon$  subunit =  $\epsilon$  subunit of bacterial FoF1-ATP synthase, FRET = Förster resonance energy transfer.

To investigate ATP levels in gametocytes, NF54 asexual blood stage parasites were transfected with a plasmid for expression of an ATeam1.03YEMK sensor. This sensor has not been used in *P. falciparum* gametocytes previously. Plasmids for expression of these sensors in the cytoplasm were kindly gifted by Eric Springer and Jude Przyborski at the Justus Liebig University Giessen.

The constructs were designed for integration into a non-essential gene locus using site-specific integration mediated by mycobacteriophage Bxb1 integrase, which catalyses recombination between an incoming attP (phage attachment) site and a chromosomal attB (bacterial attachment) site (Nkrumah *et al.*, 2006). Therefore, to generate a transgenic parasite line with the ATP sensor fully integrated into the parasite genome, an NF54 parasite line with an attB site integrated into the genome would be required (Nkrumah *et al.*, 2006). However, it was unknown whether an NF54 transgenic line with an attB site would produce gametocytes as well as the wild type NF54 strain used in other parts of the project. Therefore, to keep the parasite line used consistent, it was decided to transfect the NF54 wild type parasites with the plasmids and select for episomal expression using blasticidin, as integration is not essential for the function of the sensor.

In the second part of this chapter, I present my preliminary data using NF54 gametocytes expressing the ATeam1.03YEMK sensor as an episome which lays the groundwork for future experiments.

## **4.2 Results**

### **4.2.1 Initial experiments comparing exflagellation under differing glucose availability**

To confirm whether glycolysis was required for exflagellation, gametocytes were triggered to exflagellate in culture medium with various glucose concentrations. Two pre-incubation times were chosen to investigate the short-term and long-term effects of each treatment – 1 hour and 24 hours respectively. These conditions were as follows:

- i) Glucose – medium containing 11 mM glucose + 10% human serum. This is the standard concentration of glucose in gametocyte culture medium.
- ii) Low glucose – glucose-free medium + 10% human serum (~1 mM glucose. The concentration of glucose in human serum is assumed to be 11 mM. However, as it's only 10% of the total medium volume, in the absence of any other glucose sources, it dilutes out to 1 mM in low glucose medium).
- iii) Low glucose + 2DG - glucose-free medium + 10% human serum (~1 mM glucose) + 11 mM 2DG. 2DG is a competitive inhibitor of glucose and so arrests glycolysis.

Following pre-incubation, the gametocytes were then transferred to media at room temperature containing these conditions plus 100  $\mu$ M xanthurenic acid (condition-matched ookinete medium) to trigger exflagellation. Samples were fixed for IFAs after 15 minutes and labelled with DAPI and an anti-alpha tubulin II antibody to visualise exflagellation centres.

In the 1-hour pre-incubation exflagellation assay (Figure 4.5), gametocytes incubated with normal concentrations of glucose (11 mM) showed morphologically normal exflagellation as expected. Gametocytes in the 'low glucose' treatment also exflagellated normally, demonstrating that, at least with 1-hour pre-incubation or less, exflagellation can proceed in low concentrations (~1 mM) of glucose. However, when 2DG was added to arrest glycolysis, male gametocytes did not progress past the 'rounding up' stage. No advanced exflagellation centres with fully formed male gametes were observed (examples of this in the glucose treatment is shown in Figure 4.5.) These results suggest that male gametocytes must use glycolysis and they do not have a sufficient 'pool' of extra ATP which they can draw upon to complete exflagellation. This supports that active glycolysis is essential for exflagellation in *P. falciparum* as well as *P. berghei*.

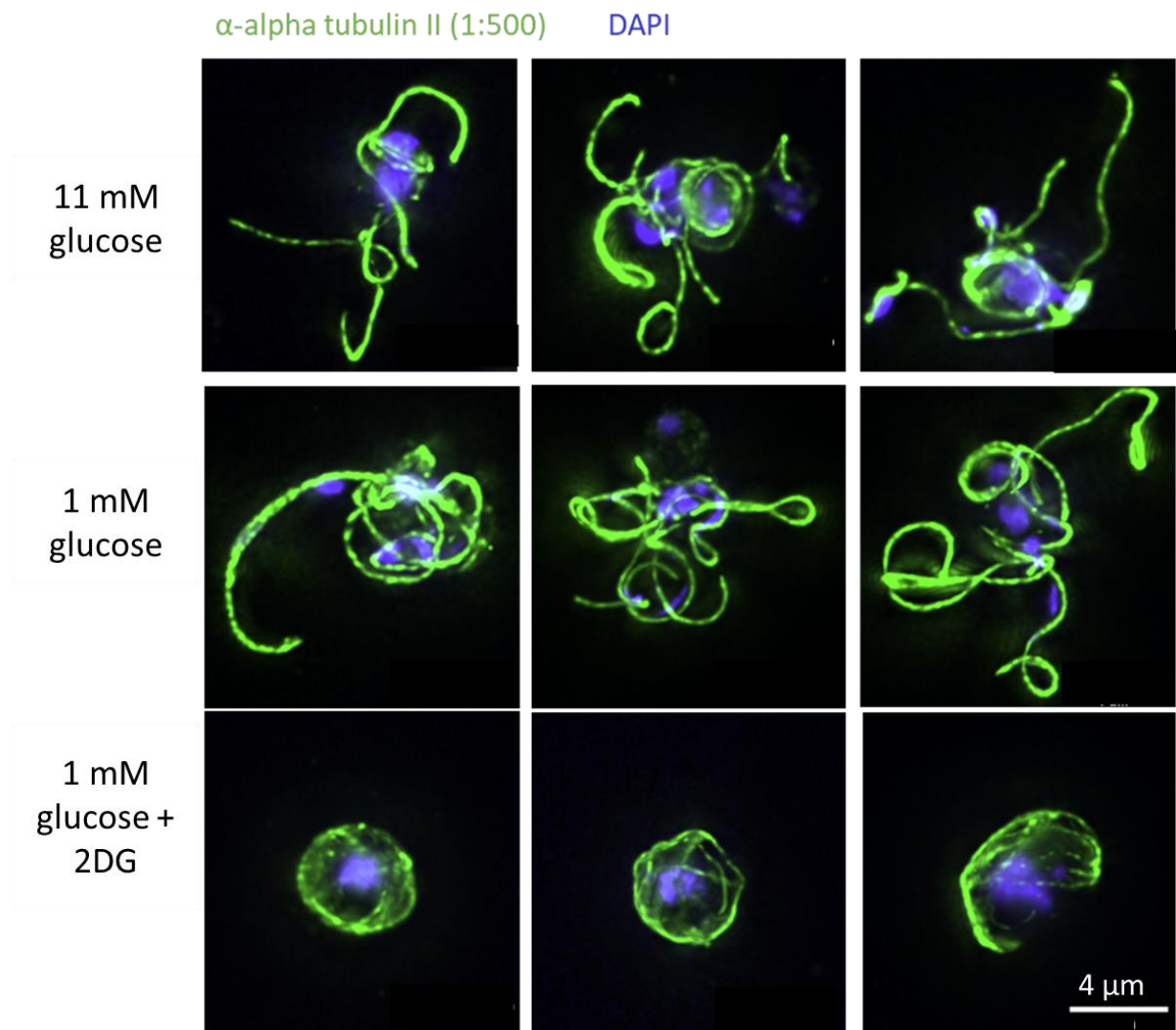


**Figure 4.5. Exflagellation male gametocytes pre-incubated for 1 hour in media with different glucose availability.** Exflagellation centres are labelled with the nuclear stain DAPI (blue) and anti-alpha tubulin II (green.)

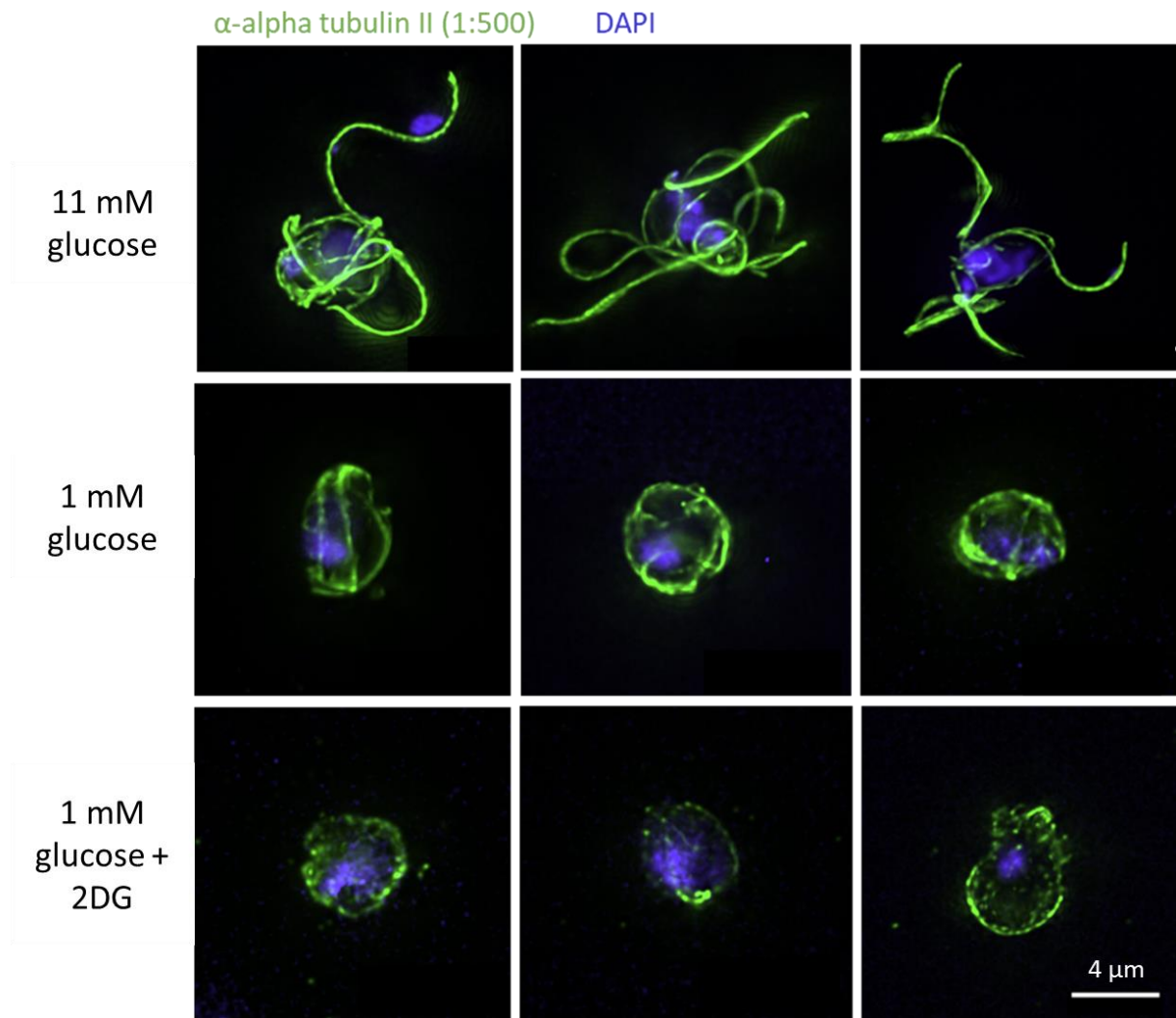


**Figure 4.6. Exflagellating male gametocytes pre-incubated for 24 hours in media with different glucose availability.** Exflagellation centres are labelled with the nuclear stain DAPI (blue) and anti-alpha tubulin II (green.)

The effect of 24-hour pre-incubation under these conditions was also compared (Figure 4.6). Gametocytes incubated for 24 hours under standard glucose concentrations showed morphologically normal exflagellation as expected. Gametocytes incubated in the 'low glucose' treatment did not proceed past 'rounding up'. Visually, the 'rounded up' cells resemble the phenotype observed in the 2DG-treated gametocytes at 1 hour. 2DG-treated gametocytes showed a similar but even more severe phenotype with faint or diffuse alpha tubulin II staining, suggesting that they fail to form flagella. However, it is interesting to note that the gametocytes have rounded up, therefore 24 hours of pre-incubation in 2DG has not killed the gametocytes. In the 'low glucose' and 'low glucose + 2DG' treatments, some gametocytes were able to replicate their DNA, the first stage of exflagellation, as shown by increased DAPI staining. However, many were not able to pass this step, showing an early arrest. This further supports that glycolysis is required for exflagellation because if the

gametocytes cannot utilise glucose (because utilisation of glucose blocked by 2DG or because the glucose has been depleted for 24 hours, in case of the low glucose treatment) then exflagellation cannot proceed.

However, several additional factors need to be considered. In *in vitro* culture of gametocytes, 10% human serum is the standard concentration used (Delves *et al.*, 2016). The concentration of glucose in the human serum used in the experiment is assumed to be ~11 mM. For comparison, the normal fasting glucose concentration in human blood is between 3.9 and 7.1 mM (70 and 130 mg/dL) (Danaei *et al.*, 2011), so the parasites in standard RPMI + 10% human serum have access to excess glucose. As the 'low glucose' treatment was composed of glucose-free medium and 10% human serum, the 'low glucose' treatment contains ~1 mM glucose. Therefore, it is possible that in the 1-hour preincubation experiment, the ~1 mM glucose provided by the serum in the 'low glucose' treatment is sufficient for exflagellation to proceed. Whereas, with 24 hours of pre-incubation the gametocytes may have already depleted the residual glucose in the medium and so were unable to complete exflagellation. In the 'low glucose + 2DG', utilisation of glucose would be blocked from the point of addition for both pre-incubation lengths, so exflagellation would be prevented in both cases.

Secondly, despite being a widely used glycolytic inhibitor, there is a considerable body of evidence that 2DG has off-target effects in eukaryotic cells (Steiner and Lester, 1972; Suzuki *et al.*, 1983; Ralser *et al.*, 2008; Zhong *et al.*, 2009). For example, in yeast, deletion of G6PD, the enzyme which links glycolysis and the pentose phosphate pathway, resulted in cells highly resistant to 2DG (Ralser *et al.*, 2008). This suggests that 2DG does not act solely by blocking glycolysis (Ralser *et al.*, 2008). This could explain why the 'low glucose + 2DG' treated gametocytes showed a more severe phenotype with 24 hours of pre-incubation as there could be more time for off-target toxic effects to occur.

These results confirm that glycolysis is essential for exflagellation. To investigate this further, experiments were designed to control for the possible confounding factors discussed above.

#### **4.2.2 Defining the minimum human serum concentration for exflagellation**

To determine whether gametocytes require exogenous glucose for exflagellation, I would ideally compare exflagellation levels of gametocytes incubated in medium containing standard levels of glucose (11 mM) to those incubated in glucose-free medium.

However, as previously stated, human serum contains glucose. Therefore, the minimum serum level at which exflagellation could occur needed to be determined to minimize glucose

as much as possible for the subsequent experiments but without other metabolic consequences to the gametocytes caused by the complete absence of serum.

Exflagellation of gametocytes was tested in glucose-containing and glucose-free medium with human serum (HS) concentrations of 10% (normal concentration), 2%, 1%, 0.1% and 0% (Figure 4.7). To do this, gametocytes were washed in warm media containing these serum levels and then activated in condition-matched ookinete medium (glucose-containing and glucose-free medium with 10%, 2%, 1% and 0.1% HS + 100  $\mu$ M xanthurenic acid) to trigger exflagellation. Exflagellation levels under different levels of HS were then compared.

In glucose-containing medium, exflagellation was observed at all serum concentrations. Exflagellation proceeded at comparable levels as long as at least 0.1% HS was present. If HS was absent, exflagellation levels were considerably lower and variable between replicates. This suggests that 0.1% HS in ookinete medium (100x lower than routinely used) is sufficient to fully support exflagellation. In the glucose-free ookinete medium, exflagellation declined in a dose-dependent manner as HS was titrated from the medium, as the amount of glucose available for glycolysis decreased. In contrast to glucose-containing medium, which provides the parasites with excess glucose, the glucose-free medium with only 0.1% HS (~0.1 mM glucose) did not support any exflagellation. This indicates that 0.1% is an appropriate serum concentration to provide male gametocytes with sufficient unknown factors required for exflagellation whilst not providing a confounding concentration of glucose for my onward experiments. Based on these results, 0.1% HS was selected as the minimum human serum level for subsequent experiments.

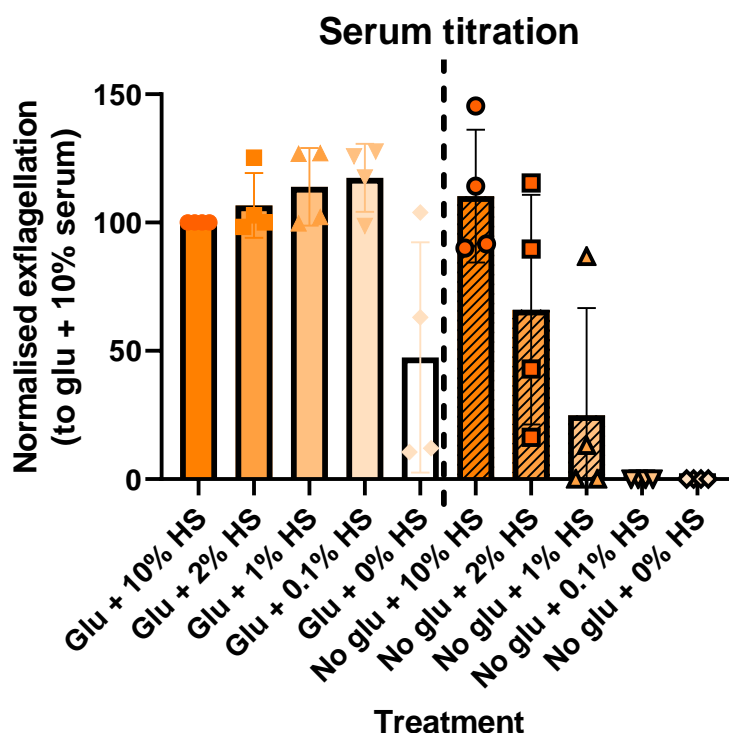


**Figure 4.7. Comparison of exflagellation of male gametocytes at different human serum concentrations.**  $n = 4$  biological replicates. The plain bars are the treatments in standard RPMI (11 mM glucose). The hatched bars are the treatments in no glucose RPMI. The glucose RPMI conditions are separated from the no glucose RPMI conditions by the dotted line. Abbreviations: glu = glucose medium (10 mM glucose), no glu = glucose-free medium, HS = human serum. In each biological replicate, exflagellation counts were normalised to the glucose + 10% human serum (Glu + 10% HS) which is the normal concentration of glucose (11 mM) and human serum in gametocyte medium. Error bars = SEM.

#### 4.2.3 Defining the minimum glucose level concentration required for exflagellation

Once the minimum serum concentration required for exflagellation to proceed under a normal glucose concentration had been determined, the next step was to define the minimum concentration of glucose required for exflagellation. Exflagellation was tested in gametocytes transferred into ookinete medium with 0.1% HS (provides ~0.1 mM glucose) and a range of concentrations of glucose from 1.1 mM (10x less than the normal glucose concentration in media, 11 mM) down to 0.03 mM (640x less than the normal glucose concentration in media). A control of glucose-free medium with no human serum was also included as a non-exflagellating control.

Gametocytes exflagellated maximally at 1.1-, 0.56- and 0.29-mM glucose. From 0.15 mM glucose (80x less than the normal glucose concentration), exflagellation reduced and was

absent by 0.05 mM. Dose response analysis calculated the concentration of glucose giving 50% exflagellation as 0.12 mM (Figure 4.8).

Overall, these results confirm that exflagellation is linked to the concentration of glucose available. This suggests that gametocytes do not have an 'energy store' of ATP and must actively use glycolysis to exflagellate successfully.

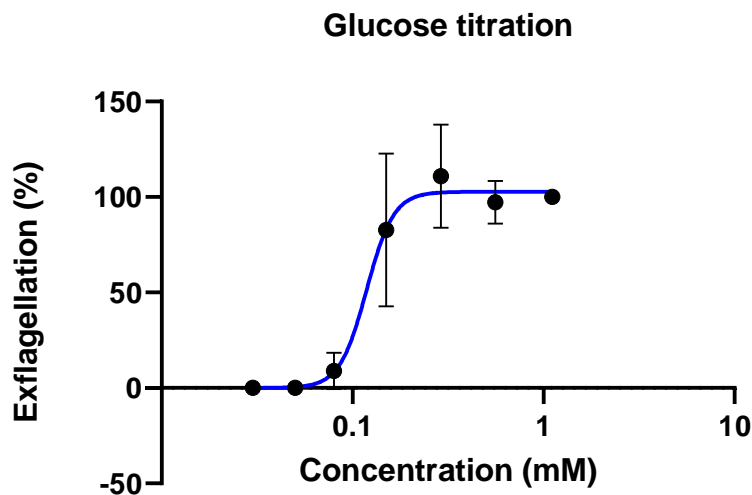


**Figure 4.8. Dose response analysis of the effect of glucose concentration on exflagellation.**  $n = 3$  independent experiments. The concentration of glucose that gave 50% exflagellation was calculated in GraphPad PRISM 9.

#### 4.2.4 Is mitochondrial respiration required for exflagellation?

By minimising confounding factors, the direct effect of glucose availability and mitochondrial respiration on male gametogenesis could now be better compared. NF54 WT gametocytes were triggered to exflagellate under the following conditions:

- i) 11 mM glucose + 0.1% human serum (HS) (~0.1 mM glucose): In this treatment, the gametocytes have access to the glucose concentration of standard RPMI. Therefore, both glycolysis and mitochondrial respiration will be unhindered. My previous experiment (Figure 4.7) showed that at this reduced concentration of human serum, exflagellation proceeded at a comparable rate to 10% serum but without substantially affecting the overall glucose concentration.
- ii) No glucose + 0.1% HS (~0.1 mM glucose): In this treatment, the gametocytes only have ~0.1 mM glucose contributed by the HS to use for glycolysis. My previous experiment (Figure 4.7) showed no exflagellation under these conditions.

- iii) 11 mM glucose + 0.1% HS (~0.1 mM glucose) + 5  $\mu$ M oligomycin A: In this treatment, the glucose concentration of standard RPMI is available to the parasites and glycolysis is unhindered but mitochondrial respiration is inhibited by oligomycin A, an ATP synthase inhibitor, which prevents the production of mitochondrial ATP. The concentration of glucose and HS used has been established to be permissive for exflagellation (Figures 4.7 and 4.8) but removes some of the confounding factors. This allows me to discriminate between the contributions of glycolysis and mitochondrial respiration to exflagellation. A concentration of 5  $\mu$ M was chosen for oligomycin A as it was the lowest concentration which consistently gave 100% inhibition in the DGFA presented in Chapter 3.

As expected, gametocytes in the 'no glucose + 0.1% HS' treatment showed no exflagellation. Gametocytes in the glucose-containing ookinete medium gave a mean exflagellation per field of 595.11 +/- 151.68 (SEM) (n= 3 independent experiments) (Figure 4.9). The exflagellation in the glucose treatment was normalised to 100% in each replicate. Addition of 5  $\mu$ M oligomycin A to glucose-containing ookinete medium considerably inhibited exflagellation, giving a mean 77.2% decrease in exflagellation. The marked reduction in male gametocytes that can successfully exflagellate suggests that mitochondrial respiration is important for exflagellation.

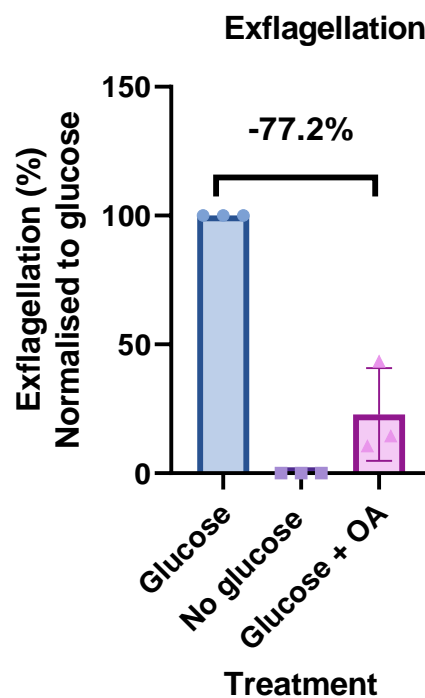


**Figure 4.9. Comparison of exflagellation in the absence of glucose and inhibition of mitochondrial respiration.** n = 3 independent experiments. Glucose = 11 mM glucose + 0.1% HS, no glucose = no glucose + 0.1% HS, glucose + OA = 11 mM glucose + 0.1% HS + 5  $\mu$ M oligomycin A. For each replicate, exflagellation levels for the low glucose and glucose + OA treatments are normalised to those observed in the glucose control. Error bars = SEM.

| Treatment                                      | % exflagellation (normalised to glucose) |        |        |        |
|--|--|--------|--------|--------|
|  | 1  | 2      | 3      | Mean   |
| <b>Glucose + 0.1% HS</b>                       | 100.00                                   | 100.00 | 100.00 | 100.00 |
| <b>No glucose + 0.1% HS</b>                    | 0.00                                     | 0.00   | 0.00   | 0.00   |
| <b>Glucose + 0.1% HS + 5 <math>\mu</math>M</b> | 10.53                                    | 43.45  | 14.41  | 22.80  |

**Table 4.1. % exflagellation with inhibition in the absence of glucose and inhibition of mitochondrial respiration.** n = 3 independent experiments. Abbreviations: HS = human serum, OA = oligomycin A, rep = technical replicate.

Exflagellation IFAs were also carried out on gametocytes activated under the three conditions to visualise the point of arrest during male gametogenesis. The results of the exflagellation assay are reflected in the morphology of the exflagellation centres observed in the exflagellation IFAs. Representative images of exflagellation centres observed in each treatment 20 minutes post activated are shown in Figure 4.10. Male gametocytes activated under normal glucose concentrations showed morphologically normal exflagellation. In contrast, in the ‘no glucose treatment’, male gametocytes did not progress beyond ‘rounding up’ in the 20-minute period, indicating an early arrest. However, it must be noted that rather than total arrest, the male gametocytes started the process of exflagellation. The cells also show only a small amount of DAPI staining (shown in blue in Figure 4.10), indicating that they have failed to replicate their DNA. This is consistent with the quantification of exflagellation where no exflagellation centres were observed in the ‘no glucose’ treatment (Figure 4.9, Table 4.1). The addition of oligomycin A appeared to result in aberrant or stalled gametogenesis. In the 20-minute period, male gametocytes frequently did not progress past the rounding up point as seen for the ‘no glucose’ treatment. Other cells undergoing male gametogenesis showed more advanced flagella formation but with abnormal morphology, with flagella appearing thick and as if stuck together rather than 6-8 distinct flagella. A few exflagellation centres did resemble those in the glucose condition with correctly formed

flagella, which is consistent with some gametocytes still being able to exflagellate under these conditions, as shown in the exflagellation assay.

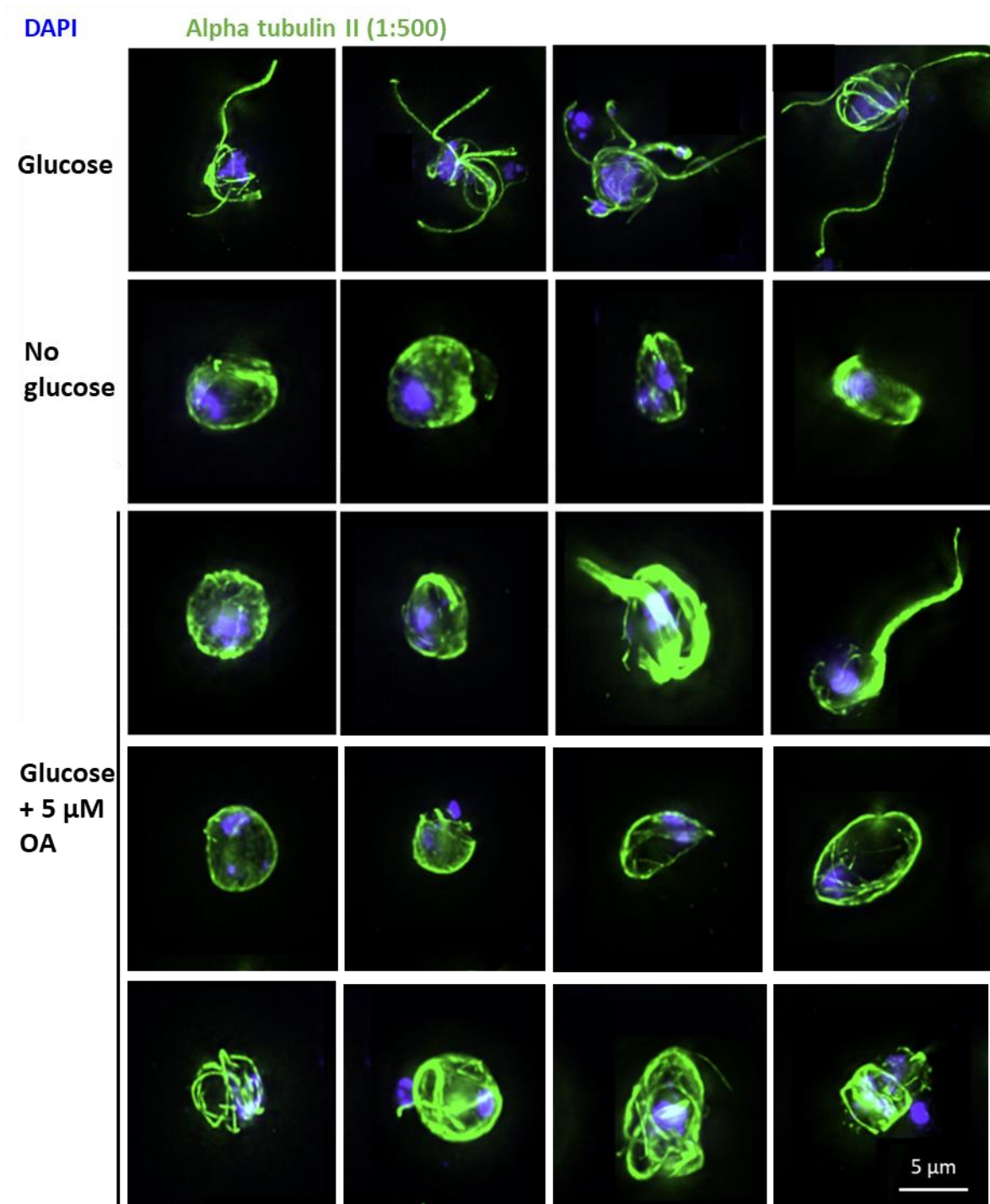


**Figure 4.10. Exflagellating male gametocytes in media with and without glucose and with inhibition of mitochondrial respiration.** Representative IFA images of male gametocytes triggered to exflagellate under the three different conditions with no pre-incubation. Cells were fixed at 20 minutes post-activation. **Top)** Glucose = 11 mM glucose + 0.1% human serum (HS). **Middle)** No glucose = No glucose + 0.1% HS. **Bottom)** Glucose + 5 μM OA = 11 mM glucose + 0.1% HS + 5 μM

oligomycin A. All exflagellation centres are labelled with DAPI (DNA stain) in blue and an anti-alpha tubulin II antibody (1:500 dilution) in green.

#### 4.2.5 Importance of glycolysis and mitochondrial respiration for female gametogenesis

Having determined that mitochondrial respiration is essential for optimal male gametogenesis, I then investigated its importance for female gametogenesis. Experiments were set up exactly as previously described for the male assay, however female gamete formation was measured by labelling with an anti-Pfs25 antibody, a protein expressed on the surface of activated female gametes. The % female activation (number of Pfs25+ve cells/number of red blood cells x 100) was compared for the different conditions.

| Condition   | % Female activation |       |       |      |
|---|---------------------|-------|-------|------|
|   | Rep 1               | Rep 2 | Rep 3 | Mean |
| <b>Glucose + 0.1% HS</b>                          | 5.43                | 6.80  | 9.35  | 7.19 |
| <b>No glucose + 0.1% HS</b>                       | 0.34                | 0.49  | 0.46  | 0.43 |
| <b>Glucose + 0.1% HS + 5 <math>\mu</math>M OA</b> | 0.75                | 2.35  | 3.68  | 2.26 |

**Table 4.2. % female activation with and without glucose and with inhibition of mitochondrial respiration.** n = 3 independent experiments. % female activation is the amount of Pfs25+ve cells (activated female gametes) as a proportion of red blood cells. Abbreviations: HS = human serum, OA = oligomycin A, rep = technical replicate.

Female gametocytes exposed to a normal glucose concentration showed mean 7.19% female activation (Figure 4.11). Female activation was markedly reduced in the ‘no glucose + 0.1% HS’ treatment which showed only 0.43% activation, a ~94% decrease compared to normal glucose levels. This reduction was statistically significant (students’ unpaired t-test, p = 0.0042). The ‘glucose + 0.1% HS + 5  $\mu$ M oligomycin A’ treatment also showed a significant reduction in female activation compared to normal glucose levels (students’ unpaired t-test, p = 0.0259), with mean female activation reduced to 2.26%, a ~69% decrease in activation.

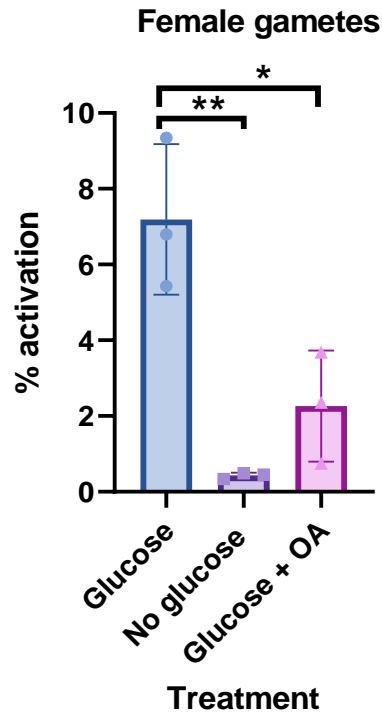


**Figure 4.11. Female gamete activation with and without glucose and with inhibition of mitochondrial respiration.** n = 3 independent experiments (range of total gametes counted: 363-942). Female gamete activation = number of Pfs25+ve cells/number of red blood cells x 100). Glucose = 10 mM glucose + 0.1% HS, no glucose = no glucose + 0.1% H, glucose + OA = 10 mM glucose + 0.1% HS + 5  $\mu$ M oligomycin A. Statistical comparisons are Student's unpaired t-tests, \*\* = p<0.005, \* = p<0.05. Error bars = SEM.

In summary, these experiments demonstrate that mitochondrial respiration is required for efficient male and female gametogenesis.

#### 4.2.6 Real time visualisation of ATP utilisation in *P. falciparum* gametocytes by FRET

##### Successful generation of NF54 parasites with episomal expression of a genetically encoded ATP indicator

NF54 asexual blood stage parasites were successfully transfected with a cassette for driving cytoplasmic expression of an ATeam1.03YEMK ATP sensor. Parasites expressing the sensor as an episome, which were visibly fluorescent, were recovered in the culture ~2 weeks after transfection under blasticidin selection (Figure 4.12).

The next step was to confirm that the transfected parasites could still form gametocytes. It was observed that the asexual blood stage parasites transfected with the ATP sensors replicate slowly compared to un-transfected NF54 asexual blood stage parasites, with

around a doubling of parasitaemia at each cycle compared to around 6-10-fold with the parental line. This suggests that the sensor imposes a fitness cost on the parasite which is detrimental to parasite growth. The ATeam1.03YEMK sensor is composed of the  $\epsilon$  subunit of a bacterial ATP synthase sandwiched between a CFP and YFP. The  $\epsilon$  subunit can bind ATP, therefore it is possible that the sensor binds ATP in the cell, diverting it away from other cellular processes important for parasite replication and thus slowing growth.

This is problematic for gametocyte formation as normally asexual blood stage parasitaemia increases rapidly to a peak on day 4 after induction (Delves *et al.*, 2016) and stress produced by high asexual parasitaemia induces gametocyte formation (Chaubey, Grover and Tatu, 2014; Delves *et al.*, 2016). ATeam1.03YEMK-expressing asexual cultures were maintained on blasticidin and gametocyte cultures seeded at 2% parasitaemia. Blasticidin was then removed from the gametocyte culture to allow the parasitaemia to increase sufficiently to induce gametocyte development.

On reaching maturity, stage V gametocytes had developed which were visibly expressing the sensor, though there was some variation in intensity (Figure 4.12). This is likely because multiple copies of episomes can be present in the parasite cell so parasites with more copies will show a greater fluorescence intensity. In addition, episomes are not necessarily stably inherited. When trophozoites segregate into schizonts, a given merozoite may end up with greater or fewer copies of the episome relative to other merozoites or none.

Considering the observed fitness costs of the ATeam1.03YEMK sensor, episomal expression is likely a more suitable approach for studying ATP levels in gametocytes than genomic integration, as the latter could result in permanent slow growth, severely hampering the ability of the line to form gametocytes. In addition, the fact that multiple copies of the episome can be present with episomal expression could also provide an advantage over integration, as a brighter signal could be observed than with integration which could have only one copy of the gene encoding the sensor.

Gametocytes expressing the ATeam1.03YEMK sensor were cultured and a series of experiments performed to i) demonstrate that the sensor could measure real-time changes in ATP levels in gametocytes and ii) to investigate the rate of ATP depletion in gametocytes which has never been investigated previously.

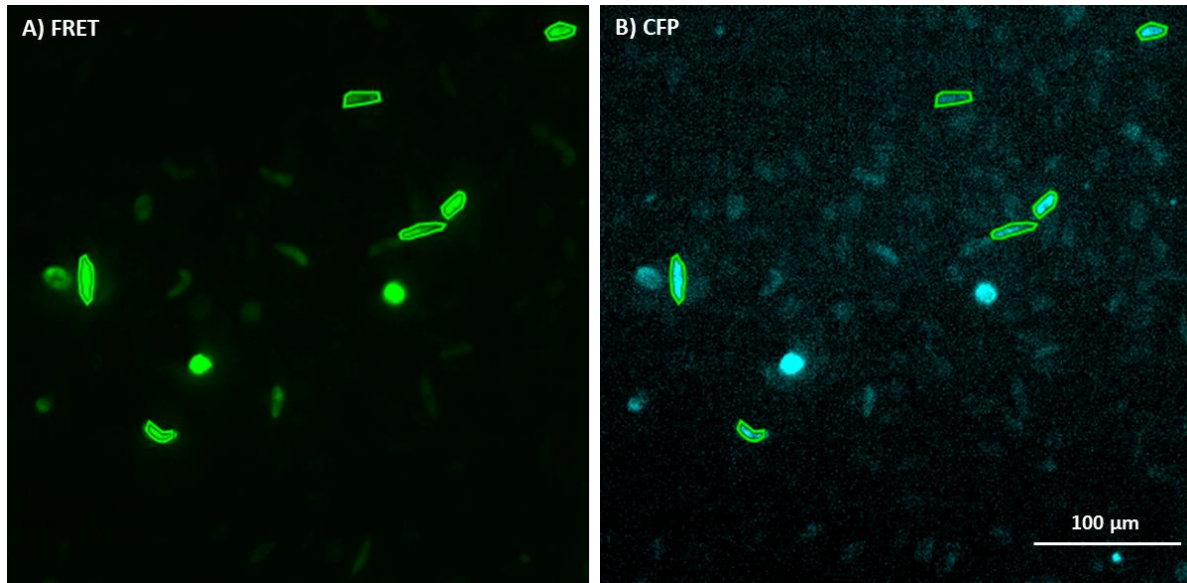


**Figure 4.12. Images of stage V gametocytes expressing the ATeam1.03YEMK sensor. A)** FRET channel: YFP FRET emission if CFP is excited, which occurs when ATP is bound to the sensor and FRET occurs. **B)** CFP channel: this channel measures CFP emission only. When ATP is unbound, the fluorophores are further away from each other, and FRET does not occur. Regions of interest (green polygons) were drawn around the gametocyte cells in ICY BioImage Analysis Software. The FRET ratio is calculated of given cell is calculated by dividing the mean intensity of fluorescence from the FRET channel by that from the CFP channel. Abbreviations = FRET = Forster resonance energy transfer, CFP = cyan fluorescent protein, YFP = yellow fluorescent protein. Images were taken on a Nikon TiE widefield fluorescence microscope.

#### **ATP depletion in gametocytes in the absence of glucose can be visualised by FRET**

The aim of this experiment was to determine whether the episomally expressed ATeam1.03YEMK sensor would enable the depletion rate of cellular ATP within the gametocytes to be measured after glucose removal. As ATP levels in gametocytes have not been previously measured using this method, it was unknown over what time scale any changes in intracellular ATP concentration would be observed. A pilot study was conducted to determine if detectable changes in intracellular ATP concentrations could be observed in gametocytes in glucose-free medium. A long-term incubation of 95 minutes was piloted first.

It was found that gametocytes in glucose maintained a stable and higher FRET (ATP/ADP) ratio (indicative of higher intracellular ATP concentration) than those in glucose-free medium (Figure 4.13). This is expected as in the 'glucose' treatment, gametocyte can utilise glucose to generate ATP using both glycolysis and mitochondrial respiration, so the ATP levels remain constant. In the absence of glucose, gametocyte cannot generate new ATP via glycolysis or mitochondrial respiration so the ATP levels in the cell are lower. The FRET ratio in the 'no glucose' treatment showed a slow decline over the 95-minute period and was

notably lower than that of the gametocytes in the 'glucose' treatment at the first measurement (20 minutes incubation). This suggests that the FRET ratio had already declined from a level seen in the glucose treatment (mean FRET ratio of ~18) within this 20-minute period. This suggests that the intracellular ATP concentration substantially drops before the first measurement 20 minutes after withdrawing glucose, and then continues to decrease gradually.

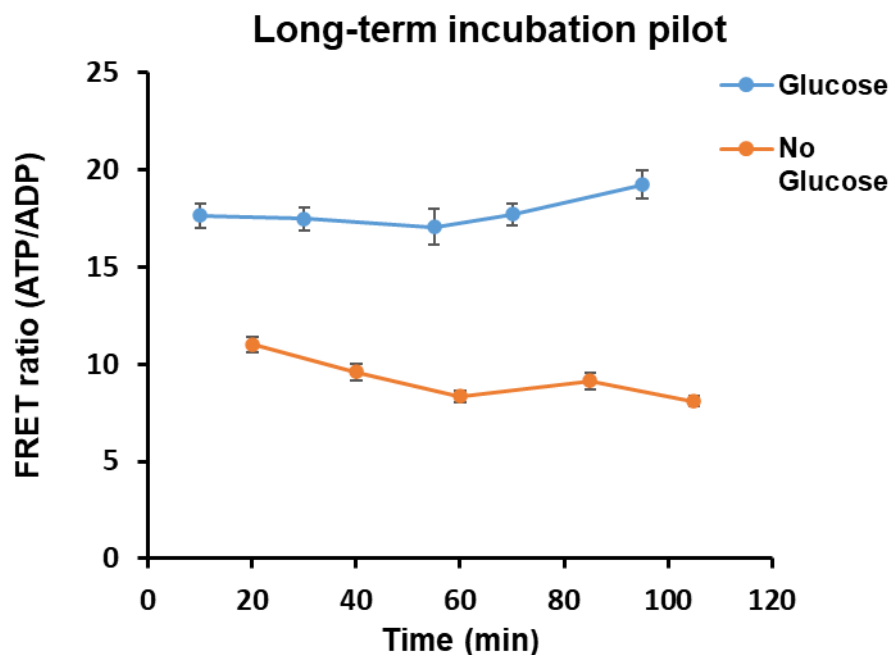
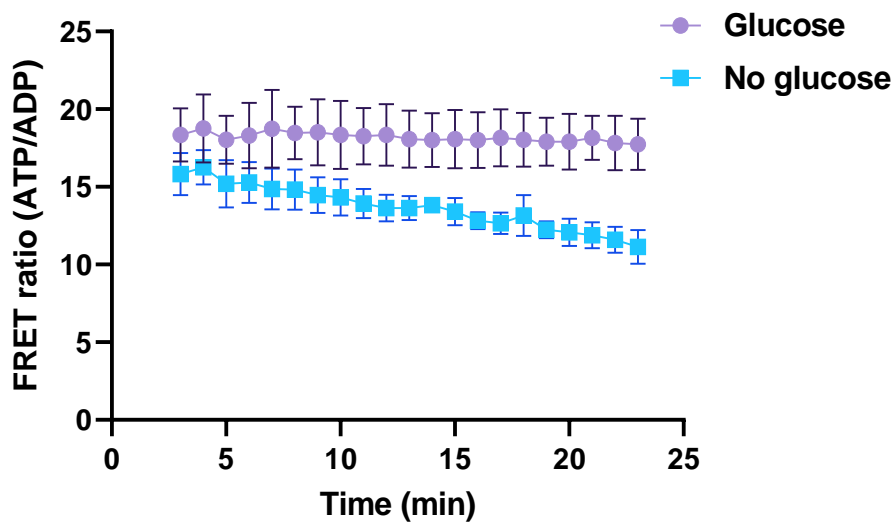


**Figure 4.13. Comparison of the FRET ratio (ATP/ADP) in gametocytes incubated in glucose versus no glucose (long-term pilot experiment).** Only 1 replicate was completed as it shows that the depletion of most of the intracellular ATP likely occurs before 20 minutes of incubation with no glucose, so a 20-minute incubation was chosen for subsequent experiments. Number of gametocytes measured per time point (min-max): glucose = 27-87, no glucose = 65-85. Error bars = SEM.

In summary, parasites with episomal expression of an ATeam1.03YEMK sensor can be used to measure the resting ATP levels in stage V gametocytes. It was concluded that 20 minutes of incubation with no glucose was too late to observe the drop in ATP levels in the gametocyte cell. Therefore, it was decided to repeat the experiment with a short-term time course, sampling at 1-minute intervals over a 20-minute period. The first reading is taken at 3 minutes after washing and transferal into PBS/PBS-glucose because this was found to be the minimum handling time to transfer the washed gametocytes to the slide and allow them to settle sufficiently for imaging.

The gametocytes in glucose maintained a constant high ATP ratio of ~18-19 over the 20-minute time course, suggesting that ATP levels did not decline over this period (Figure 4.14). This is expected as excess glucose is available for both glycolysis and mitochondrial respiration so the gametocytes should be able to maintain their ATP levels. In contrast, in the gametocytes in glucose-free medium, the FRET ratio decreased from 15 to 11 over the 20-minute period, indicating a decline in cellular ATP levels. These data are consistent with cellular ATP being depleted in the no glucose treatment as the gametocytes cannot use either glycolysis or mitochondrial respiration to generate new ATP. It must be noted that the FRET ratio in the 'no glucose' treatment does not reach a plateau which does suggest a longer time course could show the end of the decline.

### Glucose vs no glucose



### Addition of OA

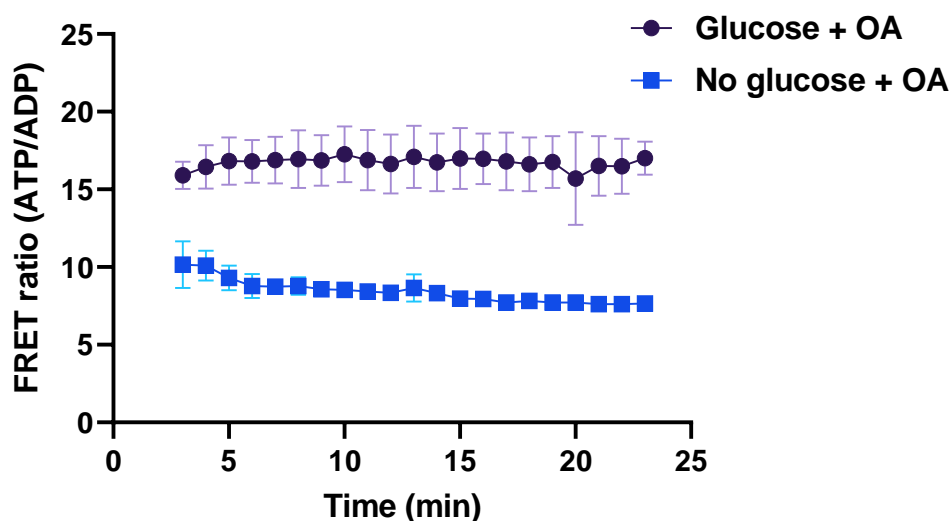


**Figure 4.14. Comparison of the FRET ratio (ATP/ADP) in gametocytes in media with and without glucose over 20 minutes. Top)** Glucose versus no glucose. Data from 3 independent experiments. Number of gametocytes per time point (min-max): no glucose = 3-20, glucose = 4-11. Error bars = SEM. **Bottom)** With and without glucose + the complex V inhibitor oligomycin A (5  $\mu$ M) over 20 minutes. Abbreviations: OA = oligomycin A. Data from 3 independent experiments. Number of gametocytes per time point (min-max): glucose + OA = 3-11, no glucose = 4-10. Error bars = SEM.

### **Blocking mitochondrial respiration further decreases ATP concentrations**

The intracellular ATP concentration was shown to steadily decline in gametocytes in conditions without available glucose over a 20-minute period. This suggests that cellular ATP is being depleted in the 'no glucose' treatment as the gametocytes cannot use either glycolysis or mitochondrial respiration to generate new ATP.

The next question was whether inhibiting mitochondrial respiration would i) reduce the amount of ATP produced under normal levels of glucose and ii) exacerbate the depletion of ATP in gametocytes without glucose available.

In the 'glucose + oligomycin A' treatment, the FRET ratio remained constant across the 20-minute period and the values were in a similar range to the 'glucose' treatment from the previous experiment (Figure 4.14, top). This suggests that if excess 'glucose' is available, intracellular ATP levels are not affected by inhibition of mitochondrial respiration. This indicates that gametocytes can meet their energy needs using glycolysis. This implies that the upregulation of mitochondrial respiration is not required to meet the needs of the gametocyte itself, which might be expected if gametocytes are quiescent in the human host.

In the 'no glucose + oligomycin A' treatment, the FRET ratio declines from  $\sim$ 10 to 7 over the 20-minute period (Figure 4.14, bottom). In the first experiment comparing glucose and no glucose (without oligomycin A) (Figure 4.14, top), the FRET ratio declined from  $\sim$ 15-11. The FRET ratio is lower at first measurements (three minutes) in the 'no glucose + oligomycin A' treatment than the 'no glucose' treatment, suggesting that the intracellular ATP concentration in the 'no glucose + oligomycin A' treatment have already declined within these first three minutes. This suggests that inhibition of mitochondrial energy metabolism with oligomycin A is having an additional detrimental effect on cellular ATP levels.

To summarise the data, ATP levels in gametocytes remain constant over a 20-minute period in excess glucose whereas a decline is observed in gametocytes in no glucose over this same period. This is because gametocytes have no available glucose for glycolysis, their intracellular ATP levels decline. When glucose is present, oligomycin A does not impact the ATP level of the gametocyte cell. This suggests that in excess glucose, glycolysis alone is

sufficient to maintain intracellular ATP levels. Whereas in the 'no glucose + oligomycin A' treatment, the ATP levels have fallen faster than my method can measure.

The slower decline in intracellular ATP observed in the 'no glucose' alone compared to the 'no glucose + oligomycin A' treatment suggests that if glucose is absent but mitochondrial respiration is unhindered, the gametocyte can prolong ATP production from the glucose it has already internalised using this route. Whereas if mitochondrial respiration is inhibited by oligomycin A, the gametocyte can only use the comparatively inefficient energy generation method of glycolysis, hence the sharp drop in the ATP/ADP ratio.

### 4.3 Discussion

The DGFA data presented in Chapter 3 indicated that mitochondrial respiration was required for optimal exflagellation. However, greater effects of the mETC inhibitors were seen with the long pre-incubation time of 24 hours compared to the 1-hour pre-incubation. To understand more about the direct effect on gametogenesis without any potentially confounding effects on the gametocyte, inhibition of energy metabolism during gametogenesis was studied in detail.

Having optimised the minimum serum level required for gametogenesis, I showed that, below a certain concentration of glucose, exflagellation is completely inhibited. This supports previously published data that active glycolysis is essential for exflagellation (Slavic *et al.*, 2011; Srivastava *et al.*, 2016). These data also suggest that there is either no intracellular 'pool' of extra ATP or, if one is present, it is not sufficient to complete exflagellation.

Female gametogenesis was markedly reduced (~94% decrease) in the absence of glucose but, at least according to the readout of proportion of Pfs25+ve cells, was not completely inhibited. However, the 'no glucose' treatment did contain ~0.1 mM glucose provided by the 0.1% human serum which may be sufficient for female gametogenesis, but not male gametogenesis, to occur. However, it was frequently observed that, while the Pfs25+ve cells in this treatment had the distinctive ring pattern of Pfs25 expression (on the gamete surface), the staining was frequently fainter than in the 'no glucose' than the 'glucose' treatment, which suggests these cells may be 'incompletely' activated female gametes which may not be fertile in the mosquito. Therefore, the difference may also reflect the different ways used to assess gametogenesis between the sexes.

The exflagellation and female activation assays with no pre-incubation with oligomycin A showed that mitochondrial respiration is important for gametogenesis. Even in the presence of excess glucose, inhibition of mitochondrial ATP production by 5  $\mu$ M oligomycin A gave a

77% reduction in exflagellation. If mitochondrial respiration was not important for exflagellation, similar levels of exflagellation would be observed between the 'glucose' and 'glucose + oligomycin A' treatments, whereas a substantial reduction was observed, suggesting mitochondrial respiration is required for efficient exflagellation. The addition of oligomycin A also inhibited female gametogenesis, though a lower decrease relative to the glucose treatment (~69%) was observed compared to exflagellation. This is consistent with the DGFA results where oligomycin A was shown to have less of an inhibitory effect on female compared to male gametogenesis.

In addition, oligomycin A is a reversible inhibitor. A follow-up experiment would be to wash the gametocytes in the 'glucose', 'no glucose' and 'glucose + oligomycin A' treatments as for the above experiment but instead of condition-matched ookinete medium, trigger exflagellation in all three treatments with 'glucose' ookinete medium. If removal of the ATP synthase inhibitor restored exflagellation, this would suggest that then results observed with oligomycin A were due to inhibition of ATP synthase rather than off-target effects of the inhibitor damaging the cell.

Immunofluorescence images of exflagellating male gametocytes treated with oligomycin A showed that they begin to undergo gametogenesis but the process stalls. As with the exflagellation IFAs of gametocytes treated with the mETC inhibitors for 24 hours presented in Chapter 3 (Figure 3.27), this demonstrates that the inhibitor is not killing the gametocyte but that it is affecting the process of exflagellation itself. This stalling indicates that when mitochondrial respiration is disrupted, male gametocytes cannot generate enough ATP to complete the process of exflagellation.

It is curious that the male gametocytes treated for 24 hours with 50  $\mu$ M oligomycin A appears to have a less severe phenotype by IFA than those treated with 5  $\mu$ M with no-preincubation. A possible explanation for this is that these two experiments were carried out with different human serum (HS) concentrations. Many drugs can bind to human serum albumin which can interfere with their pharmacokinetic properties (Banker and Clark, 1976; Koch-Weser and Sellers, 1976; Yang, Zhang and Liang, 2014). If oligomycin A binds to serum, then in the 24-hour assay, which used medium containing 10% HS, more oligomycin A could have been serum-bound and so less available to affect the cells. Whereas in the assay with no pre-incubation 0.1% HS was used, so there would be much less serum to absorb oligomycin A, allowing more to interact with the parasite. If the 24-hour IFA was repeated with 0.1% HS, a more severe phenotype may be observed.

To further investigate the exflagellation phenotypes, the IFAs could be repeated with an erythrocyte marker such as such as fluorophore-labelled wheat germ agglutinin or anti-glycophorin A, to test whether the gametes successfully egress from the erythrocyte. If it can be shown that the male gametes' axonemes can form but that they remain encased within the erythrocyte, this would suggest that inhibiting mitochondrial respiration compromises male gamete egress. To be clear, this would not be due to the male gametes lacking energy as they use glycolysis for ATP generation, but if the gametocytes cannot produce enough ATP for cellular processes to properly form flagella during gametogenesis, the resultant gametes may be damaged and not move in the correct way. Perhaps a lack of mitochondrial ATP could also affect the release of secreted proteins involved in egress so the gametes cannot escape the host cell. Live microscopy could also be used to assess whether the ability of gametes to egress from the erythrocyte is impacted or if the gametes are immotile due to the flagella being incorrectly formed. Electron microscopy of exflagellating male gametocytes treated with oligomycin A would allow the abnormal flagella morphology to be visualised in fine detail and to determine whether the individual gametes are structurally abnormal or whether multiple gametes are tangled or adhered together.

*P. falciparum* gametocytes undergo a prolonged development in the human host which takes ~10 days, whereas in most other *Plasmodium* species, it takes 1-3 days. However, following uptake into the mosquito, gametogenesis, fertilisation, and subsequent development is similar between *P. falciparum* and, for example, *P. berghei*. A possible extension to this work would be to revisit the effect of inhibiting mitochondrial respiration on exflagellation in *P. berghei*. If the upregulation of mitochondrial energy metabolism in male gametocytes is required for efficient exflagellation, it might be expected that inhibition of mitochondrial respiration would also result in impaired exflagellation in *P. berghei*. Alternatively, if inhibition of mitochondrial respiration does not affect *P. berghei* exflagellation, this might indicate that mitochondrial respiration has a role related to the prolonged development of *P. falciparum* gametocytes in the human host.

These results suggest that mitochondrial respiration is essential for efficient gametogenesis, particularly male gametogenesis.

Mature gametocytes are known to greatly reduce their metabolic activity in the human host (Sinden and Smalley, 1979; Lamour *et al.*, 2014) suggesting they require less ATP to fuel their cellular processes. However, they upregulate mitochondrial energy metabolism (MacRae *et al.*, 2013; Ke *et al.*, 2015), a more efficient form of energy generation (Kadenbach, 2003; Zheng, 2012). It has not been investigated whether upregulation of mitochondrial respiration in gametocytes could be beneficial in adverse environmental

conditions, such as low glucose availability, as it would allow them to utilise the available glucose more efficiently. To investigate this, transgenic parasites were generated which episomally express an ATP biosensor which allowed visualisation of dynamic changes in intracellular ATP concentrations by FRET microscopy in response to glucose deprivation and inhibition of mitochondrial respiration.

It was found that the ATP/ADP ratio in gametocytes remained constant over 20 minutes when excess glucose was present, even with the addition of oligomycin A, suggesting that glycolysis is sufficient to meet the energy needs of a mature gametocyte in the human host. In the 'no glucose' condition, the ATP/ADP ratio declined over a 20-minute period. In the 'no glucose + oligomycin A' treatment, the ATP/ADP ratio dropped more rapidly than can be measured with this technique. This suggests that mitochondrial respiration in gametocytes may be important for more efficient conversion of available or already internalised glucose to ATP, in conditions where glucose is limited. Taken together, these data support the hypothesis that the purpose of the upregulation of mitochondrial respiration in gametocytes is not for energy generation in the human host but is more likely to meet the energy demands of gametogenesis and onward mosquito development.

This promising preliminary set of results has raised new insights into gametocyte energy metabolism which require further investigation.

Firstly, gametocytes are known to upregulate their mitochondrial energy metabolism, but it is still unknown whether gametocytes can actively regulate their mitochondrial activity in response to reduced glucose availability so that available or already internalised glucose is utilised more efficiently. My data showed that providing mitochondrial respiration is active, intracellular ATP in gametocytes declines very slowly in the absence of glucose, whereas when mitochondrial respiration is inhibited ATP concentrations drop rapidly. This suggests that mitochondrial respiration could be enabling the maintenance of higher cellular ATP concentrations where glucose is limited.

There are potential conditions which gametocytes might encounter during their development where glucose may be limited where it would benefit them to increase their mitochondrial energy metabolism. The first of these is in the human host. Hypoglycaemia is a symptom of severe malaria (White *et al.*, 1987; Ali *et al.*, 2011; Madrid *et al.*, 2015). If glucose is depleted in the host, it may be advantageous for gametocytes to upregulate mitochondrial energy metabolism to maximise ATP production from the available glucose in the human host. Switching to a more efficient form of ATP production could be important for the prolonging the survival of gametocytes under these conditions to ensure that they survive to be transmitted to a mosquito. However, the blood glucose of human patients with severe

malaria is  $<2.2$  mM (Bruneel *et al.*, 2003). Based on my glucose titration data, this should be enough glucose for the gametocytes to lie on glycolysis. As previously discussed, it seems unlikely that glucose would be substantially depleted from the bloodmeal in the ~20 minutes needed for exflagellation. However, other environmental changes occur upon entry to the mosquito where increased mitochondrial respiration may be beneficial. For example, the decrease in temperature may slow down biological processes in the mosquito, therefore more efficient ATP generation may be required. In addition, mitochondrial respiration requires oxygen, and the parasites encounter increased oxygen levels in the mosquito midgut compared to the human host (Boysen and Matuschewski, 2011) which may make mitochondrial respiration more efficient.

To test the hypothesis that gametocytes can alter their mitochondrial activity in response to glucose availability, gametocytes could be cultured to maturity, washed, and then transferred into media containing different concentrations of glucose. MitoTracker labelling could then be used to quantify mitochondrial activity in the gametocytes to determine whether they can compensate for reduced glucose availability by modulating mitochondrial activity.

If it can be demonstrated that gametocytes can actively alter their mitochondrial activity, then this has implications for gametogenesis in the mosquito as well as during their time in the human host. For example, male gametocytes undergoing gametogenesis might need to suddenly increase their ATP production to transition from quiescence to carrying out a complex series of cellular processes which must be carefully coordinated and may require an increased contribution from mitochondrially produced ATP. The ATeam1.03YEMK line, which allows real time intracellular ATP concentrations to be visualised by FRET microscopy, could be used to visualise how ATP concentrations change in male gametocytes undergoing exflagellation. The changes observed could provide new insights into a) how energy intensive gametogenesis is compared to the 'resting' state of mature gametocytes and b) whether male gametocytes increase ATP production during the process of gametogenesis, which would imply they increase their mitochondrial activity in response to the change from the human to the mosquito environment. Some possible outcomes of this experiment are shown in Figure 4.15.

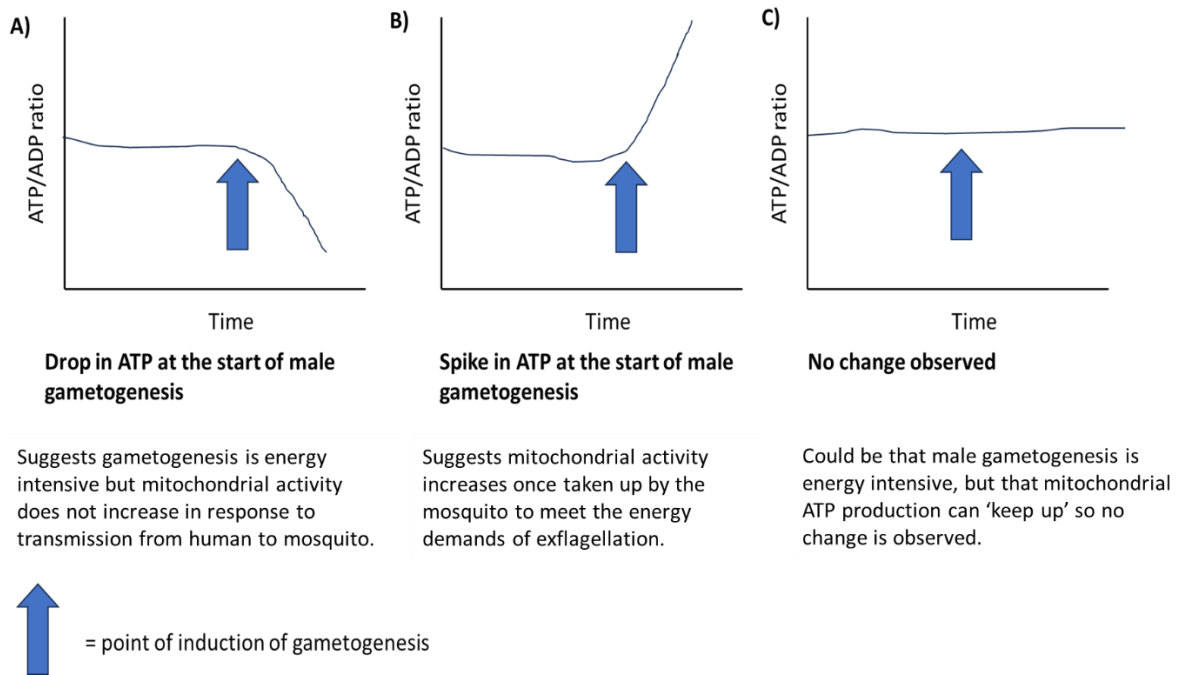


**Figure 4.15. Possible changes in intracellular ATP concentrations that might be observed on induction of male gametogenesis.** Time is not quantified as it is unknown over what timeframe during the 15-20 minutes required for exflagellation where these changes would occur.

It would also be interesting to investigate if there are changes in the ATP/ADP ratio in the presence of a treatment which increases mitochondrial activity, such as N,N,N',N'-Tetramethyl-p-phenylenediamine Dihydrochloride (TMPD) + ascorbic acid (Uyemura *et al.*, 2004). If an increase in the ATP/ADP ratio is observed in gametocytes treated with these two reagents in combination, this suggests that the gametocyte mitochondria have 'spare capacity' for ATP production, which could indicate that regulation of mitochondrial metabolism is occurring. If no increase is observed, this suggests that the gametocyte mitochondria are functioning 'at capacity' which may indicate regulation is not occurring.

My current data indicate that ATP homeostasis in gametocytes appears to be insensitive to inhibition of mitochondrial respiration providing excess glucose is available. Further experiments are needed to characterise this further. Firstly, the comparison of 'glucose' +/- oligomycin A within the same experiment will show whether the addition of oligomycin A reduces the intracellular concentration relative to 'glucose' alone. If the ATP/ADP ratio is the same +/- oligomycin A, this would suggest intracellular ATP is insensitive to inhibition of mitochondrial respiration and glycolysis is sufficient to meet the energy needs of the gametocyte. Secondly, the direct comparison of 'no glucose' +/- oligomycin A will test if the inhibition of mitochondrial respiration depletes the gametocyte of ATP faster than untreated gametocytes. If so, this supports the hypothesis that mitochondrial respiration may be

important for maintaining the intracellular ATP concentration in conditions where glucose is limited.

Gametocytes are in a non-proliferative state in the human host and thought to be minimally metabolically active, contrasting with asexual blood stage parasites which are rapidly replicating. Having established the ATP/ADP ratio in gametocytes in the presence and absence of glucose, the ATeam1.03YEMK parasite line could also be used to compare ATP consumption in gametocytes and asexual blood stage parasites to see which is more metabolically active. My experiments indicated that the gametocytes show a slow decline in ATP in 'no glucose' conditions providing mitochondrial respiration is active. Asexual blood stages rely on glycolysis and operate a minimal TCA cycle (MacRae *et al.*, 2013; Ke *et al.*, 2015; Srivastava *et al.*, 2016), therefore it might be expected that their ATP concentrations would drop rapidly in 'no glucose' conditions, as glycolysis would not be able to produce ATP so efficiently, therefore ATP would be quickly consumed.

Another possible extension to this work would be generate a parasite line episomally expressing an ATeam targeted specifically to the mitochondrial compartment. This would allow measurement of the ATP/ADP in the mitochondrion itself and may provide a clearer picture of mitochondrial ATP production in gametocytes, either in response to environmental conditions, or in males during exflagellation. ATP levels in the mitochondria could also be compared between the sexes using either a parasite line expressing an ATeam sensor and a sex-specific gametocyte protein tagged with mCHERRY or alternatively a line expressing the sensor under the control of a sex-specific promoter. Given that males have lower mitochondrial activity as measured by MitoTracker, it would be interesting to determine whether they show reduced mitochondrial ATP production compares to females.

In summary, these preliminary data suggest that glycolysis is sufficient to meet the energy needs of the gametocyte in the human host but that increased mitochondrial energy metabolism may allow them to generate ATP more efficiently in adverse conditions where glucose is limited. The generation of the ATeam1.03YEMK line has also created a valuable new tool for studying intracellular ATP concentrations in gametocytes under different conditions, making a wealth of future experiments for furthering our understanding of gametocyte energy metabolism possible.

# Chapter 5 Identification and characterisation of putative regulators of gametocyte energy metabolism

## 5.1 Introduction

As disruption of mitochondrial respiration in gametocytes has been shown to abrogate transmission downstream in the mosquito (MacRae *et al.*, 2013; Ke *et al.*, 2015; Srivastava *et al.*, 2016), gametocyte energy metabolism represents a potentially rich source of targets for transmission-blocking drugs (Birkholtz, Alano and Leroy, 2022). Drugs that target gametocytes in the human host are preferable to those specifically targeting later mosquito stages as the drug would need a long half-life to be effective against these stages if administered to a human (Delves, Angrisano and Blagborough, 2018; Birkholtz, Alano and Leroy, 2022). Although, activity against ookinetes from carry-over in the bloodmeal has been shown for some drugs e.g. atovaquone (Delves, Angrisano and Blagborough, 2018).

The gametocyte must balance survival in the human host with remaining viable for onward development once taken up a mosquito. Gametogenesis and mosquito stage development are complex and vulnerable to upstream disruption. Mitochondrial respiration is a more efficient method of generating ATP than glycolysis (Kadenbach, 2003; Zheng, 2012) but may lead to increased production of reactive oxygen species (ROS) (Oliveira and Oliveira, 2002) which could potentially harm the developing gametocytes. My hypothesis is that mitochondrial respiration in gametocytes is upregulated to a level where the parasite is ready for the mosquito environment, but that energy metabolism is regulated to minimise ROS production in the gametocyte cell. No regulatory mechanisms have been identified to date.

The proteomes of sex-separated male and female gametocytes have been published for *P. falciparum* (Lasonder *et al.*, 2016; Miao *et al.*, 2017) and the rodent malaria *P. berghei* (Khan *et al.*, 2005) which show divergent biology between male and female gametocytes. Proteins involved in energy metabolism and mitochondrial proteins are among the groups of proteins enriched in female gametocytes (Khan *et al.*, 2005; Lasonder *et al.*, 2016; Miao *et al.*, 2017). This is consistent with the different fates of male and female gametocytes once taken up by the mosquito. The male gametocyte is terminally differentiated and preparing 'only' for gametogenesis and fertilisation, whereas the female gametocyte is preparing for gametogenesis, fertilisation and provides all the organelles for onward development in the mosquito (Talman *et al.*, 2004). Female gametocytes provide most of the cellular 'biomass' to ookinetes and downstream mosquito development. If there are regulatory proteins involved in protecting gametocytes from increased ROS production, one could speculate that such proteins might be upregulated in female gametocytes.

The third aim of the PhD project was to identify and characterise proteins with evidence to suggest a role in energy metabolism. The criteria for proteins of interest were that they were a) expressed in gametocyte stages, b) assigned Gene Ontology (GO) terms to suggest a role in energy metabolism, c) differentially expressed between male and female gametocytes. Proteins of interest would first be identified by data mining of published proteomic data. Once identified, parasite lines with the proteins of interest tagged with a fluorescent protein would be generated to study subcellular localisation and expression across the parasite life cycle. Knockout lines would subsequently be generated to study whether deletion of these genes resulted in a transmission-blocking phenotype in the parasites.

To identify proteins putatively important for gametocyte energy metabolism, the proteome reported by Lasonder *et al.* (2016) was examined in detail (section 5.2.1). Six proteins of interest were identified for study. Constructs for tagging were generated for all six genes of interest. However, due to time constraints caused by COVID-19 related delays to the project, the decision was made to focus on tagging and phenotyping two of the genes selected for study.

## 5.2 Results

### 5.2.1 Identification of candidate proteins

The workflow of selection of candidate proteins is shown in Figure 5.1. Of the 2241 proteins identified in Lasonder and colleagues' proteome (2016), 469 were found to be upregulated in female gametocytes (FG) and 466 in male gametocytes (MG). Of these, 135 proteins in FG and 225 in MG showed greater than 10-fold difference in protein abundance. After identifying those genes assigned GO Terms linked to energy metabolism (e.g., glycolysis, carbohydrate metabolic process, mitochondrial TCA cycle), this shortlist was reduced to 14 genes in female gametocytes. Of these, a further nine genes were eliminated due to either well-studied activity in gametocytes or predicted essentiality to all parasite stages (i.e., not gametocyte-specific functionality). The remaining five genes were selected for study. An additional gene identified from literature searches, a putative ADP-forming acetyl-CoA synthetase (ACS-ADP, PlasmoDB ID: PF3D7\_1437700) was also included. ACS-ADP was not differentially expressed between the sexes but was selected to study a potential link between glycolysis and acetate production in gametocytes. All six genes were predicted to be non-essential for asexual growth according to published essentiality screens in *P. falciparum* (Zhang *et al.*, 2018) and *P. berghei* (Bushell *et al.*, 2017). A list of the six genes is

shown in Table 5.1. Information on the expression of these proteins can be found in Table 2.1 in Chapter 2.

#### Selection of candidate proteins

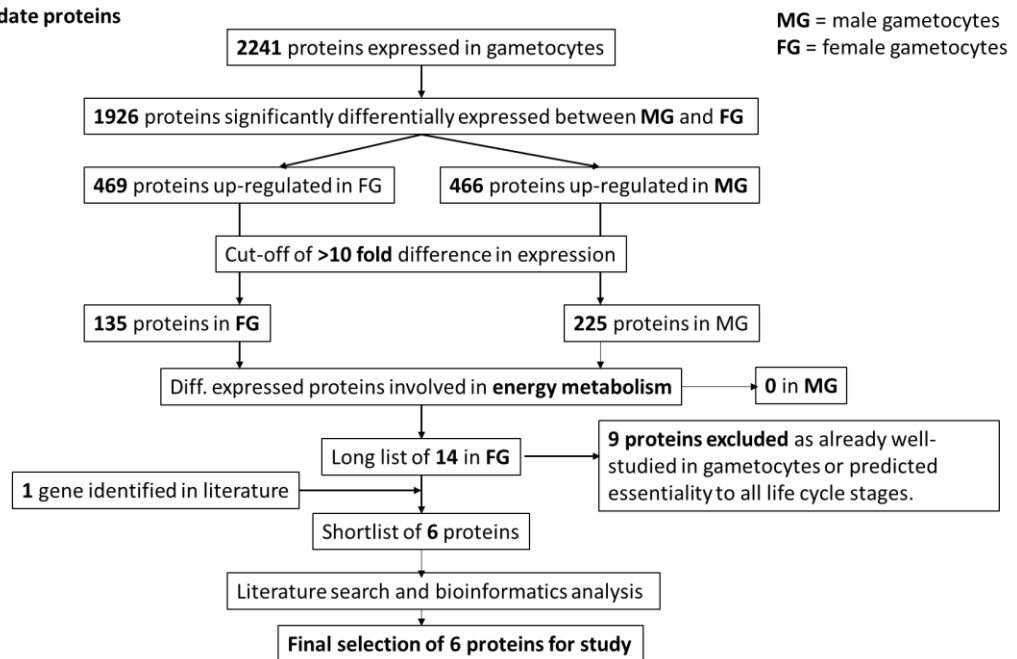


**Figure 5.1. Workflow for selection of candidate proteins.** MG = male gametocytes. FG = female gametocytes. Sex-specific gametocyte protein expression data from Lasonder *et al.* (2016).

| Plasmo DB ID   | Predicted to encode   |
|----------------|---|
| PF3D7_1128300* | Phosphofructokinase 11 (PFK11)  |
| PF3D7_1012500  | Putative phosphoglucomutase (PGM)   |
| PF3D7_0310300  | Putative phosphoglycerate mutase (PGM3)   |
| PF3D7_0306400  | Putative FAD-dependent glycerol-3-phosphate dehydrogenase (FAD-G3PDH)   |
| PF3D7_0802000  | Glutamate dehydrogenase 3 (GDH3)  |
| PF3D7_1437700* | Putative ADP-forming acetyl-CoA synthetase (ACS-ADP)<br>Annotated as: putative succinyl-CoA ligase but predicted to be an ACS-ADP due to sequence homology with ACS-ADP in other organisms. |

**Table 5.1. List of candidate proteins of interest.** \* = Taken forward for characterisation.

### 5.2.2 Bioinformatic analysis of candidate proteins

Bioinformatic analysis and literature searches were performed to find more information on the proteins of interest and find evidence to support a role in gametocyte energy metabolism.

#### Phosphofructokinase 11 (PF3D7\_1128300)

Phosphofructokinase (EC 2.7.1.11) (PFK) catalyses the conversion of fructose 6-phosphate and ATP to fructose 1,6-bisphosphate and ADP, an important regulatory step in glycolysis which commits glucose to the glycolytic pathway.

Two PFK enzymes are present in *Plasmodium*, PFK9 (PF3D7\_0915400) and PFK11 (PF3D7\_1128300). Transcriptomic data suggests that PFK9 is mostly expressed in trophozoite stages whereas PFK11 is expressed in stage V gametocytes and ookinetes and minimally expressed in asexual blood stage parasites (Aurrecochea *et al.*, 2009; López-Barragán *et al.*, 2011). Proteomic data suggests that PFK9 is expressed at all life cycle stages whereas PFK11 is predicted to be expressed in gametocytes (Florens *et al.*, 2002; Silvestrini *et al.*, 2010; Lasonder *et al.*, 2016). Notably, PFK11 protein was reported as being ~330-fold more highly abundant in female gametocytes than males (Lasonder *et al.*, 2016). This suggests that PFK11 may be important for transmission to mosquitoes.

PFK enzymes can be ATP- or P<sub>Pi</sub>-dependent. A previous study (Mony *et al.*, 2009) found that *Plasmodium* PFKs contain domains homologous to the pyrophosphate (P<sub>Pi</sub>)-dependent PFK  $\beta$  and  $\alpha$  subunits found in plants. In plants, the relative expression levels of the  $\alpha$  and  $\beta$  subunits are thought to regulate the rate of glycolysis in different tissues through oligomerization regulation (Wong *et al.*, 1990; Suzuki *et al.*, 2004; Mony *et al.*, 2009). However, unlike plant PFKs, where  $\alpha$  and  $\beta$  domains are separate subunits encoded by different genes, PFK9 and its orthologues were found to contain the two domains fused together as a single, large protein (Mony *et al.*, 2009).

In addition, despite the homology to plant-like P<sub>Pi</sub>-dependent PFKs, PFK9 was demonstrated to possess ATP-dependent phosphofructokinase activity. The  $\beta$  domain of PFK9 was found to possess catalytic activity whereas the  $\alpha$  domain (which is homologous to the  $\alpha$  regulatory subunit in plant PFKs) showed only marginal activity (Mony *et al.*, 2009). These data suggest that PFK9 can function as a PFK. In contrast, multiple sequence alignment of apicomplexan PFKs found that PFK11 and its orthologues in other *Plasmodium* species lack most of the residues in the ATP, fructose-6-phosphate and magnesium binding sites essential for catalysis (Mony *et al.*, 2009).

Table 5.2 shows a comparison of the amino acid residues important for catalysis in *Plasmodium* PFK9 and PFK11 enzymes. The residues in the *Plasmodium* PFKs were compared with the two PFKs in *E. histolytica*, one of which is ATP-dependent and the other is P<sub>Pi</sub>-dependent and which have been well-studied (Bruchhaus *et al.*, 1996; Deng *et al.*, 1998; Chi *et al.*, 2001). The residues found in the *Plasmodium* PFK9 orthologues are common to either the ATP-dependent or P<sub>Pi</sub>-dependent PFKs in *E. histolytica*, whereas

most of the residues at these positions in *Plasmodium* PFK11 orthologues are not common to those found in either *E. histolytica* PFK. This lack of key residues makes it highly unlikely that PFK11 and its orthologues could perform the normal glycolytic function of PFK (Mony *et al.*, 2009). However, the presence of homologous gene ORFs of PFK11 orthologues in other *Plasmodium* species (38–46% identity), suggests a possible function, most likely in gametocytes (Mony *et al.*, 2009).

|                                      | Length<br>(aa) | PPi/ATP binding |          |          |          | Mg2+ binding |          | Fructose 6-phosphate binding |          |          |          |          |
|--------------------------------------|----------------|-----------------|----------|----------|----------|--------------|----------|------------------------------|----------|----------|----------|----------|
|                                      |                | D               | N        | K        | G        | D            | D        | D                            | M        | E        | Y        | R        |
|                                      |                | 175             | 177      | 201      | 205      | 174          | 206      | 204                          | 249      | 310      | 420      | 423      |
| <i>E. histolytica</i><br>PFKI (PPi)  | 546            | D               | N        | K        | G        | D            | D        | D                            | M        | E        | Y        | R        |
| <i>E. histolytica</i><br>PFKII (ATP) | 439            | <b>G</b>        | <b>L</b> | K        | <b>N</b> | D            | D        | D                            | M        | E        | Y        | R        |
| <b>Plasmodium</b>                    |                |                 |          |          |          |              |          |                              |          |          |          |          |
| <b>PFK9</b>                          |                |                 |          |          |          |              |          |                              |          |          |          |          |
| <i>P. falciparum</i>                 | 1418           | <b>G</b>        | N        | K        | G        | D            | D        | D                            | M        | E        | Y        | R        |
| <i>P. reichenowi</i>                 | 1417           | <b>G</b>        | N        | K        | G        | D            | D        | D                            | M        | E        | Y        | R        |
| <i>P. malariae</i>                   | 1422           | <b>G</b>        | N        | K        | G        | D            | D        | D                            | M        | E        | Y        | R        |
| <i>P. ovale</i>                      | 1387           | <b>G</b>        | N        | K        | G        | D            | D        | D                            | M        | E        | Y        | R        |
| <i>P. chabaudi</i>                   | 1306           | <b>G</b>        | N        | K        | G        | D            | D        | D                            | M        | E        | Y        | R        |
| <i>P. berghei</i>                    | 1299           | <b>G</b>        | N        | K        | G        | D            | D        | D                            | M        | E        | Y        | R        |
| <i>P. knowlesi</i>                   | 1417           | <b>G</b>        | N        | K        | G        | D            | D        | D                            | M        | E        | Y        | R        |
| <i>P. relictum</i>                   | 1395           | <b>G</b>        | N        | K        | G        | D            | D        | D                            | M        | E        | Y        | R        |
| <b>PFK11</b>                         |                |                 |          |          |          |              |          |                              |          |          |          |          |
| <i>P. falciparum</i>                 | 1570           | <b>S</b>        | N        | <b>T</b> | <b>N</b> | <b>V</b>     | <b>E</b> | <b>Y</b>                     | M        | <b>D</b> | <b>K</b> | <b>T</b> |
| <i>P. reichenowi</i>                 | 1584           | <b>S</b>        | N        | <b>T</b> | <b>N</b> | <b>V</b>     | <b>E</b> | <b>Y</b>                     | M        | <b>D</b> | <b>K</b> | <b>T</b> |
| <i>P. malariae</i>                   | 1535           | <b>N</b>        | N        | K        | <b>N</b> | <b>V</b>     | <b>E</b> | <b>H</b>                     | <b>I</b> | E        | <b>N</b> | <b>T</b> |
| <i>P. chabaudi</i>                   | 1381           | <b>N</b>        | N        | K        | <b>N</b> | <b>T</b>     | <b>E</b> | <b>H</b>                     | <b>V</b> | E        | <b>N</b> | <b>T</b> |
| <i>P. berghei</i>                    | 1377           | D               | <b>S</b> | <b>T</b> | <b>N</b> | <b>V</b>     | <b>E</b> | <b>H</b>                     | <b>V</b> | E        | <b>N</b> | <b>T</b> |
| <i>P. knowlesi</i>                   | 1344           | D               | <b>H</b> | K        | <b>N</b> | <b>G</b>     | <b>E</b> | <b>H</b>                     | <b>I</b> | E        | <b>D</b> | <b>T</b> |
| <i>P. relictum</i>                   | 1307           | <b>K</b>        | N        | K        | <b>N</b> | <b>V</b>     | <b>E</b> | <b>Y</b>                     | M        | E        | <b>S</b> | <b>T</b> |

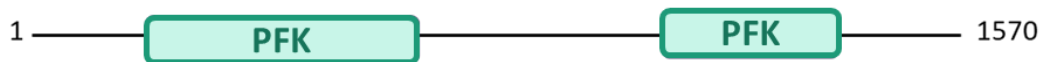
**Table 5.2. Comparison of catalytic residues between PFK9 and PFK11 orthologues in different *Plasmodium* species.** PFK9 orthologues are indicated by the blue background and PFK11 orthologues by the purple background. The residues in *Plasmodium* PFKs are compared with the two PFKs in *E. histolytica* (pink background.) The residues and position in the top of panel of the table refer to those in *E. histolytica* PFKI (PPi-dependent.) Residues identical to those in the *E. histolytica* PFKI are in plain text, those that differ are indicated in bold. Pink shaded residues are specific to ATP-dependent PFKs (Mony *et al.*, 2009). The yellow residues in the PFK11 orthologues do not correspond to those found in either ATP-dependent or PPi-dependent PFKs. *P. falciparum* PFK11, the gene of interest, is indicated by the blue box. aa = amino acids

A BLASTP search showed that outside of the *Plasmodium* genus, PFK11 shared most homology with PPi-dependent phosphofructokinase in *Theileria orientalis*, ATP- and PPi-dependent PFKs in *Cryptosporidium* species (all c. 35% identity) and ATP-dependent PFKs found in bacteria (30-34%). The sequence of PFK11 has a low level of similarity to PFK9 (20% identity) but is highly conserved between PFK11 orthologues in other *Plasmodium*

species suggesting a specific conserved function (subgenus *Laverania* (83-98% sequence identity), other *Plasmodium* species (45-72% identity)). An InterPro search of the PFK11 protein sequence predicted it to be part of the phosphofructokinase superfamily and to possess a phosphofructokinase domain based on sequence homology. Unlike PFK9, the search returned no family-level domain or motif predictions (Figure 5.2), however this is likely to be due to the missing catalytic residues.

### Comparison of PFK11 and PFK9

#### PfPFK11 (PF3D7\_1128300)



#### PfPFK9 (PF3D7\_0915400)

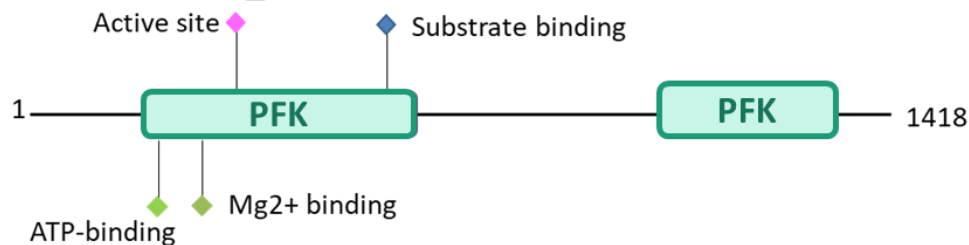


**Figure 5.2. Comparison of predicted domain architecture and active sites for PFK11 and PFK9.** Predictions were generated with InterPro. Abbreviations: PFK = phosphofructokinase domain (IPR000023).

The reason for the presence of two isoforms of PFK in *Plasmodium* is unclear. Interestingly, mammals also possess multiple isoforms of PFK (Sola-Penna *et al.*, 2010; Ausina *et al.*, 2018), termed PFK-M, PFK-L, and PFK-P (also called PFK-C) because of their major expression in muscle, liver, and platelets (or cerebrum), respectively (Sola-Penna *et al.*, 2010). Like *Plasmodium* PFKs, the catalytic and regulatory subunits of mammalian PFKs are fused together (Mony *et al.*, 2009). Distinct levels of the three isoforms are expressed in different tissues (Dunaway *et al.*, 1988; Fernandes *et al.*, 2020) and this is thought to contribute to glycolytic rates in different tissues (Sola-Penna *et al.*, 2010). For example, glycolytic efficiency was shown to be enhanced in more aggressive tumour cells and this was attributed to a higher expression of PFK-L over the other two isoforms (Zancan *et al.*, 2010).

In addition, mammalian PFKs are inactive as monomers and dimers, but active as tetramers (Sola-Penna *et al.*, 2010). Notably, heteromeric tetramers (comprising more than one isoform) can form but the biological significance of this is unknown (Fernandes *et al.*, 2020).

Therefore, it seems plausible that having two different isoforms of PFK in *Plasmodium* parasites, one of which is likely catalytically inactive, allows oligomerization regulation of glycolysis. One might imagine that a *Plasmodium* PFK heteromeric tetramer is composed of a greater proportion of the PFK11 isoforms, the overall catalytic activity might be reduced. The predicted upregulation of PFK11 in female gametocytes warrants further investigation of this protein as a possible regulator of gametocyte energy metabolism.

### **Putative phosphoglucomutase (PF3D7\_1012500)**

PF3D7\_1012500 is predicted to encode the sole phosphoglucomutase (EC 5.4.2.2) (PGM) in the *P. falciparum* genome. PGM facilitates the interconversion of glucose 1-phosphate (G1P) and glucose 6-phosphate (G6P), which can enter glycolysis or the pentose phosphate pathway (PPP) depending on the energy needs of the cell (Saha *et al.*, 2017). Surprisingly, this protein is predicted to be non-essential in asexual blood stage parasites (Bushell *et al.*, 2017; Zhang *et al.*, 2018), suggesting asexual blood stage parasites may have compensatory mechanisms.

It is estimated to be more highly expressed in gametocytes than asexual stages (30 spectra in mature gametocytes as opposed to 3 in trophozoites and 1 in early (stage I-II) gametocytes (Silvestrini *et al.*, 2010) and ~110-fold more highly expressed in female gametocytes than male gametocytes (Lasonder *et al.*, 2016). The *P. berghei* orthologue of this protein was identified in a sex-specific egress secretome of male and female gametocytes and was shown by immunofluorescence to be female gametocyte-specific (Grasso *et al.*, 2020). Therefore, it is plausible it may be female specific in *P. falciparum* as well.

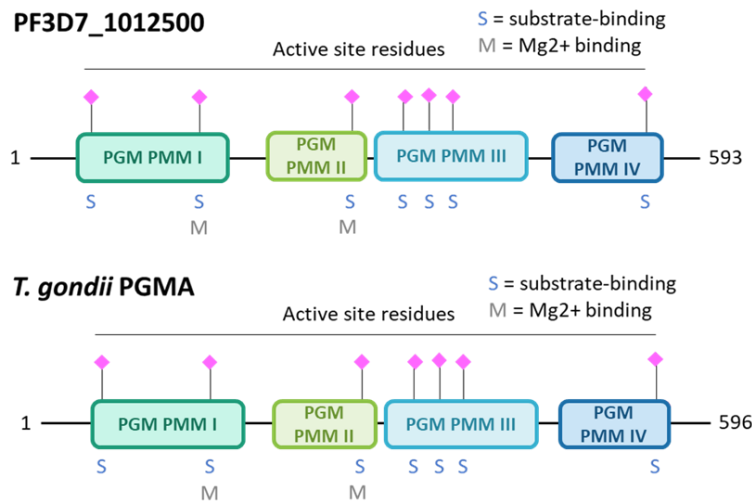
The reason for this is unclear. A major function of the PPP is to regenerate NADPH as a reducing agent for biosynthetic reactions and to protect against oxidative damage (Horecker, 2002; Wamelink, Struys and Jakobs, 2008; Riganti *et al.*, 2012; Stincone *et al.*, 2015). This could explain why it is upregulated in gametocytes relative to asexual blood stage parasites as antioxidant defence may be important during their long development of ~7-10 days in the human host (whereas as the asexual replication cycle in *P. falciparum* is 48 hours.) This may be even more important for female gametocytes which provide the cellular biomass to the zygote which must persist in the vector to survive to be transmitted, whereas male gametes have a lifespan of 30-40 minutes (Talman *et al.*, 2014) and so are short-lived in the vector.

A BLASTP search showed that PF3D7\_1012500 shows homology to known or putative phosphoglucomutases in other Apicomplexa and alveolates (41-74% identity), including

*Toxoplasma gondii* phosphoglucomutase 2 (PGMA) which has been found to have the “classical” phosphoglucomutase properties, namely pH dependency, α-D-glucose 1,6-bisphosphate necessity and Mg<sup>2+</sup> necessity (Imada *et al.*, 2010). Outside of the Apicomplexa, PF3D7\_1012500 has similarity (39-43% identity) with known or predicted phosphoglucomutase-2 and glucose 1,6-bisphosphate synthases in various fungi and metazoans.

An InterPro search predicted that PF3D7\_1012500 possesses PGM/PMM domains I-IV found in phosphoglucomutases (PGM) and phosphomannomutases (PMM) (Figure 5.4 A). Furthermore, the PGM\_PMM phosphoserine (PS00710) and PGMPMM PRINTS family signatures (PPR00509) are both found in PF3D7\_1012500 (Figure 5.4 B and C). These features are shared with bacterial phosphomannomutases, phosphomannomutase/ phosphoglucomutases (PMM/PGM) and phosphoacetylglucosamine mutases (PAGM). However, PGM seems like the most likely identity for PF3D7\_1012500 as 1) PMM/PGMs are mostly found in bacteria and archaea and 2) other genes in the *P. falciparum* genome are predicted to code for phosphomannomutase (PF3D7\_1017400) and PAGM (PF3D7\_1130000.) *T. gondii* PGMA, which has an identical domain architecture and active site to PF3D7\_1012500, was found not to possess phosphomannomutase activity (Imada *et al.*, 2010). The evidence supports that PF3D7\_1012500 is the *P. falciparum* phosphoglucomutase. Direct study is needed to elucidate this protein’s role in gametocytes and its higher expression in female gametocytes.

### A) Comparison of PF3D7\_1012500 and *Toxoplasma gondii* PGMA



### B) Phosphoglucomutase and phosphomannomutase phosphoserine signature

[GSA]-[LIVFMF]-x-[LIVM]-[ST]-[PGA]-**S**-H-[NIC]-P

PF3D7\_1012500 G V M V T A **S** H N P

### C) Comparison with human PGM2 and *Toxoplasma gondii* PGMA

|                       |   |     |
|-----------------------|---|-----|
| Human PGM2            | RFARLAATTFISQGI PVYLFSDITPTPFVPTVSHLKLKLCAGIMITA <b>SHNP</b> KQDNGYKVYW | 178 |
| <i>T. gondii</i> PGMA | RFAQLTAAVFLSKGFRVQLFSDIVHTPMVPTYVVAANCIAGIMITA <b>SHNP</b> KADNGYKVYA   | 171 |
| <i>P. falciparum</i>  | SFAHVAASVCLSKGFRVYLFQAQTVATPILCYSNLKKNCLC <b>GVMVTA</b> SHNPKLDNGYKVYA  | 168 |
|                       | **::*: . :*: * **:: . **:: : : : .*:*:***** *****                       |     |

### Figure 5.4. Bioinformatic analysis of putative phosphoglucomutase in *P. falciparum*. A)

Schematic of predicted domain architecture and active site residues in PF3D7\_1012500 in *P.*

*falciparum*. A known PGM in *T. gondii* is shown below for comparison. PGM PMM I-IV =

Phosphoglucomutase and phosphomannomutase domains 1-IV (IPR005843-6). **B)** Diagram showing

the phosphoglucomutase and phosphomannomutase phosphoserine (PROSITE PS00710) in present

in PF3D7\_1012500 in *P. falciparum*. **C)** Comparison of PF3D7\_1012500 in *P. falciparum* with human

PGM2 and *T. gondii* PGMA. The conserved signature is highlighted in orange. In both **B)** and **C)** the

serine residue at the active site is highlighted in pink.

### Putative phosphoglycerate mutase (PF3D7\_0310300)

Phosphoglycerate mutases (PGAM) (EC 5.4.2.11) catalyse the reversible conversion of 2-phosphoglycerate (2-PG) to 3-phosphoglycerate (3-PG), an essential component (step 8) of the glycolysis pathway (Rigden, 2008). They are part of the histidine phosphatase superfamily, a large and functionally diverse group of proteins which share a conserved catalytic core centred on a histidine which becomes phosphorylated during the reaction (Rigden, 2008; Coker *et al.*, 2013).

PF3D7\_0310300 is one of six proteins in the *Plasmodium* genome predicted to possess a phosphoglycerate mutase domain (Hills *et al.*, 2011). Of these, PGM1 and PGM2 have been previously studied. PGM1 is thought to be a co-factor dependent PGAM involved in glycolysis whereas PGM2 is a phosphatase with residual mutase activity (Hills *et al.*, 2011). Unlike PF3D7\_0310300, PGM1 and PGM2 are expressed across the life cycle (Silvestrini *et al.*, 2010) and show no marked difference in expression between male and female gametocytes (Lasonder *et al.*, 2016). In contrast, PF3D7\_0310300 is of interest as it shows greater expression in gametocytes than asexual parasites (84 spectra in late gametocytes, 1 in early gametocytes (stage I-II) and 3 in trophozoites (Silvestrini *et al.*, 2010) and is 87.48-fold more highly expressed in female gametocytes than males (Lasonder *et al.*, 2016). PF3D7\_0310300 will be referred to as PGM3 for simplicity.

Interestingly, PGM3 is specific to *Plasmodium* (*Laverania* subgenus: 79-89% identity, other *Plasmodium* species: 43-65%) and the closely related primate apicomplexan parasite, *Hepatocystis sp.* (62%). PGM3 is unrelated to PGM1 and PGM2 (4.5% and 4.7% identity respectively). An InterPro search predicts that PGM3 possesses a histidine phosphatase superfamily domain (IPR029033) at amino acid (aa) positions 164-400 (Figure 5.5 A.)

Unlike PGM1, PGM3 is also predicted to be a transmembrane protein (PHOBIUS prediction) with a cytoplasmic domain (aa 1-557), a transmembrane domain (aa 558-580) and a non-cytoplasmic domain (581-1165), suggesting a possible cell signalling role (Figure 5.5 B). It is known that a large proportion of PGAM family members are involved in cell signalling and/or regulation (Hills *et al.*, 2011) so it is plausible that this could be the case for PGM3 .

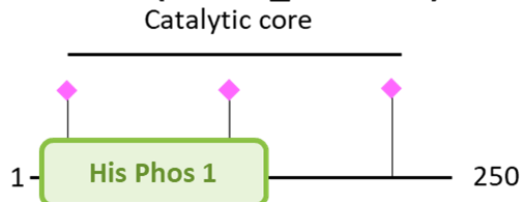
The role of PGM3 is unclear, but the fact it is largely *Plasmodium* specific and has higher protein expression in female gametocytes relative to males warrants further investigation. However, due to the diverse roles of enzymes in the histidine phosphatase superfamily, direct study is required to determine whether PGM3 plays a role in energy metabolism.

## A. Comparison of PfPGM3 with other PfPGMs

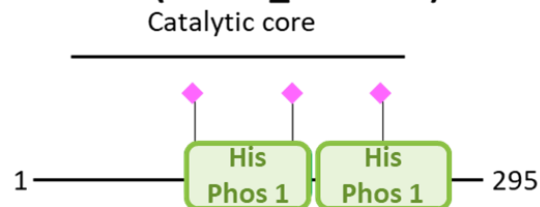
### PfPGM3 (PF3D7\_0310300)



### PfPGM1 (PF3D7\_1120100)



### PfPGM2 (PF3D7\_0413500)



## B. PHOBIUS prediction for PF3D7\_0310300

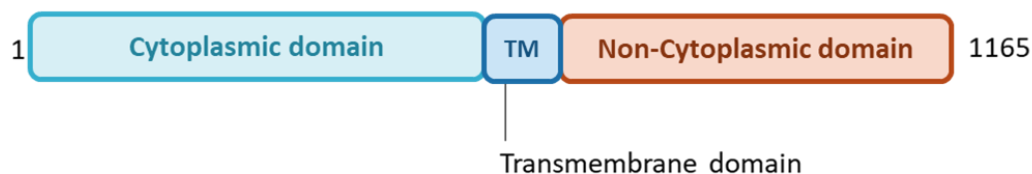


**Figure 5.5. Bioinformatic analysis of PGM3 (PF3D7\_0310300) in *P. falciparum*.** **A)** Comparison of predicted domain architecture and catalytic core residues for PGM3 and PGM1 and PGM2. **B)** PHOBIUS prediction for PGM3. Abbreviations: His\_PPase\_superfam = histidine phosphatase superfamily (IPR029033), His Phos 1 = histidine phosphatase superfamily branch 1 (PF00300), TM = transmembrane domain.

### Putative FAD-dependent glycerol-3-phosphate dehydrogenase (PF3D7\_0306400)

PF3D7\_0306400 is predicted to catalyse the reversible conversion of dihydroxyacetone phosphate to *sn*-glycerol 3-phosphate in a FAD-dependent manner. In eukaryotes, the FAD-dependent G3PDH partakes in the glycerol-3-phosphate shuttle, which functions to re-oxidise cytosolic NADH produced by glycolysis, leading to the transport of reducing equivalents to the respiratory chain for mitochondrial ATP production and maintenance of redox homeostasis (Larsson *et al.*, 1998; Shen *et al.*, 2003; Lian *et al.*, 2009) (Figure 5.6.)

PF3D7\_0306400 has greater expression in mature gametocytes (38 spectra as opposed to 9 in trophozoites and 12 in early gametocytes (Silvestrini *et al.*, 2010)) and 68.03-fold more highly expressed in female gametocytes compared to males (Lasonder *et al.*, 2016). Mitochondrial respiration increases in gametocytes so FAD-G3PDH expression may increase to direct more reducing equivalents to feed the respiratory chain. In addition, FAD-G3PDH's role in maintaining redox balance may be important during the long development of gametocytes and particularly in female gametocytes, which provide the cytoplasm and other organelles to the zygote which must persist in the vector.

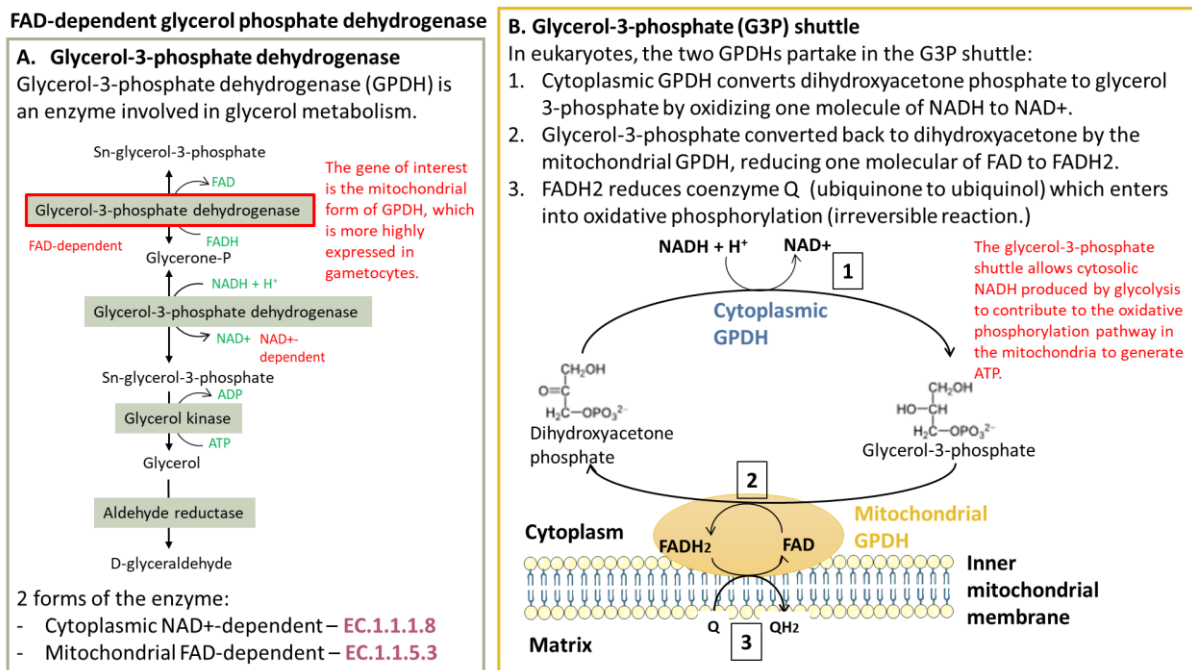
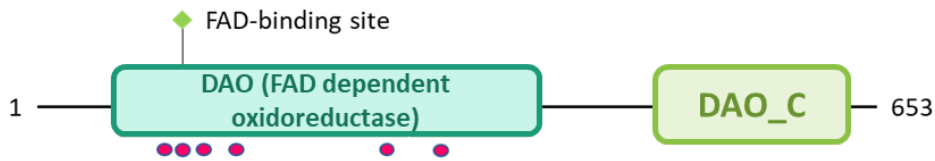


**Figure 5.6. Glycerol metabolism and the function of FAD-G3PDH.** **A)** Diagram of glycerol metabolism with the gene of interest, FAD-dependent G3PDH outlined in red. Enzymes are indicated by the grey boxes, co-factors in green text and enzyme EC numbers in pink text. **B)** Diagram of the glycerol-3-phosphate shuttle.

PF3D7\_0306400 showed sequence homology to known or predicted FAD-G3PDHs in other Apicomplexans (39-66% identity), and various fungi and metazoans (39-43% identity). PF3D7\_0306400 is predicted to contain all the necessary domains for FAD-G3PDH activity (Figure 5.7.)

## Comparison of PF3D7\_0306400 and yeast GUT2

### PF3D7\_0306400



### *Saccharomyces cerevisiae* GUT2



**Figure 5.7. Comparison of predicted domain architecture and motifs in PF3D7\_0306400 in *P. falciparum* and the FAD-dependent G3PDH in *Saccharomyces cerevisiae* (baker's yeast), GUT 2.** The pink dots indicate the positions of the FADG3PDH PRINTS family signature (PR01001) in both sequences. The conserved FAD-binding site (PS00977B) was also present in both sequences. Abbreviations: DAO = FAD-dependent oxidoreductase (IPR006076), DAO-C = alpha-glycerophosphate oxidase C-terminal domain (IPR031656).

### Glutamate dehydrogenase 3 (PF3D7\_0802000)

Glutamate dehydrogenase 3 (GDH3, PF3D7\_0802000) is one of three glutamate dehydrogenases (GDHs) annotated in the *Plasmodium* genome. It is predicted to be an NAD<sup>+</sup>-dependent GDH catalysing the breakdown of glutamate to ammonia and alpha-ketoglutarate (Storm *et al.*, 2011), which distinguishes it from GDH1 and GDH2 which are predicted to be NADP<sup>+</sup>-dependent.

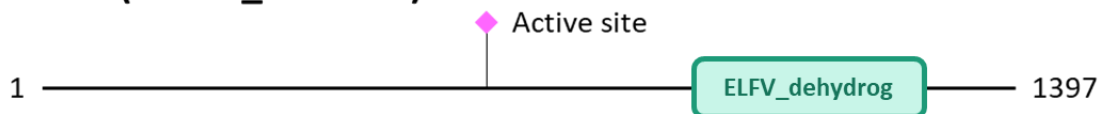
Unlike the other candidate proteins, GDH3 is similarly expressed in trophozoites (22 spectra) and mature gametocytes (18 spectra) (Silvestrini *et al.*, 2010), however it does show a female-biased expression, being 37.74-fold higher expression in female gametocytes compared to males (Lasonder *et al.*, 2016). Unlike GDH3, the expression of GDH1 and GDH2 does not differ between male and female gametocytes (Lasonder *et al.*, 2016). GDHs are thought to be involved in antioxidant defence (Zocher *et al.*, 2012) which may be important for combatting oxidative stress in the parasite in general which may be why it is expressed across the life cycle. It may be more highly expressed in female gametocytes because once it has been activated and fertilised, the resultant zygote must survive its development in the mosquito to be transmitted, whereas male gametes are short-lived in the vector.

According to a BLASTP search, GDH3 shows greatest homology to other known or predicted NAD<sup>+</sup>-dependent GDHs in apicomplexan parasites (23-77% identity). GDH3 also shows homology (29-50%) with NAD<sup>+</sup>-dependent glutamate dehydrogenases in bacteria and fungi.

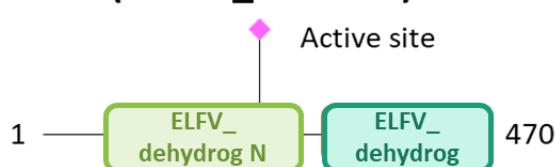
PF3D7\_0802000 possesses the necessary domains to act as a GDH (Figure 5.8). The active site in Glu/Leu/Phe/Val dehydrogenases contains a lysine residue surrounded by a glycine-rich conserved region. Pairwise comparison with *Saccharomyces cerevisiae* GDH2 (a known NAD<sup>+</sup>-dependent GDH) identified the lysine active site and glycine-rich conserved region in GDH3, corresponding to amino acids 633-646 (Figure 5.8). Interestingly, the GDH3 sequence differs from the signature at residues 641 and 646 (Figure 5.8) This might reflect evolutionary differences which may alter its function. These differences in *P. falciparum* could be beneficial as drugs designed to target the GDH3 active site might not cross-react with human GDH enzymes.

### A) Comparison of GDH3 and GDH1 in *P. falciparum*

#### GDH3 (PF3D7\_0802000)



#### GDH1 (PF3D7\_1416500)



### B) Pairwise comparison of the active site and surrounding glycine-rich region

|         |     |                |                |                        |     |
|---------|-----|----------------|----------------|------------------------|-----|
| Pf_GDH3 | 619 | AYNLAYTQNFKNKD | IPEGGSKGIILLDA | DVCNVANTKYIKNLSFYSYVNS | 668 |
|         |     | . .  .         | :    :..:..... | ..: ..   ::            |     |
| Sc_GDH2 | 606 | NYQLASTQQRKNKD | IPEGGSKGVILLNP | GLVEHDQT----FVAFSQYVDA | 651 |

### C) Glu / Leu / Phe / Val dehydrogenases active site:

[LIV]-x(2)-G-G-[SAG]-K-x-[GV]-x(3)-[DNST]-[PL]

PfGDH3            I   P E   G G   S   K G   I   I L L   D   A

**Figure 5.8. Bioinformatic analysis of GDH3 in *P. falciparum*.** **A)** Comparison of predicted domain architecture and active site for GDH3 with GDH1, an NADP<sup>+</sup>-dependent GDH., for comparison. Abbreviations: ELFV\_dehydrog = Glutamine/ leucine/phenylalanine/valine dehydrogenase domain (PF00208), N= N-terminal domain. **B)** Excerpt from pairwise comparison of the protein sequences from GDH3 and *S. cerevisiae* GDH2. The active site lysine residue is highlighted in pink, and the conserved region is shaded in purple. **C)** Comparison of the conserved region with the Glu/Leu/Phe/Val dehydrogenase active site pattern (Prosite: PS00074). The active site lysine residue is highlighted in pink. Plain text indicates residues that match the signature. Residues that differ from the signature are indicated in bold.

### **Putative ADP-forming acetyl-CoA synthetase (PF3D7\_1437700)**

Acetate is a common glycolytic endpoint in many parasitic protists and helminths (Grinsven *et al.*, 2008; Tielens *et al.*, 2010; Millerioux *et al.*, 2012). During gametocytogenesis, for reasons not yet clear, *P. falciparum* gametocytes shift their main endpoint of glycolysis from lactate towards acetate (MacRae *et al.*, 2013; Lamour *et al.*, 2014). In protozoa and some helminths, acetate is formed from acetyl-CoA through two different reactions, catalysed by either an acetyl-CoA synthetase (ACS, also known as acetate-CoA ligase) or an acetate:succinate CoA-transferase (ASCT) (Sánchez, Galperin and Müller, 2000; Tielens *et al.*, 2010; Millerioux *et al.*, 2012) (Figure 5.9 A.)

There are two different forms of ACS enzymes (Figure 5.9 B, Figure 5.10): ADP-forming ACS (EC, 6.2.1.13) involved in acetate formation, which catalyses the reaction acetyl-CoA + ADP ↔ acetate + CoA + ATP; and ATP-forming ACS (EC, 6.2.1.1), which catalyses the reaction acetyl-CoA + AMP + PPi ↔ acetate + CoA + ATP, involved in the activation of acetate to acetyl-CoA. ATP-forming ACS has a broad distribution across eubacteria, some archaea, and eukaryotes whereas ADP-forming ACS is restricted to thermophilic bacteria, archaea, and anaerobic protists. Both forms of ACS have been annotated in the *Plasmodium* genome. PF3D7\_0627800 is annotated as the ATP-forming ACS (ACS-ATP).

PF3D7\_1437700 is annotated as a putative succinyl-CoA ligase but is hypothesised to be an ADP-forming ACS (ACS-ADP) based on sequence homology with ACS-ADP enzymes in other organisms (Sánchez, Galperin and Müller, 2000.)

ACS-ADP genes are highly conserved across *Plasmodium* species (Sánchez, Galperin and Müller, 2000; Tielens *et al.*, 2010). Among eukaryotes, ACS-ADP is largely restricted to type 1 amitochondriate protozoa lacking mitochondria or a complete TCA cycle, where it plays a role comparable to succinyl-CoA synthetase in organisms with mitochondria (Sánchez, Galperin and Müller, 2000). Therefore, it is quite surprising that ACS-ADP is present in

*Plasmodium* parasites which possess mitochondria and can operate a full TCA cycle (Sánchez, Galperin and Müller, 2000).

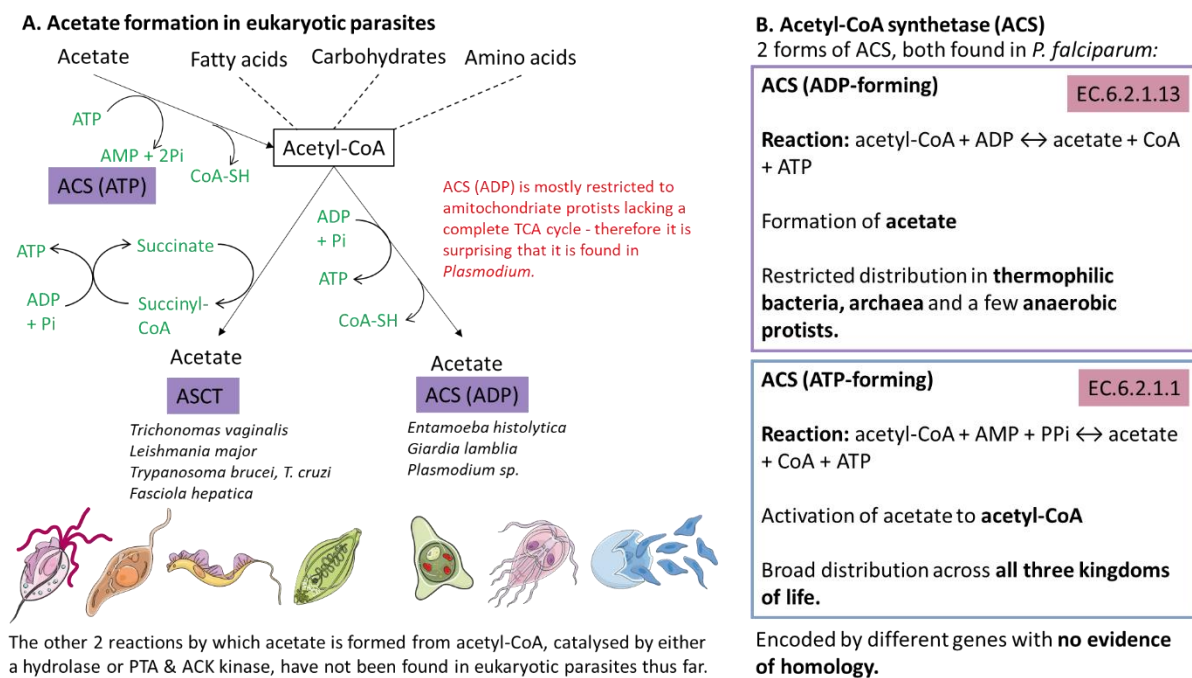


**Figure 5.9. Acetate formation in parasitic protozoa and helminths.** **A)** Reactions involved in the utilisation and formation of acetate in eukaryotic parasites. Enzymes are shaded in purple; co-factors are in green text. **B)** Key differences between ACS-ADP and ACS-ATP enzymes. Abbreviations: CoA = coenzyme A, ASCT = acetate: succinate CoA transferase, ACS = acetyl-CoA synthetase, PTA = phosphate-acetyltransferase, ACK = acetate kinase, ADP = adenine diphosphate, AMP= adenine monophosphate, Pi = inorganic phosphate, CoA-SH = reduced coenzyme A. Comparison of the two forms of ACS. EC numbers are shaded in pink. Images of parasites from Servier Medical Art.

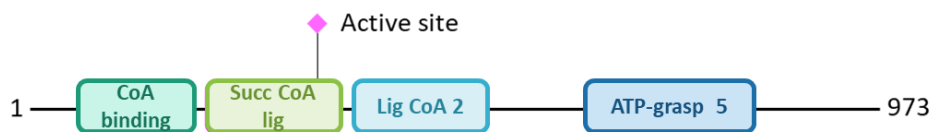
Transcriptomic (Lopez-Rubio, Mancio-Silva and Scherf, 2009) and proteomic studies (Silvestrini *et al.*, 2010) have shown that ACS-ATP is expressed at all parasite life cycle stages and likely to be an essential gene (Silvestrini *et al.*, 2010), whereas ACS-ADP is upregulated in gametocytes relative to asexual blood stage parasites (Sánchez, Galperin and Müller, 2000; Silvestrini *et al.*, 2010). It also predicted to be dispensable in asexual blood stages according to published essentiality screens (Bushell *et al.*, 2017; Zhang *et al.*, 2018). The protein is predicted to possess all the necessary domains to be an ACS-ADP involved in acetate formation and shows homology with ACS-ADP genes in other parasitic protozoa (Reeves *et al.*, 1977; Sánchez, Galperin and Müller, 2000; Tielens *et al.*, 2010).

The function of ACS-ADP in *P. falciparum* gametocytes is unknown. Gametocytes produce significant amounts of acetate, indicative of increased conversion of glucose into acetyl-CoA synthesis (Lamour *et al.*, 2014). Perhaps ACS-ADP functions to capture excess acetyl-CoA

produced by the gametocyte via glycolysis, diverting it away from the TCA cycle and mitochondrion (this model is elaborated on in the discussion 5.3). This may be important for allowing gametocyte mitochondrial development to progress in the absence of higher levels of mitochondrial respiration, which could result in greater generation of ROS which might limit the lifespan of the gametocyte during its long development and ultimately prevent it from transmitting the disease.

### Comparison of ADP-forming and ATP-forming ACS

#### ACS-ADP (PF3D7\_1437700)



#### ACS-ATP (PF3D7\_0627800)

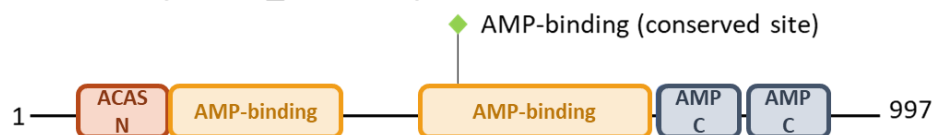


**Figure 5.10. Comparison of ACS-ADP and ACS-ATP in *P. falciparum*.** Abbreviations: CoA-binding domain (IPR003781), AMP-binding = AMP-dependent synthetase/ligase (IPR000873), Succ CoA lig = Succinyl-CoA synthetase-like flavodoxin domain (IPR032875), Lig CoA 2 = Ligase CoA domain (PF19045), ATP-grasp 5 = ATP grasp fold subdomain 1 (IPR013815), ACAS N = Acetyl-CoA synthetase N-terminal domain (IPR032387), AMP C = AMP-binding enzyme C-terminal domain (IPR025110)

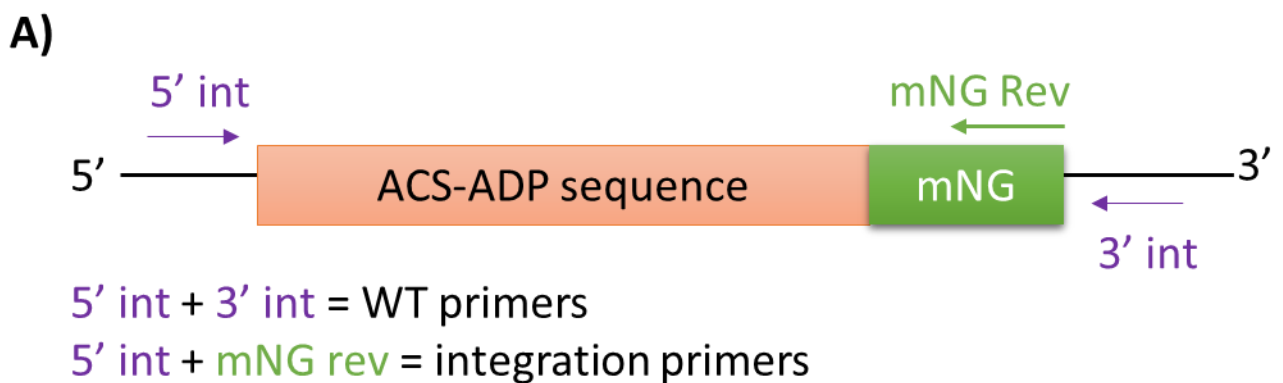
### 5.2.3 Characterisation of ACS-ADP expression

#### ACS-ADP was successfully tagged with mNeonGreen (mNG)

To characterise the expression of ACS-ADP and investigate its subcellular localisation, a construct was generated for tagging of this protein with mNeonGreen (mNG). NF54 asexual blood stage parasites were transfected with the ACS-ADP mNG construct. Parasites were subjected to drug selection with WR92210 and geneticin (G418) to obtain parasites with the construct integrated into the genome. Parasites resistant to both drugs were found to possess visible green fluorescence in a pattern which resembled small foci or filaments as shown in the images in Figure 5.13.

Samples of culture were taken for genomic DNA (gDNA) extraction and PCRs to confirm integration (Figure 5.11). The primers for the WT 5' and 5' homology regions showed

fragments of the expected sizes. WT NF54 gave a fragment size of 1.15 kb (Figure 5.12). ACS-ADP mNG gave a large band of ~7 kb as expected for integrated parasites, along with a fainter band of 1.15 kb consistent with some WT parasites in the culture that had reverted following removal of G418. The integration primers which amplified the region between the 5' integration site and the end of the mNeonGreen protein gave an expected fragment size of 1.8 kb for ACS-ADP mNG parasites, suggesting correct integration of the construct into the parasite genome. No band was observed for WT gDNA as the WT parasites do not express mNeonGreen.



**B)**

| Primer pair                                | Expected fragment size (kb) |             |
|--|-----------------------------|-------------|
|  | WT NF54                     | ACS-ADP mNG |
| WT primers (5' int + 3' int)               | 1.15                        | ~7          |
| Integration primers (5' int + mNG reverse) | No band                     | 1.8 kb      |

**Figure 5.11. Integration primers for the ACS-ADP mNG line.** **A)** Schematic showing where the primers bind on the sequence. 5' + 3' int = WT primers which amplify the 3' and 5' integration sites. 5' + mNG Rev = integration primers which amplify from the 5' integration site to the end of the mNeonGreen tag. **B)** Table of expected fragment sizes for WT NF54 and ACS-ADP mNG gDNA.

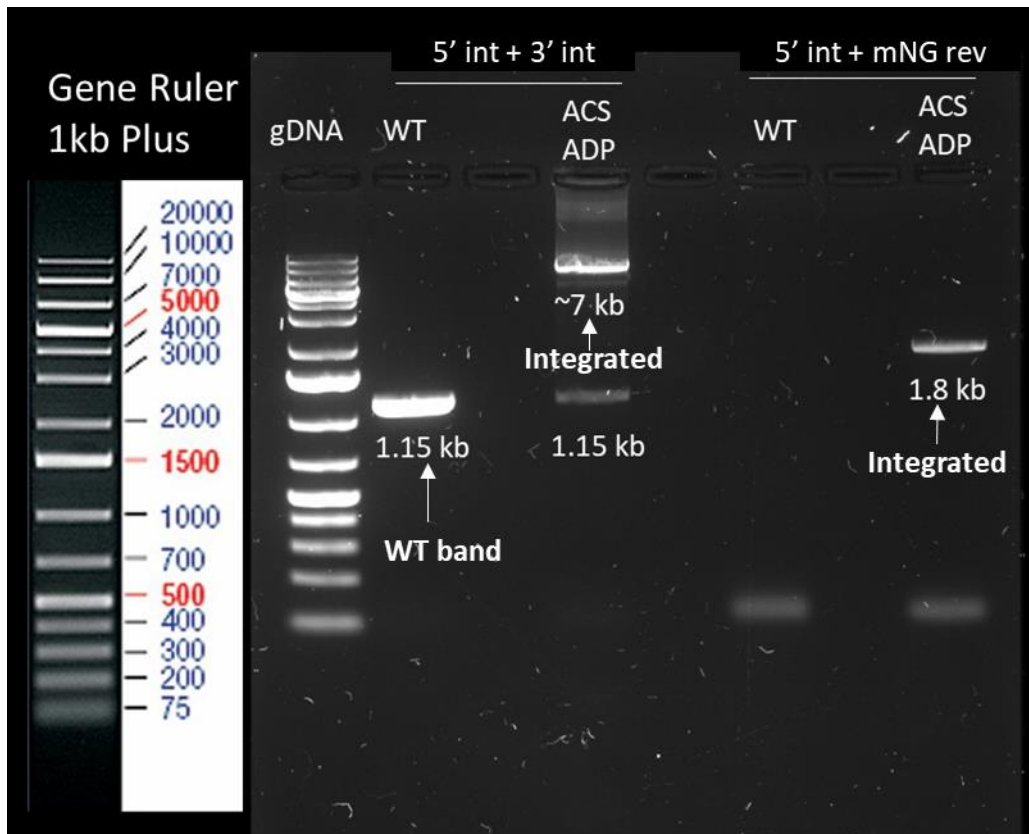


**Figure 5.12. Integration PCR gel for the ACS-ADP mNG-tagged line.** Abbreviations: gDNA = genomic DNA, kb = kilobases, WT = NF54 WT parasites and ACS-ADP= ACS-ADP mNG transgenic line. 5p + 3p int = WT primers which amplify the 3' and 5' integration sites. 5p + mNG Rev = integration primers which amplify from the 5' integration site to the end of the mNeonGreen tag. This fragment should be present in the ACS-ADP mNG gDNA sample only.

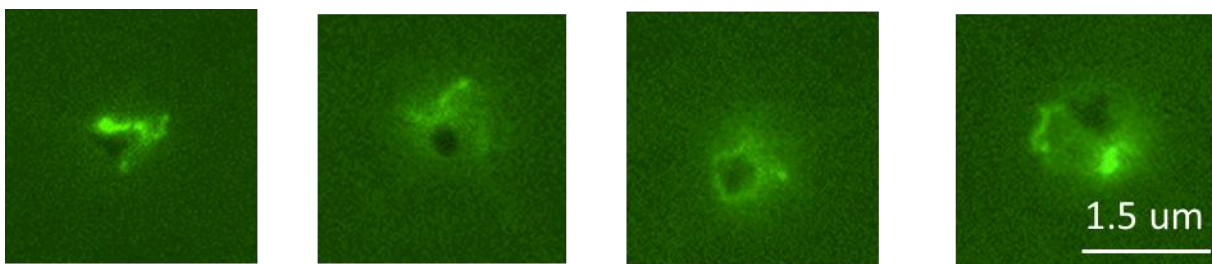


**Figure 5.13. Live images of asexual blood stage ACS-ADP mNG parasites showing mNG fluorescence.**

### Tagging and localisation of ACS-ATP

As previously mentioned, *Plasmodium* also possesses ATP-forming ACS (ACS-ATP). ACS-ATP was successfully tagged in the 3D7/iGP parasite line (Boltryk *et al.*, 2021) and its expression in asexual blood stage parasites and gametocytes investigated. ACS-ATP was expressed in asexual blood stage parasites and gametocytes (Figure 5.14). In asexual blood

stage parasites, the mNG fluorescence was concentrated in multiple, rounded foci (Figure 5.15 A). ACS-ATP mNG gametocytes were cultured and co-labelled with DAPI and MitoTrackerRed CMXRos to investigate the subcellular localisation of this protein (Figure 5.15). The mNG fluorescence was found to co-localised with DAPI, suggesting a nuclear localisation (Figure 5.15 B). This nuclear localisation was confirmed in a recent publication (Summers *et al.*, 2022) so this protein was not studied further.

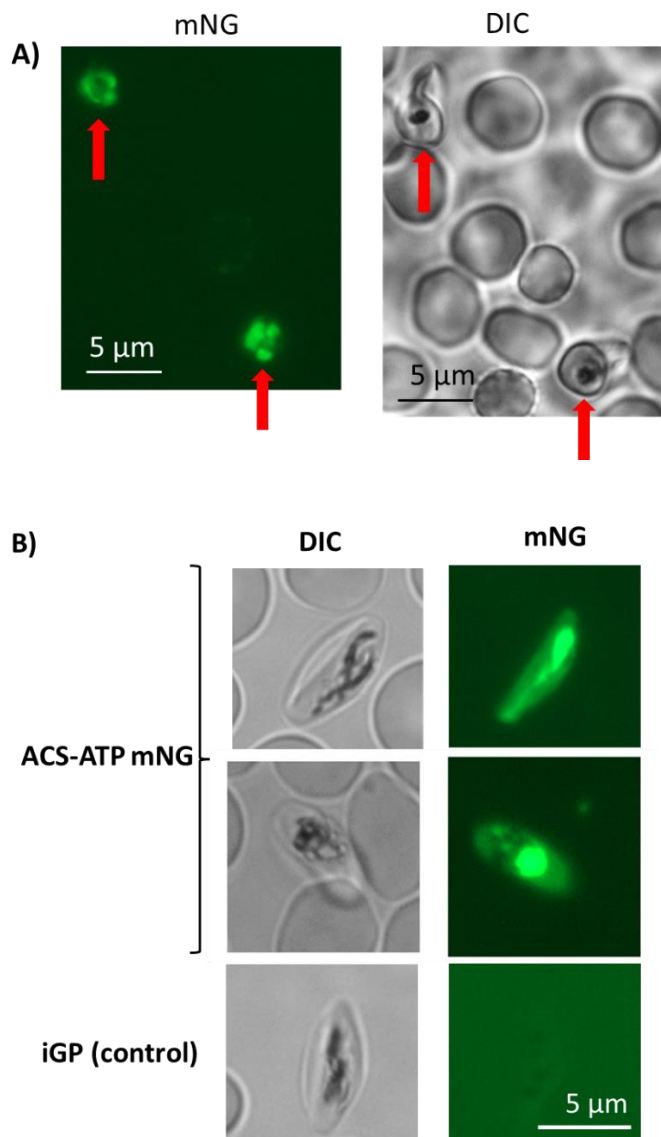


**Figure 5.14. Expression of ACS-ATP mNG in 3D7-iGP *P. falciparum* parasites. A)** Live imaging of ACS-ATP mNG fluorescence in asexual blood stage parasites. **B)** Live imaging of ACS-ATP mNG fluorescence in gametocytes. DIC (brightfield) and mNG channels are shown. Abbreviations: mNG = mNeonGreen, DIC = differential interference contrast.

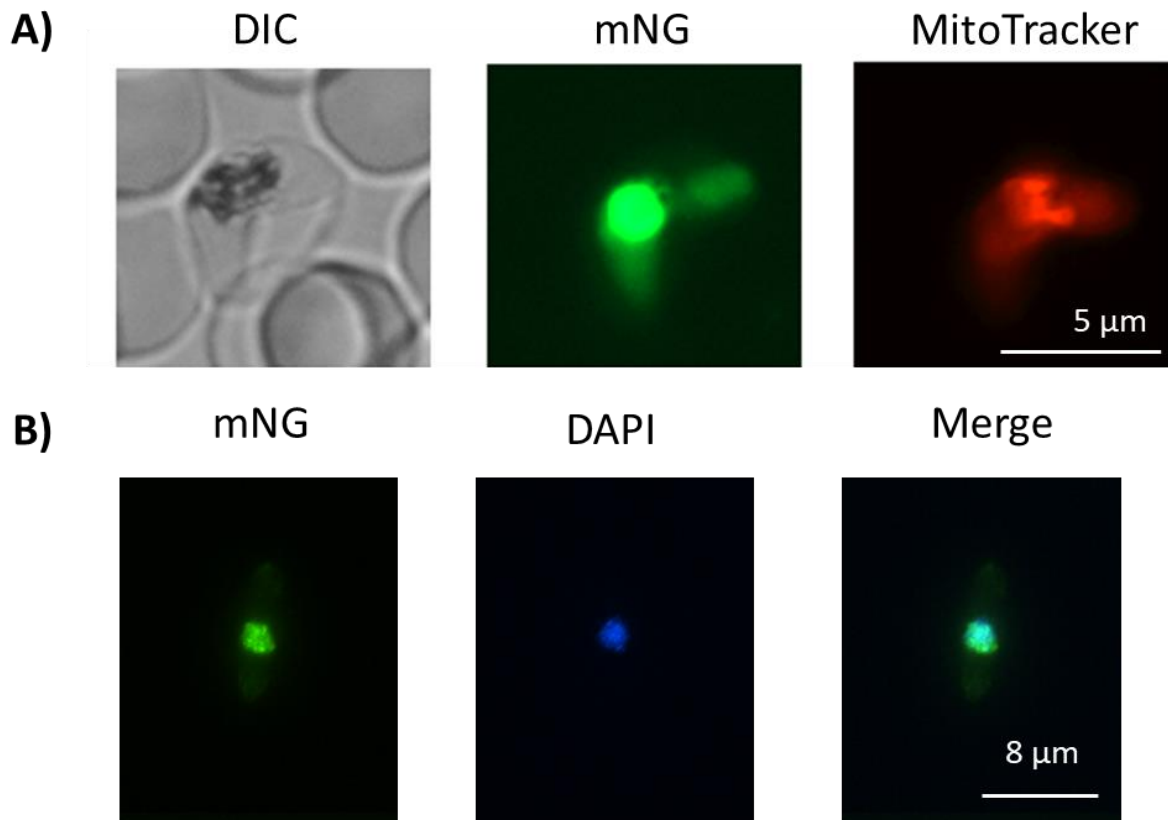


**Figure 5.15. Subcellular localisation of ACS-ATP in stage V gametocytes.** **A)** Live imaging of ACS-ATP mNG (green) parasites co-labelled with MitoTrackerRed CMXRos (red). **B)** IFA image of ACS-ATP mNG (green) co-labelled with DAPI (blue.) Abbreviations: mNG = mNeonGreen, DIC = differential interference contrast, MitoTracker = MitoTrackerRed CMXRos, merge = merged image.

### **ACS-ADP is mitochondrially localised and expressed throughout the life cycle**

The mNG-tagged ACS-ADP line was used to characterise expression of this protein across the parasite life cycle. The mNG fluorescence was present in both asexual blood stage parasites (Figure 5.13) and gametocytes (Figure 5.16 A). The mNG fluorescence is brighter in gametocytes, which supports that this protein is upregulated in gametocytes, consistent with proteomic data (Silvestrini *et al.*, 2010; Lasonder *et al.*, 2016). The mNG fluorescence was of a filament-like shape, resembling the mitochondria, particularly in gametocytes (Figure 5.16 A). This was subsequently confirmed by live imaging and fluorescence microscopy to be a mitochondrial localisation. ACS-ADP mNG fluorescence co-localises with MitoTracker Red CMXRos labelling in both asexual blood stage parasites (data not shown) and gametocytes (Figure 5.16 B), supporting that the protein is localised to the mitochondria.

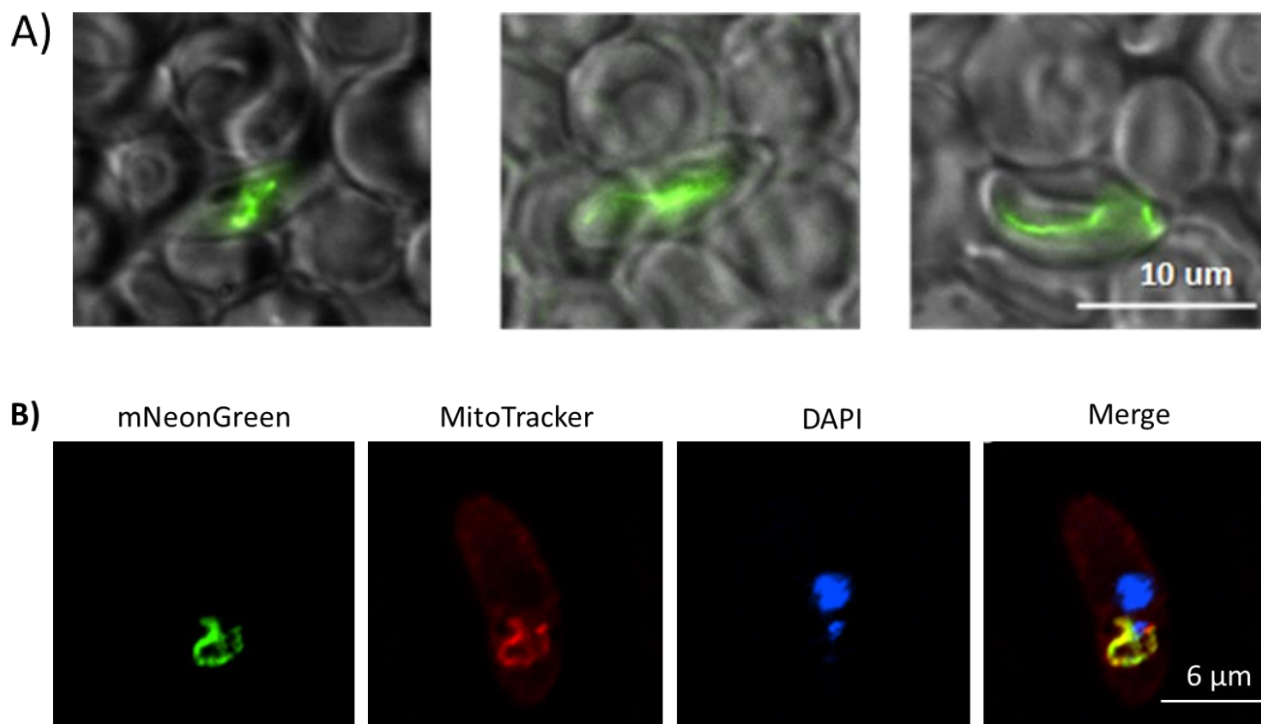


**Figure 5.16. Localisation of ACS-ADP in stage V gametocytes. A)** Live imaging of mNG fluorescence in stage V gametocytes. **B)** Fluorescence image of a stage V gametocyte showing that mNG fluorescence co-localises with MitoTracker Red CMXRos labelling.

ACS-ADP mNG gametocytes were then activated to check for expression of ACS-ADP post-activation. To assess whether ACS-ADP was expressed in activated female gametes and *in vitro* retorts (an intermediate stage between a fertilised zygote and an ookinete), mature gametocytes were activated using ookinete medium and left overnight at room temperature. The next day, the cells were labelled with an anti-Pfs25 antibody conjugated to a Cy3 red fluorophore and examined by fluorescence microscopy. Pfs25 is a protein expressed on the surface of activated female gametes, retorts and ookinetes and can be used to label these stages. In the female gametes, only fully activated gametes express the protein on their surface, so a Pfs25+ve cell is an indicator of successful activation, e.g., in dual gamete activation assays to assess activity of a compound against female gametogenesis. It was found that the mNG fluorescence was also present in activated female gametes and *in vitro* retorts (Figure 5.17).

ACS-ADP mNG gametocytes were also fed to *Anopheles stephensi* mosquitoes in a standard membrane feeding assay (SMFA) and mNG fluorescence was also observed in midgut retorts, suggesting that ACS-ADP is present in the mitochondria of fertilised zygotes and ookinetes. Mosquitoes were dissected at 24 hours post feeding. At this timepoint *in vivo* retorts possessing mitochondria-restricted ACS-ADP localisation was observed (data not

shown) as seen with *in vitro* generated retorts. Interestingly, in some of the retorts, the mitochondrion appeared to be in two parts (Figure 5.17 B). A recent 3D ultrastructural study challenged the widely held notion of a single mitochondrion in gametocytes, demonstrating multiple mitochondria which did not share a continuous lumen (Evers *et al.*, 2023). If this is the case, the two foci of mNG fluorescence could represent two different groups of mitochondria in the developing ookinete. At this timepoint it was not possible to identify any mature ookinetes, however, ACS-ADP mNG fluorescence was observed in oocysts 7 days post feeding.

The fact retorts (rather than ookinetes) were observed in both WT and the transgenic, suggests that this is due to the time point of dissection and not due to the tagging of ACS-ADP having adverse effects on transmission. The presence of retorts shows that the transgenic is capable of being fertilised normally. The mosquito feeds will be repeated later to confirm the presence of morphologically normal ookinetes and the localisation of ACS-ADP in this stage.

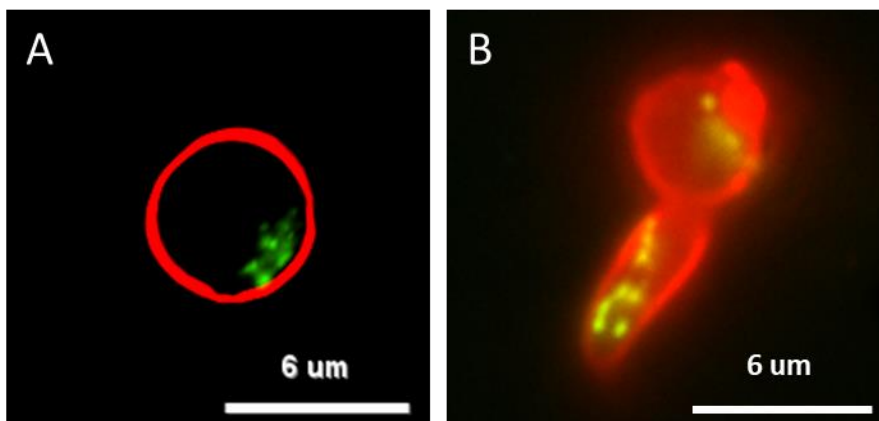


**Figure 5.17. ACS-ADP expression in activated female gametes and *in vitro* generated retorts.**

**A)** A slice through an IFA of an activated female gamete showing anti-Pfs25 staining in red and ACS-ADP mNG fluorescence in green. **B)** IFA of ACS-ADP mNG fluorescence (green) in a retort, with anti-Pfs25 staining in red.

To determine whether mNG expression was present in oocysts and sporozoites, mosquitoes fed with ACS-ADP mNG and NF54 WT gametocytes were dissected on day 7 post feeding to check for the presence of oocysts and on day 16 post feeding for sporozoites. On day 7, ACS-ADP mNG oocysts were found to have mNG labelling concentrated in the centre of the oocyst (Figure 5.18) which was absent from WT NF54 oocysts (data not shown). The expression of ACS-ADP mNG in retorts and oocysts supports that it is most likely expressed in ookinetes. On day 16, sporozoites were dissected from salivary glands with a single dot of mNG which co-localised with MitoTrackerRed CMX Ros, further supporting a mitochondrial

localisation across the life cycle (Figure 5.19). The mosquito cells possess mitochondria which would label with MitoTrackerRed CMXRos. Therefore, it was not possible to use this dye to confirm whether the mNG fluorescence in the oocysts was mitochondrial. However, the mitochondrial localisation in asexual blood stage parasites, gametocytes and the subsequent sporozoite stage supports that this is also the subcellular localisation in oocysts.

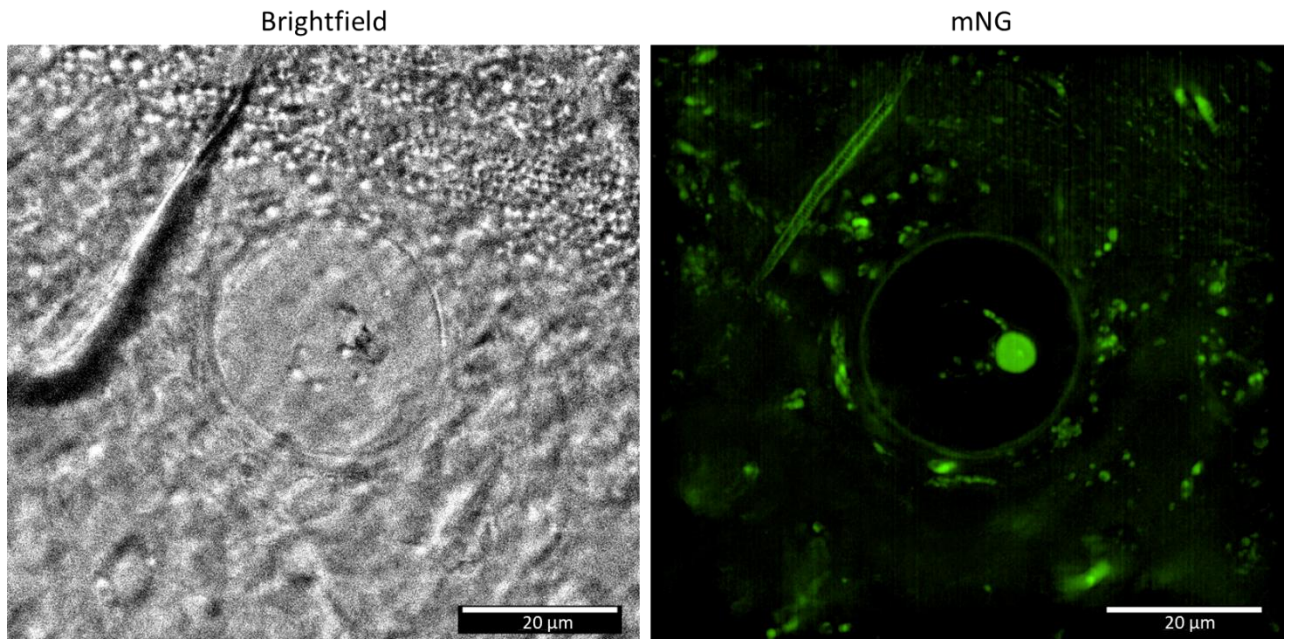


**Figure 5.18. Fluorescence image of an ACS-ADP mNG oocyst in the midgut of a mosquito dissected at day 7.** Brightfield is on the left and mNG is on the right. mNG staining is localised to the centre of the oocyst.

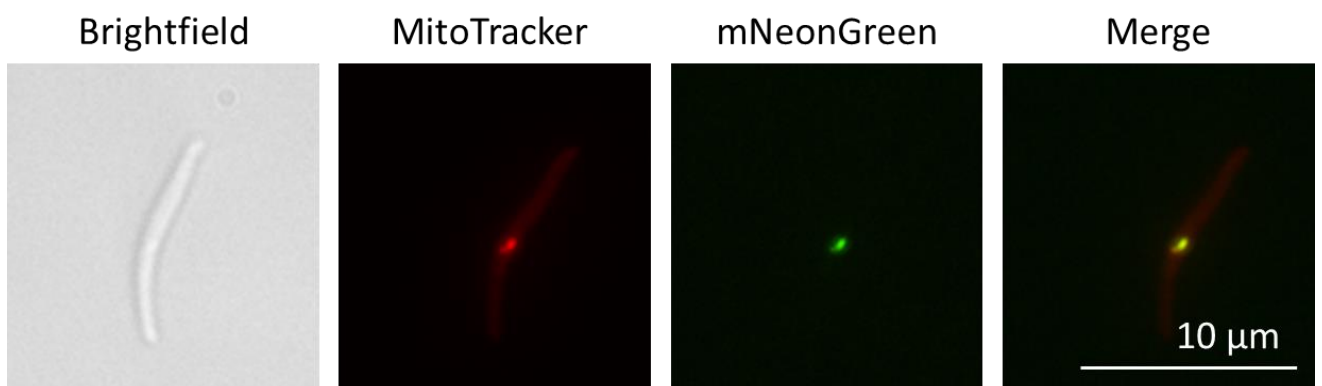


**Figure 5.19. Live image of ACS-ADP mNG sporozoites showing co-localisation between ACS-ADP mNG (green) and MitoTrackerRed CMX Ros (red).** Sporozoites are 10-15 µm in length.

## 5.2.4 Successful generation of an ACS-ADP-KO line

NF54 asexual blood stage parasites were transfected with the ACS-ADP-TGD construct and selected for by WR92210 and geneticin (G418) as described for the ACS-ADP-mNG line. G418-resistant parasites were recovered two weeks after transfection and samples taken for gDNA for integration PCR. Integration PCR gave bands of the expected sizes, suggesting correct integration of the construct into the parasite genome and successful KO of ACS-ADP (Figure 5.20.) There was not time to phenotype this line during the PhD project.

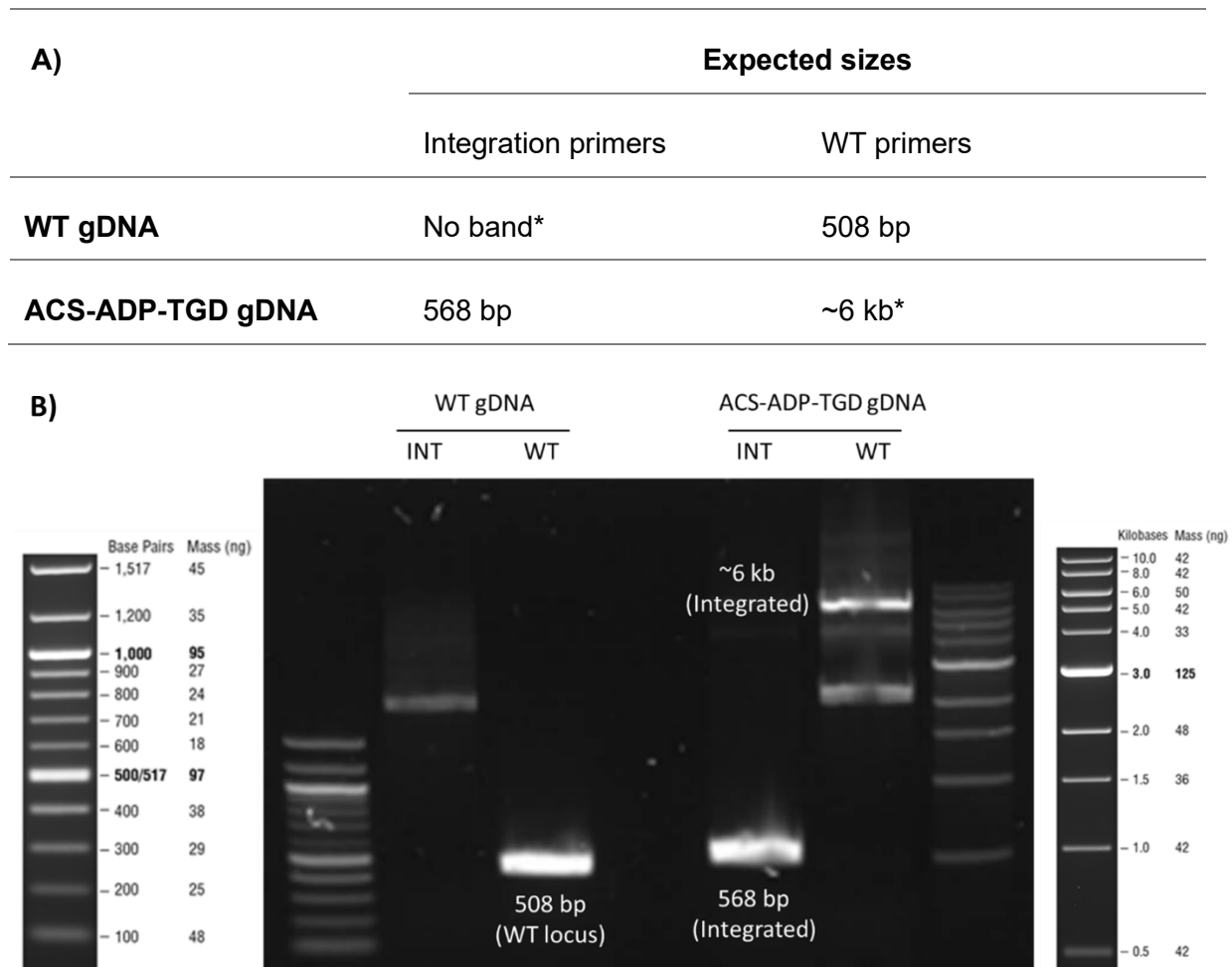


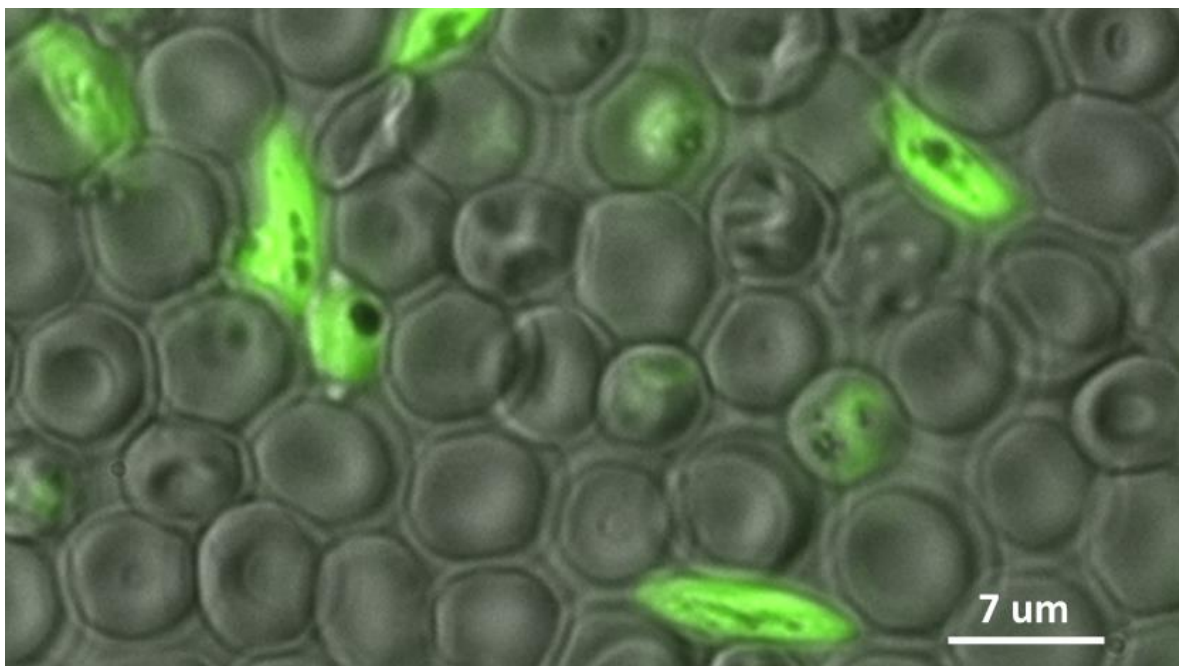
**Figure 5.20. Successful gene disruption of ACS-ADP by SLI-TGD. A)** Table showing the expected band sizes of the fragments amplified by the WT and integration primers. \* = The bands seen at 2 kb in the gel are non-specific bands. **B)** Integration PCR showing successful integration of the ACS-ADP-TGD vector.

## 5.2.5 Preliminary phenotyping of PFK11-KO parasites

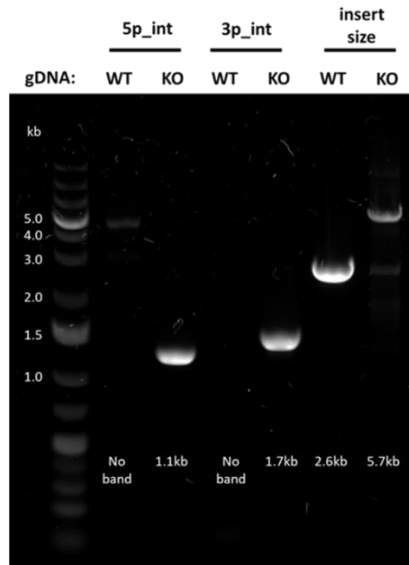
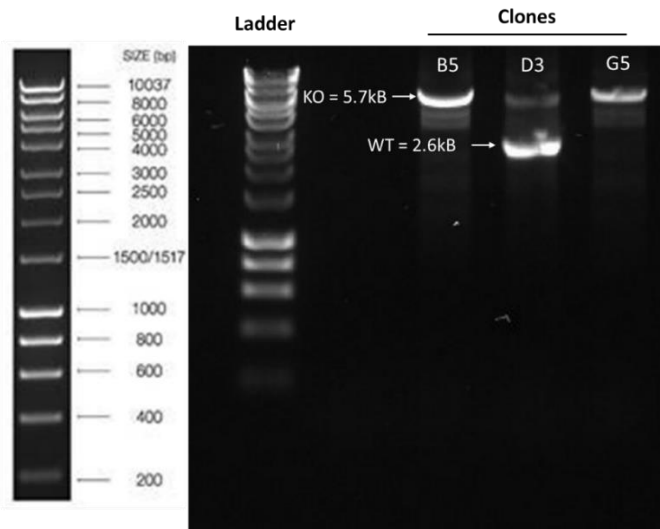
### Successful KO of PFK11

To investigate the function of PFK11, a KO line was generated using CRISPR gene editing and integration selected for directly using the drug blasticidin (BSD). The plasmid was designed so that transfected parasites would express GFP so KO parasites could be clearly identified. As both parasites with the integrated construct and the construct as an episome would express GFP, the plasmid was linearized into two fragments prior to transfection. This minimised the chance that the DNA could recombine and form an episome, therefore GFP expression would be a good indicator of integration.

Within a few weeks of transfection, asexual blood stage parasites expressing GFP reappeared in the culture. Asexual blood stage parasites and gametocytes expressing GFP are shown in Figure 5.21. To confirm integration, samples of asexual blood stage culture were taken for genomic DNA extraction for integration PCR. The integration PCR (Figure 5.22 A) for PFK11-KO showed bands for the 5' and 3' integration sites and the insert were of the expected sizes, indicating successful integration into the parasite genome. However, detectable WT contamination was observed in the knockout so dilution cloning by plaque assay (Thomas *et al.*, 2016) was carried out and two clones with a pure KO population (B5 and G5) were obtained (Figure 5.22 B.) For subsequent phenotyping, the dilution-cloned KO line was compared to the WT NF54 parent line.



**Figure 5.21. Live imaging of asexual blood stage parasites and gametocytes of the PFK11-KO line.** Expression of GFP suggests that most of the parasites have the plasmid integrated.

**A) Initial integration PCR (non-cloned)****B) Integration PCR for a sample of the dilution cloned lines****Figure 5.22. Integration PCR showing successful KO of PFK11 by CRISPR gene editing. A)**

Initial integration PCR for the PFK11-KO line. WT = NF54 WT parasites and KO = PFK11-KO transgenic line. There is detectable WT contamination in the KO so dilution cloning by plaque assay

was carried out to obtain a pure KO population. **B)** Integration PCR of three clones obtained from single parasites from plaque assays. Clones B5 and G5 are pure KO populations with one 5.7kB band whereas D3 is a mixed population and shows both the WT (2.6 kB) and KO (5.7 kB) bands.

**PFK11-KO show no defects in growth or development prior to the oocyst stage**

As PFK11 is predicted to be expressed specifically in female gametocytes, it was not expected that deletion of PFK11 would impact asexual blood stage growth. Asexual blood stage growth was assessed by seeding WT and KO asexual parasites at 0.1% parasitaemia and counting the parasitaemia on subsequent days. Parasitaemia counts were performed on three independent paired cultures of WT and KO set up in tandem. PFK11-KO and NF54 WT culture parasitaemia at each time point were compared by Student's t-tests. No significant difference in parasitaemia was observed at any time point, suggesting PFK11-KO parasites show no deficiency in asexual blood stage growth compared to WT parasites (Figure 5.23).

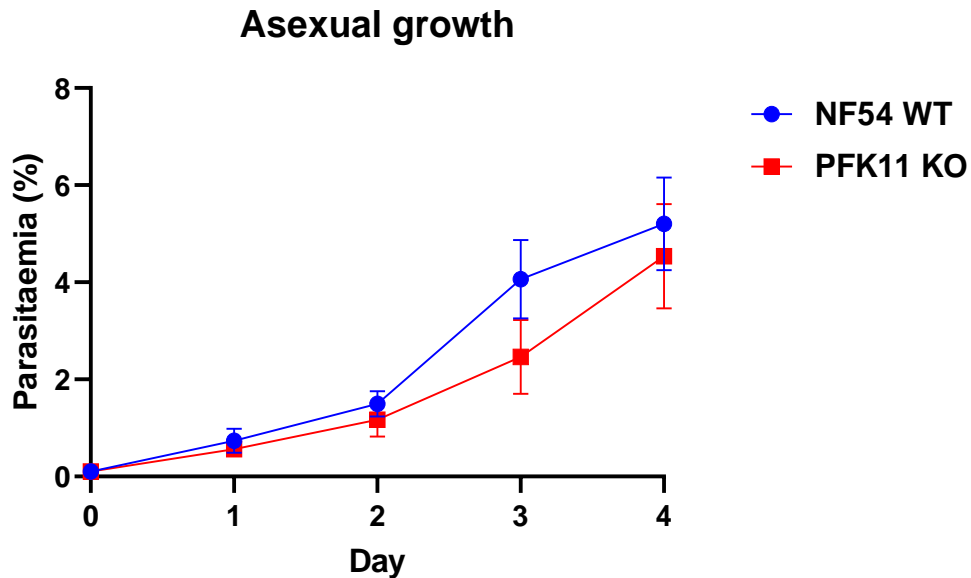


**Figure 5.23. Asexual blood stage growth in NF54 WT and PFK11-KO parasites.** Asexual blood stage parasitaemia was measured over 4 days of culture, n = 3 independent experiments. Measurements were also taken on days 5 and 6 but the parasitaemia was too high to count accurately. There were no significant differences in parasitaemia between NF54 WT and PFK11-KO parasites at any time point by Student's t-test. Error bars = SEM.

To assess whether PFK11 is required for gametocyte development, stage V gametocytaemia was compared between WT NF54 and PFK11-KO gametocyte cultures. PFK11-KO and WT gametocytes were added 1:1 to gametocyte medium containing 1  $\mu$ M ML10. ML10 is a highly specific inhibitor of the cGMP-dependent protein kinase (PKG) (Ressurreição *et al.*, 2020) which inhibits both male and female gametogenesis (Baker *et al.*, 2017) as PKG is essential for the initial stages of gametogenesis (McRobert *et al.*, 2008). Addition of ML10 prevented the mature gametocytes from exflagellating thus they retain their distinctive crescent shape, allowing gametocytes to be counted and gametocytaemia quantified. The number of gametocytes and number of red blood cells counted was used to calculate % gametocytaemia of the cultures. Variability in gametocytaemia was observed between cultures, but PFK11-KO parasites showed no deficiency in proportion of gametocytes compared to WT controls (Table 5.3). This suggests that PFK11-KO can form gametocytes as well as WT and that PFK11 is not required for gametocyte development.

Having established gametocyte development is unaffected by knocking out PFK11, it was next determined whether PFK11-KO gametocytes showed any deficiency in either male or female gametogenesis. Male gametogenesis (exflagellation) was assessed by triggering gametocytes to activate with ookinete medium and counting the number of exflagellation

centres and red blood cells in a Neubauer haemocytometer. The percentage exflagellation was then calculated. As with gametocytaemia, % exflagellation varied between the cultures for both WT and PFK11-KO but the PFK11-KO gametocytes showed no deficiency in exflagellation compared to their WT counterparts, suggesting that PFK11-KO has no effect on male gametogenesis (Table 5.3).

| Replicate | % gametocytaemia |      |      |             | % exflagellation |      |      |             |
|-----------|------------------|------|------|-------------|------------------|------|------|-------------|
|           | 1                | 2    | 3    | Mean        | 1                | 2    | 3    | Mean        |
| NF54 WT   | 3.76             | 1.05 | 1.00 | <b>1.94</b> | 0.17             | 0.78 | 0.22 | <b>0.39</b> |
| PFK11-KO  | 4.79             | 3.68 | 2.04 | <b>3.50</b> | 0.61             | 0.32 | 0.21 | <b>0.38</b> |

**Table 5.3. Gametocytaemia and exflagellation of 3 independent, matched NF54 WT and PFK11-KO gametocyte cultures.** % exflagellation = number of exflagellation centres per ml/red blood cells per ml x 100, % gametocytaemia = number of gametocyte per ml/red blood cells per ml x 100.

To assess female gametogenesis, gametocytes from the same culture were triggered in ookinete medium and incubated overnight at room temperature. The next day, the gametocytes were labelled with an anti-Pfs25-Cy3 antibody and female gamete activation quantified by calculating the proportion of Pfs25+ve cells. No difference was found in female activation between WT and KO, suggesting that knocking out PFK11 has no effect on female gametogenesis.

| Replicate | % female activation |       |              |
|-----------|---------------------|-------|--------------|
|           | 1                   | 2     | Mean         |
| WT NF54   | 8.11                | 6.06  | <b>7.08</b>  |
| PFK11-KO  | 8.87                | 14.49 | <b>11.68</b> |

**Table 5.4. % female activation of 2 independent, matched NF54 WT and PFK11-KO gametocyte cultures.** % female activation = number of Pfs25+ve cells/number of red blood cells x 100.

It was also observed that PFK11-KO parasites can form retorts *in vitro*, showing that fertilisation of female gametes by males can occur. PFK11-KO and WT NF54 gametocytes were subsequently fed to *A. stephensi* mosquitoes and PFK11-KO parasites were also found to form midgut retorts. The midgut retorts of PFK11-KO parasites show no morphological differences to those of NF54 WT, as shown in Figure 5.24.

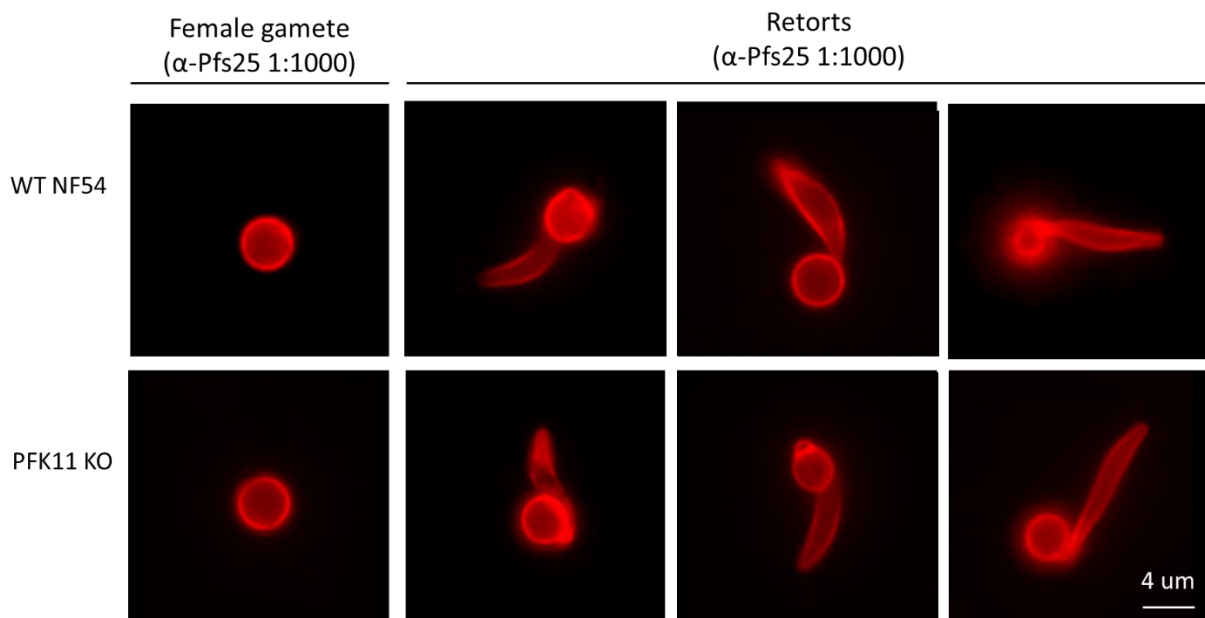
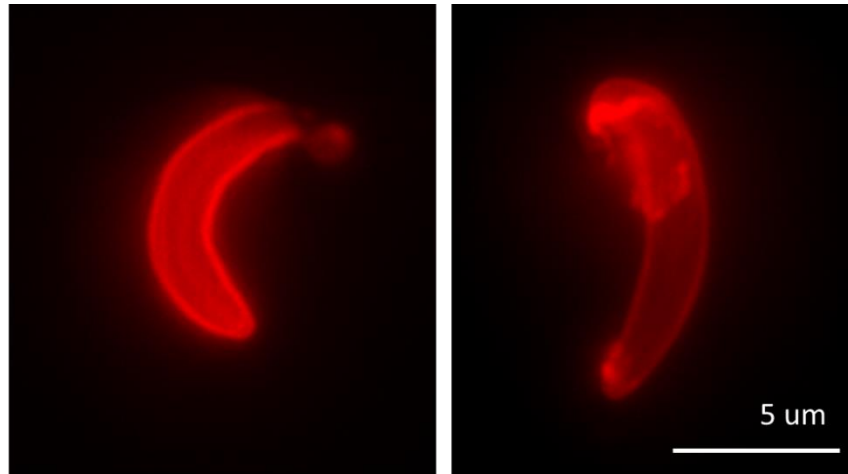


**Figure 5.24. Images of *in vivo* activated female gametes and midgut retorts of WT NF54 and PFK11-KO parasites.** Activated female gametes and retorts are labelled with an anti-Pfs25 antibody, visualised in red.

To assess whether PFK11-KO parasites arrested during insect stage development, mosquito feeding experiments were carried out in collaboration with the Malaria Transmission Facility at LSHTM. WT and PFK11-KO gametocytes cultures were checked for exflagellation to confirm maturity and then fed to female *A. stephensi* mosquitoes in a standard membrane feeding assay.

Fed mosquitoes were dissected at 24 hours post-feeding and midguts homogenised and labelled with an anti-Pfs25 antibody to search for ookinetes. Ookinetes were found in the midguts of both WT and PFK11-KO-fed mosquitoes (Figure 5.25). The PFK11-KO ookinetes showed no obvious morphological differences compared to their WT counterparts. These results suggest that PFK11 is not required for ookinete formation. Follow-up experiments will be required to determine whether PFK11-KO infections form fewer ookinetes compared to WT or whether PFK11-KO ookinetes show reduced ability to penetrate the midgut wall.

**PFK11 KO**



**NF54 WT**

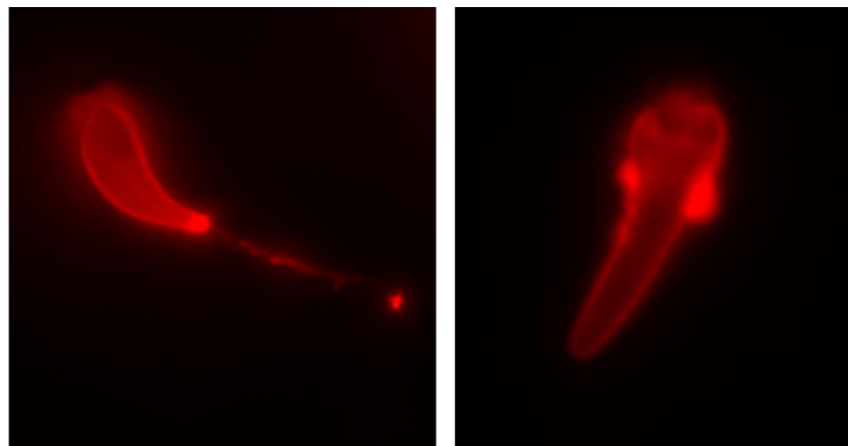


**Figure 5.25. Live fluorescence images of ookinetes from midguts of mosquitoes fed PFK11-KO and NF54 WT gametocytes.** Ookinetes are labelled with an anti-Pfs25 antibody, visualised in red.

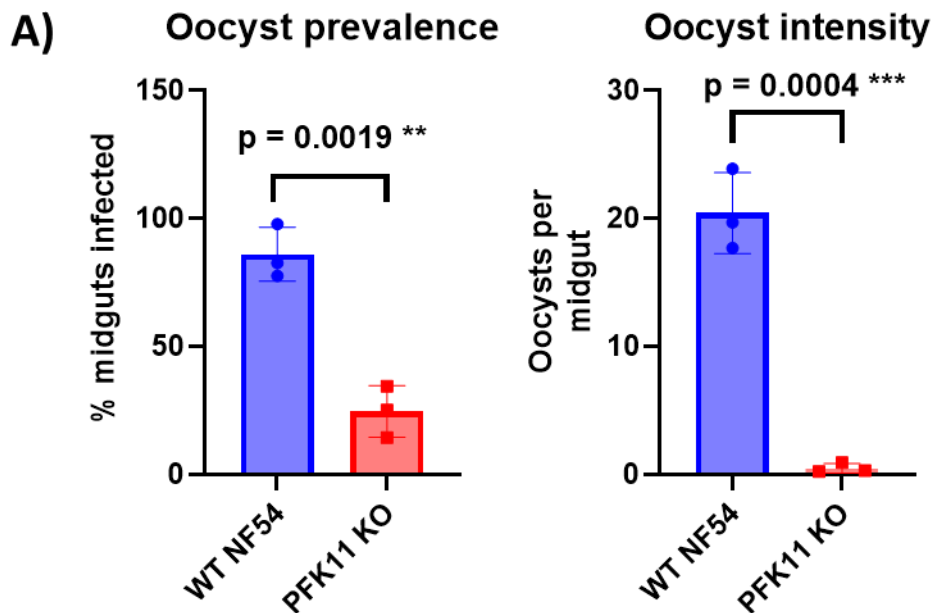
Note: The left-hand WT ookinete is demonstrating gliding motility, shown by the red trail behind it as it glides along the glass slide.

In summary, the data demonstrates that PFK11-KO parasites develop normally up until the point of ookinete formation.

### **PFK11-KO parasites show markedly reduced production of oocysts**

Having demonstrated that PFK11 is not essential for ookinete formation, its ability to generate fully formed midgut oocysts was assessed. Infected guts at day 7 post-feeding were visualised under a light microscope to count oocysts in triplicate independent experiments. Oocyst production was quantified by two measures i) oocyst prevalence – whether oocysts were present in the mosquito midgut or not (% mosquitoes infected) and ii) oocyst intensity – the mean number of oocysts per midgut. It was found that PFK11-KO parasites showed marked reductions in both oocyst prevalence and intensity compared to WT.

Mosquitoes fed NF54 WT gametocytes had a mean oocyst prevalence of 86.0 % and a mean oocyst intensity of 23.7, whereas PFK11-KO parasites had a mean prevalence of 24.6% and a mean intensity of only 0.5 (Figure 5.26). This represents a 71.4 % decrease in prevalence and a 98.0 % decrease in oocyst intensity. This dramatic decrease suggests that PFK11 is critical for ookinete development into oocysts.



**B)**

|                 | Oocyst prevalence (% mosquitoes infected) |       |      |             | Oocyst intensity (oocysts per midgut) |      |      |             |
|-----------------|---|-------|------|-------------|---------------------------------------|------|------|-------------|
| Replicate       | 1   | 2     | 3    | Mean        | 1                                     | 2    | 3    | Mean        |
| <b>NF54 WT</b>  | 82.6                                      | 97.9  | 77.5 | <b>86.0</b> | 23.8                                  | 24.4 | 22.8 | <b>23.7</b> |
| <b>PFK11-KO</b> | 34.5                                      | 25.00 | 14.3 | <b>24.6</b> | 0.9                                   | 0.3  | 0.2  | <b>0.5</b>  |

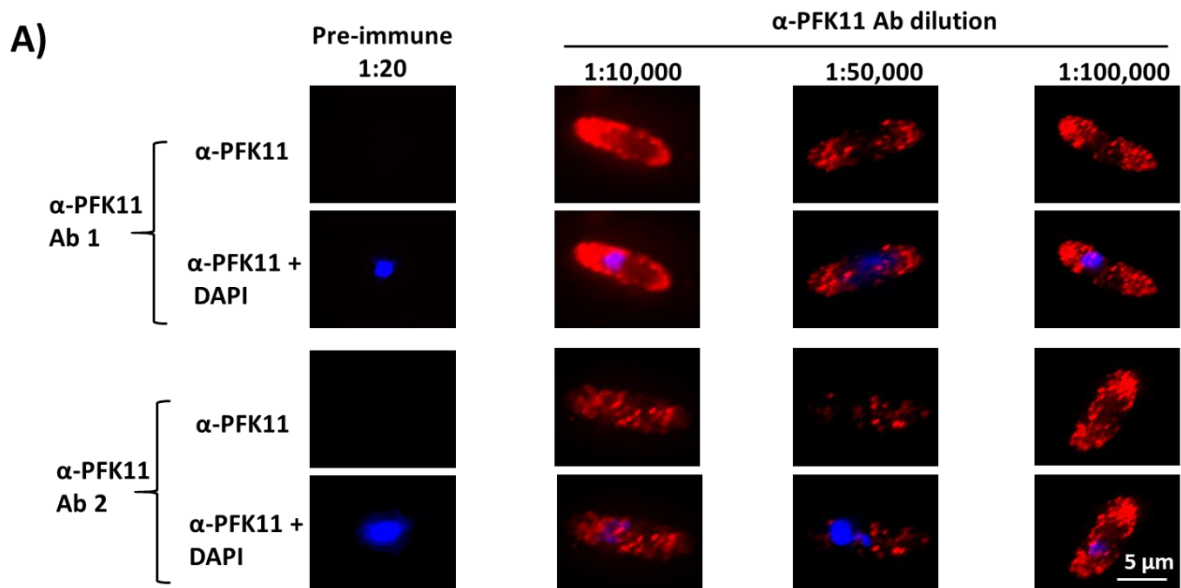
**Figure 5.26. Oocyst prevalence and intensity on NF54 WT and PFK11-KO parasites. A)** Graphs showing mean oocyst prevalence (left) and oocyst intensity (right) of WT NF54 (blue) and PFK11-KO (red) parasites, n = 3 independent experiments. Error bars = SEM. Both parameters are markedly reduced in the PFK11-KO parasites compared to WT. Statistical analyses are student's unpaired t-tests, \*\* = p<0.005, \*\*\* p<0.0005. **B)** Table of oocyst prevalence and intensity in NF54 WT and PFK11-KO parasites, n = 3 independent experiments. Oocyst prevalence is defined as the proportion of mosquitoes dissected with midguts positive for one or more oocysts. Oocyst intensity is the number

of oocysts per midgut. Both oocyst prevalence and intensity were consistent across the experimental replicates.

The experiment would also need to be repeated with a complementation line to confirm that restoring PFK11 expression in the KO line at least partially restores oocyst production. This would confirm that the observed phenotype is due to KO of PFK11 as opposed to an unrelated adverse effect of genetic modification. In addition, as oocysts are not completely absent from the PFK11-KO, follow-up experiments would be needed to check for the presence of sporozoites in the salivary glands at day 16 post-feeding. The implications of the preliminary phenotyping and future work to explore the function of this gene will be elaborated on in the discussion (5.3). Nonetheless, this is the first exciting indication that KO of PFK11 can disrupt transmission.

### 5.2.5 PFK11 antibody

Attempts to tag PFK11 with mNG are still ongoing. An antibody was raised to PFK11 to start studying PFK11 expression. The antibody showed punctate staining in the cytoplasm of both male and female gametocytes (Figure 5.27). However, once the antibody was tested against the PFK11 KO it was found that the punctate staining was also present in the KO parasites, suggesting that the antibody was non-specific (Appendix 4).



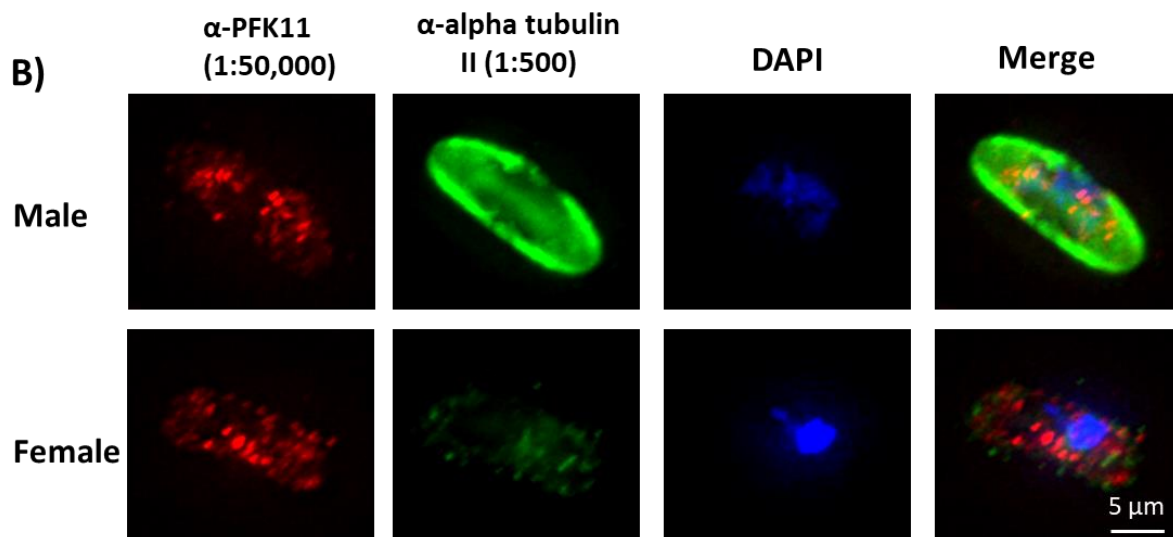


**Figure 5.27. Staining of stage V gametocytes with an antibody raised to PFK11. A)** IFA image showing punctate antibody staining of stage V gametocytes with anti-PFK11 antibodies. Anti-PFK11 is visualised in red and DAPI in blue. Antibodies were raised in two rabbits (Ab 1 + Ab 2) to PFK11 to study its expression in gametocytes. No PFK11 antibody staining was present in the IFAs using pre-immune sera. **B)** IFA image showing stage V gametocytes co-labelled with anti-alpha tubulin II (green) and anti-PFK11 (red). DAPI is shown in blue. Using the assumption that males have higher alpha tubulin II expression, there is no difference in labelling between male and female gametocytes. Unfortunately, when this antibody was tested against PFK11-KO parasites it was found to be non-specific.

### 5.2.6 Preliminary localisation of a mitochondrial FAD-dependent G3PDH in *P. falciparum*

Along with ACS-ATP, a putative FAD-dependent G3PDH (FAD-G3PDH) was tagged in the 3D7-iGP line. These results are pending integration PCR as there was not time to complete this within the time constraints of the PhD as the primary focus was on characterising ACS-ADP and PFK11. FAD-G3PDH mNG fluorescence was present in asexual blood parasites (Figure 5.28) and gametocytes (Figure 5.29 A) and appeared to be mitochondrial, resembling the pattern of mNG fluorescence in the ACS-ADP mNG line. This was confirmed by co-localisation of FAD-G3PDH mNG fluorescence with MitoTrackerRed CMXRos, strongly suggesting a mitochondrial localisation (Figure 5.29 B.) This localisation supports that this protein is a FAD-dependent G3PDH as predicted, as this form of G3PDH is usually mitochondrially-located.

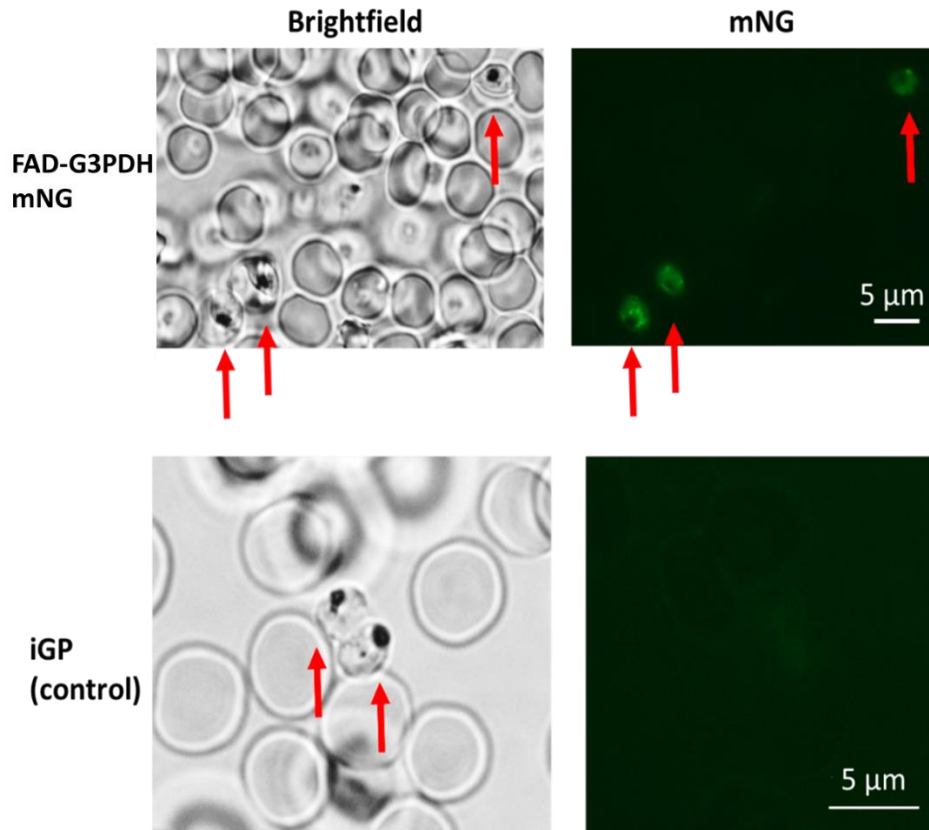
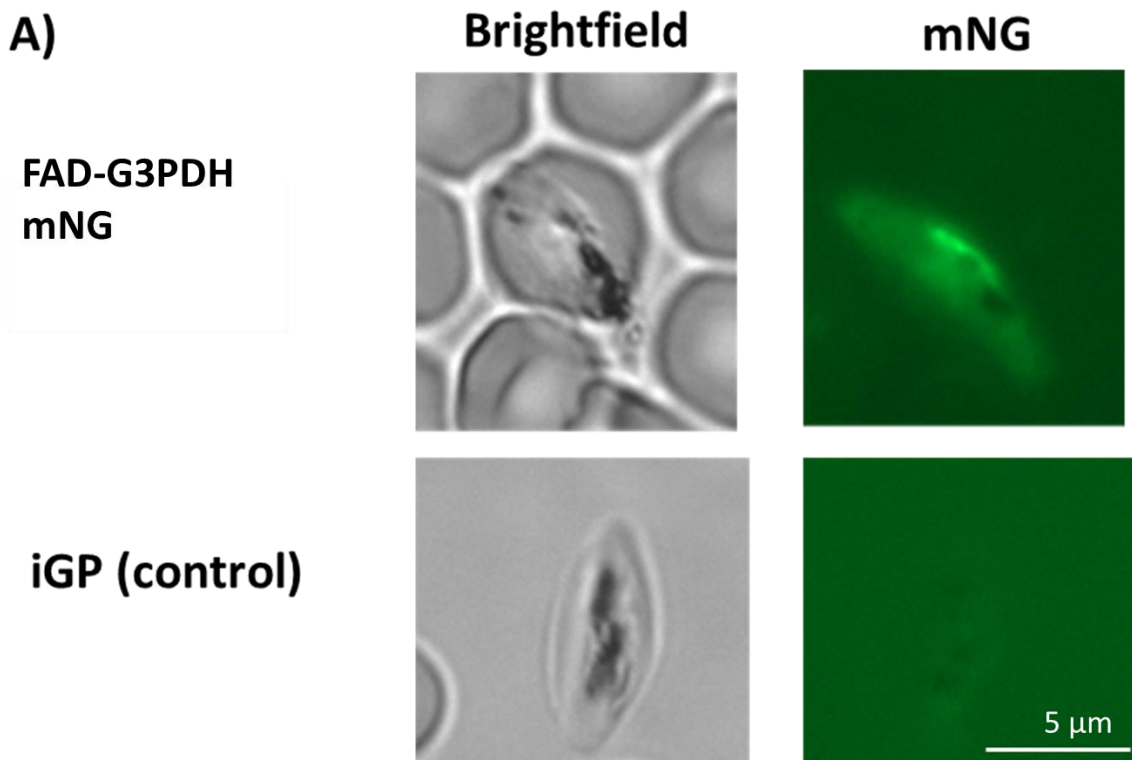
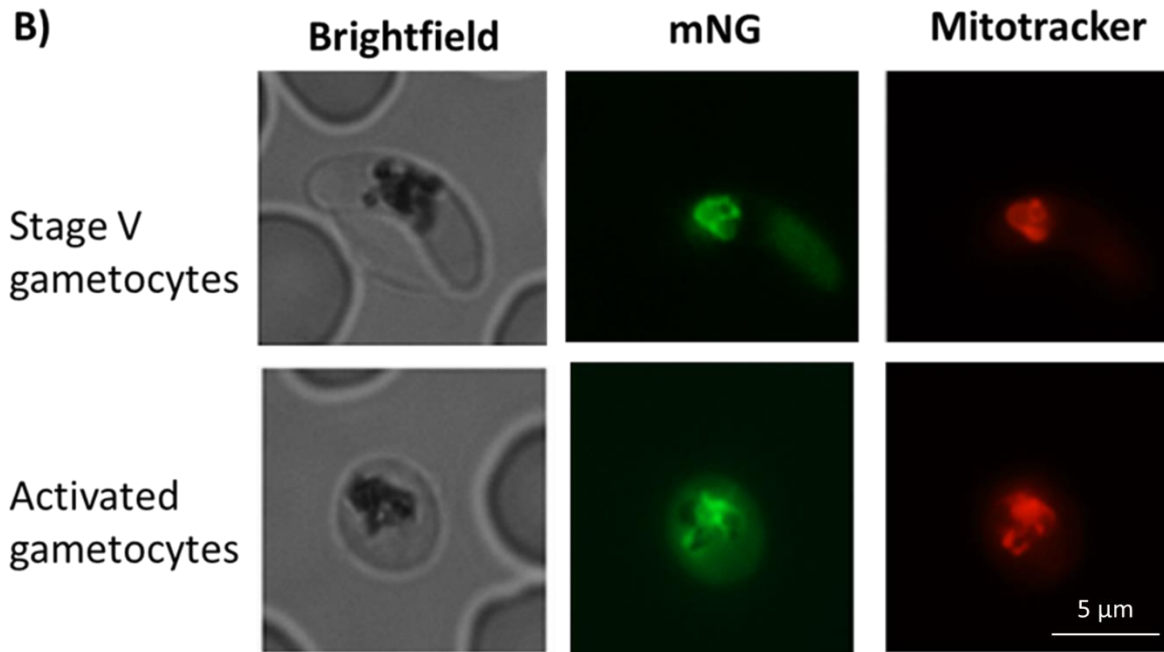


Figure 5.28. FAD-G3PDH expression in asexual blood stage parasites in the 3D7-iGP *P. falciparum* line. **Top**) FAD-G3PDH mNG parasites. **Bottom**) 3D7-iGP parent line (control.) Parasites are indicated by the red arrows.





**Figure 5.29. FAD-G3PDH expression and localisation in *P. falciparum* gametocytes.** **A)** Live image of stage V gametocytes of the FAD-G3PDH mNG line and the 3D7-iGP parent line (control). **B)** Live images of a stage V gametocytes (top) and activated gametocyte (bottom) of the FAD-G3PDH mNG line (mNG is the green channel) co-labelled with MitoTracker Red CMXRos (red channel.)

### 5.3 Discussion

Through data mining of published proteomic data and bioinformatic analyses, I have identified six proteins with evidence to suggest they may be important for gametocyte energy metabolism, five of which show a female gametocyte-biased expression. Tagging constructs were generated for all six genes, but due to time constraints caused by COVID-19, only two candidate genes were taken forward for characterisation.

The first of these was ACS-ADP, a putative ADP-forming acetyl-CoA synthetase. As part of this PhD project, ACS-ADP was successfully tagged with the green fluorescent protein mNeonGreen (mNG). It was found to be expressed throughout the life cycle and localised to the parasite mitochondrion. ACS-ADP-mNG fluorescence appeared to be brighter in gametocytes, consistent with upregulation in this stage predicted by proteomic studies. An ACS-ADP-KO line has now been generated but is yet to be characterised.

My hypothesis is that ACS-ADP is upregulated in gametocytes to deflect excess acetyl-CoA produced by glycolysis away from the TCA cycle by converting it into acetate. This could limit the production of ROS which could potentially damage the cell. Mosquito stages also use the TCA cycle, so conversion of excess acetyl-CoA to acetate may also be important for them to minimize damage to optimally complete their eventual differentiation into infectious

sporozoites to transmit to a new host. In contrast, asexual blood stage parasites rely on glycolysis and their mitochondrial activity is required only for the function of DHODH for *de novo* pyrimidine biosynthesis rather than mitochondrial respiration. However, the TCA cycle does still operate in asexual blood stage parasites where the environment is under considerable oxidative stress from haemoglobin metabolism which generates ROS (Oliveira and Oliveira, 2002; Jacot *et al.*, 2016) so perhaps this process would be still important in asexual blood stages to minimize excess ROS, but at lower levels than in gametocytes where mitochondrial respiration is upregulated (a model is shown in Figure 5.30).

The hypothesis that the upregulation of ACS-ADP in gametocytes could protect against oxidative stress could be tested as follows. The ACS-ADP-KO would undergo phenotypic analysis as performed on the PFK11-KO to first determine if deletion of this gene impacts gametocyte development or ability to transmit to mosquitoes. If a phenotype was observed, the KO and WT parasites could be treated with drugs which affect the redox balance, such as methylene blue, to see if the KO parasites are more sensitive. The assay could be performed as a DGFA to allow direct comparison of the male and female KO gametocytes to determine if there are sex differences in sensitivity.

Another possible experiment is to study the effect of 'ageing' on the viability of mature gametocytes. ACS-ADP-KO and WT gametocytes could be cultured to maturity and then left in culture to age. Male and female gametogenesis could be sampled at different time points post maturity to determine if gametogenesis is compromised as gametocytes get older. As gametocytes get older, damage from ROS would be expected to increase. If these proteins have a role in controlling oxidative damage, KO parasites may be expected to become unviable before their WT counterparts. To extend this experiment, these aged gametocytes could also be fed to mosquitoes to see if the KO phenotype worsens the older the gametocytes get. For example, the PFK11-KO parasites produced fewer oocysts, but if the gametocytes were allowed to age, perhaps even fewer oocysts or eventually no oocysts at all would be observed.

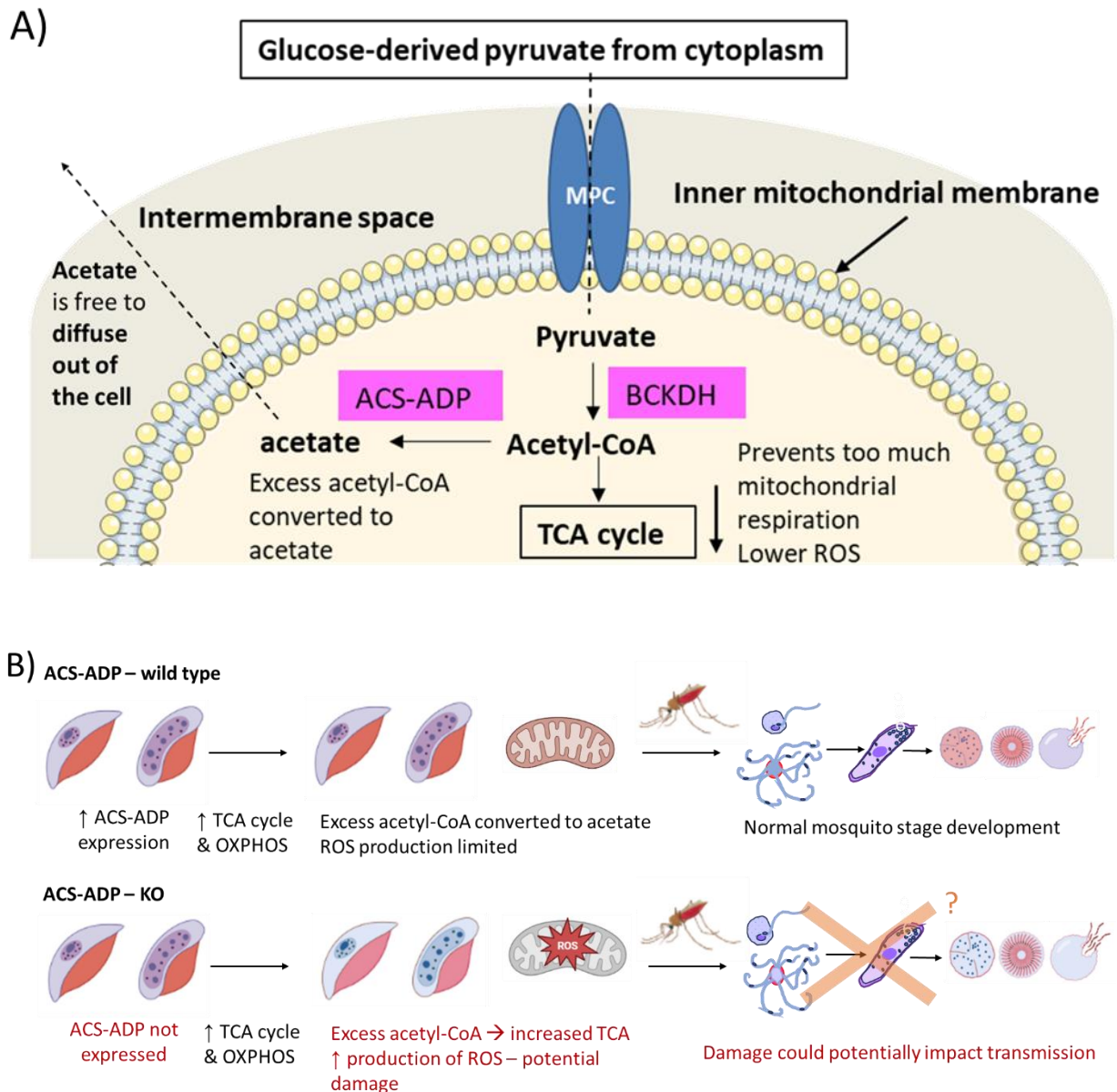


**Figure 5.30. Model of a possible role of ACS-ADP in *P. falciparum* gametocytes.** **A)** Proposed mechanism of regulation of energy metabolism. Glycolysis-derived pyruvate is taken up into the mitochondrial matrix via the mitochondrial pyruvate carrier (MPC) and is converted into acetyl-CoA by branched ketoacid dehydrogenase (BCKDH). Acetyl-CoA can enter the mitochondrial TCA cycle which can lead to generation of reactive oxygen species (ROS). ACS-ADP could convert excess acetyl-CoA to acetate preventing it from partaking in the TCA cycle and mitochondrial respiration and reducing ROS produced. **B)** If ACS-ADP limits excess ROS production by mitochondrial respiration in gametocytes, then KO of ACS-ADP could lead to overproduction of ROS which could damage the gametocyte which make them less viable and transmissible. Created with BioRender.

A further experiment to investigate the model of ACS-ADP's function would be to use metabolomic analysis to compare acetate formation between ACS-ADP-KO and WT. If

acetate formation is reduced in the KO, this suggests that ACS-ADP is responsible for the shift in the glycolytic endpoint from lactate towards acetate observed across gametocyte development (Lamour *et al.*, 2014).

In addition to quantification of acetate, mitochondrial activity between WT and ACS-ADP-KO could be compared using the image analysis methodology developed in Chapter 3. If ACS-ADP functions to shunt acetyl-CoA away from the mitochondrial TCA cycle, increased mitochondrial activity might be observed in the KO compared to the WT.

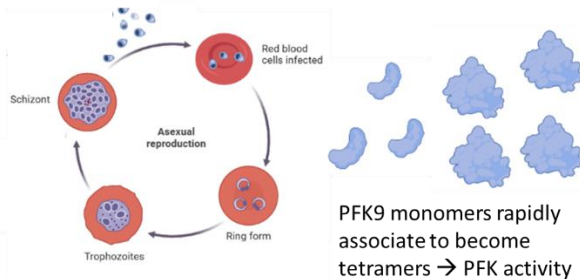
The second gene to be studied for the project was PFK11, an unusual, conserved phosphofructokinase (PFK) in *Plasmodium* spp. PFK11-KO parasites were successfully generated, and phenotyping carried out. PFK11-KO parasites showed no defect in growth or development prior to the oocyst stage, where a marked reduction in oocyst prevalence and intensity was observed in the KO compared to WT. It must be noted that for phenotypic analysis, the PFK11-KO line was compared to the WT NF54 parent line, which is an imperfect control, so these preliminary phenotyping results must be treated with caution. A suitable control would be a complementation line where the PFK11-KO parasites are transfected with a construct that restores expression of PFK11. If any observed phenotypes are due to KO of PFK11 rather than other unintended effects of genetically modifying the parasites, complementation should restore any observed phenotypes. Unfortunately, there was not sufficient time to generate a complementation line within the time limits of the PhD. The following experiments will be repeated with a complementation line as a formal control prior to publishing the data.

Pending complementation, these results suggest that PFK11 is important for ookinete development into oocysts. However, as oocysts were not completely absent from the PFK11-KO, follow-up experiments would be needed to dissect mosquito salivary glands at day 16 to check for the presence of sporozoites in the PFK11-KO. Due to the marked reduction of oocysts, it would be expected that either no sporozoites or greatly reduced numbers of sporozoites compared to WT would be seen. If the reduction in sporozoites is proportional to the reduction in oocysts, then this would suggest that while the transition from ookinete to oocyst is impaired in the PFK11-KO, sporozoite production is not affected. This would suggest PFK11 is not involved in sporozoite development. If no sporozoites are produced in the KO, then this suggests that PFK11 also has a role in sporozoite development within oocysts and it can be concluded that PFK11 is essential for transmission.

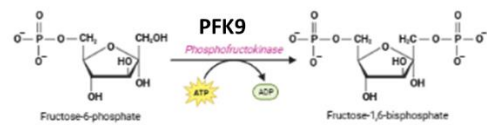
The mechanism for this phenotype is still unknown. I hypothesize that PFK11 regulates glycolysis, which may also lead to regulation of mitochondrial respiration. If PFK11 'slows'

glycolysis, this could result in a reduction in glycolysis-derived pyruvate entering the TCA cycle, thereby limiting production of ROS (a model is shown in Figure 5.31). Therefore, its role could be in limiting potential damage caused by increased mitochondrial respiration which could be harmful to the parasite later in development. It is possible that this damage takes time to accumulate so while no defect is seen in gametocytes, gametogenesis or ookinete formation, by the time the parasite reaches the oocyst stage, it is too damaged for oocysts to properly develop. The hypothesis that PFK11 may limit ROS production can be tested through the same methodology as described above for ACS-ADP.

**A) 1. Asexual blood stage parasites (ABS) – PFK9 expressed**

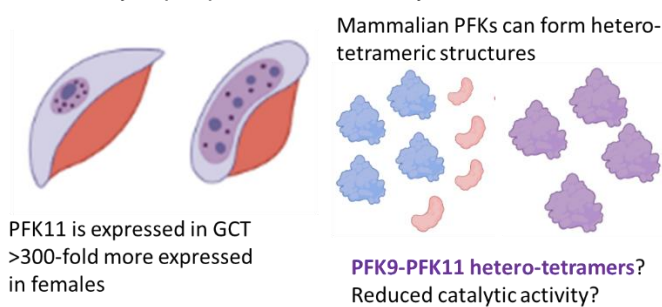


**Step 3 of glycolysis is catalysed by PFK9**

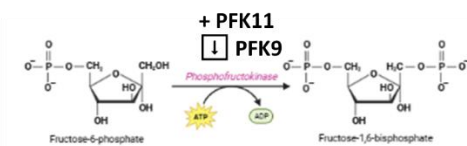


ABS operate a minimal TCA cycle and generate their ATP via glycolysis

**2. Gametocytes (GCT) – PFK11 and PFK9 expressed**



**PFK11 reduces PFK9's catalytic activity ...**



Slows glycolysis → limits glycolysis-derived pyruvate that enters the TCA cycle

Keeps mitochondrial ROS production at a 'safe' level while awaiting transmission

**B) PFK11 – wild type**

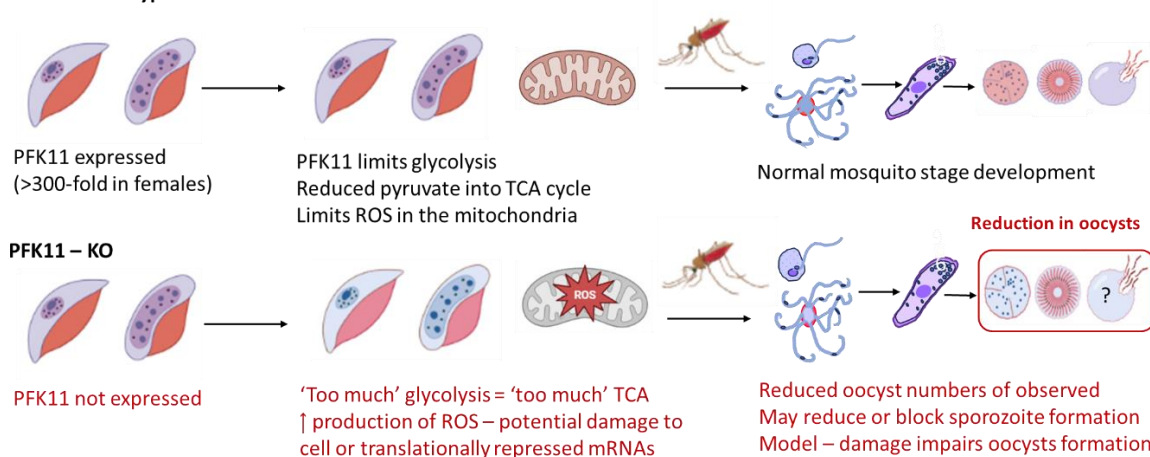


**Figure 5.31. Model for the role of PFK11 in *P. falciparum* gametocytes. A)** Proposed mechanism of regulation of gametocytes energy metabolism by PFK11. **B)** KO of PFK11 has been shown to impact oocyst numbers. If PFK11 'slows' glycolysis, thereby limiting the amount of glycolysis-derived

pyruvate entering the TCA cycle and in turn limiting mitochondrial respiration, then it could limit harmful ROS production to 'safe' levels. When PFK11 is knocked out, this could result in overproduction of ROS which could harm the gametocytes during their time in their host, and this damage could accumulate to result in the reduction in oocyst production observed in the KO. These ROS could also potentially damage translationally repressed mRNAs held in female gametocytes which could be important for oocyst development, leading to the observed arrest. Created with BioRender.

An experiment which would provide strong evidence that PFK11 regulates glycolysis in gametocytes would be metabolomic analysis. <sup>13</sup>C-glucose utilisation could be compared between WT and PFK11-KO. If the labelling of glycolytic intermediates and end points differed between WT and KO, then this would demonstrate that PFK11 expression affects glycolysis in gametocytes, lending support to the hypothesis that it acts as a regulator of gametocyte energy metabolism.

If deletion of PFK11 results in increased mitochondrial energy metabolism and overproduction of ROS, this could damage translationally repressed mRNA in female gametocytes. If these repressed transcripts are for proteins important for ookinete development into oocysts, then this could explain the reduction in oocyst production with deletion of PFK11. This hypothesis can be investigated using an antibody to 8-hydroxyguanosine, which allows the measurement of DNA and RNA damage by oxidative stress (Cattley and Glover, 1993). Intensity of anti-8-hydroxyguanosine labelling could be compared between PFK11-KO and WT gametocytes to determine whether there is any difference in staining. Increased labelling in the KO would imply that PFK11-KO parasites are experiencing greater levels of oxidative stress which could cause DNA and RNA damage to the cell. The anti-8-hydroxyguanosine antibody could be used in combination with anti-LDH2 to determine if this is a sex-specific effect which only occurs in female gametocytes. If a difference is observed, the anti-8-hydroxyguanosine antibody could be coupled to beads and used to precipitate the damaged RNA, which can be isolated and converted back to cDNA. The cDNA can then be amplified using PCR and sequenced to determine i) whether certain damaged RNAs are enriched in the PFK11-KO compared to WT and ii) whether any of these are known to be translationally repressed RNAs. WT and PFK11-KO parasites treated with hydrogen peroxide (H<sub>2</sub>O<sub>2</sub>) could be included as control conditions where the parasite will have been subject to oxidative stress.

PFK11 is predicted to be >300-fold more expressed in female gametocytes than males (Lasonder *et al.*, 2016). Tagging of this protein would allow me to determine whether PFK11 is expressed in female gametocytes as predicted, as well as its subcellular localisation. An

antibody raised to PFK11 appeared to show a punctate staining pattern in both male and female gametocytes. However, use of the antibody on PFK11-KO parasites unfortunately showed the antibody to be non-specific.

As previously mentioned, *Plasmodium* notably possesses two PFKs, PFK11 and PFK9. Unlike PFK11, which lacks the amino acid residues required for catalysis and is likely expressed in female gametocytes, PFK9 has been demonstrated to possess phosphofructokinase activity and is expressed across the life cycle (Mony *et al.*, 2009). It is known that mammals have multiple isoforms of PFK which can form hetero-tetrameric structures (Sola-Penna *et al.*, 2010; Fernandes *et al.*, 2020). I hypothesise that, although PFK11 does not possess catalytic activity, it may interact with PFK9 by forming such a hetero-tetramer with less catalytic activity, thereby acting as a regulator of glycolysis in female gametocytes. If it could be demonstrated that PFK11 and PFK9 interact, this would lend support to this hypothesis.

A PFK11-mNG line could be used to test this hypothesis through antibody pulldowns using anti-mNG antibodies coupled to magnetic beads to pull down PFK11 and any interacting partners. An antibody to PFK9 (kindly gifted by Audrey Odom John, Children's Hospital of Philadelphia) could also be chemically coupled to magnetic beads with protein A and then used to perform pulldowns with PFK9. If PFK11 pulls down PFK9 and vice versa, this suggests that they interact. Mass spectrometry would be required to prove the existence of a PFK11-PFK9 complex. Another approach which could be used to determine whether PFK11 interacts with PFK9 is proximity biotinylation. A transgenic line with PFK11 tagged with TurboID (Branon *et al.*, 2018; Ambekar, Beck and Mair, 2022; Lamb *et al.*, 2022) could be used to study whether PFK11 and PFK9 are interacting partners. If the two are interacting partners, then it strengthens the hypothesis that PFK11 could alter the catalytic activity of PFK9 through oligomerization regulation of PFK activity through formation of heteromeric tetramers. X-ray crystallography or cryoEM would be required to resolve the structures of PFK9 and PFK11 (whether they are dimers, tetramers etc.) and subsequently show if and how PFK9 and PFK11 bind.

Another possible approach to investigate PFK11's function is the generation of DiCre parasites which conditionally overexpress PFK11 and PFK9 in asexual blood stage parasites ('misexpression' lines) with the addition of the drug rapamycin (RAP). Experiments could then be carried out +/- RAP. The -RAP parasites would be functionally WT, providing an internal positive control. However, there is a possibility that overexpressing these proteins, particularly PFK11 which is not normally expressed in asexual blood stage parasites, will be toxic and prevent parasite growth. Providing the overexpression of these proteins isn't toxic

to the parasites, these lines have several applications to study PFK11. To investigate the hypothesis that PFK11 regulates glycolysis, <sup>13</sup>C-glucose utilisation could be compared in the PFK11 misexpression line +/- RAP to determine if certain glycolytic or TCA cycle intermediates are differentially labelled between +/- RAP, indicating what enzyme(s) or step of glycolysis PFK11 is regulating. If PFK11 slows glycolysis as I hypothesise, an accumulation of the intermediates just upstream of the step catalysed by PFK9 and depletion of those downstream may be observed.

In addition, correctly folded full-length PFK9 and PFK11 have not yet been successfully expressed in bacteria (Delves, unpublished observations). The DiCre plasmid which will be used generate these lines has a C-terminal Strep-tag can be used for protein purification as it has a high affinity for being pulled down. This could potentially be a way to obtain full-length PFK11 and PFK9 in sufficient quantities for purification which could then be used for functional, interaction and structural studies. If protein purification is successful, enzymatic assays (if the hypothesis is correct then PFK9 activity should reduce with the addition of PFK11) and cryoEM structural studies could be possible.

In conclusion, a putative ACS-ADP enzyme in *P. falciparum* was found to have a mitochondrial localisation and to be expressed throughout the life cycle. Metabolomic analysis of WT and KO parasites is required to determine whether ACS-ADP is involved in the shift in glycolytic endpoint from lactate towards acetate in gametocytes. Efforts to tag PFK11 are ongoing and will be needed to determine if it the protein is female gametocyte upregulated as indicated by proteomic data. PFK11 was successfully disrupted in *P. falciparum*, where it showed no defects in growth or development until the oocyst stage, where it showed a marked reduction in oocyst prevalence and density. This preliminary phenotyping data suggests that that PFK11 is important for ookinete development into oocysts. Further experiments are required to determine whether sporozoite production is reduced or completely abrogated. Future work on this parasite line will investigate how PFK11-KO leads to impaired mosquito transmission and to address the hypothesis that PFK11 regulates ('limits') glycolysis in *P. falciparum* gametocytes to avoid excess oxidative stress.

## Chapter 6

## Conclusions

Advances in metabolomics and experimental genetics have transformed our understanding of energy metabolism in *Plasmodium* parasites, showing their energy metabolism undergoes a series of changes across their complex life cycle. Whereas asexual blood stage parasites rely primarily on glycolysis for ATP generation, gametocytes upregulate mitochondrial energy metabolism and disruption of mitochondrial energy metabolism in *P. falciparum* has been shown to abrogate transmission through arrest of gametocyte development or failure to develop through the insect stages of the life cycle. This reliance on mitochondrial energy metabolism makes gametocyte energy metabolism a potentially rich source of transmission-blocking drug targets. However, our knowledge of the cell biology of gametocyte energy metabolism is sparse. This project set out to investigate 1) whether energy metabolism differs between male and female gametocytes, 2) whether the upregulation of mitochondrial energy metabolism in male gametocytes could be required for gametogenesis and 3) to identify potential regulators of gametocyte energy metabolism.

### 6.1 Male and female gametocytes differ in their energy metabolism

This study has demonstrated for the first time that male gametocyte mitochondria are less active than those of females. This seems consistent with published proteomic data which suggests that proteins involved in energy metabolism are among those enriched in female gametocytes compared to males, suggesting that mitochondrial energy metabolism may be more active. While metabolomics of sex-pure populations of gametocytes is required to confirm whether mitochondrial respiration is more active in female gametocytes, these data provide the first evidence that male and female gametocytes differ in their mitochondrial energy metabolism.

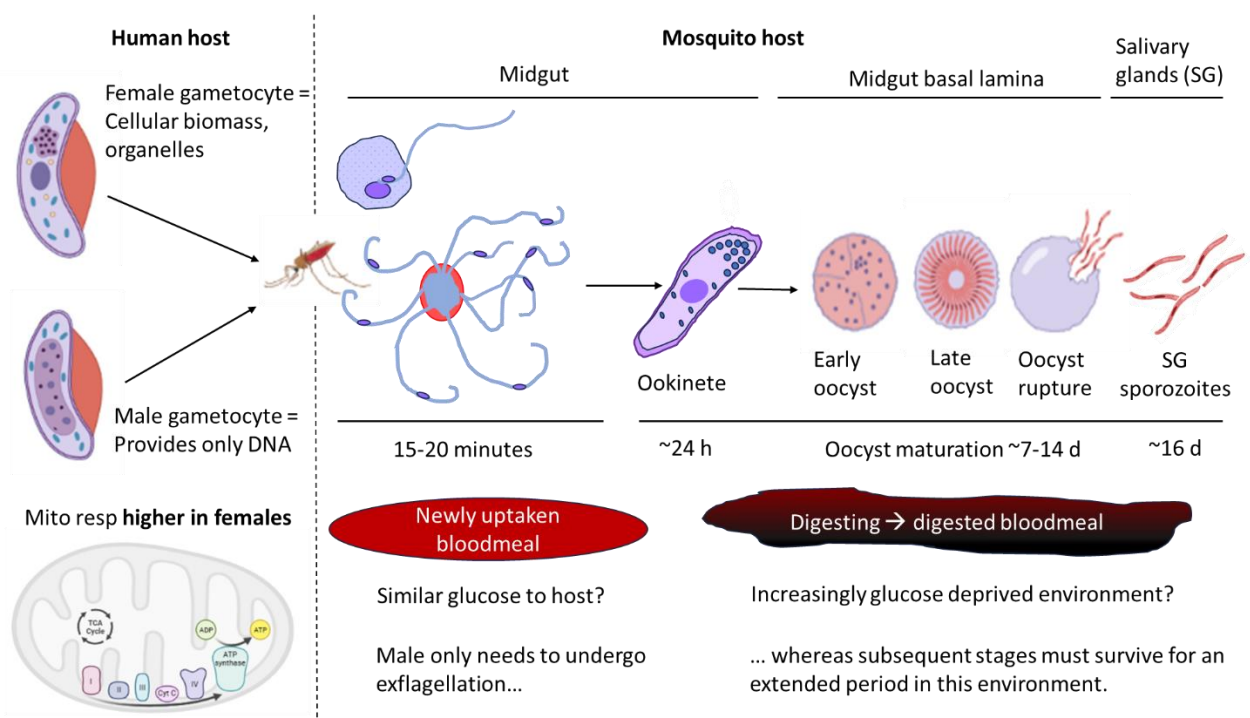
Male and female gametocytes are found in the same environment in the human host and have the same access to glucose and oxygen for mitochondrial respiration. Therefore, it seems unlikely that the increased mitochondrial activity (which presumably means a more active TCA cycle) in females is related to their time in the human host. I have two main hypotheses to explain the increased mitochondrial activity in female gametocytes.

The first is that the differences in mitochondrial activity reflect differences in energy demands of the sexes for onward development in the mosquito. This would be expected to be greater in females which are preparing for differentiation into ookinetes, oocysts and subsequently sporozoites whereas males 'only' need to undergo exflagellation. This might seem contradictory as the DGFA data presented in chapter 3 indicates, again for the first time, that

male gametogenesis is more susceptible to disruption of the mETC than that of females, suggesting male gametogenesis may be more energy intensive than female gametogenesis. However, while the process of male gametogenesis may require more energy than female gametogenesis, the energy required for onward differentiation into the subsequent developmental stages might be higher overall, explaining the higher mitochondrial activity in female gametocytes.

The second hypothesis is that the male gametocyte is limiting mitochondrial respiration to limit ROS production. It makes physiological sense not to risk damage by excess ROS production if the mitochondrion is only needed for 15-20 minutes once in the vector. Perhaps females must risk an increased level of ROS as this amount of mitochondrial energy metabolism is needed to progress through mosquito development. In addition, several of the genes I identified as part of the project which are putatively important for gametocyte energy metabolism are thought to be directly or indirectly involved in maintaining redox homeostasis or in antioxidant defence. Therefore, female gametocytes may have mechanisms to compensate for their increased mitochondrial activity.

Overall, my model is that the lower activity of male gametocyte mitochondria reflects lower energy requirements for onward development in the mosquito relative to females and may offer the added advantage of minimising oxidative stress.



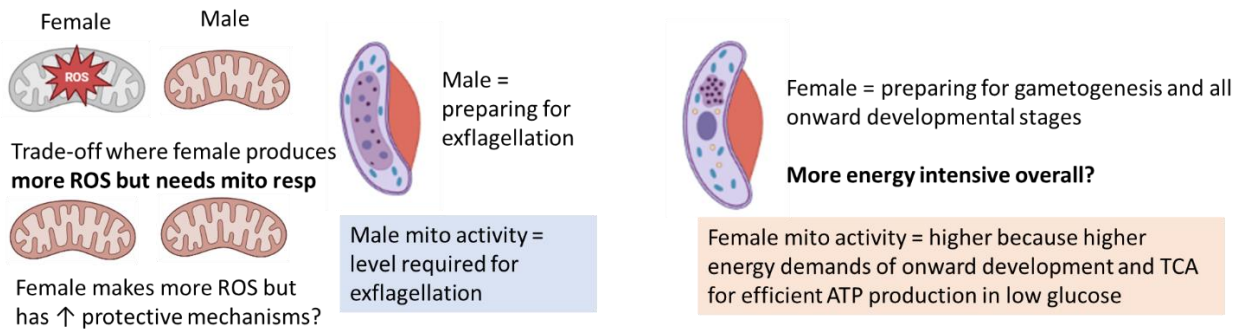


**Figure 6.2. Models for the increased activity of female gametocyte mitochondria compared to those of males.** Abbreviations: mito = mitochondrial, h = hours post-feeding, d = days post-feeding. Created with BioRender.

## 6.2 Energy for exflagellation – a role for increased mitochondrial energy metabolism in male gametocytes?

Despite being quiescent in the human host, both sexes of gametocytes grow a large, complex mitochondrion indicative of increased mitochondrial function. Prior to the start of the project, it was unclear why the male gametocyte invests in growing a large, complex mitochondrion, particularly one that could produce harmful ROS, only to discard it at the next developmental stage.

The male mitochondrion is discarded during gametogenesis, therefore its role in male gametocytes must be related to either their time in the human host or to meet the energy demands of gametogenesis. The data presented in this thesis provide evidence for the latter. DGFA analysis of male and female gametocytes treated with mETC inhibitors demonstrated a direct link between disruption of energy metabolism and inhibition of exflagellation, suggesting for the first time that mitochondrial energy metabolism is important for meeting the energy demands of male gametogenesis. Subsequent experiments testing the effect of inhibition of ATP synthase with oligomycin A on gametogenesis directly (with no pre-incubation) further supported this hypothesis, showed marked reductions in both male and female gametogenesis. These data strongly suggest that mitochondrial energy metabolism is essential for efficient gametogenesis, particularly male gametogenesis. Given the rapidity and complexity of exflagellation, it seems plausible that the process may require support from mitochondrially produced ATP. In addition, while not a sex-specific analysis, my preliminary data with the ATeam1.03YEMK line suggests that intracellular ATP concentrations in gametocytes are insensitive to inhibition of ATP synthase by oligomycin A in excess glucose. This indicates that glycolysis is sufficient to meet the energy needs of mature gametocytes and that the enlargement of gametocyte mitochondria is not related to

their time in the human host, further supporting the enlargement of the male gametocyte mitochondrion is for gametogenesis.

In the DGFA analysis, the inhibitors showed a higher activity (lower IC<sub>50</sub> values) against male gametogenesis than female gametogenesis. The reason for this sex difference to disruption of mitochondrial energy metabolism in terms of onward viability is still unknown. My hypothesis is that due to the relative complexity of exflagellation compared to female gametogenesis, the process could be more energetically costly and require a greater contribution from mitochondrially generated ATP. Female gametogenesis 'only' requires de-repression of translationally repressed transcripts and egress from the erythrocyte so this may have lower energy requirements or, alternatively, it may require the same amount of ATP but over a longer period, so inefficient glycolysis can support it. This may allow the process of female gametogenesis to be more tolerant of mitochondrial disruption providing glycolysis is active. Perhaps both sexes enlarge their mitochondrion but for different reasons, for females to support onward development in the mosquito whereas for males it may be for meeting the energy demands of gametogenesis.

IFA images of male gametocytes treated with mETC inhibitors have shown that male gametocytes start the process of gametogenesis but this subsequently stalls, either at an early 'rounded up' stage or later in the process where flagella have been formed but the flagellar morphology is aberrant. The fact that the male gametocytes try to exflagellate, even after 24 hours incubation with mETC inhibitors as shown in Chapter 3, demonstrates that disruption of mitochondrial energy metabolism does not kill mature gametocytes. The ATP sensor data showed that oligomycin A does not perturb intracellular ATP in gametocytes providing glycolysis is active. In addition, the effect of mETC inhibitors on mitochondrial activity as measured by MitoTracker labelling was found not to differ between male and female gametocytes, with the sexes showing the same responses. Taken together, these data further support that upregulating of mitochondrial respiration is not related to their time in the vertebrate host but for gametogenesis. In addition, the fact male gametogenesis starts but arrests during the process of exflagellation, as opposed to never starting, could be seen to support the hypothesis that male gametogenesis is energy intensive, and the observed arrest is the gametocytes 'running out of energy.' One could speculate that, if male gametogenesis is energy intensive, without the more efficient mitochondrial ATP production, the ATP produced by glycolysis is depleted more quickly than new ATP can be generated and the cell runs out of ATP, arresting gametogenesis.

Further experiments are required to determine the exact mechanism(s) by which disruption of mitochondrial energy metabolism results in failure of male gametocytes to exflagellate.

However, this thesis provides the first evidence that mitochondrial energy metabolism is required for optimal gametogenesis. The seemingly counterintuitive enlargement (and presumably increased activity) of the male gametocyte mitochondria may be because, for most male gametocytes, mitochondrially produced ATP is essential to meet the energy demands of gametogenesis.

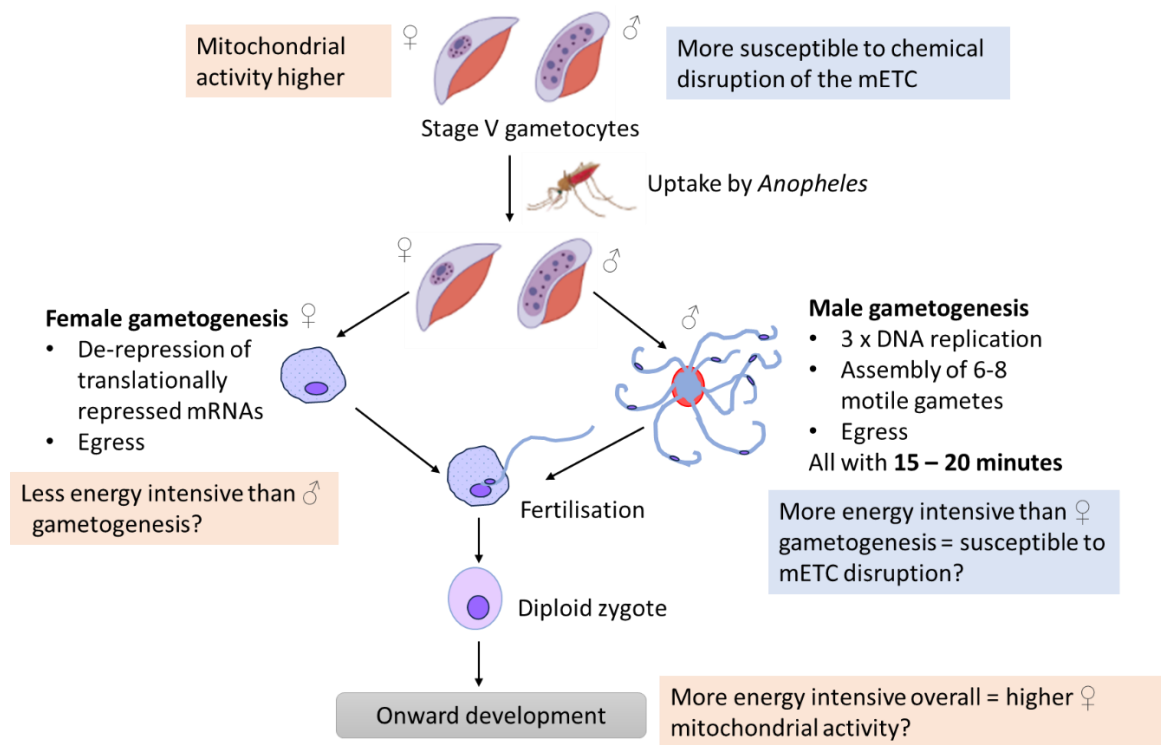


**Figure 6.3. Model for the increased susceptibility of male gametocytes to chemical inhibition of the mETC. Created with BioRender.**

### 6.3 Avoiding oxidative stress – a model for regulation of gametocyte energy metabolism

As part of the project, I identified six candidate proteins putatively important for regulating gametocyte energy metabolism. It is currently unknown why these six proteins have significantly higher (or specific) protein expression in gametocytes. However, this strongly suggests that they play roles critical for parasite transmission.

Production of ROS is an inevitable consequence of increased mitochondrial respiration. I hypothesize that gametocytes must strike a balance between preparedness for uptake into the mosquito and limiting ROS whilst in the human host to ensure the gametocytes remain reliable and transmissible. Intriguingly, three of the proteins – phosphoglucosmutase (PGM), FAD-G3PDH and GDH3 – are thought to be involved, directly or indirectly, in maintaining redox homeostasis and antioxidant defence. Similarly, I hypothesize that ACS-ADP and

PFK11 may also have roles in preventing oxidative stress. ACS-ADP may function to divert excess acetyl-CoA away from the mitochondrial TCA cycle by converting it to acetate, thus limiting mitochondrial respiration and ROS production. PFK11 is unlikely to possess catalytic activity itself but may interact with PFK9 as hetero-tetrameric structure to regulate (limit) the activity of PFK9 in gametocytes. This could 'limit' glycolysis, in turn limiting mitochondrial respiration and preventing excess ROS.

Gametocytes grow a large, complex mitochondria and drive an active TCA cycle. However, an inevitable consequence of mitochondrial respiration is the production of ROS (Oliveira and Oliveira, 2002; Sturm et al., 2015), therefore excess mitochondrial respiration may be detrimental to gametocytes. Perhaps these proteins are upregulated in gametocytes to mitigate the effects of increased mitochondrial respiration, which may be important in gametocytes during their long development and subsequently once released into the peripheral blood as mature gametocytes awaiting uptake into the mosquito.

Interestingly, PFK11, PGM, FAD-G3PDH and GDH3 are all upregulated in females (fold differences from Lasonder *et al.* (2016) are shown in Table 5.1). My image analysis using MitoTracker staining indicates that female gametocytes have a higher mitochondrial activity than male gametocytes. These proteins may be upregulated in females relative to males to compensate for their increased mitochondrial activity (and potentially increased ROS production) compared to males. However, if this is the case, it would be expected that this would also be the case for ACS-ADP which is upregulated in gametocytes but is not differentially expressed between the sexes (Lasonder *et al.*, 2016).

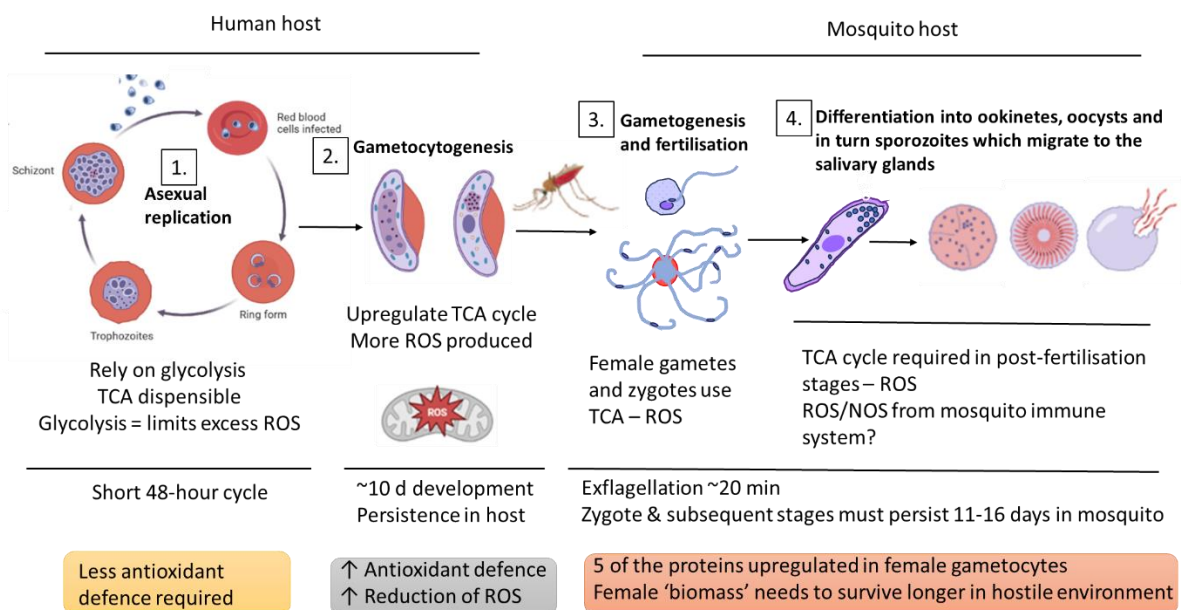


**Figure 6.4. Model of possible roles of candidate proteins in regulating gametocyte energy**

**metabolism. Hypothesised roles of candidate proteins:** PGM, FAD-G3PDH and GDH3 are thought to be involved directly or indirectly in maintaining the redox balance or in antioxidant defence. In addition, I hypothesise that ACS-ADP and PFK11 could limit TCA activity and in turn limit mitochondrial ROS production. **1) Asexual blood stage replication** – Asexual blood stage parasites rely on glycolysis (Srivastava *et al.*, 2016), which is thought to be advantageous to the parasites as it limits mitochondrial ROS production (Oliveira and Oliveira, 2002; Sturm *et al.*, 2015). **2) Gametocytogenesis** – Gametocytes upregulate their mitochondrial energy metabolism (MacRae *et al.*, 2013; Srivastava *et al.*, 2016) which would lead to increased mitochondrial ROS production. Therefore, these proteins may be upregulated in gametocytes to provide increased defence against ROS or to limit the amount of ROS produced. This may allow gametocytes to survive longer in the host to be taken up by a mosquito and to avoid damage which may affect their downstream development. **3) Gametogenesis and fertilisation** – male gametocytes are preparing for exflagellation whereas female gametocytes are preparing for functions after fertilisation (Talman *et al.*, 2004). Therefore, proteins involved in protecting against oxidative stress may be important in females as the zygote must persist in the vector, whereas males only need to survive to undergo exflagellation and pass on their DNA. **4) Onward development in the mosquito** – female gametocytes provide most of the cellular ‘biomass’ to the new zygote which must persist in the host environment of the mosquito to complete its development into sporozoites which can be transmitted to a new host. These proteins may be upregulated in female gametocytes to ensure the survival of post-zygote stages and transmission through the mosquito. Created with BioRender.

Proteins in *P. falciparum* and *P. berghei* with the highly female-biased expression in mature gametocytes have been demonstrated to be important or essential for insect stage development. Examples include LCCL domain containing proteins (CCPs) (Pradel *et al.*, 2004), G377 (Alano *et al.*, 1995; Severini *et al.*, 1999; De Koning-Ward *et al.*, 2008), P47 (Molina-Cruz, Canepa and Barillas-Mury, 2017; Ukegbu *et al.*, 2017), ABCG2 (Tran *et al.*, 2014) and actin-related protein 1 (Siden-Kiamos *et al.*, 2010). Therefore, although expressed in gametocytes, the energy metabolism proteins with the most female-biased expression (PGM = ~110-fold, PGM3 = ~87-fold) may be important for insect stage development. This appears to be the case for PFK11. This could be because their role in gametocytes becomes important downstream in development i.e., if energy metabolism is not regulated, then parasites accumulate damage which eventually prevents them progressing through the insect stages of the life cycle. Alternatively, it cannot be ruled out that these proteins could have moonlighting roles outside of energy metabolism which are important for female gametogenesis or insect stage development. For example, PGM was found to be associated with female gamete egress in *P. berghei* (Grasso *et al.*, 2022).

During the selection of candidate genes, there was a notable absence of male gametocyte upregulated proteins (proteins with >10-fold greater expression in males than females) with

GO terms associated with energy metabolism. This is perhaps not unexpected as previous sex-separated proteomes have shown that the male gametocyte proteome is enriched for proteins required for exflagellation (e.g. chromatin assembly, axoneme formation and DNA replication) whereas females are enriched for proteins involved in post-fertilisation functions, among them energy metabolism (Khan *et al.*, 2005; Lasonder *et al.*, 2016; Miao *et al.*, 2017). Many of the most male upregulated proteins in Lasonder and colleagues' proteomes (2016) are annotated as 'conserved *Plasmodium* protein of unknown function' and do not have GO terms assigned. Therefore, it cannot be ruled out that there are proteins important for male gametocyte energy metabolism among them. However, the fact some glycolysis enzymes and most TCA cycle enzymes are more highly expressed in females suggests that energy metabolism may be more active in females, coupled with my finding reported in Chapter 3 that males have a lower mitochondrial activity. As previously mentioned, female gametocytes outnumber males (Smalley and Sinden, 1977) and so previous metabolomic studies on mixed populations of gametocytes may be female-biased. Sex-specific metabolomics on transgenic lines which produce only male or only female gametocytes will be the best method to conclusively demonstrate if there are differences in energy metabolism between the sexes.

Many of these proteins putatively important for gametocyte energy metabolism are divergent from the human enzymes or not found in humans at all (e.g., ACS-ADP is not found in mammals, PGM3 is specific to the *Plasmodium* genus and *Hematocystis* spp.) which has potential for selectivity when targeted with drugs, should they be found to be important for mosquito transmission. PFK11 shares little similarity (~15% identity) with human PFKs (Mony *et al.*, 2009) and its deletion has shown to reduce oocyst production. If follow-up experiments find that sporozoite production is abrogated, PFK11 could be explored as a transmission-blocking drug target against gametocytes. Although detailed characterisation of all six proteins of interest was not possible in the time frame of the PhD, this research has uncovered several potential genes of interest in gametocytes and allowed the generation of hypotheses for further investigation. Direct study using transgenic parasite lines is required to determine the function of these proteins.

## 6.4 Final conclusions

The data presented in this thesis strongly suggest energy metabolism differs between male and female *P. falciparum* gametocytes. Male gametocyte mitochondria were found to be less active than those of females and to show greater susceptibility to chemical disruption of mETC. In addition, inhibition of ATP synthase was shown to markedly reduce

gametogenesis in both male and female gametocytes, suggesting that mitochondrial respiration is essential for optimal gametogenesis in *P. falciparum*. Possible hypotheses to explain these data are that exflagellation is highly complex and may be more energy intensive than female gametogenesis, requiring greater contributions to its energy needs from mitochondrially produced ATP. Another key finding is that inhibition of ATP synthase does not affect intracellular ATP conditions in gametocytes providing excess glucose is available, suggesting that mitochondrial respiration is not required to meet the energy needs of mature gametocytes. Taken together, these results support the notion that increased mitochondrial respiration in gametocytes is not related to their time in the human host. This work has allowed the formation of the hypothesis that both male and female gametocytes upregulate mitochondrial energy metabolism in preparation for uptake into the mosquito but for different reasons. In females, the mitochondrion is passed to the new zygote, where it is required to support the energy demands of differentiation into subsequent developmental stages, whereas in males, the mitochondrion is solely required to meet the energy demands of exflagellation, after which it is discarded. In terms of wider implications, these data suggests that mitochondrial respiration is a vulnerability of gametocytes which could be exploited for transmission-blocking drugs.

## References

- Adams, J.H. and Mueller, I. (2017) 'The Biology of *Plasmodium vivax*', *Cold Spring Harbor Perspectives in Medicine*, 7(9), p. a025585. Available at: <https://doi.org/10.1101/cshperspect.a025585>.
- Aguilar, R. *et al.* (2014) 'Molecular evidence for the localization of *Plasmodium falciparum* immature gametocytes in bone marrow', *Blood*, 123(7), pp. 959–966. Available at: <https://doi.org/10.1182/blood-2013-08-520767>.
- Aikawa, M. *et al.* (1978) 'Erythrocyte entry by malarial parasites. A moving junction between erythrocyte and parasite', *Journal of Cell Biology*, 77(1), pp. 72–82. Available at: <https://doi.org/10.1083/jcb.77.1.72>.
- Alano, P. *et al.* (1995) 'COS cell expression cloning of Pfg377, a *Plasmodium falciparum* gametocyte antigen associated with osmiophilic bodies', *Molecular and Biochemical Parasitology*, 74(2), pp. 143–156. Available at: [https://doi.org/10.1016/0166-6851\(95\)02491-3](https://doi.org/10.1016/0166-6851(95)02491-3).
- Alano, P. (2007) 'Plasmodium falciparum gametocytes: still many secrets of a hidden life', *Molecular Microbiology*, 66(2), pp. 291–302. Available at: <https://doi.org/10.1111/j.1365-2958.2007.05904.x>.
- Alano, P. and Carter, R. (1990) 'Sexual Differentiation in Malaria Parasites', *Annual Review of Microbiology*, 44(1), pp. 429–449. Available at: <https://doi.org/10.1146/annurev.mi.44.100190.002241>.
- Ali, A.A. *et al.* (2011) 'Hypoglycaemia and severe plasmodium falciparum malaria among pregnant sudanese women in an area characterized by unstable malaria transmission', *Parasites & Vectors*, 4(1), p. 88. Available at: <https://doi.org/10.1186/1756-3305-4-88>.
- Ambekar, S.V., Beck, J.R. and Mair, G.R. (2022) 'TurboID Identification of Evolutionarily Divergent Components of the Nuclear Pore Complex in the Malaria Model *Plasmodium berghei*', *mBio*, 13(5), pp. e01815-22. Available at: <https://doi.org/10.1128/mbio.01815-22>.
- Amino, R. *et al.* (2006) 'Quantitative imaging of *Plasmodium* transmission from mosquito to mammal', *Nature Medicine*, 12(2), pp. 220–224. Available at: <https://doi.org/10.1038/nm1350>.
- Andolina, C. *et al.* (2021) 'Sources of persistent malaria transmission in a setting with effective malaria control in eastern Uganda: a longitudinal, observational cohort study', *The Lancet Infectious Diseases*, 21(11), pp. 1568–1578. Available at: [https://doi.org/10.1016/S1473-3099\(21\)00072-4](https://doi.org/10.1016/S1473-3099(21)00072-4).
- Arora, N., C Anbalagan, L. and Pannu, A.K. (2021) 'Towards Eradication of Malaria: Is the WHO's RTS,S/AS01 Vaccination Effective Enough?', *Risk Management and Healthcare Policy*, 14, pp. 1033–1039. Available at: <https://doi.org/10.2147/RMHP.S219294>.
- Ashley, E.A. *et al.* (2014) 'Spread of Artemisinin Resistance in *Plasmodium falciparum* Malaria', *New England Journal of Medicine*, 371(5), pp. 411–423. Available at: <https://doi.org/10.1056/NEJMoa1314981>.

- Aulner, N. *et al.* (2019) 'Next-Generation Phenotypic Screening in Early Drug Discovery for Infectious Diseases', *Trends in Parasitology*, 35(7). Available at: <https://doi.org/10.1016/j.pt.2019.05.004>.
- Aurrecoechea, C. *et al.* (2009) 'PlasmoDB: a functional genomic database for malaria parasites', *Nucleic Acids Research*, 37(suppl\_1), pp. D539–D543. Available at: <https://doi.org/10.1093/nar/gkn814>.
- Ausina, P. *et al.* (2018) 'Insulin specifically regulates expression of liver and muscle phosphofructokinase isoforms', *Biomedicine & Pharmacotherapy*, 103, pp. 228–233. Available at: <https://doi.org/10.1016/j.biopha.2018.04.033>.
- Baer, K. *et al.* (2007) 'Release of Hepatic Plasmodium yoelii Merozoites into the Pulmonary Microvasculature', *PLOS Pathogens*, 3(11), p. e171. Available at: <https://doi.org/10.1371/journal.ppat.0030171>.
- Baker, D.A. (2010) 'Malaria gametocytogenesis | Elsevier Enhanced Reader', *Molecular and Biochemical Parasitology*, 172, pp. 57–65. Available at: <https://doi.org/10.1016/j.molbiopara.2010.03.019>.
- Baker, D.A. *et al.* (2017) 'A potent series targeting the malarial cGMP-dependent protein kinase clears infection and blocks transmission', *Nature Communications*, 8(1), p. 430. Available at: <https://doi.org/10.1038/s41467-017-00572-x>.
- Bancells, C. *et al.* (2019) 'Revisiting the initial steps of sexual development in the malaria parasite Plasmodium falciparum', *Nature Microbiology*, 4(1), pp. 144–154. Available at: <https://doi.org/10.1038/s41564-018-0291-7>.
- Banker, M.J. and Clark, T.H. (1976) 'Plasma / Serum Protein Binding Determinations', *Current Drug Metabolism*, 9(9), pp. 854–859.
- Bannister, L.H. *et al.* (1975) 'Structure and invasive behaviour of Plasmodium knowlesi merozoites in vitro', *Parasitology*, 71(3), pp. 483–491. Available at: <https://doi.org/10.1017/S0031182000047247>.
- Bannister, L.H. *et al.* (2000) 'A Brief Illustrated Guide to the Ultrastructure of Plasmodium falciparum Asexual Blood Stages', *Parasitology Today*, 16(10), pp. 427–433. Available at: [https://doi.org/10.1016/S0169-4758\(00\)01755-5](https://doi.org/10.1016/S0169-4758(00)01755-5).
- Bantuchai, S., Imad, H. and Nguitragee, W. (2022) 'Plasmodium vivax gametocytes and transmission', *Parasitology International*, 87, p. 102497. Available at: <https://doi.org/10.1016/j.parint.2021.102497>.
- Bartoloni, A. and Zammarchi, L. (2012) 'Clinical Aspects of Uncomplicated and Severe Malaria', *Mediterranean Journal of Hematology and Infectious Diseases*, 4(1), p. e2012026. Available at: <https://doi.org/10.4084/MJHID.2012.026>.
- Basco, L.K. and Le Bras, J. (1994) 'In Vitro Activity of Mitochondrial ATP Synthetase Inhibitors Against Plasmodium falciparum', *Journal of Eukaryotic Microbiology*, 41(3), pp. 179–183. Available at: <https://doi.org/10.1111/j.1550-7408.1994.tb01493.x>.
- Baton, L.A. and Ranford-Cartwright, L.C. (2012) 'Ookinete destruction within the mosquito midgut lumen explains Anopheles albimanus refractoriness to Plasmodium falciparum (3D7A) oocyst infection', *International Journal for Parasitology*, 42(3), pp. 249–258.

- Bhatt, S. *et al.* (2015) 'The effect of malaria control on *Plasmodium falciparum* in Africa between 2000 and 2015', *Nature*, 526(7572), pp. 207–211. Available at: <https://doi.org/10.1038/nature15535>.
- Billker, O. *et al.* (1997) 'The roles of temperature, pH and mosquito factors as triggers of male and female gametogenesis of *Plasmodium berghei* in vitro', *Parasitology*, 115(1), pp. 1–7. Available at: <https://doi.org/10.1017/S0031182097008895>.
- Billker, O. *et al.* (1998) 'Identification of xanthurenic acid as the putative inducer of malaria development in the mosquito', *Nature*, 392(6673), pp. 289–292. Available at: <https://doi.org/10.1038/32667>.
- Birkholtz, L.-M., Alano, P. and Leroy, D. (2022) 'Transmission-blocking drugs for malaria elimination | Elsevier Enhanced Reader', *Trends in Parasitology*, 38(5). Available at: <https://doi.org/10.1016/j.pt.2022.01.011>.
- Birnbaum, J. *et al.* (2017) 'A genetic system to study *Plasmodium falciparum* protein function', *Nature Methods*, 14(4), pp. 450–456. Available at: <https://doi.org/10.1038/nmeth.4223>.
- Birth, D., Kao, W.-C. and Hunte, C. (2014) 'Structural analysis of atovaquone-inhibited cytochrome bc1 complex reveals the molecular basis of antimalarial drug action', *Nature Communications*, 5(1), p. 4029. Available at: <https://doi.org/10.1038/ncomms5029>.
- Blume, M. *et al.* (2011) 'A constitutive pan-hexose permease for the *Plasmodium* life cycle and transgenic models for screening of antimalarial sugar analogs', *The FASEB Journal*, 25(4), pp. 1218–1229. Available at: <https://doi.org/10.1096/fj.10-173278>.
- Boltryk, S.D. *et al.* (2021) 'CRISPR/Cas9-engineered inducible gametocyte producer lines as a valuable tool for *Plasmodium falciparum* malaria transmission research', *Nature Communications*, 12(1), p. 4806. Available at: <https://doi.org/10.1038/s41467-021-24954-4>.
- Bousema, T. and Drakeley, C. (2011) 'Epidemiology and Infectivity of *Plasmodium falciparum* and *Plasmodium vivax* Gametocytes in Relation to Malaria Control and Elimination', *Clinical Microbiology Reviews*, 24(2). Available at: <https://doi.org/10.1128/CMR.00051-10>.
- Boyd, M.F. and Kitchen, S.F. (1937) 'On the Infectiousness of Patients infected with *Plasmodium vivax* and *Plasmodium falciparum*.', *American Journal of Tropical Medicine*, 17(2). Available at: <https://www.cabdirect.org/cabdirect/abstract/19371000426> (Accessed: 2 May 2023).
- Boyle, M.J. *et al.* (2010) 'Isolation of viable *Plasmodium falciparum* merozoites to define erythrocyte invasion events and advance vaccine and drug development', *Proceedings of the National Academy of Sciences*, 107(32), pp. 14378–14383. Available at: <https://doi.org/10.1073/pnas.1009198107>.
- Boysen, K.E. and Matuschewski, K. (2011) 'Arrested Oocyst Maturation in *Plasmodium* Parasites Lacking Type II NADH:Ubiquinone Dehydrogenase \*', *Journal of Biological Chemistry*, 286(37), pp. 32661–32671. Available at: <https://doi.org/10.1074/jbc.M111.269399>.
- Brancucci, N.M.B. *et al.* (2014) 'Heterochromatin Protein 1 Secures Survival and Transmission of Malaria Parasites', *Cell Host & Microbe*, 16(2), pp. 165–176. Available at: <https://doi.org/10.1016/j.chom.2014.07.004>.

Brancucci, N.M.B. *et al.* (2017) 'Lysophosphatidylcholine Regulates Sexual Stage Differentiation in the Human Malaria Parasite *Plasmodium falciparum*', *Cell*, 171(7), pp. 1532-1544.e15. Available at: <https://doi.org/10.1016/j.cell.2017.10.020>.

Branon, T.C. *et al.* (2018) 'Efficient proximity labeling in living cells and organisms with TurboID', *Nature Biotechnology*, 36(9), pp. 880–887. Available at: <https://doi.org/10.1038/nbt.4201>.

Brooks, S.R. and Williamson, K.C. (2000) 'Proteolysis of *Plasmodium falciparum* surface antigen, Pfs230, during gametogenesis', *Molecular and Biochemical Parasitology*, 106(1), pp. 77–82. Available at: [https://doi.org/10.1016/S0166-6851\(99\)00201-7](https://doi.org/10.1016/S0166-6851(99)00201-7).

Bruce, M.C. *et al.* (1990) 'Commitment of the malaria parasite *Plasmodium falciparum* to sexual and asexual development', *Parasitology*, 100(2), pp. 191–200. Available at: <https://doi.org/10.1017/S0031182000061199>.

BRUCHHAUS, I. *et al.* (1996) 'Pyrophosphate-dependent phosphofructokinase of *Entamoeba histolytica*: molecular cloning, recombinant expression and inhibition by pyrophosphate analogues', *Biochemical Journal*, 316(1), pp. 57–63. Available at: <https://doi.org/10.1042/bj3160057>.

Bruneel, F. *et al.* (2003) 'The Clinical Spectrum of Severe Imported *Falciparum* Malaria in the Intensive Care Unit', *American Journal of Respiratory and Critical Care Medicine*, 167(5), pp. 684–689. Available at: <https://doi.org/10.1164/rccm.200206-631OC>.

Buchholz, K. *et al.* (2008) 'Interactions of Methylene Blue with Human Disulfide Reductases and Their Orthologues from *Plasmodium falciparum*', *Antimicrobial Agents and Chemotherapy*, 52(1), pp. 183–191. Available at: <https://doi.org/10.1128/AAC.00773-07>.

Burgess, R.W. and Bray, R.S. (1961) 'The effect of a single dose of primaquine on the gametocytes, gametogony and sporogony of *Laverania falciparum*', *Bulletin of the World Health Organization*, 24(4–5), pp. 451–456.

Bushell, E. *et al.* (2017) 'Functional Profiling of a *Plasmodium* Genome Reveals an Abundance of Essential Genes', *Cell*, 170(2), pp. 260-272.e8. Available at: <https://doi.org/10.1016/j.cell.2017.06.030>.

Butcher, G.A. (1997) 'Antimalarial drugs and the mosquito transmission of *Plasmodium*', *International Journal for Parasitology*, 27(9), pp. 975–987. Available at: [https://doi.org/10.1016/S0020-7519\(97\)00079-9](https://doi.org/10.1016/S0020-7519(97)00079-9).

Carrasquilla, M. *et al.* (2020) 'Defining multiplicity of vector uptake in transfected *Plasmodium* parasites', *Scientific Reports*, 10(1), p. 10894. Available at: <https://doi.org/10.1038/s41598-020-67791-z>.

Cattley, R.C. and Glover, S.E. (1993) 'Elevated 8-hydroxydeoxyguanosine in hepatic DNA of rats following exposure to peroxisome proliferators: relationship to carcinogenesis and nuclear localization', *Carcinogenesis*, 14(12), pp. 2495–2499. Available at: <https://doi.org/10.1093/carcin/14.12.2495>.

CDC - Centers for Disease Control and Prevention (2021) *CDC - Malaria - Malaria Worldwide - Impact of Malaria*. Available at: [https://www.cdc.gov/malaria/malaria\\_worldwide/impact.html](https://www.cdc.gov/malaria/malaria_worldwide/impact.html) (Accessed: 17 April 2023).

Chaubey, S., Grover, M. and Tatu, U. (2014) 'Endoplasmic Reticulum Stress Triggers Gametocytogenesis in the Malaria Parasite', *Journal of Biological Chemistry*, 289(24), pp. 16662–16674. Available at: <https://doi.org/10.1074/jbc.M114.551549>.

Chi, A.S. *et al.* (2001) 'The Two Phosphofructokinase Gene Products of *Entamoeba histolytica*', *Journal of Biological Chemistry*, 276(23), pp. 19974–19981. Available at: <https://doi.org/10.1074/jbc.M011584200>.

Churcher, T.S. *et al.* (2012) 'Measuring the blockade of malaria transmission – An analysis of the Standard Membrane Feeding Assay', *International Journal for Parasitology*, 42(11), pp. 1037–1044. Available at: <https://doi.org/10.1016/j.ijpara.2012.09.002>.

Chutmongkonkul, M., Maier, W.A. and Seitz, H.M. (1992) 'A new model for testing gametocytocidal effects of some antimalarial drugs on *Plasmodium falciparum* in vitro', *Annals of Tropical Medicine & Parasitology*, 86(3), pp. 207–215. Available at: <https://doi.org/10.1080/00034983.1992.11812656>.

Cobbold, S.A. *et al.* (2013) 'Kinetic Flux Profiling Elucidates Two Independent Acetyl-CoA Biosynthetic Pathways in *Plasmodium falciparum*', *Journal of Biological Chemistry*, 288(51), pp. 36338–36350. Available at: <https://doi.org/10.1074/jbc.M113.503557>.

Cogswell, F.B. (1992) 'The hypnozoite and relapse in primate malaria', *Clinical Microbiology Reviews*, 5(1), pp. 26–35. Available at: <https://doi.org/10.1128/CMR.5.1.26>.

Coker, O.O. *et al.* (2013) 'Functional characterization of two members of histidine phosphatase superfamily in *Mycobacterium tuberculosis*', *BMC Microbiology*, 13(1), p. 292. Available at: <https://doi.org/10.1186/1471-2180-13-292>.

Coleman, B.I. *et al.* (2014) 'A *Plasmodium falciparum* Histone Deacetylase Regulates Antigenic Variation and Gametocyte Conversion', *Cell Host & Microbe*, 16(2), pp. 177–186. Available at: <https://doi.org/10.1016/j.chom.2014.06.014>.

Collins, C.R. *et al.* (2013) 'Robust inducible Cre recombinase activity in the human malaria parasite *Plasmodium falciparum* enables efficient gene deletion within a single asexual erythrocytic growth cycle', *Molecular Microbiology*, 88(4), pp. 687–701. Available at: <https://doi.org/10.1111/mmi.12206>.

Cowman, A.F. and Crabb, B.S. (2006) 'Invasion of Red Blood Cells by Malaria Parasites', *Cell*, 124(4), pp. 755–766. Available at: <https://doi.org/10.1016/j.cell.2006.02.006>.

Cox-Singh, J. and Singh, B. (2008) 'Knowlesi malaria: newly emergent and of public health importance?', *Trends in Parasitology*, 24(9), pp. 406–410. Available at: <https://doi.org/10.1016/j.pt.2008.06.001>.

Daily, J.P. *et al.* (2007) 'Distinct physiological states of *Plasmodium falciparum* in malaria-infected patients', *Nature*, 450(7172), pp. 1091–1095. Available at: <https://doi.org/10.1038/nature06311>.

Danaei, G. *et al.* (2011) 'National, regional, and global trends in fasting plasma glucose and diabetes prevalence since 1980: systematic analysis of health examination surveys and epidemiological studies with 370 country-years and 2.7 million participants', *The Lancet*, 378(9785), pp. 31–40. Available at: [https://doi.org/10.1016/S0140-6736\(11\)60679-X](https://doi.org/10.1016/S0140-6736(11)60679-X).

Das, A. *et al.* (1997) 'Molecular characterization and ultrastructural localization of *Plasmodium falciparum* Hsp 601: Nucleotide sequence data reported in this paper is

available in the GenBank™ database under accession No. U94594.1', *Molecular and Biochemical Parasitology*, 88(1), pp. 95–104. Available at: [https://doi.org/10.1016/S0166-6851\(97\)00081-9](https://doi.org/10.1016/S0166-6851(97)00081-9).

Datoo, M.S. *et al.* (2022) 'Efficacy and immunogenicity of R21/Matrix-M vaccine against clinical malaria after 2 years' follow-up in children in Burkina Faso: a phase 1/2b randomised controlled trial', *The Lancet Infectious Diseases*, 22(12), pp. 1728–1736. Available at: [https://doi.org/10.1016/S1473-3099\(22\)00442-X](https://doi.org/10.1016/S1473-3099(22)00442-X).

De Koning-Ward, T.F. *et al.* (2008) 'The role of osmiophilic bodies and Pfg377 expression in female gametocyte emergence and mosquito infectivity in the human malaria parasite *Plasmodium falciparum*', *Molecular Microbiology*, 67(2), pp. 278–290. Available at: <https://doi.org/10.1111/j.1365-2958.2007.06039.x>.

De Niz, M. *et al.* (2018) '*Plasmodium* gametocytes display homing and vascular transmigration in the host bone marrow', *Science Advances*, 4(5), p. eaat3775. Available at: <https://doi.org/10.1126/sciadv.aat3775>.

Dearnley, M.K. *et al.* (2012) 'Origin, composition, organization and function of the inner membrane complex of *Plasmodium falciparum* gametocytes', *Journal of Cell Science*, 125(8), pp. 2053–2063. Available at: <https://doi.org/10.1242/jcs.099002>.

Deitsch, K.W., Driskill, C.L. and Wellems, T.E. (2001) 'Transformation of malaria parasites by the spontaneous uptake and expression of DNA from human erythrocytes', *Nucleic Acids Research*, 29(3), pp. 850–853.

Delves, M. *et al.* (2012) 'The Activities of Current Antimalarial Drugs on the Life Cycle Stages of *Plasmodium*: A Comparative Study with Human and Rodent Parasites', *PLoS Medicine*, 9(2), p. e1001169. Available at: <https://doi.org/10.1371/journal.pmed.1001169>.

Delves, M.J. *et al.* (2013) 'Male and Female *Plasmodium falciparum* Mature Gametocytes Show Different Responses to Antimalarial Drugs', *Antimicrobial Agents and Chemotherapy*, 57(7), pp. 3268–3274. Available at: <https://doi.org/10.1128/AAC.00325-13>.

Delves, M.J. *et al.* (2016) 'Routine in vitro culture of *P. falciparum* gametocytes to evaluate novel transmission-blocking interventions', *Nature Protocols*, 11(9), pp. 1668–1680. Available at: <https://doi.org/10.1038/nprot.2016.096>.

Delves, M.J. *et al.* (2017) 'Failure of in vitro differentiation of *Plasmodium falciparum* gametocytes into ookinetes arises because of poor gamete fertilisation'. bioRxiv, p. 216721. Available at: <https://doi.org/10.1101/216721>.

Delves, M.J. *et al.* (2018) 'A high throughput screen for next-generation leads targeting malaria parasite transmission', *Nature Communications*, 9(1), p. 3805. Available at: <https://doi.org/10.1038/s41467-018-05777-2>.

Delves, M.J., Angrisano, F. and Blagborough, A.M. (2018) 'Antimalarial Transmission-Blocking Interventions: Past, Present, and Future', *Trends in Parasitology*, 34(9), pp. 735–746. Available at: <https://doi.org/10.1016/j.pt.2018.07.001>.

Dembélé, L. *et al.* (2014) 'Persistence and activation of malaria hypnozoites in long-term primary hepatocyte cultures', *Nature Medicine*, 20(3), pp. 307–312. Available at: <https://doi.org/10.1038/nm.3461>.

DENG, Z. *et al.* (1998) 'Cloning and expression of the gene for the active PPI-dependent phosphofructokinase of *Entamoeba histolytica*', *Biochemical Journal*, 329(3), pp. 659–664. Available at: <https://doi.org/10.1042/bj3290659>.

Dicko, A. *et al.* (2018) 'Efficacy and safety of primaquine and methylene blue for prevention of *Plasmodium falciparum* transmission in Mali: a phase 2, single-blind, randomised controlled trial', *The Lancet Infectious Diseases*, 18(6), pp. 627–639. Available at: [https://doi.org/10.1016/S1473-3099\(18\)30044-6](https://doi.org/10.1016/S1473-3099(18)30044-6).

van Dijk, M.R. *et al.* (2001) 'A Central Role for P48/45 in Malaria Parasite Male Gamete Fertility', *Cell*, 104(1), pp. 153–164. Available at: [https://doi.org/10.1016/S0092-8674\(01\)00199-4](https://doi.org/10.1016/S0092-8674(01)00199-4).

Dixon, M.W.A. *et al.* (2008) 'Sex in *Plasmodium*: a sign of commitment', *Trends in Parasitology*, 24(4), pp. 168–175. Available at: <https://doi.org/10.1016/j.pt.2008.01.004>.

Drakeley, C.J. *et al.* (1999) 'Host haematological factors influencing the transmission of *Plasmodium falciparum* gametocytes to *Anopheles gambiae* s.s. mosquitoes', *Tropical Medicine & International Health*, 4(2), pp. 131–138. Available at: <https://doi.org/10.1046/j.1365-3156.1999.00361.x>.

Dunaway, G.A. *et al.* (1988) 'Analysis of the phosphofructokinase subunits and isoenzymes in human tissues', *Biochemical Journal*, 251(3), pp. 677–683. Available at: <https://doi.org/10.1042/bj2510677>.

Eichner, M. *et al.* (2001) 'Genesis, sequestration and survival of *Plasmodium falciparum* gametocytes: parameter estimates from fitting a model to malariatherapy data', *Transactions of The Royal Society of Tropical Medicine and Hygiene*, 95(5), pp. 497–501. Available at: [https://doi.org/10.1016/S0035-9203\(01\)90016-1](https://doi.org/10.1016/S0035-9203(01)90016-1).

Eksi, S. *et al.* (2002) 'Targeting and sequestration of truncated Pfs230 in an intraerythrocytic compartment during *Plasmodium falciparum* gametocytogenesis', *Molecular Microbiology*, 44(6), pp. 1507–1516. Available at: <https://doi.org/10.1046/j.1365-2958.2002.02986.x>.

Eksi, S. *et al.* (2012) 'Plasmodium falciparum Gametocyte Development 1 (Pfgdv1) and Gametocytogenesis Early Gene Identification and Commitment to Sexual Development', *PLOS Pathogens*, 8(10), p. e1002964. Available at: <https://doi.org/10.1371/journal.ppat.1002964>.

Eksi, S. and Williamson, K.C. (2002) 'Male-specific expression of the paralog of malaria transmission-blocking target antigen Pfs230, PfB0400w', *Molecular and Biochemical Parasitology*, 122(2), pp. 127–130. Available at: [https://doi.org/10.1016/S0166-6851\(02\)00091-9](https://doi.org/10.1016/S0166-6851(02)00091-9).

Evers, F. *et al.* (2021) 'Composition and stage dynamics of mitochondrial complexes in *Plasmodium falciparum*', *Nature Communications*, 12(1), p. 3820. Available at: <https://doi.org/10.1038/s41467-021-23919-x>.

Evers, F. *et al.* (2023) 'Comparative 3D ultrastructure of *Plasmodium falciparum* gametocytes'. *bioRxiv*, p. 2023.03.10.531920. Available at: <https://doi.org/10.1101/2023.03.10.531920>.

Färber, P. *et al.* (1998) 'Recombinant *Plasmodium falciparum* glutathione reductase is inhibited by the antimalarial dye methylene blue', *FEBS Letters*, 422(3), pp. 311–314. Available at: [https://doi.org/10.1016/S0014-5793\(98\)00031-3](https://doi.org/10.1016/S0014-5793(98)00031-3).

- Farrance, C.E. *et al.* (2011) 'Antibodies to plant-produced *Plasmodium falciparum* sexual stage protein Pfs25 exhibit transmission blocking activity', *Human Vaccines*, 7(sup1), pp. 191–198. Available at: <https://doi.org/10.4161/hv.7.0.14588>.
- Fernandes, P.M. *et al.* (2020) 'Biochemical and transcript level differences between the three human phosphofructokinases show optimisation of each isoform for specific metabolic niches', *Biochemical Journal*, 477(22), pp. 4425–4441. Available at: <https://doi.org/10.1042/BCJ20200656>.
- Filarsky, M. *et al.* (2018) 'GDV1 induces sexual commitment of malaria parasites by antagonizing HP1-dependent gene silencing', *Science*, 359(6381), pp. 1259–1263. Available at: <https://doi.org/10.1126/science.aan6042>.
- Florens, L. *et al.* (2002) 'A proteomic view of the *Plasmodium falciparum* life cycle', *Nature*, 419(6906), pp. 520–526. Available at: <https://doi.org/10.1038/nature01107>.
- Fowler, R.E., Sinden, R.E. and Pudney, M. (1995) 'Inhibitory Activity of the Anti-Malarial Atovaquone (566C80) against Ookinetes, Oocysts, and Sporozoites of *Plasmodium berghei* on JSTOR', *The Journal of Parasitology*, 38(3), pp. 452–458.
- Frevert, U. *et al.* (2005) 'Intravital Observation of *Plasmodium berghei* Sporozoite Infection of the Liver', *PLOS Biology*, 3(6), p. e192. Available at: <https://doi.org/10.1371/journal.pbio.0030192>.
- Fry, M., Webb, E. and Pudney, M. (1990) 'Effect of mitochondrial inhibitors on adenosinetriphosphate levels in *Plasmodium falciparum*', *Comparative Biochemistry and Physiology Part B: Comparative Biochemistry*, 96(4), pp. 775–782. Available at: [https://doi.org/10.1016/0305-0491\(90\)90230-Q](https://doi.org/10.1016/0305-0491(90)90230-Q).
- Galinski, M.R., Meyer, E.V.S. and Barnwell, J.W. (2013) 'Chapter One - *Plasmodium vivax*: Modern Strategies to Study a Persistent Parasite's Life Cycle', in S.I. Hay, R. Price, and J.K. Baird (eds) *Advances in Parasitology*. Academic Press (The Epidemiology of *Plasmodium vivax*), pp. 1–26. Available at: <https://doi.org/10.1016/B978-0-12-407826-0.00001-1>.
- Garcia, G.E. *et al.* (1998) 'Xanthurenic Acid Induces Gametogenesis in *Plasmodium*, the Malaria Parasite\*', *Journal of Biological Chemistry*, 273(20), pp. 12003–12005. Available at: <https://doi.org/10.1074/jbc.273.20.12003>.
- Garnham, P.C.C. (1966) 'Malaria Parasites and other Haemosporidia.', *Malaria Parasites and other Haemosporidia*. [Preprint]. Available at: <https://www.cabdirect.org/cabdirect/abstract/19672901312> (Accessed: 2 May 2023).
- Gebru, T., Mordmüller, B. and Held, J. (2014) 'Effect of Fluorescent Dyes on In Vitro-Differentiated, Late-Stage *Plasmodium falciparum* Gametocytes', *Antimicrobial Agents and Chemotherapy*, 58(12), pp. 7398–7404. Available at: <https://doi.org/10.1128/AAC.03772-14>.
- Geneva: World Health Organisation (2022) 'World malaria report 2022'. Available at: <https://www.who.int/publications-detail-redirect/9789240064898> (Accessed: 14 March 2023).
- Ghorbal, M. *et al.* (2014) 'Genome editing in the human malaria parasite *Plasmodium falciparum* using the CRISPR-Cas9 system', *Nature Biotechnology*, 32(8), pp. 819–821. Available at: <https://doi.org/10.1038/nbt.2925>.
- Goldberg, D.E. *et al.* (1990) 'Hemoglobin degradation in the malaria parasite *Plasmodium falciparum*: an ordered process in a unique organelle.', *Proceedings of the National*

*Academy of Sciences*, 87(8), pp. 2931–2935. Available at: <https://doi.org/10.1073/pnas.87.8.2931>.

Gomes, A.R. *et al.* (2022) 'A transcriptional switch controls sex determination in *Plasmodium falciparum*', *Nature*, 612(7940), pp. 528–533. Available at: <https://doi.org/10.1038/s41586-022-05509-z>.

Gonçalves, B.P. *et al.* (2016) 'Single low dose primaquine to reduce gametocyte carriage and *Plasmodium falciparum* transmission after artemether-lumefantrine in children with asymptomatic infection: a randomised, double-blind, placebo-controlled trial', *BMC Medicine*, 14(1), p. 40. Available at: <https://doi.org/10.1186/s12916-016-0581-y>.

Goodman, C.D. *et al.* (2016) 'Parasites resistant to the antimalarial atovaquone fail to transmit by mosquitoes', *Science*, 352(6283), pp. 349–353. Available at: <https://doi.org/10.1126/science.aad9279>.

Grasso, F. *et al.* (2020) 'A Comprehensive Gender-related Secretome of *Plasmodium berghei* Sexual Stages', *Molecular & Cellular Proteomics*, 19(12), pp. 1986–1997. Available at: <https://doi.org/10.1074/mcp.RA120.002212>.

Grasso, F. *et al.* (2022) 'Identification and preliminary characterization of *Plasmodium falciparum* proteins secreted upon gamete formation', *Scientific Reports*, 12(1), p. 9592. Available at: <https://doi.org/10.1038/s41598-022-13415-7>.

Greenspan, P., Mayer, E.P. and Fowler, S.D. (1985) 'Nile red: a selective fluorescent stain for intracellular lipid droplets.', *Journal of Cell Biology*, 100(3), pp. 965–973. Available at: <https://doi.org/10.1083/jcb.100.3.965>.

Grinsven, K.W.A. van *et al.* (2008) 'Acetate:Succinate CoA-transferase in the Hydrogenosomes of *Trichomonas vaginalis*: IDENTIFICATION AND CHARACTERIZATION \*', *Journal of Biological Chemistry*, 283(3), pp. 1411–1418. Available at: <https://doi.org/10.1074/jbc.M702528200>.

Hale, V.L. *et al.* (2017) 'Parasitophorous vacuole poration precedes its rupture and rapid host erythrocyte cytoskeleton collapse in *Plasmodium falciparum* egress | PNAS', *Proceedings of the National Academy of Sciences*, 114(13), pp. 3439–3444. Available at: <https://doi.org/10.1073/pnas.1619441114>.

Harris, C.T. *et al.* (2023) 'Metabolic competition between lipid metabolism and histone methylation regulates sexual differentiation in human malaria parasites'. bioRxiv, p. 2022.01.18.476397. Available at: <https://doi.org/10.1101/2022.01.18.476397>.

Hawking, F., Wilson, M.E. and Gammage, K. (1971) 'Evidence for cyclic development and short-lived maturity in the gametocytes of *Plasmodium falciparum*.' , *Transactions of the Royal Society of Tropical Medicine and Hygiene*, 65(5), pp. 549–59.

Hearne, A. *et al.* (2020) 'Oligomycin-induced proton uncoupling', *Toxicology in Vitro*, 67, p. 104907. Available at: <https://doi.org/10.1016/j.tiv.2020.104907>.

Hendrickse, R.G. and Adeniyi, A. (1979) 'Quartan malarial nephrotic syndrome in children', *Kidney International*, 16(1), pp. 64–74. Available at: <https://doi.org/10.1038/ki.1979.103>.

Hills, T. *et al.* (2011) 'Characterization of a new phosphatase from *Plasmodium*', *Molecular and Biochemical Parasitology*, 179(2), pp. 69–79. Available at: <https://doi.org/10.1016/j.molbiopara.2011.06.001>.

Hino, A. *et al.* (2012) 'Critical roles of the mitochondrial complex II in oocyst formation of rodent malaria parasite *Plasmodium berghei*', *The Journal of Biochemistry*, 152(3), pp. 259–268. Available at: <https://doi.org/10.1093/jb/mvs058>.

Hliscs, M. *et al.* (2015) 'Organization and function of an actin cytoskeleton in *Plasmodium falciparum* gametocytes', *Cellular Microbiology*, 17(2), pp. 207–225. Available at: <https://doi.org/10.1111/cmi.12359>.

Hogh, B. *et al.* (1998) 'The differing impact of chloroquine and pyrimethamine/sulfadoxine upon the infectivity of malaria species to the mosquito vector.', *The American Journal of Tropical Medicine and Hygiene*, 58(2), pp. 176–182. Available at: <https://doi.org/10.4269/ajtmh.1998.58.176>.

Hopert, A. *et al.* (1993) 'Mycoplasma detection by PCR analysis', *In Vitro Cellular & Developmental Biology - Animal*, 29(10), pp. 819–821. Available at: <https://doi.org/10.1007/BF02634350>.

Horecker, B.L. (2002) 'The Pentose Phosphate Pathway', *Journal of Biological Chemistry*, 277(50), pp. 47965–47971. Available at: <https://doi.org/10.1074/jbc.X200007200>.

Howes, R.E. *et al.* (2012) 'G6PD Deficiency Prevalence and Estimates of Affected Populations in Malaria Endemic Countries: A Geostatistical Model-Based Map', *PLoS Medicine*. Edited by L. Von Seidlein, 9(11), p. e1001339. Available at: <https://doi.org/10.1371/journal.pmed.1001339>.

Idro, R. *et al.* (2010) 'Cerebral Malaria: Mechanisms of Brain Injury and Strategies for Improved Neurocognitive Outcome', *Pediatric Research*, 68(4), pp. 267–274. Available at: <https://doi.org/10.1203/PDR.0b013e3181eee738>.

Imada, M. *et al.* (2010) 'Characterization of  $\alpha$ -phosphoglucosyltransferase isozymes from *Toxoplasma gondii*', *Parasitology International*, 59(2), pp. 206–210. Available at: <https://doi.org/10.1016/j.parint.2010.01.007>.

Imamura, H. *et al.* (2009) 'Visualization of ATP levels inside single living cells with fluorescence resonance energy transfer-based genetically encoded indicators', *Proceedings of the National Academy of Sciences*, 106(37), pp. 15651–15656. Available at: <https://doi.org/10.1073/pnas.0904764106>.

Imbert, P., Rapp, C. and Buffet, P.A. (2009) 'Pathological rupture of the spleen in malaria: Analysis of 55 cases (1958–2008)', *Travel Medicine and Infectious Disease*, 7(3), pp. 147–159. Available at: <https://doi.org/10.1016/j.tmaid.2009.01.002>.

Jacot, D. *et al.* (2016) 'Apicomplexan Energy Metabolism: Carbon Source Promiscuity and the Quiescence Hyperbole', *Trends in Parasitology*, 32(1), pp. 56–70. Available at: <https://doi.org/10.1016/j.pt.2015.09.001>.

Janse, Chris J. *et al.* (1986) 'DNA synthesis in *Plasmodium berghei* during asexual and sexual development', *Molecular and Biochemical Parasitology*, 20(2), pp. 173–182. Available at: [https://doi.org/10.1016/0166-6851\(86\)90029-0](https://doi.org/10.1016/0166-6851(86)90029-0).

Janse, C.J. *et al.* (1986) 'Rapid repeated DNA replication during microgametogenesis and DNA synthesis in young zygotes of *Plasmodium berghei*', *Transactions of The Royal Society of Tropical Medicine and Hygiene*, 80(1), pp. 154–157. Available at: [https://doi.org/10.1016/0035-9203\(86\)90219-1](https://doi.org/10.1016/0035-9203(86)90219-1).

- Janse, C.J. *et al.* (1988) 'DNA synthesis in gametocytes of *Plasmodium falciparum*', *Parasitology*, 96(1), pp. 1–7. Available at: <https://doi.org/10.1017/S0031182000081609>.
- Jiang, X. (2022) 'An overview of the *Plasmodium falciparum* hexose transporter and its therapeutic interventions', *Proteins: Structure, Function, and Bioinformatics*, 90(10), pp. 1766–1778. Available at: <https://doi.org/10.1002/prot.26351>.
- Jiménez, B.C. *et al.* (2007) 'Spontaneous Splenic Rupture due to *Plasmodium vivax* in a Traveler: Case Report and Review', *Journal of Travel Medicine*, 14(3), pp. 188–191. Available at: <https://doi.org/10.1111/j.1708-8305.2007.00112.x>.
- Jogdand, P.S. *et al.* (2012) 'Flow cytometric readout based on Mitotracker Red CMXRos staining of live asexual blood stage malarial parasites reliably assesses antibody dependent cellular inhibition', *Malaria Journal*, 11(1), p. 235. Available at: <https://doi.org/10.1186/1475-2875-11-235>.
- Joice, R. *et al.* (2014) '*Plasmodium falciparum* transmission stages accumulate in the human bone marrow', *Science Translational Medicine*, 6(244), pp. 244re5–244re5. Available at: <https://doi.org/10.1126/scitranslmed.3008882>.
- Josling, G.A. and Llinás, M. (2015) 'Sexual development in *Plasmodium* parasites: knowing when it's time to commit', *Nature Reviews Microbiology*, 13(9), pp. 573–587. Available at: <https://doi.org/10.1038/nrmicro3519>.
- Kadenbach, B. (2003) 'Intrinsic and extrinsic uncoupling of oxidative phosphorylation', *Biochimica et Biophysica Acta (BBA) - Bioenergetics*, 1604(2), pp. 77–94. Available at: [https://doi.org/10.1016/S0005-2728\(03\)00027-6](https://doi.org/10.1016/S0005-2728(03)00027-6).
- Kafsack, B.F.C. *et al.* (2014) 'A transcriptional switch underlies commitment to sexual development in malaria parasites', *Nature*, 507(7491), pp. 248–252. Available at: <https://doi.org/10.1038/nature12920>.
- Kagawa, Y. and Racker, E. (1966) 'Partial Resolution of the Enzymes Catalyzing Oxidative Phosphorylation: VIII. PROPERTIES OF A FACTOR CONFERRING OLIGOMYCIN SENSITIVITY ON MITOCHONDRIAL ADENOSINE TRIPHOSPHATASE', *Journal of Biological Chemistry*, 241(10), pp. 2461–2466. Available at: [https://doi.org/10.1016/S0021-9258\(18\)96640-8](https://doi.org/10.1016/S0021-9258(18)96640-8).
- Kappe, S.H.I., Kaiser, K. and Matuschewski, K. (2003) 'The *Plasmodium* sporozoite journey: a rite of passage', *Trends in Parasitology*, 19(3), pp. 135–143. Available at: [https://doi.org/10.1016/S1471-4922\(03\)00007-2](https://doi.org/10.1016/S1471-4922(03)00007-2).
- Ke, H. *et al.* (2015) 'Genetic Investigation of Tricarboxylic Acid Metabolism during the *Plasmodium falciparum* Life Cycle', *Cell Reports*, 11(1), pp. 164–174. Available at: <https://doi.org/10.1016/j.celrep.2015.03.011>.
- Ke, H. *et al.* (2019) 'Mitochondrial type II NADH dehydrogenase of *Plasmodium falciparum* (PfNDH2) is dispensable in the asexual blood stages', *PLOS ONE*, 14(4), p. e0214023. Available at: <https://doi.org/10.1371/journal.pone.0214023>.
- Kent, R.S. *et al.* (2018) 'Inducible developmental reprogramming redefines commitment to sexual development in the malaria parasite *Plasmodium berghei*', *Nature Microbiology*, 3(11), pp. 1206–1213. Available at: <https://doi.org/10.1038/s41564-018-0223-6>.

- Khan, S.M. *et al.* (2005) 'Proteome Analysis of Separated Male and Female Gametocytes Reveals Novel Sex-Specific Plasmodium Biology', *Cell*, 121(5), pp. 675–687. Available at: <https://doi.org/10.1016/j.cell.2005.03.027>.
- Kibbe, W.A. (2007) 'OligoCalc: an online oligonucleotide properties calculator', *Nucleic Acids Research*, 35(Web Server), pp. W43–W46. Available at: <https://doi.org/10.1093/nar/gkm234>.
- Koch-Weser, J. and Sellers, E.M. (1976) 'Binding of Drugs to Serum Albumin', *New England Journal of Medicine*, 294(6), pp. 311–316. Available at: <https://doi.org/10.1056/NEJM197602052940605>.
- Krishna, S., Webb, R. and Woodrow, C. (2001) 'Transport proteins of Plasmodium falciparum: defining the limits of metabolism', *International Journal for Parasitology*, 31(12), pp. 1331–1342. Available at: [https://doi.org/10.1016/S0020-7519\(01\)00254-5](https://doi.org/10.1016/S0020-7519(01)00254-5).
- Krotoski, W.A. *et al.* (1982) 'Demonstration of hypnozoites in sporozoite-transmitted Plasmodium vivax infection', *The American journal of tropical medicine and hygiene*, 31(6), pp. 1291–1293. Available at: <https://doi.org/10.4269/ajtmh.1982.31.1291>.
- Krungkrai, J., Prapunwattana, P. and Krungkrai, S.R. (2000a) 'Ultrastructure and function of mitochondria in gametocytic stage of Plasmodium falciparum', *Parasite*, 7(1), pp. 19–26. Available at: <https://doi.org/10.1051/parasite/2000071019>.
- Krungkrai, J., Prapunwattana, P. and Krungkrai, S.R. (2000b) 'Ultrastructure and function of mitochondria in gametocytic stage of Plasmodium falciparum', *Parasite*, 7(1), pp. 19–26. Available at: <https://doi.org/10.1051/parasite/2000071019>.
- Kumar, N. and Zheng, H. (1990) 'Stage-specific gametocytocidal effect in vitro of the antimalaria drug qinghaosu on Plasmodium falciparum', *Parasitology Research*, 76(3), pp. 214–218. Available at: <https://doi.org/10.1007/BF00930817>.
- Lamb, I.M. *et al.* (2022) 'Mitochondrially targeted proximity biotinylation and proteomic analysis in Plasmodium falciparum', *PLOS ONE*, 17(8), p. e0273357. Available at: <https://doi.org/10.1371/journal.pone.0273357>.
- Lambros, C. and Vanderberg, J.P. (1979) 'Synchronization of Plasmodium falciparum Erythrocytic Stages in Culture', *The Journal of Parasitology*, 65(3), pp. 418–420. Available at: <https://doi.org/10.2307/3280287>.
- Lamour, S.D. *et al.* (2014) 'Changes in metabolic phenotypes of Plasmodium falciparum in vitro cultures during gametocyte development', *Malaria Journal*, 13(1), p. 468. Available at: <https://doi.org/10.1186/1475-2875-13-468>.
- Lane, K.D. *et al.* (2018) 'Selection of Plasmodium falciparum cytochrome B mutants by putative PfNDH2 inhibitors', *Proceedings of the National Academy of Sciences*, 115(24), pp. 6285–6290. Available at: <https://doi.org/10.1073/pnas.1804492115>.
- Lardy, H.A., Johnson, D. and McMurray, W.C. (1958) 'Antibiotics as tools for metabolic studies. I. A survey of toxic antibiotics in respiratory, phosphorylative and glycolytic systems', *Archives of Biochemistry and Biophysics*, 78(2), pp. 587–597. Available at: [https://doi.org/10.1016/0003-9861\(58\)90383-7](https://doi.org/10.1016/0003-9861(58)90383-7).
- Larsson, C. *et al.* (1998) 'The importance of the glycerol 3-phosphate shuttle during aerobic growth of Saccharomyces cerevisiae', *Yeast*, 14(4), pp. 347–357. Available at: [https://doi.org/10.1002/\(SICI\)1097-0061\(19980315\)14:4<347::AID-YEA226>3.0.CO;2-9](https://doi.org/10.1002/(SICI)1097-0061(19980315)14:4<347::AID-YEA226>3.0.CO;2-9).

- Lasonder, E. *et al.* (2016) 'Integrated transcriptomic and proteomic analyses of *P. falciparum* gametocytes: molecular insight into sex-specific processes and translational repression', *Nucleic Acids Research*, 44(13), pp. 6087–6101. Available at: <https://doi.org/10.1093/nar/gkw536>.
- Lelièvre, J. *et al.* (2012) 'Activity of Clinically Relevant Antimalarial Drugs on Plasmodium falciparum Mature Gametocytes in an ATP Bioluminescence "Transmission Blocking" Assay', *PLOS ONE*, 7(4), p. e35019. Available at: <https://doi.org/10.1371/journal.pone.0035019>.
- Lerchundi, R. *et al.* (2019) 'FRET-based imaging of intracellular ATP in organotypic brain slices', *Journal of Neuroscience Research*, 97(8), pp. 933–945. Available at: <https://doi.org/10.1002/jnr.24361>.
- Lerchundi, R., Huang, N. and Rose, C.R. (2020) 'Quantitative Imaging of Changes in Astrocytic and Neuronal Adenosine Triphosphate Using Two Different Variants of ATeam', *Frontiers in Cellular Neuroscience*, 14. Available at: <https://www.frontiersin.org/articles/10.3389/fncel.2020.00080> (Accessed: 3 April 2023).
- LeRoux, M., Lakshmanan, V. and Daily, J.P. (2009) 'Plasmodium falciparum biology: analysis of in vitro versus in vivo growth conditions', *Trends in Parasitology*, 25(10), pp. 474–481. Available at: <https://doi.org/10.1016/j.pt.2009.07.005>.
- Levine, N. (1970) 'Taxonomy of the Sporozoa', *Journal of Parasitology*, 56(4), pp. 208–9.
- Lian, L.-Y. *et al.* (2009) 'Glycerol: An unexpected major metabolite of energy metabolism by the human malaria parasite', *Malaria Journal*, 8(1), p. 38. Available at: <https://doi.org/10.1186/1475-2875-8-38>.
- Liu, Y. *et al.* (2008) 'The conserved plant sterility gene HAP2 functions after attachment of fusogenic membranes in Chlamydomonas and Plasmodium gametes', *Genes & Development*, 22(8), pp. 1051–1068. Available at: <https://doi.org/10.1101/gad.1656508>.
- Lobo, C.A. and Kumar, N. (1998) 'Sexual Differentiation and Development in the Malaria Parasite', *Parasitology Today*, 14(4), pp. 146–150. Available at: [https://doi.org/10.1016/S0169-4758\(97\)01210-6](https://doi.org/10.1016/S0169-4758(97)01210-6).
- López-Barragán, M.J. *et al.* (2011) 'Directional gene expression and antisense transcripts in sexual and asexual stages of Plasmodium falciparum', *BMC genomics*, 12, p. 587. Available at: <https://doi.org/10.1186/1471-2164-12-587>.
- Lopez-Rubio, J.-J., Mancio-Silva, L. and Scherf, A. (2009) 'Genome-wide Analysis of Heterochromatin Associates Clonally Variant Gene Regulation with Perinuclear Repressive Centers in Malaria Parasites', *Cell Host & Microbe*, 5(2), pp. 179–190. Available at: <https://doi.org/10.1016/j.chom.2008.12.012>.
- Lovegrove, F.E. *et al.* (2008) 'Plasmodium falciparum shows transcriptional versatility within the human host', *Trends in Parasitology*, 24(7), pp. 288–291. Available at: <https://doi.org/10.1016/j.pt.2008.04.004>.
- Mackintosh, C.L., Beeson, J.G. and Marsh, K. (2004) 'Clinical features and pathogenesis of severe malaria', *Trends in Parasitology*, 20(12), pp. 597–603. Available at: <https://doi.org/10.1016/j.pt.2004.09.006>.

- Maclean, A.E. *et al.* (2022) 'The mystery of massive mitochondrial complexes: the apicomplexan respiratory chain', *Trends in Parasitology*, 38(12). Available at: <https://doi.org/10.1016/j.pt.2022.09.008>.
- MacRae, J.I. *et al.* (2013) 'Mitochondrial metabolism of sexual and asexual blood stages of the malaria parasite *Plasmodium falciparum*', *BMC Biology*, 11(1), p. 67. Available at: <https://doi.org/10.1186/1741-7007-11-67>.
- Madrid, L. *et al.* (2015) 'Malaria-associated hypoglycaemia in children', *Expert Review of Anti-infective Therapy*, 13(2), pp. 267–277. Available at: <https://doi.org/10.1586/14787210.2015.995632>.
- Mai, M.S. and Allison, W.S. (1983) 'Inhibition of an oligomycin-sensitive ATPase by cationic dyes, some of which are atypical uncouplers of intact mitochondria', *Archives of Biochemistry and Biophysics*, 221(2), pp. 467–476. Available at: [https://doi.org/10.1016/0003-9861\(83\)90165-0](https://doi.org/10.1016/0003-9861(83)90165-0).
- Mair, G.R., Braks, J.A.M., Garver, L.S., Wiegant, J.C.A.G., *et al.* (2006) 'Regulation of Sexual Development of *Plasmodium* by Translational Repression', *Science*, 313(5787), pp. 667–669. Available at: <https://doi.org/10.1126/science.1125129>.
- Mair, G.R., Braks, J.A.M., Garver, L.S., Dimopoulos, G., *et al.* (2006) 'Translational Repression is essential for *Plasmodium* sexual development and mediated by a DDX6-type RNA helicase', *Science (New York, N.Y.)*, 313(5787), pp. 667–669. Available at: <https://doi.org/10.1126/science.1125129>.
- Mairet-Khedim, M. *et al.* (2021) 'Clinical and In Vitro Resistance of *Plasmodium falciparum* to Artesunate-Amodiaquine in Cambodia', *Clinical Infectious Diseases*, 73(3), pp. 406–413. Available at: <https://doi.org/10.1093/cid/ciaa628>.
- Mariebernard, M., Mohanty, A. and Rajendran, V. (2022) 'A comprehensive review on classifying fast-acting and slow-acting antimalarial agents based on time of action and target organelle of *Plasmodium* sp', *Pathogens and Disease*, 80(1), p. ftac015. Available at: <https://doi.org/10.1093/femspd/ftac015>.
- McKee, R.W. *et al.* (1946) 'STUDIES ON MALARIAL PARASITES', *The Journal of Experimental Medicine*, 84(6), pp. 569–582.
- McRobert, L. *et al.* (2008) 'Gametogenesis in Malaria Parasites Is Mediated by the cGMP-Dependent Protein Kinase', *PLoS Biology*. Edited by G.E. Ward, 6(6), p. e139. Available at: <https://doi.org/10.1371/journal.pbio.0060139>.
- Medley, G.F. *et al.* (1993) 'Heterogeneity in patterns of malarial oocyst infections in the mosquito vector', *Parasitology*, 106(5), pp. 441–449. Available at: <https://doi.org/10.1017/S0031182000076721>.
- Miao, J. *et al.* (2017) 'Sex-Specific Biology of the Human Malaria Parasite Revealed from the Proteomes of Mature Male and Female Gametocytes\*', *Molecular & Cellular Proteomics*, 16(4), pp. 537–551. Available at: <https://doi.org/10.1074/mcp.M116.061804>.
- Millerioux, Y. *et al.* (2012) 'ATP Synthesis-coupled and -uncoupled Acetate Production from Acetyl-CoA by Mitochondrial Acetate:Succinate CoA-transferase and Acetyl-CoA Thioesterase in *Trypanosoma*\*', *Journal of Biological Chemistry*, 287(21), pp. 17186–17197. Available at: <https://doi.org/10.1074/jbc.M112.355404>.

Miura, K. *et al.* (2013) 'Qualification of Standard Membrane-Feeding Assay with *Plasmodium falciparum* Malaria and Potential Improvements for Future Assays', *PLoS ONE*. Edited by D.J. Diemert, 8(3), p. e57909. Available at: <https://doi.org/10.1371/journal.pone.0057909>.

Modica-Napolitano, J.S. *et al.* (1984) 'Rhodamine 123 inhibits bioenergetic function in isolated rat liver mitochondria', *Biochemical and Biophysical Research Communications*, 118(3), pp. 717–723. Available at: [https://doi.org/10.1016/0006-291X\(84\)91453-0](https://doi.org/10.1016/0006-291X(84)91453-0).

Molina-Cruz, A., Canepa, G.E. and Barillas-Mury, C. (2017) 'Plasmodium P47: a key gene for malaria transmission by mosquito vectors', *Current Opinion in Microbiology*, 40, pp. 168–174. Available at: <https://doi.org/10.1016/j.mib.2017.11.029>.

Montagna, G.N., Matuschewski, K. and Buscaglia, C.A. (2012) 'Plasmodium sporozoite motility: an update', *Frontiers in Bioscience (Landmark Edition)*, 17(2), pp. 726–744. Available at: <https://doi.org/10.2741/3954>.

Mony, B.M. *et al.* (2009) 'Plant-like phosphofructokinase from *Plasmodium falciparum* belongs to a novel class of ATP-dependent enzymes', *International Journal for Parasitology*, 39(13), pp. 1441–1453. Available at: <https://doi.org/10.1016/j.ijpara.2009.05.011>.

Moorthy, V. and Binka, F. (2021) 'R21/Matrix-M: a second malaria vaccine?', *The Lancet*, 397(10287), pp. 1782–1783. Available at: [https://doi.org/10.1016/S0140-6736\(21\)01065-5](https://doi.org/10.1016/S0140-6736(21)01065-5).

Mota, M.M. *et al.* (2001) 'Migration of Plasmodium Sporozoites Through Cells Before Infection', *Science*, 291(5501), pp. 141–144. Available at: <https://doi.org/10.1126/science.291.5501.141>.

Nagy, M., Lacroute, F. and Thomas, D. (1992) 'Divergent evolution of pyrimidine biosynthesis between anaerobic and aerobic yeasts.', *Proceedings of the National Academy of Sciences*, 89, pp. 8966–8970. Available at: <https://doi.org/10.1073/pnas.89.19.8966>.

Ng, C.L. *et al.* (2016) 'CRISPR-Cas9-modified pfmdr1 protects *Plasmodium falciparum* asexual blood stages and gametocytes against a class of piperazine-containing compounds but potentiates artemisinin-based combination therapy partner drugs', *Molecular Microbiology*, 101(3), pp. 381–393. Available at: <https://doi.org/10.1111/mmi.13397>.

van Niekerk, D.D. *et al.* (2016) 'Targeting glycolysis in the malaria parasite *Plasmodium falciparum*', *The FEBS Journal*, 283(4), pp. 634–646. Available at: <https://doi.org/10.1111/febs.13615>.

Nilsen, A. *et al.* (2013) 'Quinolone-3-Diarylethers: A new class of drugs for a new era of malaria eradication', *Science translational medicine*, 5(177), p. 177ra37. Available at: <https://doi.org/10.1126/scitranslmed.3005029>.

Nilsson, S.K. *et al.* (2015) 'Targeting Human Transmission Biology for Malaria Elimination', *PLOS Pathogens*. Edited by C.E. Chitnis, 11(6), p. e1004871. Available at: <https://doi.org/10.1371/journal.ppat.1004871>.

Nina, P.B. *et al.* (2011) 'ATP Synthase Complex of *Plasmodium falciparum*', *Journal of Biological Chemistry*, 286(48), pp. 41312–41322. Available at: <https://doi.org/10.1074/jbc.M111.290973>.

Nixon, G.L. *et al.* (2013) 'Targeting the mitochondrial electron transport chain of *Plasmodium falciparum*: new strategies towards the development of improved antimalarials for the

elimination era', *Future Medicinal Chemistry*, 5(13), pp. 1573–1591. Available at: <https://doi.org/10.4155/fmc.13.121>.

Nkrumah, L.J. *et al.* (2006) 'Efficient site-specific integration in *Plasmodium falciparum* chromosomes mediated by mycobacteriophage Bxb1 integrase', *Nature Methods*, 3(8), pp. 615–621. Available at: <https://doi.org/10.1038/nmeth904>.

Noedl, H. *et al.* (2008) 'Evidence of Artemisinin-Resistant Malaria in Western Cambodia', *New England Journal of Medicine*, 359(24), pp. 2619–2620. Available at: <https://doi.org/10.1056/NEJMc0805011>.

Okamoto, N. *et al.* (2009) 'Apicoplast and Mitochondrion in Gametocytogenesis of *Plasmodium falciparum*', *Eukaryotic Cell*, 8(1), pp. 128–132. Available at: <https://doi.org/10.1128/EC.00267-08>.

Oliveira, P.L. and Oliveira, M.F. (2002) 'Vampires, Pasteur and reactive oxygen species: Is the switch from aerobic to anaerobic metabolism a preventive antioxidant defence in blood-feeding parasites?', *FEBS Letters*, 525(1), pp. 3–6. Available at: [https://doi.org/10.1016/S0014-5793\(02\)03026-0](https://doi.org/10.1016/S0014-5793(02)03026-0).

Olivieri, A. *et al.* (2015) 'Distinct properties of the egress-related osmiophilic bodies in male and female gametocytes of the rodent malaria parasite *Plasmodium berghei*', *Cellular Microbiology*, 17(3), pp. 355–368. Available at: <https://doi.org/10.1111/cmi.12370>.

Oppenheim, R.D. *et al.* (2014) 'BCKDH: The Missing Link in Apicomplexan Mitochondrial Metabolism Is Required for Full Virulence of *Toxoplasma gondii* and *Plasmodium berghei*', *PLOS Pathogens*, 10(7), p. e1004263. Available at: <https://doi.org/10.1371/journal.ppat.1004263>.

Painter, H.J. *et al.* (2007) 'Specific role of mitochondrial electron transport in blood-stage *Plasmodium falciparum*', *Nature*, 446(7131), pp. 88–91. Available at: <https://doi.org/10.1038/nature05572>.

Pajak, B. *et al.* (2020) '2-Deoxy-d-Glucose and Its Analogs: From Diagnostic to Therapeutic Agents', *International Journal of Molecular Sciences*, 21(1), p. 234. Available at: <https://doi.org/10.3390/ijms21010234>.

Parkyn Schneider, M. *et al.* (2017) 'Disrupting assembly of the inner membrane complex blocks *Plasmodium falciparum* sexual stage development', *PLOS Pathogens*. Edited by T.W. Gilberger, 13(10), p. e1006659. Available at: <https://doi.org/10.1371/journal.ppat.1006659>.

Paton, D.G. *et al.* (2019) 'Exposing *Anopheles* mosquitoes to antimalarials blocks *Plasmodium* parasite transmission', *Nature*, 567(7747), pp. 239–243. Available at: <https://doi.org/10.1038/s41586-019-0973-1>.

Phillips, M.A. *et al.* (2015) 'A long-duration dihydroorotate dehydrogenase inhibitor (DSM265) for prevention and treatment of malaria | Science Translational Medicine', *Science Translational Medicine*, 7(296), p. 296ra111. Available at: <https://doi.org/DOI:10.1126/scitranslmed.aaa6645>.

Plouffe, D.M. *et al.* (2016) 'High-Throughput Assay and Discovery of Small Molecules that Interrupt Malaria Transmission', *Cell Host & Microbe*, 19(1), pp. 114–126. Available at: <https://doi.org/10.1016/j.chom.2015.12.001>.

Ponzi, M. *et al.* (2009) 'Egress of Plasmodium berghei gametes from their host erythrocyte is mediated by the MDV-1/PEG3 protein', *Cellular Microbiology*, 11(8), pp. 1272–1288. Available at: <https://doi.org/10.1111/j.1462-5822.2009.01331.x>.

Posayapisit, N. *et al.* (2021) 'Transgenic pyrimethamine-resistant plasmodium falciparum reveals transmission-blocking potency of P218, a novel antifolate candidate drug', *International Journal for Parasitology*, 51(8), pp. 635–642. Available at: <https://doi.org/10.1016/j.ijpara.2020.12.002>.

Pradel, G. *et al.* (2004) 'A Multidomain Adhesion Protein Family Expressed in Plasmodium falciparum Is Essential for Transmission to the Mosquito', *Journal of Experimental Medicine*, 199(11), pp. 1533–1544. Available at: <https://doi.org/10.1084/jem.20031274>.

Pradel, G. and Frevert, U. (2001) 'Malaria sporozoites actively enter and pass through rat Kupffer cells prior to hepatocyte invasion', *Hepatology*, 33(5), pp. 1154–1165. Available at: <https://doi.org/10.1053/jhep.2001.24237>.

Puta, C. and Manyando, C. (1997) 'Enhanced gametocyte production in Fansidar-treated Plasmodium falciparum malaria patients: implications for malaria transmission control programmes', *Tropical Medicine & International Health*, 2(3), pp. 227–229. Available at: <https://doi.org/10.1046/j.1365-3156.1997.d01-267.x>.

Raabe, A.C. *et al.* (2009) 'Quantitative assessment of DNA replication to monitor microgametogenesis in Plasmodium berghei', *Molecular and Biochemical Parasitology*, 168(2), pp. 172–176. Available at: <https://doi.org/10.1016/j.molbiopara.2009.08.004>.

Radfar, A. *et al.* (2009) 'Synchronous culture of Plasmodium falciparum at high parasitemia levels', *Nature Protocols*, 4(12), pp. 1899–1915. Available at: <https://doi.org/10.1038/nprot.2009.198>.

Rajaram, K. *et al.* (2022) 'Metabolic changes accompanying the loss of fumarate hydratase and malate–quinone oxidoreductase in the asexual blood stage of Plasmodium falciparum', *Journal of Biological Chemistry*, 298(5). Available at: <https://doi.org/10.1016/j.jbc.2022.101897>.

Ralser, M. *et al.* (2008) 'A catabolic block does not sufficiently explain how 2-deoxy-d-glucose inhibits cell growth', *Proceedings of the National Academy of Sciences*, 105(46), pp. 17807–17811. Available at: <https://doi.org/10.1073/pnas.0803090105>.

Rawlings, D.J. *et al.* (1992) 'α-Tubulin II is a male-specific protein in Plasmodium falciparum', *Molecular and Biochemical Parasitology*, 56(2), pp. 239–250. Available at: [https://doi.org/10.1016/0166-6851\(92\)90173-H](https://doi.org/10.1016/0166-6851(92)90173-H).

Reeves, R.E. *et al.* (1977) 'An energy-conserving pyruvate-to-acetate pathway in Entamoeba histolytica. Pyruvate synthase and a new acetate thiokinase.', *Journal of Biological Chemistry*, 252(2), pp. 726–731. Available at: [https://doi.org/10.1016/S0021-9258\(17\)32778-3](https://doi.org/10.1016/S0021-9258(17)32778-3).

Ressurreição, M. *et al.* (2020) 'Use of a highly specific kinase inhibitor for rapid, simple and precise synchronization of Plasmodium falciparum and Plasmodium knowlesi asexual blood-stage parasites', *PLOS ONE*. Edited by G. Langsley, 15(7), p. e0235798. Available at: <https://doi.org/10.1371/journal.pone.0235798>.

- Richter, J. *et al.* (2010) 'What is the evidence for the existence of Plasmodium ovale hypnozoites?', *Parasitology Research*, 107(6), pp. 1285–1290. Available at: <https://doi.org/10.1007/s00436-010-2071-z>.
- Riganti, C. *et al.* (2012) 'The pentose phosphate pathway: An antioxidant defense and a crossroad in tumor cell fate', *Free Radical Biology and Medicine*, 53(3), pp. 421–436. Available at: <https://doi.org/10.1016/j.freeradbiomed.2012.05.006>.
- Rigden, D.J. (2008) 'The histidine phosphatase superfamily: structure and function | Biochemical Journal | Portland Press', *Biochemical Journal*, 409(2), pp. 333–348.
- Rivadeneira, E.M., Wasserman, M. and Espinal, C.T. (1983) 'Separation and Concentration of Schizonts of Plasmodium falciparum by Percoll Gradients<sup>1</sup>', *The Journal of Protozoology*, 30(2), pp. 367–370. Available at: <https://doi.org/10.1111/j.1550-7408.1983.tb02932.x>.
- Rosenberg, R. and Rungsiwongse, J. (1991) 'The number of sporozoites produced by individual malaria oocysts', *The American journal of tropical medicine and hygiene*, 45(5), pp. 574–577. Available at: <https://doi.org/10.4269/ajtmh.1991.45.574>.
- Roth, E.F. (1987) 'Malarial parasite hexokinase and hexokinase-dependent glutathione reduction in the Plasmodium falciparum-infected human erythrocyte.', *Journal of Biological Chemistry*, 262(32), pp. 15678–15682. Available at: [https://doi.org/10.1016/S0021-9258\(18\)47780-0](https://doi.org/10.1016/S0021-9258(18)47780-0).
- RTS'S Clinical Trials Partnership (2015) 'Efficacy and safety of RTS,S/AS01 malaria vaccine with or without a booster dose in infants and children in Africa: final results of a phase 3, individually randomised, controlled trial', *The Lancet*, 386(9988), pp. 31–45. Available at: [https://doi.org/10.1016/S0140-6736\(15\)60721-8](https://doi.org/10.1016/S0140-6736(15)60721-8).
- Ruecker, A. *et al.* (2014) 'A Male and Female Gametocyte Functional Viability Assay To Identify Biologically Relevant Malaria Transmission-Blocking Drugs', *Antimicrobial Agents and Chemotherapy*, 58(12), pp. 7292–7302. Available at: <https://doi.org/10.1128/AAC.03666-14>.
- Saha, S. *et al.* (2017) 'Two Phosphoglucomutase Paralogs Facilitate Ionophore-Triggered Secretion of the Toxoplasma Micronemes', *mSphere*, 2(6), pp. e00521-17. Available at: <https://doi.org/10.1128/mSphere.00521-17>.
- Salcedo-Sora, J.E. *et al.* (2014) 'The proliferating cell hypothesis: a metabolic framework for Plasmodium growth and development', *Trends in Parasitology*, 30(4), pp. 170–175. Available at: <https://doi.org/10.1016/j.pt.2014.02.001>.
- Saliba, K.J. and Kirk, K. (1999) 'pH Regulation in the Intracellular Malaria Parasite, Plasmodium falciparum: H<sup>+</sup> EXTRUSION VIA A V-TYPE H<sup>+</sup>-ATPase<sup>\*</sup>', *Journal of Biological Chemistry*, 274(47), pp. 33213–33219. Available at: <https://doi.org/10.1074/jbc.274.47.33213>.
- Saliba, K.J., Krishna, S. and Kirk, K. (2004) 'Inhibition of hexose transport and abrogation of pH homeostasis in the intraerythrocytic malaria parasite by an O-3-hexose derivative', *FEBS Letters*, 570(1–3), pp. 93–96. Available at: <https://doi.org/10.1016/j.febslet.2004.06.032>.
- Sánchez, L.B., Galperin, M.Y. and Müller, M. (2000) 'Acetyl-CoA Synthetase from the Amitochondriate Eukaryote Giardia lamblia Belongs to the Newly Recognized Superfamily of Acyl-CoA Synthetases (Nucleoside Diphosphate-forming)<sup>\*</sup>', *Journal of Biological Chemistry*, 275(8), pp. 5794–5803. Available at: <https://doi.org/10.1074/jbc.275.8.5794>.

Santos, J.M. *et al.* (2017) 'Malaria parasite LIMP protein regulates sporozoite gliding motility and infectivity in mosquito and mammalian hosts', *eLife*, 6, p. e24109. Available at: <https://doi.org/10.7554/eLife.24109>.

Schmidt, M.C. and O'Donnell, A.F. (2021) "'Sugarcoating" 2-deoxyglucose: mechanisms that suppress its toxic effects', *Current Genetics*, 67(1), pp. 107–114. Available at: <https://doi.org/10.1007/s00294-020-01122-7>.

Schwank, S., Sutherland, C.J. and Drakeley, C.J. (2010) 'Promiscuous Expression of  $\alpha$ -Tubulin II in Maturing Male and Female Plasmodium falciparum Gametocytes', *PLoS ONE*. Edited by A.C. Gruner, 5(12), p. e14470. Available at: <https://doi.org/10.1371/journal.pone.0014470>.

Severini, C. *et al.* (1999) 'The production of the osmiophilic body protein Pfg377 is associated with stage of maturation and sex in Plasmodium falciparum gametocytes', *Molecular and biochemical parasitology*, 100(2), pp. 247–252. Available at: [https://doi.org/10.1016/s0166-6851\(99\)00050-x](https://doi.org/10.1016/s0166-6851(99)00050-x).

Shang, X. *et al.* (2021) 'A cascade of transcriptional repression determines sexual commitment and development in Plasmodium falciparum', *Nucleic Acids Research*, 49(16), pp. 9264–9279. Available at: <https://doi.org/10.1093/nar/gkab683>.

Shen, W. *et al.* (2003) 'Identification of a mitochondrial glycerol-3-phosphate dehydrogenase from Arabidopsis thaliana: evidence for a mitochondrial glycerol-3-phosphate shuttle in plants', *FEBS Letters*, 536(1–3), pp. 92–96. Available at: [https://doi.org/10.1016/S0014-5793\(03\)00033-4](https://doi.org/10.1016/S0014-5793(03)00033-4).

Sherman, I.W. (1979) 'Biochemistry of Plasmodium (malarial parasites)', *Microbiological Reviews*, 43(4), pp. 453–495. Available at: <https://doi.org/10.1128/mr.43.4.453-495.1979>.

Siden-Kiamos, I. *et al.* (2010) 'Arp1, an actin-related protein, in Plasmodium berghei', *Molecular and Biochemical Parasitology*, 173(2), pp. 88–96. Available at: <https://doi.org/10.1016/j.molbiopara.2010.05.008>.

Sidjanski, S. and Vanderberg, J.P. (1997) 'Delayed migration of Plasmodium sporozoites from the mosquito bite site to the blood', *The American journal of tropical medicine and hygiene*, 57(4), pp. 426–429. Available at: <https://doi.org/10.4269/ajtmh.1997.57.426>.

Silvestrini, F. *et al.* (2010) 'Protein Export Marks the Early Phase of Gametocytogenesis of the Human Malaria Parasite Plasmodium falciparum\*', *Molecular & Cellular Proteomics*, 9(7), pp. 1437–1448. Available at: <https://doi.org/10.1074/mcp.M900479-MCP200>.

Sinden, R.E. *et al.* (1978) 'Gametocyte and gamete development in Plasmodium falciparum', *Proceedings of the Royal Society of London. Series B. Biological Sciences*, 201, pp. 375–399. Available at: <https://doi.org/10.1098/rspb.1978.0051>.

Sinden, R.E. (1982a) 'Gametocytogenesis of Plasmodium falciparum in vitro: an electron microscopic study', *Parasitology*, 84(1), pp. 1–11. Available at: <https://doi.org/10.1017/S003118200005160X>.

Sinden, R.E. (1982b) 'Gametocytogenesis of Plasmodium falciparum in vitro: ultrastructural observations on the lethal action of chloroquine', *Annals of Tropical Medicine & Parasitology*, 76(1), pp. 15–23. Available at: <https://doi.org/10.1080/00034983.1982.11687500>.

- Sinden, R.E. (1982c) 'Gametocytogenesis of *Plasmodium falciparum* in vitro: ultrastructural observations on the lethal action of chloroquine', *Annals of Tropical Medicine & Parasitology*, 76(1), pp. 15–23. Available at: <https://doi.org/10.1080/00034983.1982.11687500>.
- Sinden, R.E. (1983) 'Sexual Development of Malarial Parasites', in J.R. Baker and R. Muller (eds) *Advances in Parasitology*. Academic Press, pp. 153–216. Available at: [https://doi.org/10.1016/S0065-308X\(08\)60462-5](https://doi.org/10.1016/S0065-308X(08)60462-5).
- Sinden, R.E. (2017) 'Developing transmission-blocking strategies for malaria control', *PLOS Pathogens*. Edited by L.J. Knoll, 13(7), p. e1006336. Available at: <https://doi.org/10.1371/journal.ppat.1006336>.
- Sinden, R.E. and Croll, N.A. (1975) 'Cytology and Kinetics of microgametogenesis and fertilization in *Plasmodium yoelii nigeriensis*', *Parasitology*, 70(1), pp. 53–65. Available at: <https://doi.org/10.1017/S0031182000048861>.
- Sinden, R.E., Hartley, R.H. and Winger, L. (1985) 'The development of *Plasmodium* ookinetes in vitro: an ultrastructural study including a description of meiotic division', *Parasitology*, 91(2), pp. 227–244. Available at: <https://doi.org/10.1017/S0031182000057334>.
- Sinden, R.E. and Smalley, M.E. (1979) 'Gametocytogenesis of *Plasmodium falciparum* in vitro: the cell-cycle', *Parasitology*, 79(2), pp. 277–296. Available at: <https://doi.org/10.1017/S003118200005335X>.
- Sinha, A. *et al.* (2014) 'A cascade of DNA-binding proteins for sexual commitment and development in *Plasmodium*', *Nature*, 507(7491), pp. 253–257. Available at: <https://doi.org/10.1038/nature12970>.
- Siqueira, A.M. *et al.* (2012) 'Spleen Rupture in a Case of Untreated *Plasmodium vivax* Infection', *PLOS Neglected Tropical Diseases*, 6(12), p. e1934. Available at: <https://doi.org/10.1371/journal.pntd.0001934>.
- Slavic, K. *et al.* (2011) 'Use of a Selective Inhibitor To Define the Chemotherapeutic Potential of the Plasmodial Hexose Transporter in Different Stages of the Parasite's Life Cycle', *Antimicrobial Agents and Chemotherapy*, 55(6), pp. 2824–2830. Available at: <https://doi.org/10.1128/AAC.01739-10>.
- Smalley, M.E. (1977) '*Plasmodium falciparum* gametocytes: the effect of chloroquine on their development', *Transactions of the Royal Society of Tropical Medicine and Hygiene*, 71(6), pp. 526–529. Available at: [https://doi.org/10.1016/0035-9203\(77\)90149-3](https://doi.org/10.1016/0035-9203(77)90149-3).
- Smalley, M.E. and Sinden, R.E. (1977) '*Plasmodium falciparum* gametocytes: their longevity and infectivity', *Parasitology*, 74(1), pp. 1–8. Available at: <https://doi.org/10.1017/S0031182000047478>.
- Sola-Penna, M. *et al.* (2010) 'Regulation of mammalian muscle type 6-phosphofructo-1-kinase and its implication for the control of the metabolism', *IUBMB Life*, 62(11), pp. 791–796. Available at: <https://doi.org/10.1002/iub.393>.
- Srivastava, A. *et al.* (2016) 'Stage-Specific Changes in *Plasmodium* Metabolism Required for Differentiation and Adaptation to Different Host and Vector Environments', *PLOS Pathogens*. Edited by A.R. Odom, 12(12), p. e1006094. Available at: <https://doi.org/10.1371/journal.ppat.1006094>.

- Srivastava, I.K., Rottenberg, H. and Vaidya, A.B. (1997) 'Atovaquone, a Broad Spectrum Antiparasitic Drug, Collapses Mitochondrial Membrane Potential in a Malarial Parasite \*', *Journal of Biological Chemistry*, 272(7), pp. 3961–3966. Available at: <https://doi.org/10.1074/jbc.272.7.3961>.
- Srivastava, I.K. and Vaidya, A.B. (1999) 'A Mechanism for the Synergistic Antimalarial Action of Atovaquone and Proguanil', *Antimicrobial Agents and Chemotherapy*, 43(6), pp. 1334–1339. Available at: <https://doi.org/10.1128/AAC.43.6.1334>.
- Steiner, S. and Lester, R.L. (1972) 'Studies on the Diversity of Inositol-Containing Yeast Phospholipids: Incorporation of 2-Deoxyglucose into Lipid', *Journal of Bacteriology*, 109(1), pp. 81–88. Available at: <https://doi.org/10.1128/jb.109.1.81-88.1972>.
- Stepniewska, K. *et al.* (2008) 'Plasmodium falciparum gametocyte dynamics in areas of different malaria endemicity', *Malaria Journal*, 7(1), p. 249. Available at: <https://doi.org/10.1186/1475-2875-7-249>.
- Stickles, A.M. *et al.* (2015) 'Subtle Changes in Endochin-Like Quinolone Structure Alter the Site of Inhibition within the Cytochrome bc1 Complex of Plasmodium falciparum', *Antimicrobial Agents and Chemotherapy*, 59(4), pp. 1977–1982. Available at: <https://doi.org/10.1128/AAC.04149-14>.
- Stincone, A. *et al.* (2015) 'The return of metabolism: biochemistry and physiology of the pentose phosphate pathway', *Biological Reviews*, 90(3), pp. 927–963. Available at: <https://doi.org/10.1111/brv.12140>.
- Storm, J. *et al.* (2011) 'Plasmodium falciparum glutamate dehydrogenase a is dispensable and not a drug target during erythrocytic development', *Malaria Journal*, 10(1), p. 193. Available at: <https://doi.org/10.1186/1475-2875-10-193>.
- Sturm, A. *et al.* (2006) 'Manipulation of Host Hepatocytes by the Malaria Parasite for Delivery into Liver Sinusoids', *Science*, 313(5791), pp. 1287–1290. Available at: <https://doi.org/10.1126/science.1129720>.
- Sturm, A. *et al.* (2015) 'Mitochondrial ATP synthase is dispensable in blood-stage Plasmodium berghei rodent malaria but essential in the mosquito phase', *Proceedings of the National Academy of Sciences*, 112(33), pp. 10216–10223. Available at: <https://doi.org/10.1073/pnas.1423959112>.
- Summers, R.L. *et al.* (2022) 'Chemogenomics identifies acetyl-coenzyme A synthetase as a target for malaria treatment and prevention', *Cell Chemical Biology*, 29(2), pp. 191-201.e8. Available at: <https://doi.org/10.1016/j.chembiol.2021.07.010>.
- Suzuki, J. *et al.* (2004) 'Putative pyrophosphate phosphofructose 1-kinase genes identified in sugar cane may be getting energy from pyrophosphate', *Genetics and Molecular Research* [Preprint].
- Suzuki, M. *et al.* (1983) '2-Deoxyglucose as a substrate for glutathione regeneration in human and ruminant red blood cells', *Comparative biochemistry and physiology B, Comparative biochemistry*, 75(2), pp. 195–197. Available at: [https://doi.org/10.1016/0305-0491\(83\)90312-7](https://doi.org/10.1016/0305-0491(83)90312-7).
- Symersky, J. *et al.* (2012) 'Oligomycin frames a common drug-binding site in the ATP synthase', *Proceedings of the National Academy of Sciences*, 109(35), pp. 13961–13965. Available at: <https://doi.org/10.1073/pnas.1207912109>.

- Talman, A.M. *et al.* (2004) 'Gametocytogenesis : the puberty of Plasmodium falciparum', *Malaria Journal*, 3(1), p. 24. Available at: <https://doi.org/10.1186/1475-2875-3-24>.
- Talman, A.M. *et al.* (2014) 'Proteomic analysis of the Plasmodium male gamete reveals the key role for glycolysis in flagellar motility', *Malaria Journal*, 13(1), p. 315. Available at: <https://doi.org/10.1186/1475-2875-13-315>.
- Tantama, M. *et al.* (2013) 'Imaging energy status in live cells with a fluorescent biosensor of the intracellular ATP-to-ADP ratio', *Nature Communications*, 4(1), p. 2550. Available at: <https://doi.org/10.1038/ncomms3550>.
- Tavares, J. *et al.* (2013) 'Role of host cell traversal by the malaria sporozoite during liver infection', *Journal of Experimental Medicine*, 210(5), pp. 905–915. Available at: <https://doi.org/10.1084/jem.20121130>.
- Thomas, J.A. *et al.* (2016) 'Development and Application of a Simple Plaque Assay for the Human Malaria Parasite Plasmodium falciparum', *PLOS ONE*. Edited by T. Spielmann, 11(6), p. e0157873. Available at: <https://doi.org/10.1371/journal.pone.0157873>.
- Thomson, D. (1914) 'The Origin and Development of Gametes (Crescents) in Malignant Tertian Malaria: Some Observations on Flagellation, Etc.', *Annals of Tropical Medicine & Parasitology*, 8(1), pp. 85–104. Available at: <https://doi.org/10.1080/00034983.1914.11687643>.
- Tibúrcio, M. *et al.* (2012) 'A switch in infected erythrocyte deformability at the maturation and blood circulation of Plasmodium falciparum transmission stages', *Blood*, 119(24), pp. e172–e180. Available at: <https://doi.org/10.1182/blood-2012-03-414557>.
- Tielens, A.G.M. *et al.* (2010) 'Acetate formation in the energy metabolism of parasitic helminths and protists', *International Journal for Parasitology*, 40(4), pp. 387–397. Available at: <https://doi.org/10.1016/j.ijpara.2009.12.006>.
- Torrentino-Madamet, M. *et al.* (2010) 'Microaerophilic Respiratory Metabolism of Plasmodium falciparum Mitochondrion as a Drug Target', *Current Molecular Medicine*, 10(1), pp. 29–46. Available at: <https://doi.org/10.2174/156652410791065390>.
- Toyé, P.J., Sinden, R.E. and Canning, E.U. (1977) 'The action of metabolic inhibitors on microgametogenesis in Plasmodium yoelii nigeriensis', *Zeitschrift für Parasitenkunde*, 53(2), pp. 133–141. Available at: <https://doi.org/10.1007/BF00380457>.
- Trager, W. (2005) 'What triggers the gametocyte pathway in Plasmodium falciparum?', *Trends in Parasitology*, 21(6), pp. 262–264. Available at: <https://doi.org/10.1016/j.pt.2005.04.005>.
- Tran, P.N. *et al.* (2014) 'A female gametocyte-specific ABC transporter plays a role in lipid metabolism in the malaria parasite', *Nature Communications*, 5(1), p. 4773. Available at: <https://doi.org/10.1038/ncomms5773>.
- Tsebriy, O. *et al.* (2023) 'Machine Learning-based Phenotypic Imaging to Characterise the Targetable Biology of Plasmodium falciparum Male Gametocytes for the Development of Transmission-Blocking Antimalarials'. bioRxiv, p. 2023.04.22.537818. Available at: <https://doi.org/10.1101/2023.04.22.537818>.

Ukegbu, C.V. *et al.* (2017) 'Plasmodium berghei P47 is essential for ookinete protection from the Anopheles gambiae complement-like response', *Scientific Reports*, 7(1), p. 6026. Available at: <https://doi.org/10.1038/s41598-017-05917-6>.

Usui, M. *et al.* (2019) 'Plasmodium falciparum sexual differentiation in malaria patients is associated with host factors and GDV1-dependent genes', *Nature Communications*, 10(1), p. 2140. Available at: <https://doi.org/10.1038/s41467-019-10172-6>.

Uyemura, S.A. *et al.* (2004) 'Oxidative Phosphorylation and Rotenone-insensitive Malate- and NADH-Quinone Oxidoreductases in Plasmodium yoelii yoelii Mitochondria in Situ\*', *Journal of Biological Chemistry*, 279(1), pp. 385–393. Available at: <https://doi.org/10.1074/jbc.M307264200>.

Vanderberg, J.P. and Frevort, U. (2004) 'Intravital microscopy demonstrating antibody-mediated immobilisation of Plasmodium berghei sporozoites injected into skin by mosquitoes', *International Journal for Parasitology*, 34(9), pp. 991–996. Available at: <https://doi.org/10.1016/j.ijpara.2004.05.005>.

Vaughan, A.M. *et al.* (2012) *Complete Plasmodium falciparum liver-stage development in liver-chimeric mice*. American Society for Clinical Investigation. Available at: <https://doi.org/10.1172/JCI62684>.

Vizioli, J. *et al.* (2001) 'Blood digestion in the malaria mosquito Anopheles gambiae', *European Journal of Biochemistry*, 268(14), pp. 4027–4035. Available at: <https://doi.org/10.1046/j.1432-1327.2001.02315.x>.

Vlachou, D. *et al.* (2004) 'Real-time, in vivo analysis of malaria ookinete locomotion and mosquito midgut invasion', *Cellular Microbiology*, 6(7), pp. 671–685. Available at: <https://doi.org/10.1111/j.1462-5822.2004.00394.x>.

Wamelink, M.M.C., Struys, E.A. and Jakobs, C. (2008) 'The biochemistry, metabolism and inherited defects of the pentose phosphate pathway: A review', *Journal of Inherited Metabolic Disease*, 31(6), pp. 703–717. Available at: <https://doi.org/10.1007/s10545-008-1015-6>.

Warren, L. and Manwell, R.D. (1954) 'Rate of glucose consumption by malarial blood', *Experimental Parasitology*, 3(1), pp. 16–24. Available at: [https://doi.org/10.1016/0014-4894\(54\)90013-2](https://doi.org/10.1016/0014-4894(54)90013-2).

Webster, R. *et al.* (2023) 'Transmission Blocking Activity of Low-dose Tafenoquine in Healthy Volunteers Experimentally Infected With Plasmodium falciparum', *Clinical Infectious Diseases*, 76(3), pp. 506–512. Available at: <https://doi.org/10.1093/cid/ciac503>.

Wernsdorfer, W.H. and McGregor, I. (1988) *Malaria : principles and practice of malariology*. Churchill Livingstone. Available at: <https://ci.nii.ac.jp/ncid/BA07172937> (Accessed: 2 May 2023).

White, N.J. *et al.* (1987) 'HYPOGLYCAEMIA IN AFRICAN CHILDREN WITH SEVERE MALARIA', *The Lancet*, 329(8535), pp. 708–711. Available at: [https://doi.org/10.1016/S0140-6736\(87\)90354-0](https://doi.org/10.1016/S0140-6736(87)90354-0).

WHO (2023) *WHO recommends R21/Matrix-M vaccine for malaria prevention in updated advice on immunization*. Available at: <https://www.who.int/news/item/02-10-2023-who-recommends-r21-matrix-m-vaccine-for-malaria-prevention-in-updated-advice-on-immunization> (Accessed: 17 October 2023).

- Witmer, K. *et al.* (2018) 'An inexpensive open source 3D-printed membrane feeder for human malaria transmission studies', *Malaria Journal*, 17, p. 282.
- Witmer, K. *et al.* (2020) 'Transmission of Artemisinin-Resistant Malaria Parasites to Mosquitoes under Antimalarial Drug Pressure', *Antimicrobial Agents and Chemotherapy*, 65(1), pp. e00898-20. Available at: <https://doi.org/10.1128/AAC.00898-20>.
- Wong, J.H. *et al.* (1990) 'Pyrophosphate Fructose-6-P 1-Phosphotransferase from Tomato Fruit: Evidence for Change during Ripening', *Plant Physiology*, 94(2), pp. 499–506. Available at: <https://doi.org/10.1104/pp.94.2.499>.
- Yang, F., Zhang, Y. and Liang, H. (2014) 'Interactive association of drugs binding to human serum albumin', *International Journal of Molecular Sciences*, 15(3), pp. 3580–3595. Available at: <https://doi.org/10.3390/ijms15033580>.
- Yang, M. *et al.* (2022) 'Genetic disruption of isocitrate dehydrogenase arrests the full development of sexual stage parasites in *Plasmodium falciparum*'. bioRxiv, p. 2022.08.05.502965. Available at: <https://doi.org/10.1101/2022.08.05.502965>.
- Young, J.A. *et al.* (2005) 'The *Plasmodium falciparum* sexual development transcriptome: A microarray analysis using ontology-based pattern identification', *Molecular and Biochemical Parasitology*, 143(1), pp. 67–79. Available at: <https://doi.org/10.1016/j.molbiopara.2005.05.007>.
- Yuda, M. *et al.* (2015) 'Global transcriptional repression: An initial and essential step for *Plasmodium* sexual development', *Proceedings of the National Academy of Sciences*, 112(41), pp. 12824–12829. Available at: <https://doi.org/10.1073/pnas.1504389112>.
- Zancan, P. *et al.* (2010) 'Differential expression of phosphofructokinase-1 isoforms correlates with the glycolytic efficiency of breast cancer cells', *Molecular Genetics and Metabolism*, 100(4), pp. 372–378. Available at: <https://doi.org/10.1016/j.ymgme.2010.04.006>.
- Zhang, C. *et al.* (2017) 'Systematic CRISPR-Cas9-Mediated Modifications of *Plasmodium yoelii* ApiAP2 Genes Reveal Functional Insights into Parasite Development', *mBio*, 8(6), pp. e01986-17. Available at: <https://doi.org/10.1128/mBio.01986-17>.
- Zhang, M. *et al.* (2018) 'Uncovering the essential genes of the human malaria parasite *Plasmodium falciparum* by saturation mutagenesis', *Science*, 360(6388), p. eaap7847. Available at: <https://doi.org/10.1126/science.aap7847>.
- Zheng, J. (2012) 'Energy metabolism of cancer: Glycolysis versus oxidative phosphorylation (Review)', *Oncology Letters*, 4(6), pp. 1151–1157. Available at: <https://doi.org/10.3892/ol.2012.928>.
- Zhong, D. *et al.* (2009) 'The Glycolytic Inhibitor 2-Deoxyglucose Activates Multiple Prosurvival Pathways through IGF1R\*', *Journal of Biological Chemistry*, 284(35), pp. 23225–23233. Available at: <https://doi.org/10.1074/jbc.M109.005280>.
- Zingman, B.S. and Viner, B.L. (1993) 'Splenic Complications in Malaria: Case Report and Review', *Clinical Infectious Diseases*, 16(2), pp. 223–232. Available at: <https://doi.org/10.1093/clind/16.2.223>.
- Zocher, K. *et al.* (2012) 'Biochemical and structural characterization of *Plasmodium falciparum* glutamate dehydrogenase 2', *Molecular and Biochemical Parasitology*, 183(1), pp. 52–62. Available at: <https://doi.org/10.1016/j.molbiopara.2012.01.007>.



## Appendix

### Appendix 1. List of primers

Primers for construction of selection-linked integration (SLI) and selectable targeted gene disruption (SLI-TGD)

| Primer name     | Sequence  |
|-----------------|---|
| ACS-ADP-mNG Fwd | TCTTGTTATAAAAAGTAATGGTACCGGCGGATCCGGTGAAGCGGAGGT              |
| ACS-ADP-mNG Rev | TAAACTTCCTCTTCCTTCGTCGACTTTATACAATTCATCCATTCCCATAACATCTGT     |
| ACS-ADP-TGD Fwd | tgacactatagaataactcgcgccgctaaTGGGTGGGATACAACAAGAATGTA         |
| ACS-ADP-TGD Rev | TTCTGAGATGAGTTTTTGTTCgccggtaccTTCATTTTCTAGACGTAATCCTTCTGC     |
| ACS-ATP-mNG Fwd | gtgacactatagaataactcgcgccgctaaAATGTTAAGGGAGAAGGAATTTTATGTTT   |
| ACS-ATP-mNG Rev | tccgctgcctccaccggatccgccggtaccTTTCTTAATTTCAATATGCTTTAACTTTT   |
| PFK11-mNG Fwd   | gtgacactatagaataactcgcgccgctaaGACTTGCTCAATTATGTAACATCCATTAAAG |
| PFK11-mNG Rev   | tccgctgcctccaccggatccgccggtaccAAATATATATGAAGAATATCCAAGATTGTC  |
| PFK11-TGD Fwd   | gtgacactatagaataactcgcgccgctaaGGATATCGAGAATTCAAAAAACACCTAAG   |
| PFK11-TGD Rev   | TTCTGAGATGAGTTTTTGTTCgccggtaccCTTGAAATCCGTTCATAAATCCATAAAGAG  |
| PFK9-mNG Fwd    | gtgacactatagaataactcgcgccgctaaTTATTGAAAGTGGCTTAACAGGATATATTG  |
| PFK9-mNG Rev    | tccgctgcctccaccggatccgccggtaccGTTCAATCTTTTTCTCTGGTTTTCCCAATC  |
| PGM-mNG Fwd     | gtgacactatagaataactcgcgccgctaaGCATTAGGTTATTGGATAGAAATTGCAGT   |
| PGM-mNG Rev     | tccgctgcctccaccggatccgccggtaccTGATTTCTTTACGTTATATTTATTTGGTTG  |
| PGM3-mNG Fwd    | gtgacactatagaataactcgcgccgctaaTTAATGCATATAGAAGAAAAAATAGATAAC  |
| PGM3-mNG Rev    | tccgctgcctccaccggatccgccggtaccTTTTAAAACATTCAAATGTAAACGTTCTC   |
| FAD-GPDH Fwd    | gtgacactatagaataactcgcgccgctaaATGAAGATGATTTAACTTTGGTTGTAATA   |
| FAD-GPDH Rev    | tccgctgcctccaccggatccgccggtaccTATTGTATCTTTTAGGGATAAAGAATTAT   |
| GDH3-mNG Fwd    | gtgacactatagaataactcgcgccgctaaAGTGTAATGAGGATCAACAAGACGTTTCTG  |
| GDH3-mNG Rev    | tccgctgcctccaccggatccgccggtaccAGCACTTTGCTTTGTAATTTGTTATGTA    |
| PGM1-mNG-Fwd    | gtgacactatagaataactcgcgccgctaaGCACTATGGTTCCTTCAAGGTTTAAACAA   |

|              |   |
|--------------|---|
| PGM1-mNG-Rev | tccgctgcctccaccggatccgccggtaccTTTTGCTTTTCCTTGGTTGGCTACTTCATC  |
| PGM2-mNG Fwd | gtgacactatagaataactcgcgccgctaaACCTGACCCTCTTCCAAGACATTCAA AATT |
| PGM2-mNG Rev | tccgctgcctccaccggatccgccggtaccAAAATATGTTACACTTTCAAAGGGGAG GTG |
| GDH1-mNG Fwd | gtgacactatagaataactcgcgccgctaaTCTACAGCTAAATATTTCCCAAATGAA AAA |
| GDH1-mNG Rev | tccgctgcctccaccggatccgccggtaccAAAACAACCTTGTTCAATATATGATTC AGC |

### Primers for construction of CRISPR tagging and KO vectors for PFK11

| Primer name              | Sequence  |
|--------------------------|---|
| PFK11KO_CRISP R_5pHR_FWD | GGCGAATTGGGTACCGGGCCCCCCTCGAGATGGATATCGAGA ATTCAAAAAACAC                            |
| PFK11KO_CRISP R_5pHR_REV | ACTCCTCTTTTTATTAAGTTCAAGCTTCTCAAATATTCAGATAA GATAGCTGTAC                            |
| PFK11KO_CRISP R_3pHR_FWD | aaattgttccttttgcctccaccggatccgccggtaccAAAATATGTTACACTTTCAAAGGGGAG GTG               |
| PFK11KO_CRISP R_3pHR_REV | CCTCACTAAAGGGAACAAAAGCTGGAGCTCGTAGTTCGGTACTT AACCTAGC                               |
| PFK11KO_guide_FWD        | atTTaacttgctaTTTCtagctctaaaacTCTTGTTTACATTTTGTTTAATATT ATATACTTAATATGAAATATGTGC     |
| PFK11KO_guide_REV        | GCACATATTTTCATATTAAGTATATAATATTAACAAAATGTAAACA AGAGTTTTAGAGCTAGAAATAGCAAGTTAAAAT    |
| PFK11tag_guide_FWD       | atTTaacttgctaTTTCtagctctaaaacTGGGAACAGGTGCTACAGAGGAA TATTATACTTAATATGAAATATGTGC     |
| PFK11tag_guide_REV       | GCACATATTTTCATATTAAGTATATAATATTCCTCTGTAGCACCTG TTCCCAGTTTTAGAGCTAGAAATAGCAAGTTAAAAT |
| GFPBSD_FWD               | tattatcatatatataattcaaaagctagcAtggtagcaagggcgagg                                    |
| GFPBSD_REV               | TtttattctgcatatTTAAAAatcctgcagttagccctccacacataacca                                 |
| guideRNA_seq             | CGACAGGTTTCCCGACTGGAAAG   |
| PFK11tagnew_5p HR_FWD    | atgaccatgattacgccaagcttatactagATTTCAAGAAAATATTAAGAAAAGAA AGTGTCGAT                  |
| PFK11tag_5pHR_REV        | TTCGTTAAAATGCCCTTTATCGTCC   |
| PFK11tag_3pHR_FWD        | AGGAGAAAAAATATAAATACATTCATATATATAAATGAATG   |
| PFK11tagnew_3p HR_REV    | gaaaagaaagcggccgctagtcgaGAAAGTTAGGTATTGACGTAGAA GTTG                                |

### Primers for integration PCR

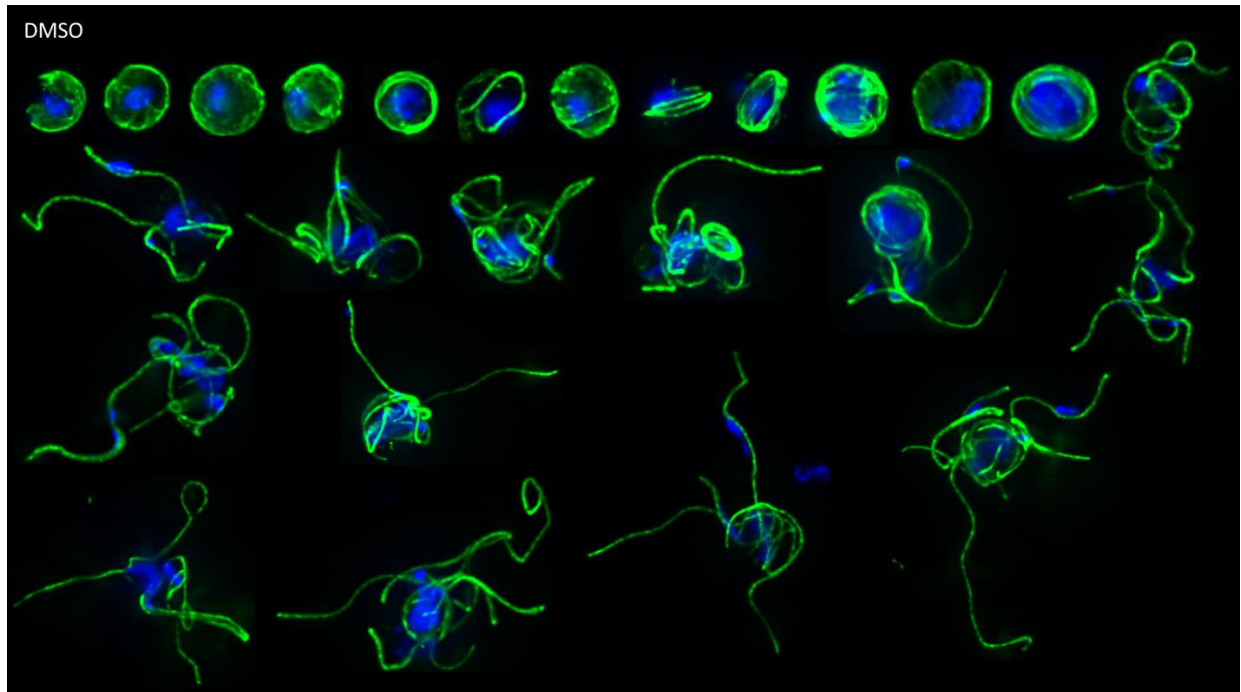
| Primer name       | Sequence                      |
|-------------------|-------------------------------|
| ACSADPmNG_int_5 p | CTTCAAAGGTGTAACAATTCAAGATATGG |
| ACSADPmNG_int_3 p | CACGAAATGGATATATTATGTATGAACAT |

|                            |   |
|----------------------------|---|
| mNeonGreen REV             | TAAACTTCCTCTTCCTTCGTCGACTTTATACAATTCATCCATTC<br>CCATAACATCTGT |
| ACSADP_TGD_int5<br>p       | GATTAGTAAAAGAACAATTCTACCTTTC                                  |
| ACSADP_TGD_int3<br>p       | gattttctctacatctccacatg                                       |
| ACSADP_TGD_int3<br>pWT     | AATTATACCTAAGCAATTCGGTCC                                      |
| PFK11KO_5p_geno<br>mic int | GTGGATCTCACATTTTACAATATAAAG                                   |
| PFK11KO_3p_geno<br>mic int | CTATTGTTGAACGTTAACGACATAG                                     |
| PFK11KO_5p_int             | CATTTTTATTTGAGGGTACATTACTC                                    |
| PFK11KO_3p_int             | CAATTTTTTTTATACCTCTAATATATTCCC                                |

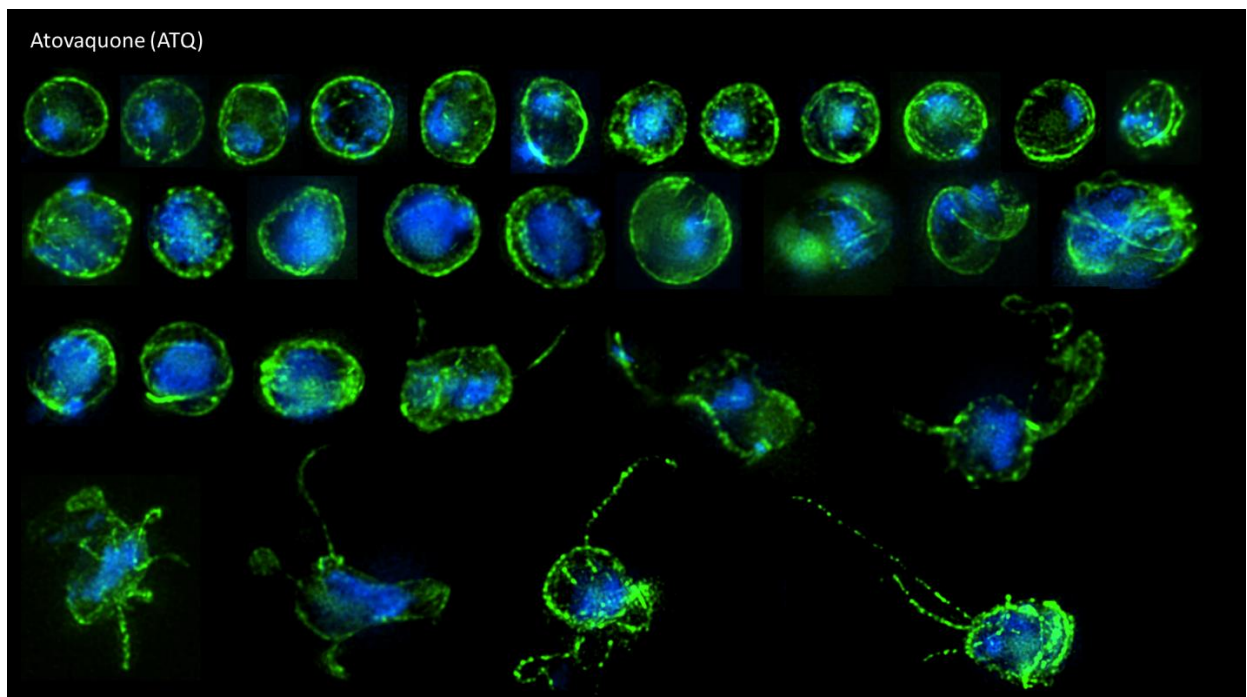
| <b>Primer name</b>        | <b>Sequence</b>                                      |
|---------------------------|--|
| ACSADPmNG_int_5p          | CTTCAAAGGTGTAACAATTCAAGATATGG                        |
| ACSADPmNG_int_3p          | CACGAAATGGATATATTATGTATGAACAT                        |
| mNeonGreen REV            | TAAACTTCCTCTTCCTTCGTCGACTTTATACAATTCATCCATTCCCATAACA |
| ACSADP_TGD_int5p          | GATTAGTAAAAGAACAATTCTACCTTTC                         |
| ACSADP_TGD_int3p          | gattttctctacatctccacatg                              |
| ACSADP_TGD_int3pWT        | AATTATACCTAAGCAATTCGGTCC                             |
| PFK11KO_5p_genomic<br>int | GTGGATCTCACATTTTACAATATAAAG                          |
| PFK11KO_3p_genomic<br>int | CTATTGTTGAACGTTAACGACATAG                            |
| PFK11KO_5p_int            | CATTTTTATTTGAGGGTACATTACTC                           |
| PFK11KO_3p_int            | CAATTTTTTTTATACCTCTAATATATTCCC                       |

**Appendix 2. Exflagellation IFAs of make gametocytes incubation for 24 hours with mETC inhibitors**

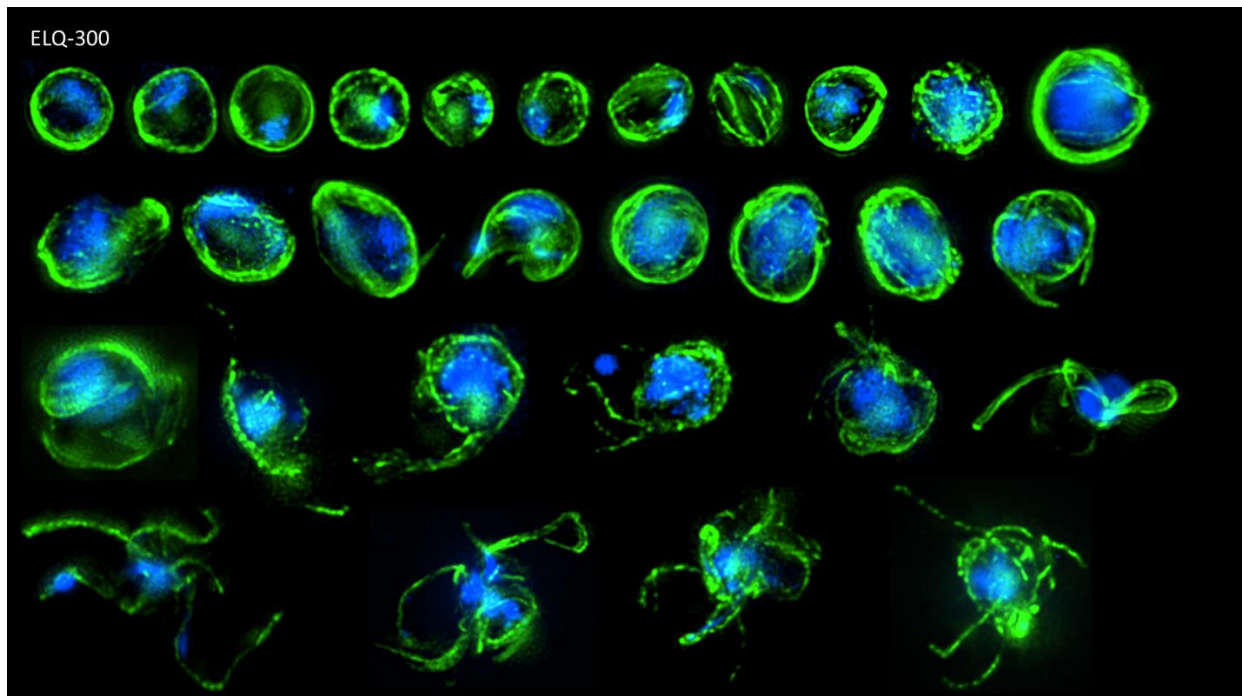
**A**



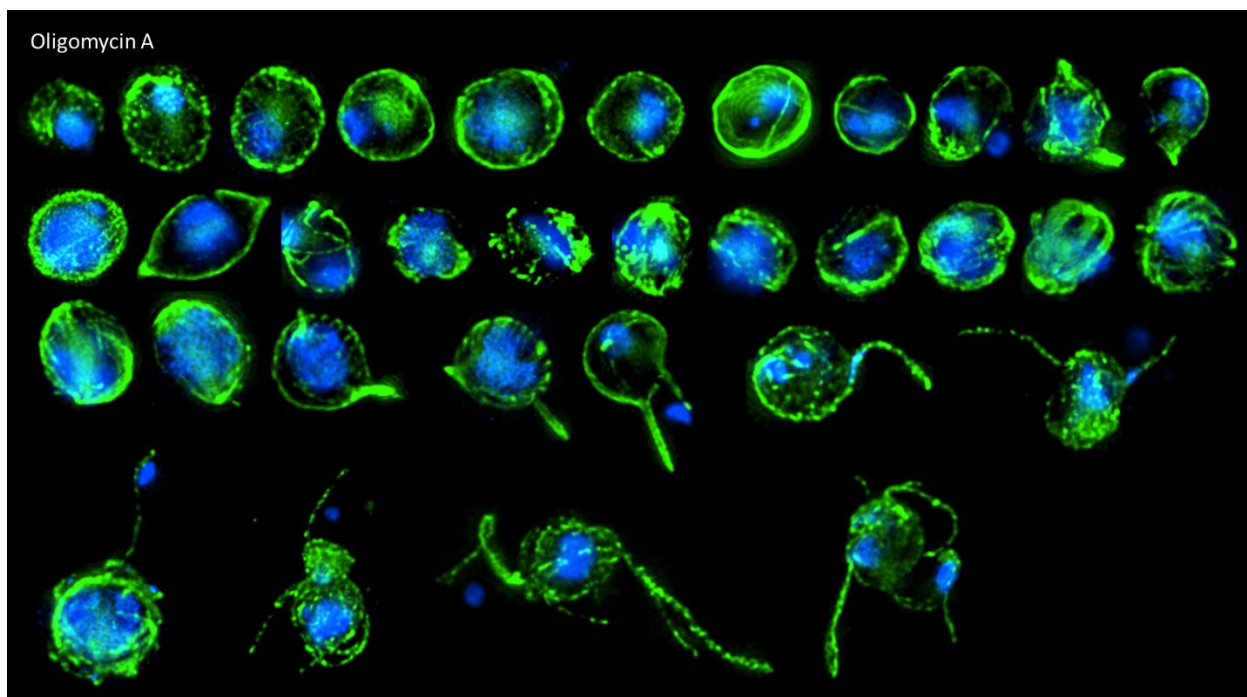
**B**



**C**



**D**



Exflagellating male gametocytes showing the flagella labelled with anti-alpha tubulin II (green) and the DNA labelled with DAPI (blue.) **A)** DMSO-treated parasites showing normal exflagellation. **B)** 10  $\mu$ M Atovaquone **C)** 10  $\mu$ M ELQ-300 **D)** 50  $\mu$ M oligomycin A. Gametocytes were pre-incubated with all three drugs for 24 hours before triggering exflagellation. The drug-treated male gametocytes start the process of exflagellation and frequently replicate their DNA but show fainter or punctate anti-alpha tubulin II staining compared to DMSO-treated gametocytes. Those in the late stages of exflagellation show fewer flagella or aberrant flagellar morphology.

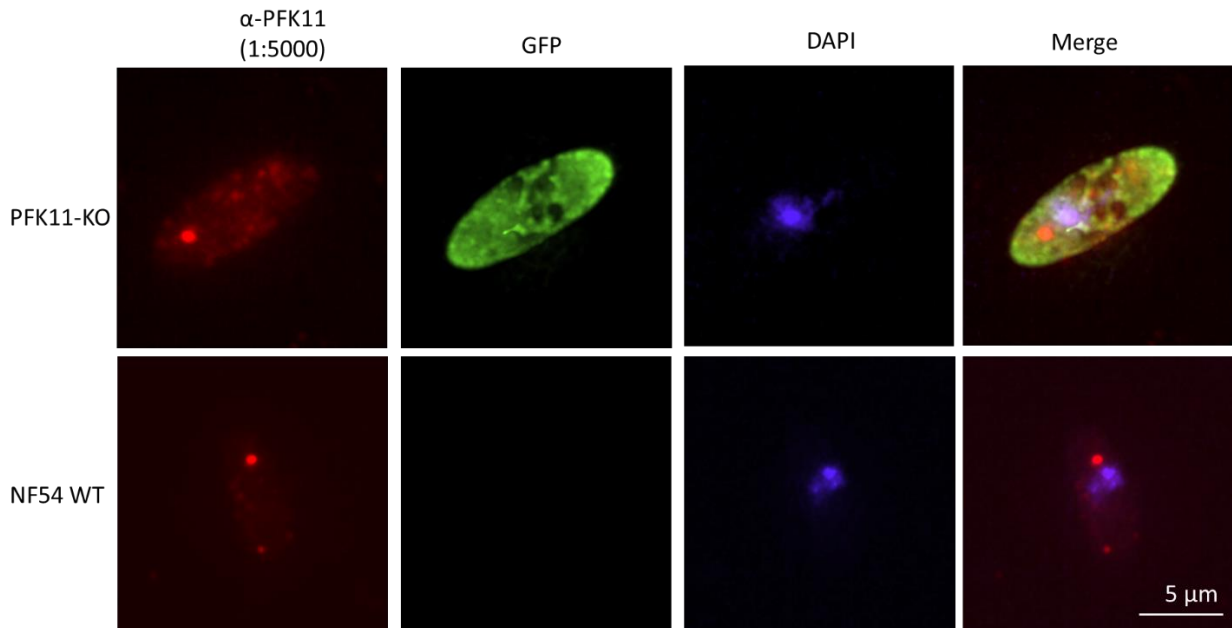
**Appendix 3. Table of oocyst counts for PFK11-KO vs NF54 WT mosquito feeding experiments**

| Mosquito Num. | Total Oocysts per midgut |                  |                 |                  |                 |                  |
|---------------|--------------------------|------------------|-----------------|------------------|-----------------|------------------|
|               | NF54 WT (rep 1)          | PFK11-KO (rep 1) | NF54 WT (rep 2) | PFK11-KO (rep 2) | NF54 WT (rep 3) | PFK11-KO (rep 3) |
| 1             | 15                       | 1                | 30              | 1                | 2               | 0                |
| 2             | 31                       | 0                | 64              | 0                | 38              | 0                |
| 3             | 14                       | 0                | 8               | 0                | 13              | 0                |
| 4             | 3                        | 0                | 20              | 1                | 15              | 0                |
| 5             | 38                       | 0                | 11              | 0                | 32              | 1                |
| 6             | 61                       | 0                | 19              | 1                | 24              | 0                |
| 7             | 2                        | 0                | 16              | 0                | 18              | 0                |
| 8             | 21                       | 0                | 40              | 0                | 18              | 0                |
| 9             | 10                       | 0                | 0               | 0                | 40              | 0                |
| 10            | 0                        | 0                | 46              | 1                | 0               | 0                |
| 11            | 1                        | 0                | 5               | 0                | 0               | 0                |
| 12            | 0                        | 4                | 34              | 1                | 0               | 0                |
| 13            | 9                        | 0                | 49              | 0                | 0               | 0                |
| 14            | 79                       | 0                | 35              | 0                | 0               | 0                |
| 15            | 29                       | 0                | 23              | 0                | 40              | 0                |
| 16            | 66                       | 1                | 19              | 0                | 5               | 0                |
| 17            | 4                        | 3                | 63              | 0                | 34              | 0                |
| 18            | 0                        | 1                | 11              | 1                | 25              | 1                |
| 19            | 36                       | 0                | 39              | 0                | 0               | 0                |
| 20            | 0                        | 0                | 25              | 0                | 0               | 0                |
| 21            | 6                        | 0                | 31              | 1                | 0               | 2                |
| 22            | 0                        | 1                | 21              | 0                | 52              | 0                |
| 23            | 35                       | 1                | 38              | 0                | 5               | 0                |
| 24            | 3                        | 0                | 11              | 1                | 12              | 0                |
| 25            | 1                        | 0                | 26              | 0                | 12              | 1                |
| 26            | 59                       | 1                | 1               | 2                | 19              | 0                |
| 27            | 17                       | 0                | 27              | 0                | 31              | 0                |
| 28            | 1                        | 0                | 1               | 2                | 13              | 0                |
| 29            | 10                       | 1                | 21              | 1                | 51              | 0                |
| 30            | 2                        | 0                | 16              | 0                | 0               | 0                |
| 31            | 0                        | 0                | 28              | 0                | 18              | 1                |
| 32            | 2                        | 0                | 39              | 0                | 19              | 0                |
| 33            | 18                       | 0                | 45              | 0                | 16              | 0                |
| 34            | 36                       | 1                | 19              | 0                | 52              | 1                |
| 35            | 27                       | 7                | 6               | 0                | 39              | 0                |

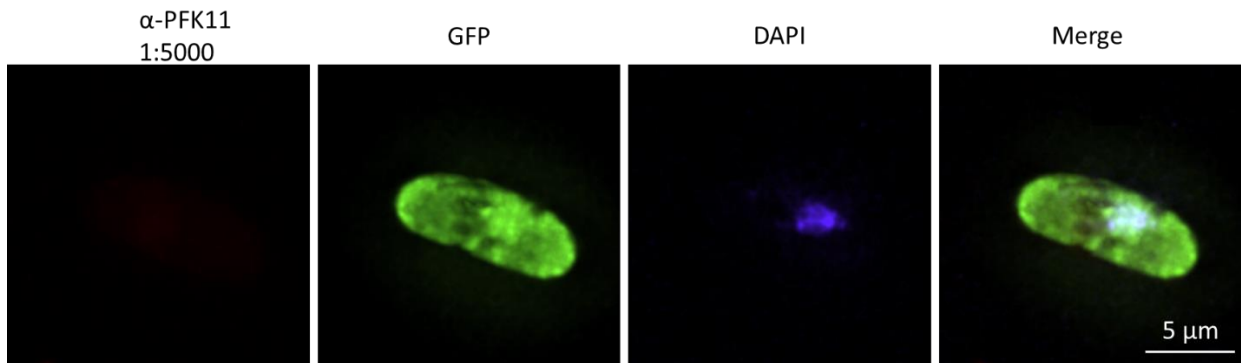
|                        |    |    |    |    |    |    |
|------------------------|----|----|----|----|----|----|
| 36                     | 0  | 0  | 27 | 0  | 24 | 0  |
| 37                     | 15 | 1  | 37 | 0  | 11 | 0  |
| 38                     | 9  | 3  | 11 | 0  | 13 | 0  |
| 39                     | 60 | 0  | 3  | 0  | 12 | 0  |
| 40                     | 23 | 5  | 4  | 0  | 4  | 0  |
| 41                     | 68 | 0  | 3  | 2  |    | 0  |
| 42                     | 0  | 0  | 10 | 0  |    | 0  |
| 43                     | 56 | 2  | 43 | 0  |    |    |
| 44                     | 6  | 0  | 9  | 0  |    |    |
| 45                     | 22 | 0  | 58 | 0  |    |    |
| 46                     | 9  | 0  | 10 | 0  |    |    |
| 47                     |    | 0  | 21 | 0  |    |    |
| 48                     |    | 5  |    | 0  |    |    |
| 49                     |    | 0  |    |    |    |    |
| 50                     |    | 0  |    |    |    |    |
| 51                     |    | 0  |    |    |    |    |
| 52                     |    | 0  |    |    |    |    |
| 53                     |    | 4  |    |    |    |    |
| 54                     |    | 2  |    |    |    |    |
| 55                     |    | 0  |    |    |    |    |
| 56                     |    | 0  |    |    |    |    |
| 57                     |    | 1  |    |    |    |    |
| 58                     |    | 7  |    |    |    |    |
| <b>Total Dissected</b> | 46 | 58 | 47 | 48 | 40 | 42 |
| <b>Total Infected</b>  | 38 | 20 | 46 | 12 | 31 | 6  |

## Appendix 4. IFA showing that PFK11 antibody is not specific.

**A**



## B. PFK11-KO secondary antibody only control



**Appendix 4. A)** IFA image showing PFK11-KO and NF54 WT stage V gametocytes stained with the anti-PFK11 antibody (visualised in red). PFK11-KO parasite express GFP, visualised in green, and DAPI is shown in blue. Punctate staining is visible in both WT and KO, suggesting that the antibody is not specific to PFK11. **B)** IFA image showing PFK11-KO line labelled with the red secondary antibody only. No red labelling is present, which suggests the antibody is parasite specific but is not specific to PFK11.





